AD-A138 761 THE DETECTION OF NONPLANAR SURFACES IN VISUAL SPACE(U) 1/3
MICHIGAN UNIV ANN ARBOR PERCEPTION LAB
W R UTTAL ET AL. 01 MAR 84 PERLAB-4 N00014-81-C-0266
UNCLASSIFIED F/G 6/16 NL

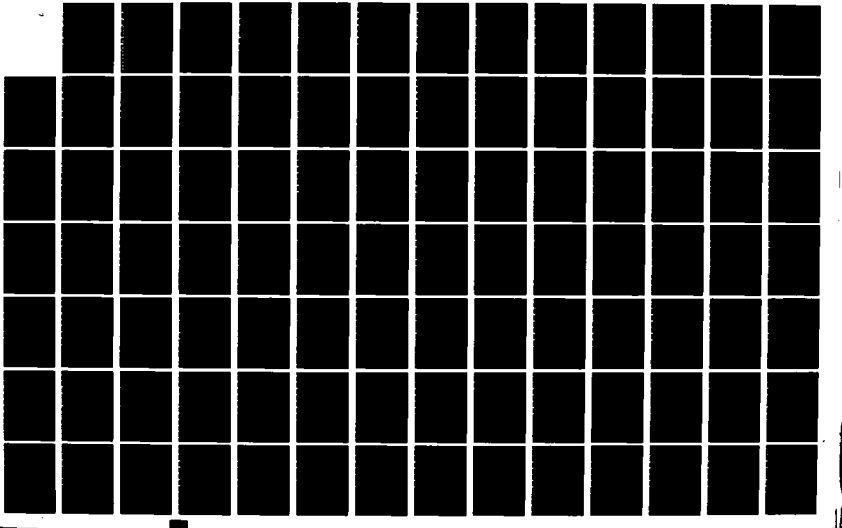

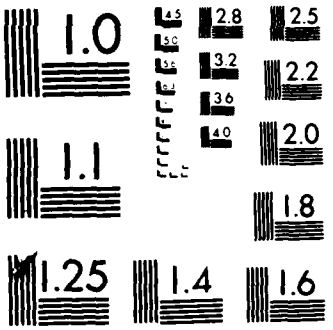

MICROCOPY RESOLUTION TEST CHART
NATIONAL BUREAU OF STANDARDS-1963-A

(12)

PERLAB-4

THE DETECTION OF NONPLANAR SURFACES IN VISUAL SPACE

William R. Uttal

with the technical collaboration of
John Brogan
Katherine McCreight
Susan Robertson
Phyllis White
Larry Spino

Perception Laboratory
Institute for Social Research
The University of Michigan
Ann Arbor, Michigan

1 MARCH 1984

PERLAB-4

THE DETECTION OF NONPLANAR SURFACES IN VISUAL SPACE

William R. Uttal

with the technical collaboration of
John Brogan
Katherine McCreight
Susan Robertson
Phyllis White
Larry Spino

Perception Laboratory
Institute for Social Research
The University of Michigan
Ann Arbor, Michigan

1 MARCH 1984

SECURITY CLASSIFICATION OF THIS PAGE (When Data Entered)

REPORT DOCUMENTATION PAGE

READ INSTRUCTIONS BEFORE COMPLETING FORM

1. REPORT NUMBER: PERLAB-4	2. GOVT ACCESSION NO.: AD A138761
	3. RECIPIENT'S CATALOG NUMBER:
4. TITLE (and Subtitle): The detection of nonplanar surfaces in visual space	5. TYPE OF REPORT & PERIOD COVERED: Technical
	6. PERFORMING ORG. REPORT NUMBER:
7. AUTHOR(s): William R. Uttal	8. CONTRACT OR GRANT NUMBER(s): N00014-81-C-0266
9. PERFORMING ORGANIZATION NAME AND ADDRESS: Institute for Social Research University of Michigan Ann Arbor, MI 48106-1248	10. PROGRAM ELEMENT, PROJECT, TASK AREA & WORK UNIT NUMBERS: 61153N 42; RR04209 RR0420902; NR 197-070
11. CONTROLLING OFFICE NAME AND ADDRESS: Office of Naval Research Engineering Psychology Programs (Code 442) Arlington, VA 22217	12. REPORT DATE: 1 March 1984
	13. NUMBER OF PAGES:
14. MONITORING AGENCY NAME & ADDRESS (if different from Controlling Office):	15. SECURITY CLASS. (of this report): U
	15a. DECLASSIFICATION/DOWNGRADING SCHEDULE:

16. DISTRIBUTION STATEMENT (of this Report)

Approved for public release; distribution unlimited.

17. DISTRIBUTION STATEMENT (of the abstract entered in Block 20, if different from Report)

18. SUPPLEMENTARY NOTES

19. KEY WORDS (Continue on reverse side if necessary and identify by block number)

Visual Perception
Form Detection
Masking
Signal-to-noise ratio
Dotted Forms
Stereopsis
Nonplanar stimuli

20. ABSTRACT (Continue on reverse side if necessary and identify by block number)

This monograph presents the results of a series of 17 experiments designed to provide a partial answer to two questions concerning the detection of dotted forms in dotted visual masks: (1) What is the effect of the spatial geometry of three-dimensional, nonplanar forms on their detectability? (2) What is the effect of the signal-to-noise ratio on their detectability? The results of the study indicate that the spatial geometry exerts virtually no effect until a threshold level of geometrical complexity is exceeded by the

DD FORM 1 JAN 73 1473 EDITION OF 1 NOV 65 IS OBSOLETE

SECURITY CLASSIFICATION OF THIS PAGE (When Data Entered)

stimulus-forms. Beyond that threshold, the effects of form are significant but modest in absolute amplitude. The results further indicate that a putative large effect of form obtained with sinusoidal stimuli actually results from a violation of the Shannon-Weaver sampling theorem from information theory and is thus due to inadequate definition of the form rather than to the nature of the form. On the other hand, the signal-to-noise ratio strongly influences detectability, regardless of whether it is manipulated by varying the number of dots in the stimulus form or by varying the number of masking-dots.

This study failed to extend a highly successful autocorrelation-type theory from two-dimensions to three-dimensions. The stereoscopic task used in this study apparently involves other factors not incorporated in the current version of the theory. Indeed, the complexity of the experimental paradigm and certain paradoxical results leave many questions unresolved. The implications and background of this study are discussed in detail.

PERLAB-4

THE DETECTION OF NONPLANAR SURFACES IN VISUAL SPACE

William R. Uttal

with the technical collaboration of
John Brogan
Katherine McCreight
Susan Robertson
Phyllis White
Larry Spino

Perception Laboratory
Institute for Social Research
The University of Michigan
Ann Arbor, Michigan

1 MARCH 1984

TABLE OF CONTENTS

ABSTRACT

This monograph presents the results of a series of 17 experiments designed to provide a partial answer to two questions concerning the detection of dotted forms in dotted visual masks: (1) What is the effect of the spatial geometry of three-dimensional, nonplanar forms on their detectability? (2) What is the effect of the signal-to-noise ratio on their detectability? The results of the study indicate that the spatial geometry exerts virtually no effect until a threshold level of geometrical complexity is exceeded by the stimulus forms. Beyond that threshold, the effects of form are significant but modest in absolute amplitude. The results further indicate that a putative large effect of form obtained with sinusoidal stimuli actually results from a violation of the Shannon-Weaver sampling theorem from information theory and is thus due to inadequate definition of the form rather than to the nature of the form. On the other hand, the signal-to-noise ratio strongly influences detectability, regardless of whether it is manipulated by varying the number of dots in the stimulus-form or by varying the number of masking-dots.

This study failed to extend a highly successful autocorrelation-type theory from two-dimensions to three-dimensions. The stereoscopic task used in this study apparently involves other factors not incorporated in the current version of the theory. Indeed, the complexity of the experimental paradigm and certain paradoxical results leave many questions unresolved. The implications and background of this study are discussed in detail.

PREFACE

This monograph is the third in a series that examines the nature of a mid-level visual process relatively uncontaminated by either peripheral receptor or central cognitive processing. The paradigm utilized in this study selectively assays what seems to be a relatively fixed algorithmic mechanism involved in the extraction of dotted stimulus-forms from masks consisting of random dots. The first book in this series (Uttal, 1975) described a study of two-dimensional patterns hidden in two-dimensional masks. The second (Uttal, 1983) dealt with an investigation of planar stimulus-forms placed in different spatial positions and orientations and masked by dots distributed throughout a solid volume. The stimulus-forms studied in the present work were no longer restricted to planes but, in general, were nonplanar surfaces distorted by means of appropriate mathematical transformations.

The purpose of this entire research program has been to answer the question: What role do specific attributes of stimulus-forms play in visual perception? Future research will examine analogous effects on discrimination and recognition performance to derive general conclusions concerning both the nature of the processes that underlie our ability to perceive and the characteristics of the visual space constructed by those processes.

During the course of this research program, I have benefitted from the advice of a number of people who deserve specific acknowledgement. Several of my colleagues at The University of Michigan have provided one or another kind of counsel at various times during the past year. J.E. Keith Smith and Lisbeth Fried from the Psychology Department and Wilfred Kincaid from the Mathematics Department (and the "vision lunch group") provided insights at times when the

pattern that now seems so evident was not yet so clear. In our Perception Laboratory, the programming skills of John Brogan and Larry Spino have been the rock upon which this work was founded. Phyllis White, Katherine McCreight, and Susan Robertson contributed their research assistance, organizational abilities, and typing-editing skills in ways that have been invaluable to the daily execution of the experiments and to the preparation of this manuscript. Behind the scenes, the guidance and continued collaborative support of John J. O'Hare of the Office of Naval Research has been always present and much appreciated. John's administrative role of Scientific Officer has expanded into a highly valued collegial relationship.

The project was supported by the financial instrument known as ONR contract #N00014-81-C-0266. I remain especially grateful for the enlightened attitude of the ONR. Their decades-long commitment to basic science plays an important role in the continuing development of perceptual research.

Part of this report was written during the summer of 1983 while I was a visiting scholar at the Rockefeller Foundation's Villa Serbelloni study center in Bellagio, Italy. I am grateful to the Foundation and for the gracious hospitality extended by Angela Barmettler and Roberto Celli and their staffs during that visit.

Finally, I could not end any acknowledgement of appreciation without mentioning the ultimate source of all that has been of value to me in life — my wife, May. Her companionship, wisdom, and positive enthusiasm about life in general have been absolute necessities for everything that I have ever accomplished.

1. INTRODUCTION

During the past decade, together with my colleagues in the Perception Laboratory at the Institute for Social Research, I have been involved in the search for answers to a relatively straightforward empirical question: What is the effect of the geometry of a dotted stimulus-form on its visual detectability when it is embedded in a field of randomly arrayed masking-dots? We have researched this question for both two-dimensional and three-dimensional visual stimuli. For the present study, we generated three-dimensional stimuli in a computer-controlled, real-time, dichoptic viewing situation in which the disparity of the two retinal images was manipulated to produce a strong and compelling experience of depth.

There are several theoretical and practical arguments for pursuing this research paradigm. The very nature of the dotted-abstraction-from-continuous-reality that is embodied in our experiments provides us with a simple and convenient domain in which to study some exceedingly interesting and complex perceptual phenomena. Indeed, the abstracted reality is simple enough that in some cases it has been possible to construct formal mathematical models of the behavior of the human observer in the dot-detection task, an accomplishment that would have been impossible in a study that used continuous forms. The relatively high degree of success previously enjoyed in applying a formal model based on the autocorrelation transform to the description of the perceptual performance in the detection of dotted stimulus-forms (Uttal, 1975; 1983) is an example of how simplification per se can carry understanding beyond where it might have been had we chosen to use more natural continuous stimuli.

The dotted-stimulus-in-dotted-mask paradigm is also both simple and specific

enough to permit us to examine an especially clearly defined intermediate stage of human visual processing that lies between the processes of the receptors and the retinal plexus, on the one hand, and higher level cognitive processes, on the other. This is a distinct advantage considering how often events occurring at multiple levels of processing are confounded using other paradigms. The essentially wholistic and algorithmic nature of the visual processes assayed in this study is sharply highlighted by the experimental paradigm and the mathematical model used to describe our results.

It should be mentioned, too, that the abstractions themselves also have immediate practical implications. The techniques used and findings obtained in these experiments are directly relevant to a variety of real-world tasks that require observers to detect signals in interferring backgrounds or that involve quasi-dotted stimuli. For example, applications may be found in fields such as air traffic control; geophysical surveys (e.g., to distinguish a region of interesting density differences from its surroundings); oceanography (e.g., to locate fish schools or inversion layers); medical diagnostics (e.g., to detect abnormal volumes and surfaces among other normal volumes and surfaces); and even atmospheric physics in which gradients must be detected amidst other gradients.

Experimental results from earlier research have shown that, for two-dimensional stimuli (i.e., stimulus-forms confined to a plane), a general rule of visual perception denoted as The Rule of Linear Periodicity seems to hold true. This rule asserts that the stimulus attributes that most strongly influence detectability of a dotted stimulus-form in a dotted masking field are the linearity of the global structure and the periodicity of the spacing between the constituent dots. To the degree that a dotted line deviates from linearity or that its dots are aperiodically spaced along the axis of the line, the detectability of a stimulus-form is substantially reduced. A corollary of this rule is that dotted stimuli that do not

contain straight-lines (i.e., planar surfaces defined by arrays of random dots, as shown in Figure 1) exhibit only a minimal differential sensitivity to the global arrangement of the constituent dots. A further corollary is that straight, periodic lines also are the main determinant of detectability of any other, more complex forms of which they are a part. The detectability of a form such as that shown in Figure 2 is strongly influenced by the linear arrangements of its constituent dots.

In spite of the ubiquity of this finding throughout our study, it must be acknowledged that this rule characterizes a highly specific stimulus situation —one in which dotted stimulus-forms are hidden in dotted masks — and by no means can it be assumed a priori that this general rule also describes the properties of the continuous stimulus-forms of which real life scenes are themselves formed. Dot arrays, ordered or random, and the experimental paradigms in which they are used are abstractions from most visual realities. Other kinds of bridging arguments and empirical data must be invoked to validate the relevance of the rule of linear periodicity to more realistic kinds of stimuli.

The main argument permitting us to generalize the rule of linear periodicity to the perception of continuous stimuli is, in fact, an empirical one. In the few instances in which research has been done with continuous figures, a similarity does appear between our results with dots and the earlier findings. Data resulting from comparable research with continuous figures are by no means abundant, and one must go far back in the literature to find such correspondences. Helson and Fehrer (1932), for example, in one of the pioneering studies on the influence of form on visual perception, found that while the global shape of the stimulus had little influence on the luminosity threshold — a conclusion also supported by much recent research -- one of their stimuli was "better" than others when the observer had to perform tasks involving recognition or discrimination. Surprising (as well as misleading) to them was the outcome that the "best" form was not the "good"

circle of the then-pervasive Gestalt tradition. Rather, it was the rectangle -- a form which lacked the same degree of the mysterious "goodness" or "pragnanz" central to the wholistic psychologies that dominated perceptual thinking in the 1920s and 1930s. Helson and Fehrer's results antedated and predicted the general results obtained in some of our earlier studies (Uttal, 1983) showing that more oblong rectangles are more easily detected than less oblong ones, but only when they are constructed from dotted outlines and not from random dot arrays. Both data speak to the prepotency of linear stimuli since outlined rectangles, whether dotted or continuous, are composed of just that kind of component part — straight lines.

Although there is much more to be said later about the significance of the rule of linear periodicity, the generalization is of sufficient import to deserve some preliminary comment here. The laboratory datum (perhaps an otherwise irrelevant empirical triviality) known as the rule of linear periodicity asserts a profound and seemingly universal fact about the perceptual system. At the macroscopic level with which we are concerned here, form vision primarily functions in a Cartesian, linear space as opposed to a polar, angular, or even a curved one. Straight lines are more detectable because of their own properties or the nature of the visual system, although other geometrical sensitivities could easily have been hypothesized. This single datum helps us to understand something fundamental about the nature of visual space and, thus, is suggestive if not definitive of the nature of our visual nervous system.

Although it is possible to assume a broader generality for the dotted-figure-in-dotted-mask results in at least some regards, such generalization may not be equally valid for some other aspects of vision. For example, it is well established that the oblique effect — the difference in performance that exists between obliquely oriented figures and horizontally or vertically oriented figures —is

observable in many different visual tasks with continuous lines (Appelle, 1972) but does not exist with dotted patterns. Dotted forms have rarely in our experiments with either two (Uttal, 1975) or three dimensions (Uttal, 1983) exhibited any evidence of an oblique effect. Indeed, this result even holds true when the form is rotated into the z (depth) dimension. The only exception to this occurs when dotted lines are used as masks (rather than single dots) and when both the masking lines and stimulus-form lines are presented at an oblique angle. This unexpected exception was recently shown to be the case by Michael Young (1984) in his master's thesis research conducted in this laboratory.

One, therefore, must display great care in asserting which aspects of dotted-form perception can be generalized to other, more continuous domains of form perception. The difficulties are compounded when other kinds of dotted-perception tasks also show orientation effects. For example, Rogers and Graham (1983) have shown that, when a Craik-O'Brien-Cornsweet illusion is established with a random-dot stereoscopic procedure, a vertically aligned stimulus may produce the illusion while a horizontally aligned one does not. This orientation effect in a depth-illusion task is quite different from the generally negative results obtained in the studies of dotted-form detection reported here.

There are many pieces of evidence that illustrate how tricky visual perception can be, and how incomplete either our knowledge or intuition about it. The extrapolation of a conclusion from one type of stimulus situation to another, or from two to three dimensions, can be fraught with unexpected conceptual and empirical hazards. It is embarrassing to realize just how often my intuitions have been mistaken and how often the data have surprised me when some apparently trivial aspect of the stimulus or experimental design is changed. For example, the degree of oblongness of rectangularity exerts no influence on detection when the rectangle is composed of arrays of randomly positioned dot, a situation in which

contours, therefore, are only suggested (Uttal, 1983; Exp.12). On the other hand, rectangularity does exert a powerful effect when the stimulus-form is defined by dotted outlines (Uttal, 1983; Supplementary Exp.1). This lack of generalizability from one stimulus situation to another when the actual differences seem only slight, exists not only vis-a-vis continuous and dotted forms or between random dot-arrays and dotted-outline forms, but also with regard to the relationship between two- and three-dimensional dotted-detection tasks. Thus, it is necessary to test specifically any putative "generalities" in the laboratory whenever one makes a change such as going from experimental situations that are primarily two-dimensional to those that are primarily three-dimensional.[1]

The Issues

The purpose of the present study is to investigate the effects of their three-dimensional form on the detectability of nonplanar surfaces. Specifically, the questions addressed in this study are:

1. Do nonplanar surfaces composed of arrays of random dots differ in their psychophysical detectability as a function of the kind of shape?
2. Do nonplanar surfaces composed of arrays of random dots differ in their psychophysical detectability as a function of the magnitude of distortion away from a plane?
3. Do nonplanar surfaces composed of regular matrices or dotted lines differ in their psychophysical detectability as a function of either the kind of shape or magnitude of distortion from a prototypical plane?
4. What is the influence of the signal-to-noise ratio (i.e., stimulus-form dot numerosity divided by masking-dot numerosity) on detectability in several different situations.

We may add, by way of a priori speculation, what the answer to these first three questions would be if what we know concerning the visual detectability of planes could simply be extrapolated to nonplanar surfaces, or what the two-dimensional rules of detectability might lead us to predict concerning the detectability of nonplanar, three-dimensional stimulus-forms. Keeping in mind that these are speculative extrapolations, these answers might be:

Predictions:

1. Given the small effect of global form when planar surfaces are composed of random-dot arrays, the kind of form of a nonplanar surface in three-dimensional space should not produce a major effect on psychophysical detectability.

2a. Given the small effect of global form when planar surfaces composed of random-dot arrays are deformed in two-dimensional space, there should be little effect of distortion away from a plane.

or

2b. Given that the plane in three-dimensional space is analogous to the line in two-dimensional space and that to distort a line greatly reduces its detectability, there should be a major effect of distortion away from the plane.

Either prediction 2a or 2b might be plausible given its particular underlying assumption. The rejection of one or both has been one of the major goals of this study. Which one remains will tell us something about the nature of visual space. As we shall see, the actual results are, in empirical fact, more complex than

indicated by either of these two hypothetical predictions.

3. Given that regular planar arrays of dots are also analogous to straight lines, regular arrays should become less detectableare as they are distorted from planar to nonplanar surfaces.

As we shall see, this third question cannot be answered to our total satisfaction with the stereoscopic technique used in this study. The dichoptic disparities and perspectives involved in generating these regular, gridlike forms produce a monocular cue (straight-lines) that cannot be controlled or negated. The impact of the rule of linear periodicity, a psychophysical property, is so great that it allows these monocular cues to swamp out the more subtle stereoscopic ones. Nevertheless, even these confounded (by the presence of monocular cues) experiments are instructive in surprising ways, and several are reported as supplementary experiments in Chapter 4.

The following pages of this report describe the results of 17 experiments. The first of these is designed to investigate the effect of different kinds of the most extreme nonplanar surfaces on visual detectability. By "most extreme" is meant the most distorted versions of a set of seven different nonplanar surfaces (i.e., surfaces produced by seven different generating functions, which are described later on). The detectabilities of these seven stimulus-forms are compared over a wide range of masking-dot densities. All of these stimulus-forms are composed of random-dot arrays without straight-line components.

The second experiment is a monocular control using the same stimuli as the first. Most of the other reported experiments, however, deal with single kinds of forms (surfaces produced by a single generating function) but with different

coefficients that are progressively varied to distort the surface to greater and greater degrees away from a prototypical plane. In general, results indicated a progressive increase in the effect of the magnitude of distortions as the complexity of the stimulus-forms increased. Complexity is defined by an aggregate measure of several attributes of the stimuli that will be more completely spelled out later in this monograph.

2. BACKGROUND

A. Previous Work from the Perception Laboratory.

The dot-masking paradigm has proven over the years to be a rich source of data and ideas related to problems of form perception. The current research is the outgrowth and continuation of over a decade of research in this laboratory (mainly reported in the series of papers cited below and in two monographs (Uttal, 1975; 1983). The purity of the stimulus-forms used in this study (that is, their freedom from both energy-driven receptor influences and context-dependent semantic and cognitive influences) allows us to examine some subtle information-processing attributes of vision that may have been hidden or overwhelmed by other energy sensitive, peripheral or meaning-dominated central effects if non-dotted, natural, or realistic stimulus-forms had been used. In short, we have chosen an ideal method for studying a particular kind of preattentive geometrical and spatio-temporal organizational influence on an intermediate level of form vision. This, it is believed, is the only context to which this work is relevant; the results are not germane to either simpler or more complex levels of visual information processing nor to the processing of continuous stimuli unless independently related.

The history of dot masking as a formal experimental procedure (it probably existed as a practical visual task in real-life, camouflage-type situations long before this date) goes back to a largely overlooked paper by R.S. French (1954). French implicitly foresaw the advantages of a methodology in which the signal-to-noise ratio (somewhat arbitrarily measured by the number of dots in the stimulus-form and in the mask, respectively) could be used to vary the detectability of a visual form. The idea of using dots was an

important breakthrough because it minimized the role of the nature of the components and emphasized the role of their arrangement. Given the ubiquity of data suggesting that this is, in fact, the way human beings see, this was not a trivial advantage.

Another main paradigmatic theme that obviously permeates this work is the concept of the random-dot stereogram, a technique that was introduced into psychology by Bela Julesz (1960, 1971). This technique helps to remove superfluous cues or complex meaning and, more important, opens up the third dimension of depth to experimental analysis. For many purposes, the random-dot stereogram is the sine qua non of an executable experiment in stereoscopic depth perception. This is so simply because it reduces the full range of possible cues, some monocular and some binocular, to solely those associated with the dichoptic disparities. Our work depends heavily upon the important contributions of both French and Julesz.

Earlier stages of this project have led to a number of insights into human visual form perception. I must qualify this sentence for precision by appending the phrase in the dot-masking context. Nevertheless, as indicated earlier, at least some of our findings generalize to more realistic and natural continuous stimuli. One of the major discoveries that we have made is the very straightforward and undeniable fact that some constellations of dots are more detectable than others, even when dot numerosity and spacing are controlled. That is, the global geometry per se of a constellation of dots, and presumably other kinds of stimulus-forms, influences their detectability above and beyond the specific details of their local features. Indeed, when dotted stimulus-forms are used, the local features have been reduced to nil. For the detection of two-dimensional forms, the general result can be formalized as the rule of linear periodicity — the prepotency of straight, periodically spaced dotted lines, to

which I have already alluded. The reasons for special visual sensitivity to straight-lines are suggested, but the underlying physiological mechanisms are not completely illuminated or explained, by the mathematical transformation embodied in the autocorrelation model that has been used to describe these data. The autocorrelation model is a means of processing simulations (but not exact copies) of stimulus-forms in a manner that has been shown in many cases to be analogous to the way in which the same stimuli are processed by the human visual system. To the degree that the autocorrelational transformation and psychophysical phenomena agree, it can be asserted that the model is sensitive to many of the same attributes of the stimulus as is the perceptual skill. Beyond this statement of analogy, however, interpretations concerning the exact details of the underlying physiological mechanisms becomes highly speculative.

It must be appreciated, furthermore, that it is the entirety of the mathematical and psychophysical processes, including the input stimuli, that are analogs of each other. Therefore, it is uncertain whether the rule of linear periodicity is a result of certain of the attributes of the stimulus configuration (lines are simpler in a certain sense than curves — fewer points are necessary to define them) or, to the contrary, a property of the transformational processes -- similarities between the autocorrelation mathematics and some inferred autocorrelation-like psychophysical processes. Even if it is the former, there is no compelling reason to suggest the presence of an actual autocorrelator in the nervous system, merely a transformational process that exhibits the same sensitivity to straight-lines and other stimulus-forms as does an autocorrelator.

Nevertheless, it is extremely instructive to apply the autocorrelation model, which has done a surprisingly competent job of actually predicting the psychophysical detectability of dotted stimuli, in this context. This is so even

though the model does not work well, as shall be seen later, in this three-dimensional paradigm. Its very failures become the basis of future, more successful, models, and thus it is worthwhile to consider it in detail.

The autocorrelation transformation is a special case of a convolution integral based on the following formula:

$$A(\Delta x,\Delta y) = \iint f(x,y) \cdot f(x + \Delta x,\ y + \Delta y)\,dy\,dx \qquad (1)$$

where Δx and Δy are shifts in the positions of the points of a stimulus-form f(x,y) required to produce a shifted replica — $f(x + \Delta x, y + \Delta y)$.

Although this formula is presented here in terms of the integral calculus and in the terminology of infinitesimals, in our actual model the transformation is implemented on the computer in the form of a discrete approximation to this equation. Indeed, some of my mathematical colleagues, more precise than I in their terminology, may prefer to call it an "autocorrelation-like" transformation, a nomenclatural purification I would happily accept. A complete description of the discrete algorithm actually used to compute the autocorrelation has been presented in Uttal (1975).

A family of $A(\Delta x,\Delta y)$ values must be computed for all possible Δx and Δy combinations to fill the autocorrelation space. Samples of two simulated stimuli that can serve as inputs to the autocorrelation processor and two photographs of the computer plot of their discrete autocorrelated outputs are shown in Figure 3. The first plate in this figure shows a straight dotted-line stimulus and its autocorrelation. The second plate shows the same dotted-line embedded in random masking-dots; it should be noted that the peaks in the

autocorrelation space most closely associated with the straight-line of dots are higher than other peaks. This is a clue as to how this mechanism might be used to discriminate a periodic line of dots from random dots in either the brain or the computer — form has been converted into amplitude and the highest peaks are associated with the most regular form. Of course, it is not this simple for other nonlinear or three-dimensional forms, but similar transformational cues may also apply in such cases.

The autocorrelational surface is made up of a number of peaks distributed in the $\Delta x, \Delta y$ space. By applying the following empirical expression:

$$F_m = \frac{\sum_{n=1}^{N} \sum_{i=1}^{I} (A_n \cdot A_i) / D}{N} \quad ; n \neq i \qquad (2)$$

a single numerical "Figure of Merit" (F_m) can be generated for each autocorrelated stimulus pattern. In this expression, A_i and A_n are the amplitudes of peaks taken pairwise, D is the Pythagorean distance in the $\Delta x, \Delta y$ space between the two peaks, and N is the number of peaks. The purely arbitrary and ad hoc Figure of Merit produces families of F_m's that are closely associated with the relative psychophysical detectability of sets of stimulus forms.

In some of the earlier studies (Uttal, 1975), the effects of variations of a number of different attributes of two-dimensional stimulus-forms were evaluated in a series of psychophysical experiments using only two-dimensional visual masks. Specifically, I considered the effects of each of the following attributes and found the results indicated for each of the following dimensions:

1. Dot numerosity — more dots, more detectable.

2. Line orientation — no effect.
3. Deformation of straight-lines into curves and angles — more deformation, less detectable.
4. Colinear dot-spacing irregularity — more irregular, less detectable.
5. Transverse dot-spacing irregularity — more irregular, less detectable.
6. Missing parts in triangles — sides more important than corners.
7. Polygonal orientation — no effect.
8. Distortions of squares into parallelograms — more distortion, less detectable.
9. Organized straight-line patterns versus "pick-up-sticks" patterns composed of the same lines — more organized, more detectable.
10. Distortions of squares and triangles by misplacing one or more corners — more distortion, less detectable.
11. Figural goodness — no effect.

The order of detectability of the forms in each of the psychophysical experiments was compared with the order of the Figures of Merit generated by the autocorrelation evaluation of the simulated stimulus-forms. In most cases, the two rank orders were in agreement. There were, however, some discrepancies between the two rank orders. Some forms that showed differences in their respective Figures of Merit in the simulation produced no comparable differences in psychophysical performance. Furthermore, while the Figure of Merit for forms that varied in "figural goodness" were in substantial agreement with the psychophysical data, there were some particular cases in which order reversals appeared. These discrepancies seemed to be mainly due to a lack of sensitivity on the part of the autocorrelation model to forms that

possessed preponderantly diagonal arrangements of the constituent dots. All of these discrepancies between theory and psychophysical findings, are probably due to deficiences in the formulation of the empirical Figure of Merit expression.

In the next series of experiments, reported in Uttal (1983), I turned from two-dimensional stimuli hidden in two-dimensional masks to stimuli that, while still two-dimensional themselves (single dots, lines, and planes) were embedded among random visual masking-dots that were arrayed in three-dimensional space. This work acjoeved a number of interesting results:

1. As an unmitigated generality, increasing the number of masking-dots monotonically reduced the detectability of a dotted stimulus-form when all other varibles are held constant. In other words, the raw signal (stimulus-dot numerosity)-to-noise (masking-dot numerosity) ratio was a powerful determinant of dotted-form detection. Although not surprising, this outcome is an important cross-referencing parameter in the present study and is of interest in its own right. This outcome confirmed and extended the findings concerning signal-to-noise ratios from the earlier study with two-dimensional stimuli.
2. The position of a repetitive flashing dot in the apparent cubical space exerted only a minor effect on its detectability. A dot placed far off the rear, lower, right-hand corner was seen slightly less well than dots at other positions, and one centered in space was seen slightly better. Although I presented no equivalent data concerning the translations of lines or planes, within similar limits and on the basis of my two-dimensional results, I believe this result also holds

for such multidimensional stimuli.

3. Repetitively flashed dots with interdot intervals of 100 msec were seen better than those with shorter or longer intervals when the number of flashed dots was held constant. The function relating single-dot detectability to interdot interval was thus nonmonotonic and suggests the existence of an optimum interval of about this duration.

4. In dotted-form discrimination, there was a substantial advantage gained by using a dichoptic viewing condition that allowed the perceptual construction of depth compared to either binocular or monocular viewing conditions in which no disparity cue to depth was present. Somewhat surprisingly, binocular viewing produced higher detection scores than did monocular viewing, in spite of the fact that there was no information difference between the stimuli in the two nondisparity viewing conditions.

5. Increasing the interdot interval between sequential dots in a plotted straight-line of dots led to a monotonic and nearly linear reduction in the detectability of the line. It is unclear whether this was a result of the increase in the interval per se or due to the increased number of masking-dots encompassed by the duration of the dot train. What is certain is that apparent movement did not substitute in any way for simultaneity.

6. Very surprisingly, irregularity of the temporal intervals between the plotting of successive dots did not appreciably diminish dotted-line detection. A high degree of interdot-interval irregularity could be tolerated without reduction in detection scores.

7. Spatial irregularity of the dots along a straight-line affected

detectability at short interdot-intervals (less than or equal to 30 msec). However, at longer dot intervals these same spatial irregularities exerted little influence on detectability. In some manner, visual mechanisms seemed to be able to compensate for these spatial distortions if sufficient time elapses between the plotting of sequential dots.

8. An increase in the disorder of the sequence in which a series of regularly spaced (in time and position) lines of dots was plotted produced only a modest, though monotonic, decrease in the detectability of the form. This form of irregularity, so extreme that it violated the spatio-temporal topology of the stimulus-form, could still be partially overcome, presumably by the same mechanisms that were capable of "smoothing" temporal and spatial irregularity.

9. Dotted-line orientation in space was ineffective in influencing detectability scores. Visual space was isotropic for diagonal lines.

10. When two planes were to be discriminated from each other with regard to their respective depths:

    a. The greater the dichoptic disparity between the two planes, the more easily one was discriminated from the other.

    b. The effect of the number of dots in the two planes was relatively small. Indeed, discrimination of a highly reduced stimulus consisting of only two dots was easily accomplished.

    c. A reduction in viewing time led to a progressive though modest reduction in the discrimination of the two planes.

    d. When a burst of masking-dots followed the presentation of a dichoptic stimulus, stereoscopic performance was especially

degraded at intervals less than 50 msec.

11. The form of a planar stimulus composed of even a relatively large number of randomly arrayed of dots had a surprisingly small effect on its detectability, given what we had previously learned in the earlier two-dimensional studies with dotted-outline forms. Even when the viewing time was reduced, further impoverishing the dot-masked stimulus, form defined in this way remained an ineffective variable and any putative effect of form was not enhanced. Furthermore, the effect of even as drastic a manipulation as changing the stimulus-form from a square to an elongated rectangle was slight. However, this conclusion did not hold for forms defined by dotted-outlines. Dotted-outline forms showed a strong increase in detectability as they became more oblong.

12. There was virtually no effect on detectability when a planar stimulus-form defined by a random array of dots was rotated around the y axis. When the form was rotated in more complex ways around two or three axes the experimental outcome was equally unaffected. Space also appeared to be isotropic for planes of this kind.

13. The gradient of form detectability was very steep between 88 and 90 deg of rotation, but virtually flat over the entire range from 0 to 88 deg.

14. When a frontoparallel-oriented plane was placed in different positions within a cubical space filled with masking-dots, it was most easily detected at the center of the cube. Detectability diminished, therefore, where disparity was greatest in either the crossed or uncrossed direction.

These, then, are the major findings that were obtained in the study of the influence of stimulus-form on the detectability of two-dimensional dotted forms in stereoscopic space.

The autocorrelation transformation also successfully modelled these psychophysical data. Because of the essentially two-dimensional nature of the stimulus-forms it was easy to represent many of the stimuli that were utilized in these experiments with the autocorrelation mathematics and to calculate the Figure of Merit. Some striking surprises emerged when this was done—most notably, evidence to support the prediction of both qualitative and quantitative differences between planes composed of random arrays of dots and those composed of dotted-outlines.

B. Related Work.

Of the two main questions motivating this research, that of greatest concern deals with the effect of form on the detectability of dotted forms in this signal-from-noise extraction task. This "specific-attribute question" asks which geometric attributes of a stimulus-form are important in its detection, discrimination, or recognition. A major corollary of this general issue is: What are the most salient attributes of a form--its local features or its global organization?

As I noted previously in the two main reports that have emanated from this program, and as other commentators (Sutherland, 1967; Zusne, 1970) have also noted, it is surprising how little effort has been directed at this central aspect of form perception by the relevant scientific community. The reasons for this lack of attention are manifold, but include: (1) Technical difficulties in the manipulation of forms (a difficulty that has largely been ameliorated by

the further development of real time control computers and novel display devices); (2) the absence of a general notational system for geometric form (the analytic geometry used here is at best a bandaide over a great wound); and (3) the complexity of geometrical forms themselves. How often researchers have generated an ideal gedanken experiment only to discover that it was impossible to implement because of some intrinsic confounding arising out of the inherant linkage of two or more attributes of the stimulus (e.g., perimeter and area). This kind of deep-seated, structural obstacle is not easily surmounted by any kind of ingenious experimental design. Rather, it is a difficulty that is built into the essential nature of the geometric forms with which we deal. Thus, there are some experiments that might well be done but that cannot without altering the experimental paradigm in such a way that dimensions other than those with which we are mainly concerned would be inadverantly manipulated. For example, some might say (as did Bela Julesz in a personal communication recently) that any stimulus-form could, in principle, be presented in a random-dot stereogram possessing no monocular cues. In fact, the process of converting something like a dotted straight-line into a random stereogram changes the essence of the line so thoroughly that it would no longer be the kind of stimulus in which we were interested. Rather, each line element would be replaced by a relatively broad array of dots that would destroy the very geometrical feature (linear dot order) that is under investigation.

Such reasons partially explain the paucity of studies in which the specific geometrical attributes of a visual stimulus have been examined to determine their effect on a visual performance task. It is also for these reasons that researchers have, in general, tended to turn to studies of other aspects of geometrical stimuli that are, in fact, only secondarily associated with the specific-attribute question. A popular alternative has been to examine

temporal effects rather than geometrical ones. For example, our laboratory, along with others, has carried out a number of studies on the temporal dynamics of the dot-masking process (Uttal, 1969a; 1969b; 1970a; 1970b; 1970c; 1971a; Uttal and Hieronymous, 1970; Uttal, Bunnell, and Corwin, 1970). Research of this kind is probably best considered to exemplify what the ethologists would call "displacement activity" — actions that are not germane to the task at hand but which keep the organism busy until it can decide what to do with the real problem it faces.

We have now, however, gone on to consider the specific-attribute question in studies that are directly concerned with geometric form. Form investigations include those reported in my earlier papers, Uttal, 1971b; 1973; 1976; 1977) and, of course, the two monographs that preceded this one (Uttal, 1975; 1983). Few others have considered the spatial geometry of stimulus-forms from the same perspective. Most notable are the works of Hughes (1982), the large body of highly relevant knowledge from T. Caelli's laboratory (e.g., Caelli, 1982), the work of Bela Julesz on textures (see especially Julesz, 1981), the studies on density discrimination carried out by Horace Barlow and his colleagues (e.g., Barlow, 1978; Burgess and Barlow, 1983) and their work specifically on form (Barlow and Reeves, 1979; Van Meeteren and Barlow, 1981), and most germanely, the work from Joseph Lappin's Laboratory (see especially Falzett and Lappin, 1983). This, we believe, is the context within which our work falls. Chen's (1982; 1983) work is also closely related in overall concept to the goals of this present work; indeed, one of the detection experiments described later in this monograph is a direct outgrowth of his work. Foster and Mason's (1979; 1980) work on local position information also is of relevance in the same way as are Foster's 1980a; 1980b) studies of form discrimination.

In Japan a number of psychologists have become interested in similar problems related to stimulus-form. Yodogawa (1982) has proposed a measure of symmetry that seems promising in defining some of the attributes of stimulus-forms. More immediately related is the work of Oshima (1983), who has specifically studied some of the geometrical attribute variables in figure-ground segregation.

Another body of work that has some interesting similarities to this topic, but which I had not until recently appreciated as salient, is the work on visual displays carried out by the group of aviation psychologists led by Stanley N. Roscoe at the University of Illinois. Scanlan and Roscoe's (1980) work on time-compressed displays is quite similar to the present study and seems to have generated some of the same conclusions.

van Oeffelen and Vos' (1983) work on the Gestalt principle of proximity also has many similarities to the present approach. In particular, both their formal model and their sample stimuli share the discrete geometric philosophy that characterizes this monograph.

It would be inappropriate, furthermore, to overlook the fine theoretical analysis carved out by Hoffman (1966; 1978; 1980), one of the few instances in which the neural microcosm and the visual-form macrocosm are interrelated in modern theory. Dodwell's (1983) tutorial on Hoffman's Lie algebra approach is especially useful in untangling the intricacies of this theoretical perspective.

There is another huge body of contemporary form-perception work that deals with the coded attributes of form from a different perspective. This is the increasingly popular approach based on Fourier spatial-frequency components that is philosophically related to, but vastly different in technique and results from, the experimental studies listed above. The Fourier approach also speaks to the problem of the specific attributes of a visual stimulus;

however, some proponents of this theory seem in some cases to be more concerned with examining the influences of attributes that are present only in the formal mathematical sense that Fourier originally suggested in 1807 than with investigating the actual geometrical attributes of a stimulus. In fact, an argument can be made that the use of real grating-like stimuli and the pursuit of hypothetical frequency-sensitive channels in the nervous system often obscure the actual properties of the stimulus within the intricacies of the mathematical formalism. It must not be forgotten that Fourier analysis allows any pattern to be analyzed into a set of orthogonal functions such as the family of sinusoids. These analytical functions now seem, however, to have become idealized, not merely as a useful mathematical construct but as anatomical realities. Indeed, physiological mechanisms purported to be selectively sensitive to narrow bands of spatial frequencies are vigorously sought in many laboratories.

In general, attacks on the specific-attribute question—which seems to be among the most important, if not the most important, of issues—are remarkably absent from other, more traditional lines of work in form perception. The heroic bibliographies compiled by Zusne (1970; 1975; 1981) not only demonstrate the enormous and varied interest in the general problem of how people see forms, but also the relative paucity of studies of the influence of the specific geometrical attributes of those forms. Instead, attack is aimed at lmost every other dimension or aspect of the problem, from perceptual development to perceptual persistance to perceptual aesthetics. Only a few items in Zusne's three bibliographies deal directly with what he refers to as stimulus varibles -- the specific-attributes. The bottom line of this brief review is that, with rare exceptions, there have been very few studies comparable to the present research that have dealt specifically with the problem of geometrical form and

its effect on detectability.

3. THE EXPERIMENTAL PARADIGM

This chapter address the procedures and equipment used to answer the version of the specific-attribute question that is the focus of this study. To reiterate, the primary issue of concern is: What is the effect of the spatial geometry of dotted, nonplanar, three-dimensional stimuli on their detectability when they are masked by a random array of dots also distributed throughout the same space. More specifically, we ask: Are the shapes of randomly dotted, nonplanar surfaces influential in determining their detectability, both with regard to qualitatively different (as defined by different generating functions) types of shapes and with regard to quantitatively different (as defined by different coefficients in a single generating function) distortions of the same type of shape? The secondary question motivating this research is: How do the relative signal-to-noise characteristics of the stimulus-form and masking-dots influence detectability?

To implement a research paradigm capable of answering these questions, it is necessary to construct random-dot stereograms as stimuli using hybrid computer techniques. The procedure used here was originally popularized and exploited by Bela Julesz (1960) and has become a mainstay of modern research on depth perception. The present adaptation of the technique is a real-time version in which computations are performed as fast as necessary to avoid any disconcerting delays in the construction of the stimuli or processing of the observer's responses. The computer system is fast enough so that the procedure is essentially paced by the observer's ability to respond.

Stimuli, consisting of dotted forms embedded among random masking-

dots, are presented dichoptically (slightly different images are sent to the two eyes on a split screen cathode ray oscilloscope — CRO) under the control of a hybrid digital and analog computer. The observer is thus faced with a signal-from-noise extraction task; performance is measured by the percentage of trials in which he is correctly able to detect the ordered stimulus in the mask.

The cubical stereoscopic space (a perceptual construct) within which both the dots of the stimulus-form and the visual mask occur is of some interest from a general conceptual point of view. The space is represented in a highly encoded and symbolic way inside the digital computer memory in the form of a table of number triplets, each triplet representing the spatial coordinates (x, y, and z) of a particular point. The stimulus space itself, therefore, does not exist inside the computer in any true physical sense; it is only represented by the numbers in the table inside the digital computer's memory.

Indeed, the space never actually exists anywhere in the sense of a tangible, solid volume even though it goes through several stages of electronic and optical transformation and representation. The digital codes are transformed by a digital-to-analog converter into three analog voltages whose magnitudes correspond in a somewhat more direct (analog) way to the spatial coordinates of a point in the perceived cubical space than does the table of numbers in the computer memory. However, even in this case, the voltages still do not reproduce the physical geometry of a real solid —they are representative in exactly the same way as are the digital numbers. The analog signals are subsequently converted, passing through several intermediate representational stages, into the dichoptic images — the two disparate, two-dimensional patterns projected from the CRO. Here, too, however, these images are not physically three-dimensional. They only represent (by virtue of the invariances represented by the disparity between the two images) the three-

dimensional nature of the represented space. Finally, these CRO images are projected onto the retina where they are encoded by neural mechanisms that are themselves also intrinsically two-dimensional throughout the early stages of neural processing. As the invariances are processed and evaluated, the represented image ultimately comes to be perceived as a solid volume filled with a spatially distributed array of dots, some of which are ordered and some of which are randomly dispersed.

The important point behind this conceptual excursion into the subtleties of coding and representation is that for all these levels of coding of which we are knowledgeable in this chain (and that most certainly does not include the latter stages of neural encoding where the percept becomes extant, a region in which our knowledge is totally deficient) the three-dimensional volume never exists in any physically solid or palpable, spatial sense. It is simply encoded or represented by several different systems of symbols and codes. The coded representations vary from one stage to the next, of course, but the critical fact is that even though the message — in this case, the concept of a three-dimensional volume — remains constant, the cubical space itself never actually exists.

A logical perplexity emerges from this line of thought: If three dimensions can be encoded (rather than exist as a real solid) and can be manipulated in those stages of representation for which we are knowledgeable, why then can we not in a similar symbolic fashion encode a representation of three dimensions within the central nervous system (where, presumably, resides the psychoneural equivalent of our perception of space)? In other words, this argument is intended to provide support for the general notion that some kind of three-dimensional isomorphic reconstruction is neither necessary nor even likely to be present in the visual nervous system. The perception of a solid need

not be associated with any kind of a "model" or "toy" solid in the brain any more than space need be represented by solids in the external electronic or mathematical apparatus of our experiment.

Philosophical esoterica of this sort arise from the details of our experimental procedure and equipment as well as from the phenomena reported by our observers. However, the main purpose of this chapter is to explicate the detailed nature of the procedures and methods that are used. These much more practical matters will now be considered.

A. General Procedure

Each of the experiments on the detectability of dotted, nonplanar surfaces reported in this monograph were carried out using a two-alternative, forced-choice detection paradigm as our psychophysical method. The percentage of the total number of trials in which the stimulus-forms were correctly detected was the main dependent measure of performance. Because this was a two-alternative task, 50 percent was the floor level of performance that would be exhibited by an observer who was detecting no better than chance. The stimulus-forms were constructed of ordered constellations of dots and are prearranged by the experimenter into a sequence varying along some well-defined dimension. John Brogan, the Perception Lab programmer from 1982 to 1983, developed some extremely powerful automatic aides for preparing tables of numbers that represent such ordered stimulus-forms. Using a graphic input device (a Houston Instrument Hi-Pad digitizer), he made it possible to create prototypical, dotted stimuli (e.g., a dotted-outline, a dotted grid, or a random array of dots of a particular shape) constrained to a planar area in two-dimensional space. These prototypes could be of virtually any regular polygonal shape (up to a decagon), be irregularly shaped, or even contain holes devoid of

dots. Once these planar prototypes were defined, Brogan's programs allowed us to transform these two-dimensional prototypes into three-dimensional nonplanar surfaces by means of appropriate programmed algorithmic distorting functions. These algorithms acted as if they were elastically stretching the two-dimensional prototypical planar surfaces into nonplanar surfaces in accord with rules of the general form:

$$z = f(x, y) \tag{3}$$

Specifically, the planar surfaces could simply be "extruded" into solids by allowing f(x,y) to be a random number generator that arbitrarily selects (between predetermined limits) z axis values. They could also be stretched or distorted into nonplanar surfaces by appropriate sinusoidal or polynomial generating functions. Sets of these transformed nonplanar stimulus-forms were then stored in a disk storage file, to be called for presentation as needed during our experiments by a master control program.

In the experiments to be reported here, dotted stimulus-forms were hidden among various numbers of randomly placed masking-dots. (As noted earlier, these formless and random arrays of masking-dots are also sometimes referred to as visual noise.) The organized stimulus-forms were interspersed both temporally and spatially among these random masking-dots and the observer's task was to detect the form as described below.

Use of this dot-masking paradigm has certain advantages. First, it enabled us to have control over the detectability of a form without varying its shape or the intensity of its constituent dots. Furthermore, dots are roughly

independent in their physiological effects on the retina since it is unlikely, even at the high-dot densities we used, that any single receptor would be repeatedly stimulated. Since dots are also known to interact only very weakly through lateral inhibitory interaction mechanisms, this independence is even greater than might have been predicted on the basis of receptor activation probabilities alone. Most advantageous of all, however, is the fact that dots have minimal attributes of their own. It is only by virtue of their spatio-temporal arrangements that they take on "meaningful" form.

Figure 4 shows a dotted stimulus-form — a parabolic arch consisting of 81 randomly distributed dots — typical of those used in this study. This figure presents the images for both the left and right eyes that generate the percept of this stimulus-form in four sample stereoscopic displays with progressively higher numbers of masking-dots present. The observer's specific task was to report which of two sequential, one-second long, stereoscopic presentations contained the stimulus-form. Each of the two presentations in each trial displayed a dichoptic pair of images that, when perceptually fused, created the impression of the cubical volume in which the dots constituting the stimulus-form and the randomly dotted visual mask appeared at positions depending on the design of the experiment and the vagaries of a random-number generator. One presentation contained the ordered form; the other contained the same number of dots but without the order.

The images for the right and left eye were presented on the right and left halves, respectively, of a single split-screen oscilloscope (Hewlett-Packard 1311-B) coated with a high speed P-24 phosphor. The observer viewed the two images through binocular rotary prisms that were individually adjusted at the beginning of each session for comfortable convergence. An opaque septum extended from the binocular prisms to the screen of the oscilloscope (a distance

of 71 cm) and thus divided the two halves of the screen so that neither eye saw the field of view of the other. Figure 5 shows the organization of the display station.

The perceptual result, when left and right eye stimuli of appropriate disparity were fused, was the appearance of a highly realistic cubical volume containing the dotted stimulus-form and the random array of masking-dots. The cubical volume was defined by the extent of the masking-dots and appeared as a region in space filled with a varying number of point-like lights arranged according to the needs of the specific experiment. There were no outlines or other cues to its spatial structure. The stimulus-forms always subtended a slightly smaller volume than did the masking-dots.

In each of the experiments reported here, all of the the dots of both the stimulus-form and the mask were illuminated constantly throughout a one-second presentation epoch by rapid, repetitive plotting. By keeping the interval between succesive replottings of each dot less than 5 msec, there was no perceptible flicker except at very large masking-dot densities (greater than 300). This small residual flicker was believed to have no effect on the results obtained in our experiments.

As shown in Figure 6, an experimental trial consisted of two such presentations; either the first or the second presentation contained a stimulus-form (e.g., an orderly plane or a nonplanar surface of random dots) plus varying numbers of masking-dots. The other presentation contained exactly the same mask along with an additional number of randomly placed dummy dots instead of the orderly stimulus-form. The number of dummy dots was equal to the number of dots in the stimulus-form and they were limited in spatial extent to the maximum and minimum x, y, and z values of the dots of the stimulus-form. Furthermore, in all of the experiments reported here, the dummy dots also had

exactly the same x and y coordinates as those of the stimulus-form; the z axis values alone were randomized to create the irregular array of dummy dots in the "other" presentation. Thus, for example, what had been dots organized in a plane (the stimulus-form) became a collection of the same number of dots (the dummy dots) distributed in depth, but with a cross-sectional (i.e., x and y) shape nearly identical to that of the stimulus-form. In this manner, both presentations contained exactly the same number of dots and had exactly the same masking-dot patterns. In addition, except for the shifts due to disparity differences, the monocular views were very similar. These disparity shifts were not negligible, however. Indeed, they became quite noticeable when regular, grid-like stimuli were used as shown in Figure 69a and b.

The purpose of the dummy dots was to maintain as constant in both presentations the total number of dots, the luminosity of the display, and, to the degree possible given the necessary disparity differences, the two-dimensional, monocular view. Therefore, the two sequential presentations were alike in all regards except one — the dummy dots did not contain the critical piece of information that was present in the stimulus-form, namely, the organization or arrangement of the surface in depth, the dimension that has been the main target of investigation in this study. It is important to remember, therefore, that when the stimulus-forms were constructed from random arr 's of dots, the spatial arrangement of those dots constituted the sole difference between the two alternative presentations. Everything else was controlled and made as equal as possible in the two presentations.

It should also be appreciated that in some instances there may have been monocular cues that allowed the task to be performed with only one eye. In the first two experiments to be reported in the next chapter, the detectability of a set of forms was compared under monocular (one side of the CRO covered with

an opaque shield), with the usual dichoptic (each eye viewing a stimulus that was disparate with the other eye's view) viewing condition used in all other experiments. (The set of observers was the same in this comparison.) Differences in detectability between these two viewing conditions, as well as the differences due to form, tell us something about the visual processes involved in detecting forms in space and act as a control for inadvertant monocular clues. As we shall see, there were some monocular cues present, but their influence was small and obscured at the high masking-dot densities. This was not, however, the case in Supplementary Experiments 14, 15, and 16 where the monocular cues contained in regular grid-like stimulus-forms produced curious results. Supplementary Experiment 17 shows that observers actually deal with grids as if they had only monocular information available.

The precise sequence of visible events in each trial was presented in an order that controlled by a master computer program, as shown in Figure 6. First, a pair of disparate dots (one for each eye) providing a single fixation-convergence dot at the geometrical and stereoscopic center of the apparent cube was illuminated for one-second. This pair of dots served to help the observer align the lines of sight of his eyes so that subsequent stimulus information could be properly registered for stereoscopic viewing. The observers' strong perceptions of a dot-filled cube obtained with our calibration patterns and under the many different conditions of the various experiments, as well at the results of the experiments themselves, indicate that registration of corresponding dots was successfully achieved.

Immediately following the display of the fixation-convergence dot, the first of the two alternative presentations was displayed. Each presentation lasted for one-second during which time the randomly positioned dots of the mask and of the stimulus-form were repeatedly intensified to produce a stable

(in time) image. This produced a snapshot-like appearance of a static array of dots without noticeable flicker (except in very high masking-dot density situations) or positional jitter. This mode of presentation has been designated as the static masking mode, as opposed to the dynamic mode in which each dot is only flashed once and a snowstorm-like perceptual experience obtains.

The first one-second presentation was then followed by another one-second period during which the solitary fixation-convergence dot was again presented. The second of the two presentations was then displayed. As noted, the stimulus-form may have been included in either the first or second presentation; the dummy dots were displayed in the other. Following the second presentation, the screen remained dark until the observer responded by depressing one of two hand-held pushbuttons indicating that he had "seen" a stimulus-form in either the first or second presentation. At that point, a "plus" or a "minus" indicating that either a correct or an incorrect choice had been made was briefly flashed on the oscilloscope. The cycle then repeated. It is important to note that the observer was required to make a choice: He could not equivocate or qualify his answer. In this manner a considerable measure of control over individual differences in criterion level was achieved.

Given the widespread application of laboratory automation by psychologists, one not-so-novel aspect of these experiments is that they were all totally controlled by real-time, on-line microcomputers. The control program was initially loaded by the experimenter from the computer's disk memory into its randomly addressable working memory at the beginnng of each experimental day. At this point the specific conditions and parameters for each session were set by the experimenter and the computer carried out certain initialization segments of the control program. Next, the observer signed on at the computer terminal with a personal code and began the experimental session

by depressing either one of the two response push buttons. At the end of 50 minutes, the observer terminated the session by typing a code letter into the computer console. The observer's performance was immediately analyzed by the computer and results were printed along with identifying and timing information. Pooled data from several observers and conditions were subsequently analyzed by another, more comprehensive data analysis program. A third program computed an analysis of variance (ANOVA) of the data.

B. Observers

In each of the experiments reported here, at least three, and usually four, undergraduate students from The University of Michigan served as paid and increasingly expert observers for periods of time that varied from one to several experiments. Each was tested for normal stereoscopic vision with an anaglyphic screening procedure using Figure 8.1-2* from Julesz (1971). We depended upon self-reports of normal or corrected refraction and any other visual anomalies. From time to time however, observers, have been dissociated from the project after having demonstrated adequate stereopsis with anaglyphs but failing to display an adequate level of discrimination performance in the computer-controlled task. All observers were extensively pretrained and familiarized with the stimuli to be used in each experiment before data collection commenced.

C. Apparatus

The stereoscopic stimuli in this experiment were generated by a hybrid computer system consisting of a Cromemco System 3 digital microcomputer

and a subsystem of Optical Electronics, Inc., analog computer components. This hybrid computer approach circumvented one of the most difficult problems in the presentation of this kind of haploscopic stimuli. While it is not particularly time consuming to generate the tabular representation for any single dot or group of dots in a digital computer (x, y, and z coordinates can be generated by simple algorithms or from prestored information), it is a much more difficult programming task to promptly construct the actual real-time analog signals required to control the left- and right-eye images on the the split-screen oscilloscopic display (the disparate cues necessary to create a stereoscopic percept). This difficulty is exacerbated in the highly demanding real-time requirements of the present study. The computer-generated and stored x, y, and z coordinates specifying the precise location in the apparent cubical space for each dot must be transformed into two sets of two-dimensional coordinates (x_L, y_L, for the left eye and x_R, y_R for the right eye) with the proper disparity, perspective, and separation to project a haploscopic pair of images at the proper locations on the oscilloscope. Each pair of dots in the left- and right-eye images must be precisely positioned so that it can be processed by the visual system into the appropriate perceptual experience associated with its designated location in three-dimensional space. The problem is that the transformation from x, y, and z, on the one hand, to x_L, y_L and x_R, y_R on the other, involves a series of trigonometric calculations that is extensive enough to quickly overload the modest-sized digital microcomputer used to control these displays should they be performed digitally. Once overloaded, the computer would not be able to maintain the timing relations required by the experiment.

The analog subsystem (shown in Figure 7) provides a means of finessing this potential digital computer processing overload difficulty. The

trigonometric problem required to transform x, y, and z into x_L, y_L and x_R, y_R is solved by means of analog circuitry (manufactured by Optical Electronics, Incorporated — OEI) in real-time whenever it is necessary to plot a haploscopic pair of dots on the oscilloscope. It is only necessary to provide this analog subsystem with the three voltages representing the three spatial coordinates x, y, and z at the appropriate time. These three analog voltages are easily and quickly obtained from the internally stored digital x, y, and z representations by means of highspeed digital-to-analog converters. The hybrid computer used as its digital-to-analog converter the California Data Corporation's DA-100, a four-channel system. Each channel is capable of converting any single dimension of the digital representation into the equivalent analog voltage in approximately three microseconds.[2] Three channels of the system are used to convert the x, y, and z dimensions and one is used to regulate the horizontal separation between the left- and right-eye images drawn on the oscilloscope. The disparity and perspective of the two images are adjusted with external regulating potentiometers and are kept constant throughout the experiments.

The speed of operation of the analog OEI subsystem is fast enough — it is designed to have a band pass of DC to 500KHz — so that the entire set of trigonometric computations required to plot the images for both eyes is carried out in a few microseconds, a duration comparable to the settling time of the entire electronic communication and display system used in the study and to one or two average digital computer instruction execution times. Thus, one has only to pause for a few computer "no operation" instructions before sending a "beam intensify" signal (obtained directly from one TTL level bit of a parallel eight bit output port of the microcomputer) to the oscilloscope to maintain good dot quality. The OEI components are, therefore, fast enough to carry out this conversion in what is easily the "real-time" of our experimental paradigm.

The speed of generation of the pairs of left- and right-eye images is constrained only by the modest digital computer instruction execution time required to read information from an internally stored table of x, y, and z values (all of which are either computed in the intervals between trials or arbitrarily specified by the experimenter prior to the session) to the digital to analog converters.

Stereoscopic depth was defined by the horizontal disparities between x_L and x_R for each dot. Horizontal retinal disparity, however, does not define absolute depths but rather cues the observer to relative depths; that is, a dot would be perceived in front of or in back of the reference depth (the point or plane in space at which the lines of sight converge and disparity is zero) by a certain amount. In such a system, even if the convergence depth is changed, the relative relationships may remain constant and no perceptual shift may occur. Furthermore, in the hybrid computer system utilized in the present study, the electronic disparity adjustment was uncalibrated and arbitrary. It was, therefore necessary to calibrate the actual disparity of dot pairs by direct measurements from photographs of special test patterns on the display screen and from measurements of the distance from the observer's eye to the display screen. These angular measurements were then related to the z axis values stored within the computer. It should be noted that this relationship between disparity and internally represented z values is accurate only for our system and only as it was adjusted for these experiments. Within this constraint, we determined that if the observer focused on the fixation-convergence dot centered in the apparent cube, then the maximum crossed relative disparity for a dot positioned on the front surface of the apparent cube was 14 min of visual angle and the maximum uncrossed disparity for a dot positioned on the rear surface of the apparent cube would also be min of visual angle. These maximum crossed and uncrossed disparity values were arbitrarily chosen so that

the perceived volume appeared to the observer to be as close to a cube as possible. Because of the several stages of transformation involved, all disparity values should be considered to be approximate. Furthermore, in some of the experiments reported here less than this full range of disparity was utilized.

In all instances for which tables of disparity values are presented, I have chosen to present them in the form of the corresponding z values. That is, the 28 min range of visual disparity is equivalent to a range of z values varying from z = 1074 (the front of the cube) to z = 3021 (the back of the cube). The center point of the cube is situated at z = 2047; this was the usual fixation point in all of the experiments presented in this monograph. Therefore, each minute of disparity is equal to 70.5 of these z-units. This is the source of the otherwise mysterious numbers in some of the yet-to-be-presented tables.

The field of view presented to each eye on the two halves of the CRO was shielded by an opaque screen through which a pair of 5.4 deg X 5.4 deg apertures had been cut for the left and right image respectively. This shielding screen was attached directly to the face of the oscilloscope. The viewing distance from the observer's cornea to the CRO surface was 71 cm. The screen was, therefore, far enough from the observer that each dot appeared to be virtually point-like in space and its angular subtense less than the point spread function of the human eye. Luminance was standardized with a Salford S.E.I. photometer to approximately 0.1 candles/m^2 and was kept constant at approximately this level from day to day.[3]

The two pushbuttons used by the observer to respond were connected to Schmitt triggers with capacitive inputs designed to smooth switch contact bounce. The outputs of the Schmitt triggers were fed to two of the bit positions on an eight-bit parallel input port of the computer for acquisition and processing.

4. EXPERIMENTAL DESIGN AND RESULTS

A. The Stimuli

In order to achieve the twin goals of this study — to determine the effects of stimulus-form and signal-to-noise ratios — it is necessary to have a means of quantifying the shape of the surfaces used as stimuli. This must be done both in terms of the degree of deformation from a prototypical plane and the particular trajectory or type of form along which the deformation occurs. In the history of interest in these and related problems, it has been unusual to have had the availability of a systematic and descriptive quantitative system;[4] many of the stimulus-forms had to be arbitrarily generated without any precise quantitative control over the shape or degree of deformation beyond the intuitive judgment of the experimenter. However, a quantitative system does exist that was perfect for our needs in this study. That system is the well-known one called "solid analytic geometry." It has allowed us to vary the type of form or trajectory as well as the magnitude of the deformation of a nonplanar surface from a planar prototype in a precisely controlled fashion.

In particular, we utilized a generalized polynomial expression of the following form to generate the needed surfaces for most of the reported experiments:

$$z = G\,(Ax^5+Bx^4+Cx^3+Dx^2+Ex+Ry^5+Sy^4+Ty^3+Uy^2+Vy+W)^F + H \qquad (4)$$

By arbitrarily selecting the coefficients (A,B,C,D,E,F,G,H,R,S,T,U,V,W) in this equation (including, of course, the option to set each to zero), it was possible to

produce a wide variety of surfaces. Indeed, the expression could be easily generalized even further if components that were the products of x and y and their powers were added to the general expression of Equation 4.

This polynomial expression was implemented within the context of the versatile, multipart computer program authored by John Brogan. Brogan's program first allowed the experimenter to create a prototypical planar surface consisting of a constellation of randomly positioned dots or an experimenter-specified regular array of dots. The second part of the program allowed the experimenter to deform this prototype into surfaces of the kinds exemplified in Figure 8. These surfaces, as well as those shown in Figure 9, are, however, only diagrammatically represented. In actual fact, the observer saw neither the grid-like surface nor the outlines of the cube. These extra lines are presented here only to help my readers visualize these forms. In the experimental presentations, the cube was defined only by the extent of the masking-dots and the nonplanar stimulus surface by the orderly distribution of its constituent dots.

The version of the surfaces shown in Figure 8 are the most extremely deformed of each type and exemplify the stimulus-forms used in Experiment 1. Figure 9, on the other hand, shows a single set of surfaces formed by evaluating Equation 7 for the specific set of coefficients shown in Table 5. In this case, only the magnitude, not the type of the distortion, is varied. Other parts of Brogan's program allowed us to rotate, translate, or even magnify the various deformed surfaces so that they could be inspected from any angle in any position under both stereoscopic and two-dimensional viewing conditions.

In some of our experiments, however, even the broadly applicable polynomial generating expression of Equation 4 would not conveniently produce the forms that were needed. In some cases, therefore, we had to turn to a

sinusoidal-generating equation of the form:

$$z = A \cos Wx \qquad (5)$$

to produce waves of spatial frequency systematically varying in width, height, and amplitude (ie., in depth) that could be used to test other attributes of these nonplanar surfaces.

Several difficulties with the type of research of concern in this study are appropriately mentioned here. The first difficulty concerns the sampling of observers. Each of the experiments described in the various sections of this chapter was roughly a two-week long (or longer) endeavor. Typically, four observers would participate each day on five or more successive days while the masking levels were progressively increased. The procedure was then repeated for an additional five or more days, during which the number of masking-dots were progressively decreased. This was a compromise strategy adopted to counterbalance any sequence effects yet not to introduce abrupt changes in masking-dot density from day to day — a tactic that often seemed to produce irregular data in this kind of experimental paradigm in the past. Because of the length of a single experiment and given the vagaries of observers' availabilities, different groups of observers tended to be used in different experiments. Given also the fact that there were considerable individual differences in performance (mainly with regard to the absolute magnitude of the obtained scores), interexperiment absolute differences cannot be considered to be accurate indicators of true performance differences and, therefore, of perceptual sensitivities. Whatever real differences may have contributed to performance

scores in different experiments and with different observers therefore, would, tend to be submerged in the interexperiment differences caused by sampling variance. Thus, the differences in performance that are utilized have always been drawn from intraexperiment findings -- findings for which the observer pool was the same and for which all other conditions of sequence and experimental protocol were held constant.

It is also for this reason that the masking-dot densities used in this experiment were not exactly the same from experiment to experiment. Some groups of observers displayed strong resistance to masking and others showed a low resistance. Thus, some experiments required more masking-dots than others to degrade performance to the same degree. This will be evident when our data is presented later. Since relative, intraexperiment performance differences are the key criteria for our conclusions, this poses only an aesthetic and not a technical difficulty for our study. That this is an acceptable strategy is strongly supported by the typical low level of interaction (it was always insignificant) between the dot density and the shape dimensions found in our ANOVA analyses.

Another difficulty, particularly for stereoscopic displays of the kind we used, should also be reiterated here: In many instances, subtle and sometimes not so subtle monocular cues may have been present. It is imperative that control experiments like those reported in Experiment 2 be carried out and that stimulus-forms composed of small numbers of dots be especially closely monitored. Both caveats are necessary to guarantee that the negligible form effects observed in some experiments are not in fact due to some overlooked monocular or ceiling effect cue and thus are not either artifactual or irrelevant to the main purpose of these experiments. In some experiments, monocular cues have in fact been identified and the value of these experiments is,

therefore, somewhat limited. However, experiments of this class are of interest in their own right, and several will be presented, although in a qualified way.

A difficulty of more mysterious origins arises from the fact that the results of individual experiments sometimes seem to depend upon the size of the stimulus set that is utilized. In experiments in which a wide variety of different stimulus-forms is used, there are often smaller differences, both relatively and absolutely, than when a narrower variety is used. It is not clear why this should be the case in the present experiment, although this kind of outcome has been reported and analyzed elsewhere (e.g., Krumhansl, 1978; Monahan, J. S. and Lockhead, G. R., 1977; Tversky, 1977). Stimulus set size, relative similarity, and diversity, therefore, may be a more important confounding varible in a wider variety of psychophysical experiments than had hitherto been appreciated.

Now, having considered some of the difficulties, let us turn to the design, rationale, and results of each of the experiments carried out in this study.

B. Experiment 1 (MIX2)

Design and rationale

Experiment 1 was the foundation experiment in this study of the influence of nonplanar shape on visual detection using a dotted-form-in-dotted mask paradigm. The main purpose of this experiment was to determine if, indeed, there is any effect of the overall shape of a dotted-nonplanar surface on its detectability. By overall shape, I refer to the particular form, type of form, or trajectory taken by a set of maximally distorted nonplanar surfaces. A number

of different nonplanar surfaces were being compared in this experiment, each of which was generated by a different version of the general polynomial expressed in Equation 4. Later experiments dealt with single types of form for which a single kind of distortion varied in magnitude. In this case, however, the type of distortion, not its magnitude, was the main concern.

Our strategy to begin to answer the fundamental question of the effect of shape in our search for an understanding of the detection process was to present the most extremely distorted versions of seven different types of surfaces. Table 1 specifically defines the particular coefficients that were used to generate each of the seven stimulus-forms. The seven surfaces used in this experiment were divided on the basis of their complexity into two groups. The first consisted of a cylinder, a parabolic arch, and a cubic in x —three stimuli that vary in only one dimension. The second group consisted of a parabolic surface of rotation, a cubic in x and y, a hemisphere, and a hyperbolic paraboloid (a saddle) — four forms that vary in two dimensions. Figure 8 displays the shape of each of the nonplanar surfaces used in this experiment. The prototypical plane from which each of the seven forms was generated was not the same. In the case of the hemisphere and the paraboloid of rotation, the prototype was a regular planar decagon defined by an array of 64 random dots. The other five stumulus-forms were produced by applying the appropriate polynomial expression to a square plane composed of a random array of 81 dots.

The number of dots used in each case was based upon the criterion that all of the nonplanar stimulus surfaces should have the same dot density in their original two-dimensional prototypes. Since the prototypes respectively, were a 5.4 deg wide square and a circle-approximating decagon of about the same radius, the dot numerosities required to keep the density constant were related to each other by the ratio $\pi/4$ or .785. Since 81 dots were used to define the

five surfaces originally generated from a prototype square, 64 dots had to be used to define the two surfaces generated from a prototype decagon to maintain equal density. Since the polynomial equation operated on the prototypical plane only to alter the apparent depth (z), the x and y extent of the prototypical plane was only slightly altered when it was distorted into one of the seven stimulus-forms. The extent of this distortion varied with the magnitudes of the horizontal disparity and the perspective contraction in both the horizontal and vertical dimensions.

The stimuli were all presented such that the observer seemed to view the prototypical plane in a fronto-parallel orientation. That is, the distorted shapes themselves were all presented in this experiment, as well as all of those subsequent to it, so that they appeared to be mainly convex from the observer's viewpoint — all distortions being in the depth dimension only. The only exceptions to this generalization were those stimulus-forms that have both maxima and minima in depth and, thus, both convexities and concavities along the line of sight. The normal viewing condition is depicted in Figure 10.

This experiment was performed on 18 successive days. For the first 9 days, the density of the visual mask was progressively increased from 50 to 500 masking-dots in 50-dot increments. On 9 succeeding days, the sequence was reversed and the masking-dot densities were presented in decreasing order in 50-dot decrements. Each day in this as well as all subsequent experiments, each observer was presented with approximately 600 trials; in this case, that meant approximately 85 randomly selected presentations of each of the seven stimuli were presented in each session.

Results

The results of foundation Experiment 1 are shown in Figures 11 and 12.

Figure 11 shows the data pooled across observers as a function of the seven shapes and presented as a parametric set of curves that vary as a function of the nine utilized masking-dot densities. It is obvious, in this case, that there is a consistent result depicted for all masking densities greater than 200 dots, a value that appears to be a threshold for the effect with this group of observers. The general effect is even more evident in Figure 12, in which the data from all levels of masking have been pooled together to emphasize the overall trend of these results. That general trend can be described in several ways.

First, the control for dot density implemented by adjusting the number of dots in the hemisphere and paraboloid of rotation stimulus-forms (the two constructed from a prototypical decagon rather than a square) appears to have worked. The two stimuli do not differ in detectablity from the equally dense but larger cylinder and single cubic.

Second, the parabolic arch seems to be more easily detected compared to the other six forms. In fact, it is the most deformed nonplanar surface with a greater range of depth generating disparities than any of the others. Thus, its three-dimensional surface area is quite large and the apparent density of the dots determining that surface quite low. On this basis, it might well have been predicted that it should be less detectable. We have no suggestion to make, based upon these results or others yet to be reported, why this enhanced detectability should be the outcome in this case. It is possible that this particular stimulus contained some micro-element that made it especially detectable to well-trained subjects, or it may simply be intrinsically more detectable. This kind of paradoxical result occurred throughout this study.

Third, both the double cubic and the saddle (the hyperbolic paraboloid) are seen less well than the other five forms. This result anticipates and predicts yet-to-be-reported data in at least one regard -- as we shall see, the double

cubic turned out to be one of the stimuli that was most affected by increasing the magnitude of the distortion away from the prototypical plane. The saddle, however, did not exhibit this characteristic. In general, however, these results are idiosyncratic and do not blend into a single conclusion concerning the effect of the type of distortion on detectability.

C. Experiment 2. (Monocular Control)

Design and rationale

Experiment 2 is a critically important control experiment. The results obtained in the preceding experiment could be seriously confounded and totally misleading if there were some subtle monocular cue that differentially distinguished the stimulus from the dummy dot conditions to any substantial degree in the two presentations. Therefore, Experiment 1 was repeated in the form of a monocular control to exclude this possibility. Only one minor, yet essential, change was made in the conditions previously used; an opaque shield was placed in the optical pathway between each observer's nondominant eye and the CRO display for that eye. Therefore, no disparity information was available to the observer — only monocular cues could be used. The experiment was intended to be self-terminating; if, as expected, performance were to be substantially degraded at relatively low masking-dot density levels, no attempt would be made to continue to the higher dot densities used in Experiment 1. As a further control, this experiment used exactly the same group of observers as did Experiment 1: it was one of the few in which this was possible. The experiment was executed immediately at the completion of Experiment 1, a point at which the observers were at their highest degree of familiarity with

the seven stimuli and, thus, most likely to be influenced by any subtle monocular cues.

Results

The results of this experiment are shown for masking-dot densities of 50, 100, and 150 dots. The experiment was run twice (once in the ascending order and once in the descending order) at each of these masking-dot densities and was then terminated because of the low level of performance at 150 dots. Figure 13 presents these results. It is obvious that there is a vast difference between the data in this graph and the three curves in Figure 11 with corresponding masking-dot densities. The monocular results exhibit much lower scores; in fact, they approach minimal performance levels at a masking-dot density (150) at which the dichoptic stimuli are detected nearly perfectly.

Indeed, the pattern of results is not even consistant with the dichoptic data. The dichoptic data show slightly elevated performance scores for the parabolic arch and slightly depressed performance scores for the double cubic and the hyperbolic paraboloid. In this monocular experiment not only is there much greater varability, but the parabolic arch, the parabola of rotation, and the saddle all produce elevated scores. It seems likely that the cues and/or strategies used in the dichoptic and monocular condition may actually be different from each other. This is a portent of the data yet to be reported in the supplementary experiments.

The important general result, that there is very poor monocular but good dichoptic performance. This outcome establishes the validity of the measures obtained in Experiment 1 and strongly supports the general stereoscopic approach taken throughout this study as a means of studying nonplanar-form detectability. This result also establishes a general principle for all

experiments in which arrays of random dots define the stimulus-form. That is, the reported effects, or absence thereof, are genuinely associated with depth and nonplanarity and are not in some cryptic way reflections of some subtle monocular artifact. The reader should, however, be prepared for quite a different outcome in the supplementary experiments. There, monocular cues and strategies are very important.

D. Experiment 3. (Cylran)

Design and rationale

The results of Experiment 1 suggest that there is some modest differential detectability as a function of the types of shape that are generated by the polynomial procedure. Different shapes do produce somewhat different detectability-performance scores even when they all exhibit roughly the same degree of distortion. This, however, is but one of the issues with which we are concerned. The other issue can be generically stated as follows: Given a single, kind, type, or more precisely, a particular polynomial form, what is the effect on detection scores of various degrees of distortion from a plane to the most extreme nonplanar surface?

The same polynomial expression (Equation 6) is used for each stimulus-form in this experiment. The degree of deformation away from the prototype plane is, however, systematically varied by varying its coefficients. This emphasis on the magnitude, rather than the specific kind, type, or trajectory of the nonplanar surfaces, constituted the main thrust of the remainder of the experiments that are to be reported in this monograph. In the series of experiments which dealt with progressively more complex stimulus patterns.

Ultimately, our discussion will address the results of experiments dealing with more complex surfaces represented by cubic polynomial or sinusoidal equations and those that vary in their topological properties.

Experiment 3 initiated the series of experiments designed to answer the magnitude of deformation question with a set of the simplest possible nonplanar surfaces — a set of five cylinders with progressively smaller radii and thus increasing nonplanarity, along with their prototypical plane. The series of stimulus-forms became more and more curved until they arrived at the maximum possible curvature, a value limited by the criterion that the cylinder must extend across the entire cubical space. The cross-sections of the set of stimuli used in this experiment are shown in Figure 14. The generic generating equation for this set of stimulus-forms is:

$$z = G(-y^2 + W)^{\frac{1}{2}} + H \qquad (6)$$

The coefficients necessary to produce this set of forms are shown in Table 2. As noted earlier, the values of these coefficients are given in terms of the digital codes used to define the extent of the cube. The somewhat mysterious numbers that appear in Table 2 and the others that follow are based upon that coordinate system. It is arbitrary, however, and any other linearly related scale could be used equally well. As also noted earlier, these numbers correspond to a range of 5.4 degrees in the x and y dimensions and 28 minutes of visual disparity in depth.

To investigate the nature of the signal-to-noise relationship, the number of dots in the test plane was also varied within each daily session. In particular,

each of the six stimulus-forms was presented as an array of dots with any one of five possible random-dot numerosities. The number of dots used were 81, 64, 49, 36, and 25, respectively. Thus, there were 30 distinct stimuli (five different dot densities times six different shapes). Each trial used a randomly selected one of these 30 stimuli in one of its two presentations and an equivalent set of dummy dots (as described earlier) in the other.

The masking-dot densities used in this experiment are 40, 100, 150, 200, and 250 randomly positioned dots respectively. Thus, the complete execution of the experiment requires that ten daily sessions be completed; five in ascending order and five in descending order of masking-dot density.[5]

Results

The results of Experiment 3 were presented in Figures 15 through 19. Figure 15 displays the results analyzed for the six shapes with the data presented parametrically as a function of the five masking-dot densities. These curves indicate that the magnitude of distortion of a plane has little effect on the detectability of the forms until the highest masking levels are used. Even then, the effect must be considered to be small, if not negligible. Indeed, the results from a two-way ANOVA showed the F ratios for this dimension to be insignificant for all masking-dot densities (See Table 3)[6]. Figure 16 summarizes the data presented in Figure 15 by pooling the response scores across all of the masking-dot densities in order to emphasize the inconsequential magnitude of the effect obtained.

The other major result of this experiment is presented in Figures 17 and 18. In the first of these two graphs the data have been analyzed with respect to the density of the stimulus-form dots and plotted parametrically as a function of the density of the masking-dots. In this case, there is obviously a strong and

significant effect of this aspect of the stimulus. Indeed, the F ratios generated by the ANOVA analysis of this part of the experiment are such large values as to be off usually available tables of significance (see Table 4). Figure 18 shows the general trend when the data are pooled across all masking densities.

In sum, there is an insignificant effect of stimulus-form as the stimulus becomes progressively more deformed from a prototypical plane to the most extreme cylinder used in this study. This result holds generally across all signal-to-noise ratios, whether stimulus-form or masking-dot densities are varied. On the other hand, the signal-to-noise ratios, as somewhat arbitrarily[7] defined by the number of dots in the stimulus-form and the mask, respectively, show the vigorously strong effect we have come to expect in this type of experiment.

It is important to note that throughout these experiments, an attempt has been made to avoid both ceiling and floor effects. In some cases, this meant that the masking-dot densities could not be raised as high as might be desired for a full-range analysis of stimulus-form. To do so would have introduced floor effects on stimuli with low stimulus-form dot densities. On the other hand, it has been necessary to be equally careful that ceiling effects are not produced by too densely dotted stimulus-forms. A potential ceiling distortion would least affect the stimulus-forms with the lowest dot densities, and it is for this reason that detailed examination of them is particularly important. Figure 19 separately plots the results for the lowest level of stimulus-form dot density (25 dots). It is clear from this graph that the insignificant effects so far obtained for all of the higher stimulus-form dot densities are not due to any putative ceiling effect resulting from inappropriately chosen signal-to-noise ratios. The insignificant effects also occur when the number of stimulus-form dots is minimal.

E. Experiment 4. (Bolran)

Design and rationale

Experiment 4 carried on the search for some effect of form on detectability by using a set of stimuli generated in the form of parabolic arches rather than cylinders. While the distortion away from the prototypical plane was still along only a single axis, the distortion was parabolic, rather than circular in cross-section. Such a parabolic deformation allows a much greater degree of distortion in depth than is permitted by a cylindrical shape, a form that is limited to an inscribed semi-circle. Thus, we increased the magnitude of possible distortions in this experiment. In particular, the generating equation used to develop these parabolic arch stimuli is:

$$z = Gy^2 + H \tag{7}$$

and the particular coefficients used are presented in Table 5. This transformation produced the set of stimuli shown in cross-section in Figure 20. Once again, six stimuli were used, a prototypical square plane and the set of five parabolic arches whose coefficients are listed in this table. Five different dot densities — 81, 64, 49, 36, and 25 — were also used for each of the forms to produce a total of 30 different stimuli, any one of which could be randomly selected for presentation by the controlling program.

The experiment was carried out over ten days. For the first five days, masking-dot densities of 40, 100, 150, 200, and 250 were presented in ascending order; for the second five days the stimuli were presented in the reverse

sequence of masking-dot densities.

Results

The results of Experiment 4 are shown in Figures 21 through 25. Figure 21 shows the results of the experiment analyzed on the basis of the six different nonplanar-surface forms — the single plane and the five parabolic arches — used in this study. Once again, the general lack of any significant effect of the shape of the stimulus-form as the stimulus changed from the prototypical plane to the most distorted parabolic arch is evident. The ANOVA analysis also produced insignificant F ratops (see Table 6) for all masking-dot densities. Figure 22 shows these same data, but in a version in which all of the scores for all masking-dot densities are pooled together to emphasize the overall trend of the data — again an inconsequential effect. Figure 23 shows the results for stimulus-forms with the smallest number of dots (25), once again analyzed separately, to show that this outcome is not an artifact due to a ceiling effect. Because many fewer trials were pooled to produce this graph, the variability is considerably larger than in Figure 21.

The data analyzed on the basis of the number of dots in the stimulus-forms and replotted in Figure 24, show the same strong relationship between signal-to-noise ratio and the detectability of the stimulus-form that has become familiar. In this case, the ANOVA produced strongly significant F scores (see Table 7). Figure 25 presents these data pooled across all masking-dot densities to emphasize this trend in the data.

F. Experiment 5. (Hemis)

Design and rationale

In both Experiment 3 and Experiment 4, the distortions introduced into the stimulus-forms occurred along only a single dimension — both cylinders and parabolic arches were generated by one-dimensional functions that varied only in y. The cross-section of the form along the x dimension was constant. It is conceivable that the general lack of any significant effect might be associated with this relatively simple kind of distortion. Therefore, other experiments with more complex stimuli were needed. The stimuli used in this experiment were more complex in the sense that variations occurred along both the x and y dimensions simultaneously. As we shall see later, there were also other ways in which complexity could be increased.

The set of six stimuli used in Experiment 5 consisted of a prototypical, decagonal-shaped plane and five hemispheres generated from it by means of the following polynomial expression:

$$z = (x^2 + y^2 - W)^{\frac{1}{2}} + H \qquad (8)$$

The specific coefficients used to generate the five hemispheres are shown in Table 8 and representations of the cross-sections of the six stimuli are displayed in Figure 26. To apply this polynomial expression to the prototype plane is to generate a set of hemispheres with differing radii, of course, but, as with the cylinders of Experiment 3, the radii available make for a rather flattened set of stimuli.

In this experiment, the number of dots in the plane or any of the five hemispheres could take on any one of five values — 81, 64, 49, 36, and 25 — and thus 30 stimulus-forms were available to be randomly selected for presentation

in any given trial. The experiment was run over ten days. First, masking-dot densities of 50, 100, 150, 200, and 250 were used in ascending order and then the sequence was repeated in descending order.

Results

The results of Experiment 5 are shown in Figures 27 through 31. Let us first, consider Figures 27 and 28, which show the results analyzed on the basis of the six shapes used in this experiment. The first figure presents the data parametric in terms of the masking-dot density, while the second plots the same data pooled for all masking-dot densities. Despite the addition of the second dimension of distortion, here, too, there is neither visual nor statistical evidence of any effect of form in the figures or in the ANOVA analysis (see Table 9). Figure 29 plots the results for the lowest level of stimulus-form dot density to show that this insignificant result is not a ceiling effect caused by an inordinately large number of dots in relation to the number of masking-dots. Figures 30 and 31 show the unpooled (parametric in masking-dot density) and pooled results when the data are analyzed on the basis of stimulus-form dot density. Here, as usual, the effects are strong and significant (see Table 10).

G. Experiment 6. (Parab)

Design and rationale

The plan in this series of experiments, as previously expressed, was to progressively enhance the complexity and magnitude of the distortions introduced into nonplanar surfaces to assay the effects of form on detectability. So far, we have discussed progress from a one-dimensional (e.g., cylinder) to a two-dimensional (e.g., a hemisphere) distortion and also have

considered the increase in the magnitude of the distortion achieved by selecting a generating equation that produces a steep parabolic arch rather than a flat cylinder. In Experiment 6, this progression was continued by combining the two manipulations. First, we used a stimulus-form varying in two dimensions to produce a surface of rotation (comparable to the hemisphere). Second, we increased the magnitude of the distortion beyond that possible with hemispheres by using a parabolic generating equation. The form of this new set of paraboloids of rotation is represented by the polynomial:

$$z = G(x^2 + y^2) + H \qquad (9)$$

Six stimulus-forms were used in this experiment. The first was a prototypical, decagonal plane and the other five were progressively greater, nonplanar, parabolic distortions of that plane characterized by the coefficients shown in Table 11. The cross-sectional shapes of these six stimuli are shown in Figure 32. Furthermore, five different levels of stimulus-form dot density were used -- 20, 35, 50, 65, and 80 — resulting in a total of 30 different stimulus-forms, any one of which could be randomly selected for presentation in any trial. In this case, the experiment was carried out at seven different masking-dot densities -- 40, 80, 120, 160, 200, 240, and 255 dots — once in ascending order and once in descending order for a total of 14 daily sessions.

Results

The results of Experiments 5 and 6 are shown in Figures 33 through 37. Figure 33 and 34 show the data analyzed on the basis of stimulus-form. The

first of these two figures presents the data parametrically as a function of masking-dot density, while the second presents all of the data for all masking-dot densities pooled into a single curve. In spite of the two-dimensional nature of the distortion and the enhancements in magnitude, here, too, the results indicate a negligible influence of the global three-dimensional shape of this kind of stimulus-form on detectability. The results of the ANOVA also indicate an insignificant effect for all of the utilized masking-dot densities (see Table 12). Figure 35 displays the results for the smallest number of stimulus-form dots alone to confirm that these results are not due to a ceiling effect. These curves are irregular due to the relatively small number of trials pooled for each plotted point, but the general trend is also clear here.

Figures 36 and 37 show the typical strong effect of signal-to-noise ratio, the former presenting the unpooled data analyzed in terms of stimulus-form dot density and displayed as a parametric function of the masking-dot density. (The ANOVA analysis is presented in Table 13).

H. Experiment 7. (Cubran1)

Design and rationale

The strategy of increasing the complexity of the stimulus-form was pursued by next turning to a polynomial-generating function of the third degree, but in one dimension, of the form:

$$z = G(Ty^3 + Vy) + H \qquad (10)$$

This polynomial expression functionally varied the shape only across the y dimension and the cross-section remained constant across the x dimension. It did differ, however, in that it had both a maximum and a minimum instead of either the single maximum or the single minimum exhibited by all of the previously generated forms. The cross-sections of the set of stimulus-forms generated by this polynomial are shown in Figure 38, and the particular coefficients used in its evaluation are presented in Table 14.

The prototypical form in this case was a square plane and, as in all other of these experiments, the stimuli were distorted along the z axis (the line of sight) of the viewing cube. Each of the six forms was presented at five different dot densities — 81, 64, 49, 36, and 25 — so that 30 stimuli were available to be randomly selected for presentation in any given trial. Ten daily sessions were necessary to complete this experiment as masking-dot densities of 50, 100, 150, 200, and 250 dots were used, first in ascending order and then in descending order to counterbalance any sequence effects.

Results

The results of Experiment 7 are shown in Figures 39 through 42. Figures 39 and 40 display the results plotted on the basis of the six shapes used in this experiment. In Figure 39 the data are plotted parametrically as a function of the masking-dot density. Figure 40 presents the data pooled across masking levels to emphasize the general trend. For the first time the curves in this graph display a significant downward trend in detectability as the form becomes more and more distorted into a cubic nonplanar surface. The ANOVA analyses of these data also indicate this result to be significant (see Table 15) for four of the masking levels used (excluding the least dense), even though the effect is only slightly greater in absolute magnitude than in some of the preceding

experiments. The analyses based upon the stimulus-form densities are shown in Figures 41 and 42 for the unpooled and pooled data, respectively. As usual, the findings are strongly significant, as evidenced both in the figures and in the ANOVA (see Table 16).

I. Experiment 8. (Cubran2)

Design and rationale

To further complicate the stimulus-forms another, more eleborate generating function was used in the next experiment. According to the complexity criteria proposed earlier, a cubic varying in two rather than one (as in Experiment 7) dimension should add even further to the stimulus complexity. The generating equation for a two-dimensional cubic was derived from our general polynomial was of the form:

$$z = G(Cx^3 + Ex + Ty^3 + Vy) + H \qquad (11)$$

The five double cubics were generated from the prototypical square plane from this equation by using the coefficients shown in Table 17. As usual, the stimulus-forms are distorted along the line of sight (the z axis) toward the observer. However, in this case the forms had both maxima and minima in depth and thus the stimuli were both concave and convex in different parts of the field of view. One set of cross-sections of these stimulus-forms is shown in Figure 43. However, this is not a completely accurate picture. Slices could be

taken elsewhere of these complex surfaces that would show different cross-sections (see Figure 8F). To vary the signal-to-noise ratio, five levels of stimulus-form dot density — 81, 64, 49, 36, and 25 — are used for each of these six forms. This produces 30 different stimulus-forms, any one of which could be randomly selected for presentation in any trial. For seven sequential days, the stimuli were presented in order of increasing masking-dot densities — 50, 100, 150, 200, 250, 300, and 350 dots, respectively. On the next seven days, the same seven masking-dot densities were progressively reduced in order to balance out sequence effects. In all, therefore, this experiment required 14 days to be completed.

Results

The results of Experiment 8 are shown in Figures 44 through 47. Figures 44 and 45 display the data analyzed on the basis of the five different double-cubic forms (and the prototype plane), first in an unpooled version that is parametric as a function of the seven masking-dot densities, and then as a single curve in which all data from all masking-dot densities have been pooled. There appears in these data, as there did for the one-dimensional cubic forms of Experiment 7, a continuation of the trend toward lower detectability as the shape became more and more distorted away from the prototypical plane. The ANOVA confirms this result (see Table 18). Indeed, the effect is much stronger than it was in Experiment 7. The significant F ratio values in this case are substantially higher than those in the one-dimensional cubic case.

The effect of stimulus-form dot density remains strongly significant. This is shown in Figure 46, as well as in the ANOVA (see Table 19) and in the pooled data of Figure 47.

J. Experiment 9 (Hyparb)

Design and rationale

An experiment was next carried out in which hyperbolic paraboloid stimuli (saddles) were generated from a prototypical square plane by applying a polynomial of the form:

$$z = G(x^2 - y^2) + H \tag{12}$$

In this experiment, six stimulus-forms were used, the prototypical square and the five progressively more extreme hyperbolic paraboloids, whose cross sections are exemplified in Figure 48. Once again, it must be remembered that these cross-sections are not inclusive — other slices could produce other pictures. Each hyperbolic paraboloid is respectively characterized by the coefficients shown in Table 20. The surfaces were distorted along the line of sight, but in a complex manner that is best described graphically (see Figure 8G). Each of the six stimulus-forms was presented at five different dot densities — 81, 64, 49, 36, and 25 — producing 30 different stimuli, any one of which could be randomly selected for presentation in any trial. The experiment took 14 days to complete; seven days with masking-dot densities of 50, 100, 150, 200, 250, 300, and 350 dots presented in ascending order on sequential days, and seven days in which these same masking levels were used in the opposite, descending order.

Results

The results of Experiment 9 are displayed in Figures 49 through 53. Figures 49 and 50 respectively, present, the unpooled data analyzed on the basis of stimulus-form and plotted as a parametric function of the masking-dot density and the pooled results. Both these figures and the ANOVA analysis of these data (see Table 21) clearly indicate that there is a negligible effect of stimulus-form for these particular nonplanar surfaces. Figure 51 presents the data for the lowest level of stimulus-form dot density — 25 dots — to support the contention that this negligible effect is not a ceiling effect.

The data analyzed on the basis of the number of stimulus-form dots are plotted in Figure 52 in an unpooled version that is parametric as a function of masking-dot density, and in Figure 53 in a pooled version. When analyzed with the ANOVA (see Table 22) and when graphed for visual inspection, strong and significant effects are evident in these data.

K. Experiment 10 (Sin1)

Design and Rationale

The positive results of Experiments 7 and 8 and the progressively less strong results of all of the others provided the incentive for our next set of experiments. Experiment 7 and 8 suggested that stimulus-form effects that do obtain may depend upon the number of maxima and minima on the generated surfaces. So far we have seen that if there is only a single maximum or minimum in depth on the nonplanar stimulus-form, then no amount of distortion (within the limits of which the currently used procedures are capable) can produce any significant differential sensitivity to form. However, a positive relationship between detectability and form appeared when more than one

maximum or minimum occured in the stimulus-form.

The obvious next step was to generate nonplanar stimulus-forms with more, and preferably controllable numbers of, maxima and minima. Such a set of stimuli could be generated by modifying the general polynominal expression of Equation 4 by introducing cross-products of x and y. However, simple repetitive waveforms could be more conveniently produced by a generating-expression of the following form:

$$z = A(\cos Wx) \tag{13}$$

The cosine form of the sinusoidal equation was chosen simply to guarantee that the maxima and minima of the stimuli would be centered in the viewing space and that the generated stimuli would thus be symmetrical about the y or vertical axis.

Stimuli generated by this expression are sinusoids in depth. That is, the undulations occur in the z dimension; all depths along any given vertical axis remain constant. Different depths occur in an oscillatory fashion across the horizontal dimensions. Figure 54 displays a sample of an undulating sinusoidal stimulus-form as it might appear in this kind of display — although of course neither the outline of the cube nor the grid would be seen, only the array of stimulus-form and masking-dots. In this experiment, sinusoidal stimuli of this kind were presented to our observers in three levels of masking-dots — 50, 100, and 200 — once in the ascending direction and once in a descending direction, for a total of six sessions. The number of dots in the prototypical square from which the sinusoids were formed was held constant at 81. The amplitudes of

the sinusoids were kept constant at 9.22 min of visual-angular disparity. The spatial frequency, however, was varied to produce six stimuli that had spatial frequencies of across the 5.4 deg width of the viewing cube (see page ____). The coefficients necessary to produce such stimuli are shown in Table 23. The prototypical square plane was also used, bringing the number of stimuli used in this experiment to seven.

Results

The results of this experiment are shown in Figures 55 and 56. Figure 55 presents the unpooled data plotted parametrically as a function of masking-dot density. This figure strongly suggests that the number of maxima and minima, or some other covarying factor, has a strong influence on detectability. As the wave length decreases and the spatial frequency of the occillations increase, there is a progressive and massive (in the context of our previous experimental results) diminution in detectability scores. The shape of the effect is comparable at all masking-dot densities, but increases in magnitude and occurs earlier as the number of masking-dots increases. When pooled (as shown in Figure 56) the data are characterized by a monotonic function that ranges over 35 percent of the 50 percent possible range — an extraordinarily large effect given the nature of the results from previous experiments. Since the amplitude of oscillation was held constant, this strong effect can only be attributed to the number of maxima or minima, the spatial wavelengths, or some other variable directly related to one or the other of these two factors. Of course, these stimulus-forms were becoming more and more random as the spatial frequency increases. Thus, it may be that we are measuring this physical property rather than a psychophysical propensity. This matter will be considered later and it will be established that, in part at least, it is the number of dots rather than the

form itself that produces the decline in performance.

L. Experiment 11 (Sin 2)

Design and rationale

The next experiment, one also using the sinusoidal stimulus-form generator, elaborated upon the simple one-way design of Experiment 10 to create a two-way design in which both frequency and amplitude were simultaneously varied. The purpose here was to give a deeper insight into the dynamics of the spatial frequency sensitivity exhibited by the visual system in this type of task. In this experiment, the same six sinusoidal spatial frequencies were utilized as in Experiment 10 namely, .09, .19, .28, .37, .56, and .93 cycles/deg across the 5.4 deg wide front surface of the cubical view space. Each of these spatial frequencies, however, was presented at one of five different peak-to-peak amplitudes corresponding to 0, 1.42, 5.32, 9.22, and 13.48 min of visual-angular disparity in a way that normally would have produced a possible total of 30 stimuli. However, since the smallest amplitude corresponding to zero disparity makes all "sinusoidal oscillations" identical, regardless of frequency -- they all become planes — there are in fact only 25 distinct stimuli. Masking-dot densities of 50, 100, 150, 200, 250, and 300 dots, respectively, were used in this experiment. The number of dots in the stimulus form was held constant at 81. Because of the exigencies of the academic year, we were able to collect data in only six sessions of this experiment -- once for each of these masking-dot densities in ascending order.

Results

The results of Experiment 11 are presented in Figures 57 through 60. The data plotted in Figure 57 were analyzed on the basis of spatial frequency and parametrically as a function of the masking-dot density. In Figure 58, the data have been pooled across masking-dot levels to emphasize the general trend of the data. This experiment replicated Experiment 10 in the form of a two-factorial design. In this case, however, the data display only a moderate decline in detectability with increases in spatial frequency. This outcome occurs because of the lessened contribution of the lower amplitude signals to variations in detectability, the magnitude of the frequency effect being much reduced in those cases than when higher amplitude stimuli were used. If the data for the largest magnitude (13.48 min of disparity) of sinusoidal amplitude are considered separately, the results of Experiment 10 are replicated. In this experiment, therefore, there is a ceiling effect that tends to obscure the functional role of spatial frequencies when performance scores are pooled for wide ranging amplitudes of sinusoidal oscillations.

Figure 59 displays the same data analyzed on the basis of the amplitude of the sinusoidal oscillation. The progressively increasing gradient of performance with increasing amplitude is clearly evident in these data.

M. Experiment 12 (Sin 4)

Design and rationale

Experiment 12 also utilizes sinusoidal-type stimuli. In this experiment, however, both sinusoidal spatial frequency and the number of dots in the target form were covaried. However, the amplitude of the oscillation was held constant at a value equivalent to 13.48 min of visual-angular disparity. The purpose of Experiment 12 was to determine the effect of both spatial frequency

and the density of the dots used to form these nonplanar sinusoidal surface in a situation in which both variable are being manipulated. The spatial frequencies used in this experiment were the same six used in Experiments 10 and 11 — 0, .09, .19, .28, .37, .56, and .93 cycles/deg across the 5.4 degree face of the viewing cube — as generated by the sinusoidal generating expression of Equation 13. Each sinusoid could be presented at any one of several stimulus-form densities, including 81, 64, 49, 36, or 25 dots. Thus, 30 distinct stimuli were available for random selection for presentation in any trial.

Masking-dot densities of 50, 100, 150, and 200 were used on four successive days in ascending order and then on four days in descending order for a total of eight experimental sessions in order to carry out the full design of this experiment.

Results

The results of Experiment 12 are plotted in Figures 60 through 63. Figures 60 and 61 present the data analyzed on the basis of spatial frequency in the unpooled (parametric in masking-dot density) and the pooled versions, respectively. Though somewhat more variable than the results of Experiments 10 and 11 (the elevated results for the .37 cycles/deg condition are believed to be idiosyncratic), the strong effect of spatial frequency is again clearly evident. This visual estimate is confirmed by the ANOVA, an analysis that produces strongly significant scores (see Table 24).

Similarily, when the data are analyzed on the basis of stimulus-form dot density, plots of both the unpooled (parametric as a function of masking-dot density) and the pooled versions of the data in Figures 62 and 63, respectively, display the usual strong effects (see Table 25 the results of the appropriate ANOVA).

N. Experiment 13 (Con1)

Design and Rationale

Thus far polynominal and sinusoidal expressions have been used as generating rules for stimulus-forms. It seems desirable at this point to consider whether there might be any other possible functional characteristics of geometrical form to which the visual system might or might not be sensitive. One plausible candidate was suggested by Chen (1982, 1983), who noted that the topological properties of a continuous stimulus-form are important in determining its discriminability from other simular-forms. The specific dimension used by Chen was the topological connectivity of the form. Connectivity (H) for surfaces has been defined by Hilbert and Cohn-Vossen (1952) with the following expression:

$$H = P+1 \qquad (14)$$

where P is the number of holes in a bounded but continuous surface.

In this experiment several planar surfaces were generated, all of which had the same area but which varied in connectivity. Their global shapes are shown in Figure 64 (but, remember, their surfaces are in fact, defined by random arrays of dots — not continuous outlines). Two of these stimulus-forms (the square and the notched square) are topologically identical and, therefore, have the same connectivity (H = 1). The other stimulus-form possess differing levels of connectivity (H = 2, 3, and 4 respectively) and are different topologically from the first two as well as from each other. The question now

confronted is: Does this topological difference affect detection scores in the present experimental design?

To answer this query, the five stimulus-forms shown in Figure 64 were presented at five levels of dot density — 81, 64, 49, 36, and 25 — producing 25 stimuli, any one of which could be randomly selected for presentation in any trial. To keep the area of all five of the stimuli constant, some had to be slightly larger than the others, but all were close to 4 deg by 4 deg in width and height. These stimuli were presented in random order in 14 daily sessions in which seven masking-dot densities (50, 100, 150, 200, 300, and 450 dots) were first presented in ascending order and then in descending order.

Results

The results of Experiment 13 exploring topological connectivity are presented in Figures 65 through 68. Figures 65 and 66 present the results in the unpooled (parametric as a function of masking-dot density) and pooled forms, respectively. The flat appearance of these curves indicates that there is no functional effect of connectivity. This outcome is quantitatively supported by the ANOVA analysis (see Table 26). Obviously connectivity is not capable of influencing detectability, at least in the context of this experimental paradigm even though it does affect discriminability.

The data were re-analyzed on this basis of the density of the masking-dots and plotted in Figures 67 and 68. Here the usual strong effect of signal-to-noise ratio appears again both visually and in the ANOVA analysis (see Table 27). This particular group of observers seemed to be somewhat more resistant to masking than were most of our other groups.

O. Supplementary Experiment 14. (Cubegrid 1)

In addition to the 13 experiments just reported, which used arrays of randomly organized dots to produce the planar and nonplanar surfaces, several other experiments were also carried out. These experiments utilized surfaces generated by applying some of the same polynominal expressions to prototype planes constructed of rectangular grids of dots rather than randomly dispersed dot arrays. In these experiments the stimulus-forms, therefore, consisted of arrays of dots that could possess one of two different kinds of regular organization. If the surface was a plane, then the grid of dots simply appeared to be composed of straight-lines. However, if the surface was deformed by applying one of the appropriate polynominal expressions described earlier, the lines of the grid appeared to be curvilinear to a degree dependent upon the perspective and disparity transformations necessary to produce stereoscopic images with depth. When the distorted images formed from grids were viewed dichoptically, a strong impression of an orderly "fishnet-like", nonplanar surface quite similar to those shown in Figure 8 (but without the interconnecting lines, of course) was created.

Even though there is a strong depth experience produced by surfaces generated from grid prototypes, it must be appreciated that these stimulus-forms are not the classic random-dot stereogram. Rather than being disorganized and random, these grid-prototype stimuli possess a regular organization that can easily be perceived monocularly. These obvious monocular cues provide an alternative means of discriminating between the dots organized on a surface and the dummy dots that are not so organized. In the former case, the lines of dots, even when viewed monocularly, lie along lines that are either straight or curve continuously and in an orderly manner from dot to dot. In the latter case, the dots are scattered (by their irregular disparity) into something much more closely approximating the masking array.

Figure 69, for example, shows a stimulus-form (a) used in Experiment 14 in which the grid is transformed into a cubic in one dimension, as well as the corresponding dummy dot array (b). The residual regularity in the case of the dummy dots is due to the fact that their positions are specified by randomizing only the z coordinate of the stimulus-form dots. Thus, except for the differences introduced by the necessary disparity and perspective shifts, the x and y coordinates of the dummy dots remain close to what they were orginally in the surface-constrained stimulus-form.

It takes no great insight to appreciate that the two kinds of stimuli shown in Figure 69 can easily be discriminated monocularly, and, thus, this type of stimulus cannot be used unequivocally to test the properties of perceived stereoscopic space. Simply put, such stimulus-forms are not examples of the monocular-cue-free, random-dot stereogram that is the essence of the important contribution made Bela Julesz to visual science. Rather, these stimulus-forms are heavily polluted with monocular cues and their use produces a much more heavily confounded experimental design than ordinarily would be acceptable. Nevertheless, in spite of this confounding — or, rather, because of it — some extremely interesting results emerged from experiments using grid prototypes, and they shall be considered here. Because of this confounding, the four experiments reported below are distingushed from the preceding ones by being designated "Supplementary Experiments."

Design and Rationale

Supplementary Experiment 14 was designed to explore the effect of the shape of grid-like stimulus-forms and the dot densities of both the form and the mask on detectability. The forms used in this experiment were distorted into cubics in one dimension (in accord with Equation 10). This experiment was

identical to Experiment 7 in all regards but two — one major and one minor. The minor exception was that the masking-dot density levels utilized included 300 as well as 50, 100, 150, 200, and 250 dots. The major difference was that the planar prototypes from which the stimulus-forms were generated were constructed of square arrays of 25, 36, 49, 64, and 81 dots, respectively, arranged in a regular grid. Given the six degrees of distortion by the polynominal of the prototype form (identical to those indicated in Table 14), 30 different stimuli were available for random order presentation in the 12 daily sessions that comprised this experiment.

Results

The results of Supplementary Experiment 14 are presented in Figures 70 through 73. Figures 70 and 71 present the data analyzed in terms of the effect of the stimulus-form in unpooled and pooled versions, respectively. Masking-dot density is the parameter in Figure 70. Unlike the outcome reported for Experiment 7, there is no evidence of any form effect in this case in which a rectangular grid is used as the prototype. This visual judgment is confirmed by the ANOVA analysis shown in Table 28 — all F ratios for the stimulus-form dimension are insignificant.

Another difference between these findings and those of Experiment 7 is that the effect of the masking-dot density, as indicated in the spacing between the various parametric curves for the different masking-dot densities, is greatly enhanced. The high sensitivity to masking is even more dramatically displayed in Figures 72 and 73, where the data are presented in terms of the number of dots in the stimulus-form for both the unpooled and pooled cases. Not only are the curves in Figure 72 steeper than those in Figure 41, but the ANOVA analysis also shows F ratios that are considerably larger, as indicated in Table 29.

Indeed, while the average F ratio for the effect of stimulus-form dot density was 115.78 for this experiment, it was 46.26 for Experiment 7. However, the detectability scores for the stimulus-forms constructed from the 81 dot grid prototype are all virtually perfect. These two characteristics lead to a fan-shaped family of curves, rather than the parallel family previously generated.

P. Supplementary Experiment 15 (Cubgrid 2)

Design and rationale

This experiment repeats all of the conditions of Experiment 8 (in which stimulus-forms were distorted into cubics in two-dimensions), with two procedural exceptions. First and trivially, the masking-dot densities used in this experiment were 50, 100, 150, 200, 250, and 300 dots and, thus, only 12 days were necessary to carry out the experiment; the 350-dot density condition was omitted. Second and more significantly, the prototype stimuli used to generate the stimulus-forms in this experiment consisted of square arrays of 25, 36 49, 64, and 81 dots, respectively, arranged in a regular grid. The stimuli in this experiment were deformed in accord with Equation 11 and Table 17 into six different shapes, any one of which could be presented at any of five different dot densities, a combination that produced 30 distinct stimuli. The particular coefficients used were the same as those presented in Table 17.

Results

The results of Supplementary Experiment 15 are presented in Figures 74 through 77. Figures 74 and 75 present the data in terms of the stimulus-form in

unpooled (parametric in masking-dot density) and pooled versions, respectively. The differences between the results for the present experiment and those of Experiment 8 are comparable to the differences between Supplementary Experiment 14 and Experiment 7. First, there is no evidence of any effect of form, in spite of the fact that distortion of the prototype plane into cubics in two-dimensions produced the strongest shape effects when randomly dotted arrays were used. Second, the effect of the number of masking-dots is stronger in the present experiment than it was in the corresponding Experiment 8, as is shown. This is also quantitatively indicated by the F ratio values shown in Table 30.

These data, re-analyzed in terms of the number of dots in the stimulus-form, are replotted in Figures 76 and 77 in the unpooled and pooled versions, respectively. The enhancement of the sensitivity to masking is clearly demonstrated both in the separation and slope of the graphs themselves and in the ANOVA analyses shown in Table 31. Indeed, the average F ratio for stimulus-form dot density for Experiment 8 was 41.23 while the average for this Experiment was 93.34. Once again, the fan-shaped family of curves obtains.

Q. Supplementary Experiment 16 (Hygrid)

Design and rationale

Supplementary Experiment 16 replicates Experiment 9, in which the stimuli were deformed in accord with a polynominal that generated a hyperbolic paraboloid. In this experiment the 350 masking-dot condition was also omitted and only masking-dot densities of 50, 100, 150, 200, 250, and 300 dots were used, once in the ascending order and once in the descending order. Twelve

days were required to carry out this experiment. The prototype stimulus-forms in this experiment were the same square arrays (consisting of 25, 36, 49, 64, and 81 dots, respectively, arranged in a regular grid) used in the previous two supplementary experiments. Each of these prototypes are deformed in accord with Equation 12 and the coefficients of Table 20 to produce a total of 30 different stimulus-forms.

Results

The results of Supplementary Experiment 16 are shown in Figures 78 through 81. Figures 78 and 79 present the data in terms of the stimulus-form in both the unpooled version, which is parametric in masking-dot density, and the pooled version. Here, as in the corresponding Experiment 9, there is no effect of form, a result also indicated in Table 32. On the other hand, the unpooled and pooled versions of the data analyzed in terms of the stimulus-form dot density and replotted in Figures 80 and 81, respectively, show that the effect of stimulus-form dot density is much greater in this experiment than in Experiment 9. This increase in the strength of the effect can be quantified by comparing the ANOVA summaries in Table 33 with those in Table 22. The average F ratio obtained in this Supplementary Experiment 16 was 70.98, as compared with 17.79 in Experiment 9.

Now, let us consider the three sets of data from Experiments 14, 15, and 16 together to see what general results have been obtained. First, results for neither Supplementary Experiments 14 or 15 displayed any indication of even the significant form effects that had been obtained in the corresponding experiments (Experiments 7 and 8) with stimulus-forms generated from random-dot array prototypes. Supplementary Experiment 16 produced results (no

stimulus-form effect) that are identical to those obtained in Experiment 9.

Second, the effect of manipulating either the stimulus-form or masking-dot densities (that is, the signal-to-noise ratio) is now much stronger than it was in all three earlier corresponding experiments. Either reductions in the number of dots in the stimulus-form or increases in the number of masking-dots produce a stronger effect now than it had previously.

Third, the shape of the families of curves in the three figures displaying the unpooled data analyzed in terms of the stimulus-form dot density for the rectangular grid-like prototypes (Figures 72, 76, and 80) are substantially different from the shapes of the families of curves in the three figures displaying the corresponding data for the random-array prototypes (Figures 41, 46, and 52). One obvious way in which the two sets of figures differ is that the family of curves generated by random-array stimulus-forms are generally parallel, while those generating grid-like arrangements fan out from left to right. The cause of this difference is twofold. First, the most dense stimulus-forms (containing 81 dots) in the latter case seem not to be affected by variations in the masking-dot density — they are all detected equally well and at a high performance level. Second, and quite surprisingly, the effect of increases in the masking-dot density is much more substantial for the less dense grid stimuli than for the equally dense random-array stimulus-forms at higher masking-dot densities. This enhanced sensitivity to masking increases progessively with the reduction in the stimulus-form dot density. The net effect is to produce a fan-shaped family of curves in the grid-prototype experiments, as opposed to the parallel set of curves in the random-dot-array experiments.

R. Supplementary Experiment 17 (Monogrid)

Design and rationale

A possible explanation of the general results of the three preceding supplementary experiments must be considered now rather than in the next chapter. One explanatory hypothesis suggests that the difference in the shapes of the families of curves in the random-dot-array and the regular-grid experiments may be due to the utilization of different criteria by the observers for the two different kinds of stimuli. For the random-dot-arrays, there is only a very weak monocular cue, as compelling shown in Experiment 2. In those experiments the observers had to depend upon the stereoscopic cues to distingush the nonplanar surfaces from arrays of random-dots. However, in the experiments using rectangular arrays, as already noted, there was certainly strong monocular cues present. The observers could and apparently did use these monocular cues at low masking-dot densities and high stimulus-form dot densities. Is it possible that they learned to also use this same monocular cue at lower signal-to-noise ratios? If so, decision criteria are being adopted in this case that are based on the monocular properties of the stimulus-form rather than on its dichoptic properties, even though the latter are present and available.

If true, this hypothesis would satisfactorily account for the fan-shaped family of curves, since the essentially two-dimensional nature of the stimulus situation, as it is used by the observer, does not allow him to enjoy the dedensification advantage obtained when the masking-dots are perceptually distributed thoughout a three- as opposed to a two-dimensional space; the masking-dots, therefore, become more influential in the latter case than in the former. Such a hypothesis would also explain the absence of the stimulus-form

effect found in the corresponding random-array: The observer was simply ignoring the cues for shape and depth present in the stereoscopic display.

How can we test the hypothesis that the observer is using only monocular criteria in the grid-prototype experiment? The most direct way is to simply repeat one of the three supplementary experiments, but with the observer limited to monocular viewing. Thus, he would not have any dichoptic stimuli available to him and would be forced to depend solely upon information available to one eye; the stereoscopic information in this case is thus not available to either be used or ignored. If the results of this monocular replication are comparable to the results of the corresponding dichoptic experiment, the argument that the observer is only using monocular information in the dichoptic situation would be supported. If, on the other hand, more complicated differences should obtain, then that hypothesis would have to be considered to be insufficent.

Supplementary Experiment 17 replicated all of the conditions of Experiment 14, in which rectangular grid-prototypes were deformed in accord with Equation 10 (a cubic in one-dimension). The only procedural change was that a shield was placed in the nondominant eye's line of sight, a minor mechanical change that produced a major stimulus change — the viewing situation became monocular rather than dichoptic but under the experimenter's control rather than the observer's.

Results

The results of Supplementary Experiment 17 are shown in Figures 82 through 85. Figures 82 and 83 show the outcome when the data are analyzed in terms of the stimulus-form, first in the unpooled version (parametric as a function of the masking-dot density) and then in the pooled version. As in

Supplementary Experiment 14 there is virtually no effect of form with these grids and deformed grids, a conclusion supported by the ANOVA analysis shown in Table 34. However, unlike Experiment 2, there is a much smaller difference between the results obtained with the monocular viewing condition and those forthcoming from the dichoptic one. In Experiment 2 the effect of eliminating dichoptic viewing was devastating — detection went from virtually perfect scores to levels that were nearly random. In Supplementary Experiment 17, however, performance is only slightly lower (approximately 10%) than in the dichoptic viewing situation.

Similarly, the fan-shaped family of curves obtained and plotted in Figures 84 and 85 for the unpooled and pooled versions (for data analyzed in terms of the number of dots in the stimulus-form) is very close to the one obtained in the dichoptic viewing condition. If anything, the influence of the number of masking-dots is even stronger as indicated by the very large F ratios emerging from the ANOVA analysis presented in Table 35.

The relatively minor differences between the results of this monocular experiment and those of the corresponding dichoptic viewing conditions of Experiment 14 suggest that it is, in fact, the case that observers are utilizing a set of monocular cues when dealing with the stimulus-forms that are generated from grid-prototypes.

5. DISCUSSION

A. A Summary of the Results

Now that the particulars of the data obtained in the various experiments carried out in this study have been presented, it is appropriate to consider their significance and implications for understanding the visual form detection process in general. As noted earlier, two major questions have motivated and guided this research program. The first is, What are the effects of form on detectability? Form, in these experiments, has been precisely quantified in terms of polynomial, sinusoidal, or topological generating functions — a somewhat unusual accomplishment in this kind of research.

The second motivating question is, What are the effects of the signal-to-noise ratio on detectability. Because "signal" attributes are complex, the signal-to-noise ratio has been "crudely" approximated by simply counting the raw number of dots in the stimulus-form and the mask, respectively. Other higher order organizational properties of the dots in the stimulus-form are important, as has been demonstrated in this study, but they are difficult to quantify in the metrics of signal or noise. Surprisingly, as we shall see, even the crude measure of numerosity accounts for a large proportion of the variance in performance produced by changes in the dot density of either the stimulus-form or the mask.

To begin, consider the empirical answers obtained to the first question concerning the influence of stimulus-form on detection. In general, it is clear from a visual inspection of the various figures, as well as from the ANOVA analyses, that the effects of stimulus-form were quite variable from one experiment to another. Indeed, performance scores varied from "insignificant" to "substantial" as a function of the sets of stimulus patterns used. In the discussion to be presented

now, we will show that what appear to be "substantial" effects of at least one measure of form (spatial frequency) obtained in the later experiments that used sinusoids are in part due to difficulties in perceptually defining the stimulus-form rather than to form per se. Once these large effects are accounted for, the overall conclusion toward which we are compelled is that form effects with randomly dotted stimuli are, in the main, quite modest, and even these small effects do not emerge until the expression generating the form crosses a certain threshold of complexity. This threshold, at first glance, appears to be associated with the number of maxima and minima present in the stimulus-form. But, as we shall see, this is also much too simplistic an explanation to be accepted at face value.

All of this is not to say that there are no stimulus-form effects; only that with the kind of dotted stimulus used in this study, the residual effects specifically attributable to form (once other signal-to-noise and sampling effects are accounted for) are in general, not huge. Indeed, statistical tests must be used to establish the existance of form effects. The use of such tests to establish subtle influence of minor magnitude is a procedure that had not been necessary with the generally large effects previously obtained in analogous two-dimensional masking studies. The necessity to do so with the three-dimensional stimuli used in this study speaks for itself. Now let us briefly review the general outcome of the various experiments.

1. Examination of the effect of different types of shapes in Experiment 1 demonstrated a systematic though modest advantage of a parabolic arch (a form varying in one dimension) and a systematic disadvantage of a double cubic and a hyperbolic paraboloid (forms varying in two dimensions) in detection scores compared to the other four forms that were tested. However, these results are ambiguous, even when

compared with the results for the other stimulus-forms (cylinder, hemisphere, paraboloid of rotation, and cubic in one dimension) utilized in this same experiment. The advantage of the parabolic arch was not replicated in the case of the paraboloid of rotation; the latter was detected at average levels. Furthermore, the disadvantage of the double cubic and hyperbolic paraboloid seems not to be correlated with their two-dimensional functionality; the paraboloid of rotation, for example, did not suffer the same diminution in detectability as did the two other forms.

2. No significant effects of form were detectable in the series of experiments that progressively distorted a single type of shape to greater and greater convexities until the stimuli became complex enough to have more than a single maximum or minimum. Table 36 presents the F ratios averaged across all masking-dot densities for all of the experiments in which this measure was computed. All nonplanar surfaces characterized by a single maximum or minimum (i.e., surfaces on which the first derivative is equal to zero in only one location) produced statistically insignificant results as their shape varied from a plane to the most distorted three-dimensional form. This summary describes the results of Experiments 3 through 6. An inspection of the graphs depicting these data indicates only a few cases (at relatively high masking-dot densities) at which some minor effects, otherwise hidden in the statistical summaries, become noticeable. For what these minor, insignificant effects are worth, in all cases they are characterized by a diminution in detectability as the deformation increases. However, when more than a single maximum or minimum is

present in depth in the stereoscopically generated images, there is a progressive increase in the effect as the geometrical complexity of the form increases. Nevertheless, even in the most complex forms generated from polynominals, the magnitude of the effect is relatively small.

3. The topological properties of a stimulus-form, as measured by its connectivity, do not affect its detectability even though it has been shown elsewhere that connectivity does influence discriminability.

4. When sinusoidal stimuli are used, a substantial decrease in detectability does occur with increases in spatial frequency. This initially suggested that the number of maxima and minima might, indeed, be the influential variable. However, this result cannot be unequivocally accepted since the distribution of the dots in the stimuli is becoming, in a certain sense, more random as the spatial frequency increases. Indeed, as we shall see later, this outcome — a decline in detectability with an increase in spatial frequency — is in fact mainly accounted for in terms of another variable, a minimum sampling density of the dots required to define the surface itself.

5. Quite unsurprisingly, the detectability of a form is closely related throughout the entire series of experiments to the signal (stimulus-form dot density)-to-noise (masking-dot density) ratio. The result of manipulating the number of dots in either the stimulus or the mask is to affect the signal-to-noise ratio and to thus strongly modify detection scores.

6. We did carry out several supplementary experiments using grid-like prototype stimuli rather than randomly dotted prototypes, although the results of these experiments are clearly confounded by the presence of monocularly detectable, dotted-straight-lines; the results are interesting in their own right. As expected, our observers did seem to use the available monocular information to detect densely dotted, grid-like stimulus-forms at a higher level than equally dense, randomly dotted surfaces. However, this advantage was quickly lost for less densely dotted grids and masking actually became more detrimental to the detection of these grids than in the case of the random-dot surfaces. This paradox of smaller, then larger, masking gives rise to a fan-shaped family of curves depicting the relationship between stimulus-form dot density and performance at various masking-dot densities, as opposed to a more parallel set of curves for random-dot-array stimulus-forms. Furthermore, the differential detectability measured for different degrees of distortion that had existed in some of the experiments using random-dot arrays disappears when regular grids are used as prototypes. Changing from a dichoptic to a monocular viewing condition only slightly affected the scores when grids were used as the prototype. The findings, as well as the increased sensitivity to masking-dots at lower stimulus-form dot densities, suggests that the stereoscopic information is either no longer available or is not being used by observers. Our speculation is that the latter explanation holds.

B. The Influence of Stimulus-Form

Now let's consider the results concerning stimulus-form in more detail. The

AD-A138 761 THE DETECTIÓN OF NONPLANAR SURFACES IN VISUAL SPACE(U) 2/3
MICHIGAN UNIV ANN ARBOR PERCEPTION LAB
W R UTTAL ET AL. 01 MAR 84 PERLAB-4 N00014-81-C-0266
UNCLASSIFIED F/G 6/16 NL

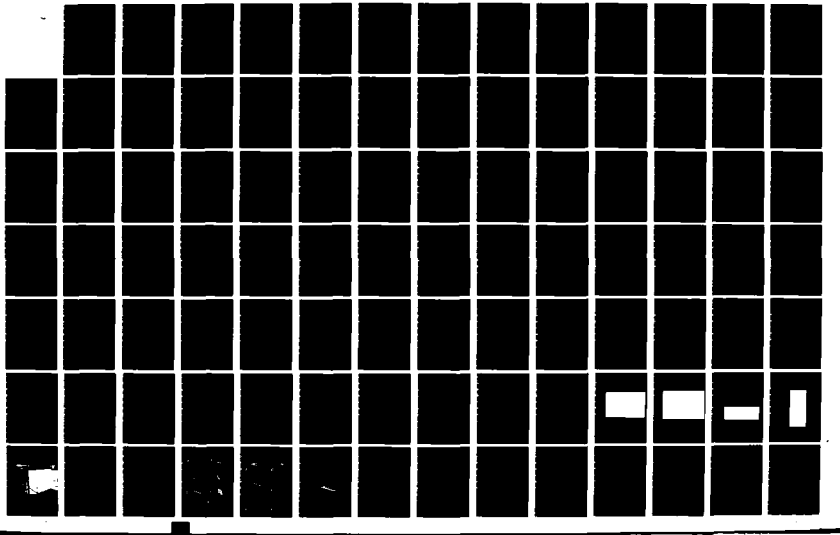

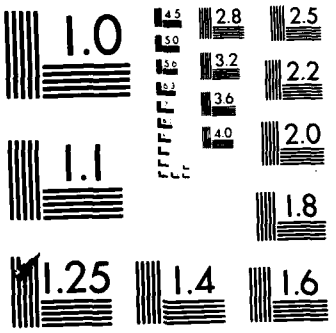

absence of form effects as the deformation progresses in all of the experiments that used stimulus-forms that had no more than one maximum or minimum is both especially surprising and deeply important with regard to the nature of stereoscopic form perception. The importance of this issue revolves around our interpretation of the nature of the perceived depth constructed from the dichoptic-disparity information. The question is: Is this depth experience, and the third dimension (z) that is constructed, similar to that of the other two dimensions (x and y)? Remember, the x and y dimensions do not require the kind of extensive computation to be encoded and perceived as does the z dimension. The x and y attributes of a stimulus are isomorphic in a dimensional sense to the retinotopic map, their initial projections into the brain, and even the perceived space, whereas depth must be created from extensive processing of the disparate images from the two eyes.

Experiments previously carried out in this laboratory (Uttal, 1983) suggested that all three dimensions are perceived and influenced in much the same way. But, one attribute of the present data now suggests otherwise. That attribute revolves around the fact that the greatly deformed nonplanar surfaces used as stimuli in this study have been "elastically" stretched into three-dimensional shapes by the polynominal and sinusoidal transformations in a way that greatly increases their perceived surface area. For example, the perceived area of a stretched hemisphere is much greater and its perceived stimulus-form dot density, therefore, much less than the corresponding features of a prototype plane. That is, 100 dots distributed across the surface of a plane produce a greater perceived density on that surface than the same number of dots distributed across a hemisphere whose surface area is much greater, at least in the perceived stereoscopic three-dimensional space. However, this reduction in perceived density seems not to influence detectability scores in many experiments in which it seemed a priori that

it should.

Results like this could be artifactual and might occur if there were a strong monocular (i.e., two-dimensional) cue that swamped out the influence of the perceived three-dimensional characteristics of the surface. However, Experiment 2 was definitive in demonstrating that if any such two-dimensional cue is available for randomly dotted stimulus-forms, it is a relatively minor perturbation and completely submerged by the masking-dots at the lowest masking-dot densities that were utilized. Indeed, the small degree of detectability that can be attributed to monocular cues has disappeared at masking-dot densities that are lower than those at which stereoscopic masking begins to become effective. Going from two eyes to one in this case is devastating to performance: Noise-dot densities that had allowed virtually perfect performance now prevent almost all detection.

It seems acceptable, therefore, to rule out monocular cues as a possible explanation of the negligible stimulus-form effects we have obtained with random-dot array stimulus-forms. The two-dimensional cues are not capable of explaining the absence of a strong global form effect in three dimensions since they are so quickly masked by relatively few dots. Rather, the relatively low level of influence exerted by the stimulus-form seems to be a true, if somewhat mysterious, property of the perceived three-dimensional perceptual space that is created by the dichoptic viewing procedure.

Incidentally, the monocular control experiment also contributes very strongly to another positive and practical conclusion concerning visual information processing. The stereoscopic procedure is exceedingly effective in greatly improving the detection of stimuli such as the ones being used here compared to a monocular viewing condition. Presumably, any other granular or quasi-dotted stimulus that might occur in a variety of applications would be similarly affected. As was seen when the regular and the Supplementary Experiments were compared,

this stereoscopic advantage holds mainly when random-dot array stimuli are being observed. The stereoscopic advantage is much less when grid stimuli are used. In fact, sparse grids seem to be even more susceptible to masking than are equivalent random array stimuli.

It seems likely that this stereoscopic improvement is accomplished because, in some way, the effective signal-to-noise ratio is reduced in the stereoscopic scene. That is, the effective density of the same number of masking-dots is less in perceived three-dimensional space than in perceived two-dimensional space. There is no question, however, that this outcome is paradoxical in light of the fact that stereoscopically stretching the stimulus-form (by manipulating disparities) does not reduce its effective density in the same way. It is not clear at this point how these seemingly contradictory and paradoxical results can be rationalized. It is also not entirely clear, although it does seem to be associated with cue selection by the observers, why sparse grid stimuli should be more affected by masking than random array stimuli.

It is only when the generating equations produce random-dot array stimulus-forms that are complex enough to display more than a single maximum or minimum that the effect of the nonplanar distortion begins to produce a modest, though statistically significant, difference in the detectability of the variously deformed (i.e., stretched from a plane to a nonplanar surface) versions of a single type of surface. The magnitude of the differential effect of nonplanar distortion increases with increases in the geometrical "complexity" of the signal as it has been somewhat artbitrarily defined as an aggregate of the number of dimensions of variation and number and order of the terms in the equation generating the surface. Specifically, the average F ratio (which is used here as a metavariable to represent the magnitude of the effect) for the one-dimensional cubic, the two-dimensional cubic, and the sinusoids -- the forms with more than a single maximum

and minimum and, thus, with statistically significant effects of form — are 5.27, 7.56, and 8.46, respectively, as shown in Table 36.[8] However, as we shall see, the high value for the sinusoids is at least partially artifactual, sampling density difficulties accounting for large portions of the effect.

In general, however, the effect of stereoscopic shape distortion does progressively increase after one crosses a threshold — that threshold being the presence of multiple maxima and minima. However, the number of maxima and minima is only one possible measure of the changes that occur as stimulus forms increase in their spatial frequency. Indeed, there are many such dimensions that could be candidates to be the critical one. The question now confronted is, What is the salient dimension of the stimulus that is determining this increase in the masking effect as the form becomes more complex — particularly as the number of maxima and minima increase.

A first suggestion, of course, is that the key variable is the number of maxima and minima itself. It is important to appreciate in this regard, however, that the decline in detectability is not directly associated with the limits of either optical resolution or with any difficulty in actually discerning the oscillations in high-frequency, stereoscopically produced depth sinusoids. The range of sinusoidal frequencies used in these experiments is lower than the threshold 3 cycles/degree for the kind of failure to discern sinusoidal oscillations in depth reported by Tyler (1973), for example. In Tyler's experiments, which used continuous (i.e., infinitely dense) stimuli, the decline in perceiving the sinusoidal undulation begans at about 1 cycle/deg and was essentially complete at about 4 cycles/deg. In the present experiments the decline in performance begins at about .37 cycles/degree (2.0 cycles/5.4 deg) and is essentially complete at about .93 cycles/degree.

Thus, the idea that the results we have obtained are assays of the limits of some kind of a depth modulation transfer function, with a relatively low high-

frequency cutoff, seems inadequate. Since the degradation in performance in the present experiments begins and ends at lower spatial frequencies than in Tyler's experiments, any constraint based on an inability to perceive depth in this situation is inadequate to explain the present results. In sum, the depth-sensitivity capabilities of the stereoscopic visual system seem not to be seriously challenged by the range of spatial frequencies that have been used in this study. We must look elsewhere for an explanation of the effects obtained here.

Another concomitantly varying nonplanar-surface attribute, closely related to but different from the simple numerosity of maxima and minima, that might be the salient characteristic is simply the perceived surface area. As the number of maxima and minima increases, the density of a constant number of dots decreases on that phenomenal surface if all other attributes are held constant. However, the possible role of this candidate attribute is mitigated by the results of other experiments in this study that serve as implicit checks of this hypothesis. Consider Experiment 6, for example, the one concerned with the detection of paraboloids of rotation. In that experiment a major change in the area of the perceived nonplanar surface (see Figure 9F and Figure 8D) occurs as the prototype plane is progressively transformed from a plane into the most extreme paraboloid. Even though the perceived three-dimensional density of the surface also declines substantially in this case, there is no corresponding decline in detectability comparable to that observed in the experiment using sinusoidal stimulus-forms. The effect of apparent density therefore, is, not obtained in an analogous situation in which it seems it should. Thus, apparent density seems an unlikely candidate to be the salient attribute accounting for the decline in performance.

Another plausible attribute of the sinusoidal nonplanar surfaces in particular deals directly with the relationship between the number of dots in the stimulus-form and the spatial frequencies per se. It is argued in this context that the dots

represent discrete samples of the sinusoidal surfaces and that, in some cases, the density of the dots may fall below the threshold necessary for their adequate definition. Shannon and Weaver's (1949) sampling theory suggests as a general rule of thumb (as well as in a more precise mathematical sense with which we need not be concerned here) that only if the sampling density (i.e., the spacing between samples) is greater than twice the highest constituent spatial frequency of a cyclic form is the necessary information available for that form to be completely reconstructed by some ideal computational engine.

Let's consider in light of the sampling theorem, the relationship between the spacing of the dots in our stimulus-forms and the spatial frequencies of the sinusoidal stimuli that were used in Experiments 10, 11, and 12. To begin, consider Figure 62, the one showing the results of Experiment 12 in which both the number of dots and the spatial frequency of a sinusoidal wave ocscillating in depth are covaried. This figure clearly shows that the variation in the number of dots in the stimulus-form — in other words, the number of samples across the stimulus-form surface — does produce a strong effect on detectability.

To pursue this argument, we must now compare two sets of numbers. The first set designates the spatial frequencies that were tested and their corresponding spatial periods. In these experiments, which used a 5.4 deg wide viewing space and stimuli with .5, 1.0, 1.5, 2.0, 3.0, and 5.0 cycles across that space, the equivalent spatial frequencies are .09, .19, .28, .37, .56, and .93 cycles/deg, respectively, and their periods are 11.1, 5.26, 3.57, 2.70, 1.79, and 1.08 deg, respectively. The separation between the dots in the stimulus-forms can be approximated by assuming that, on the average, the stimulus-form will consist of dots separated by:

$$\frac{5.4}{\sqrt{N}} \qquad (15)$$

where N is the number of dots in the 5.4 x 5.4 deg. In the case of 81, 64, 49, 36, and 25 dots, the average interdot spacing along the one dimension over which the sinusoidal nonplanar surface is varying will thus be equal to .60, .68, .77, .90, and 1.08 deg.

Given the constraint that the period or separation of the stimulus-form dots must be half the period (that is, twice the frequency) of the sampled sinusoidal surface for reconstruction to be possible, we see that this criterion is met for the four longest periods (11.1, 5.26, 3.57, and 2.70 deg) for all stimulus-form dot densities, but not for the shortest period (1.08 cycles/deg) at any of the five stimulus-form dot spacings utilized. Similarly, the second shortest period (1.79 degs) is not adequately sampled at either the 36- or 25-dot stimulus-form densities with their corresponding .90 and 1.08 deg average spacing.

In Figure 55 we see that at low masking-dot densities (50 and 100 dots) the performance begins to decline at a spatial frequency of .37 cycles/deg, a value equivalent to a period of 2.70 deg. Figure 61 shows that the decline in detectability as spatial frequency increases occurs at a slightly higher spatial frequency in the other relevant experiment — the break, in this case, appearing at .56 cycles/deg, a value equivalent to a period of 1.79 deg.

The conclusion to which we are propelled is that for at least some of the conditions of these experiments, the number of dots is theoretically insufficient to define the surface. The decline in detectability for some of the high-frequency, low-stimulus-form dot-density cases is not, therefore, due to the increase in either spatial frequency or the number of maxima and minima per se. In these extreme conditions of reduced-stimulus-form-dot-numerosity-detection failures are simply

due to the theoretical impossibility of even an ideal observer determining the nature of the surface constrained as it would be by the two samples-per-cycle criterion of the sampling theorem. For lower spatial frequencies, while not impossible, it is just more "difficult" to detect the surfaces because of the marginal sampling densities. What is happening here is that as the sparsely sampled sinusoidal stimulus-forms increase in frequency, the physical stimuli they represent are becoming increasingly random and similar to the mask. Thus, no psychophysical property is being measured; only a physical property of the stimulus. In fact, given these limits, observers do very well in detecting these undulating surfaces. The focal consideration here is that the measured limits on the detection of dotted nonplanar surfaces of high spatial frequency are not solely due to the number of maxima or minima, but to the difficulties in defining the stimulus-form. Even in the case of Experiment 11, in which the prototype plane consisted of 81 dots, some of the degradation in performance with increasing frequency must certainly be attributable to this sampling problem. The highest frequency is beyond the sampling theory criterion but, furthermore, the human observer is not an ideal reconstructor. Thus, Figures 55 and 56 depict a phenomenon that must in part be due to practical sampling difficulties if not theoretical ones.

From a purely phenomenological point of view, however, it is remarkable how strong an impression of a continuous nonplanar surface is obtained with relatively small numbers of dots under the viewing conditions of these stereoscopic displays. The perception of a continuous surface in space (typically "velvety" in texture and darker than its surrondings) is comparable in strength to the subjective contours reported in two-dimensional space by Kaniza (1974) and others. The subjective "palpability" of these stimulus-forms must be seen to be appreciated.

The general conclusion emerging from the overall trend of results of all of

the experiments in this study is that the influence of geometrical form in the three-dimensional dot-detection task is modest. It is insignificant for the simpler stimuli but does become statistically significant for more complex stimuli. However, a substantial effect of form progressively increasing with the number of maxima and minima (as regulated by the spatial frequency of a sinusoidal oscillation in depth) is illusory and is actually attributable to violations of the sampling theorem defined limits. Within those limits, the human observer functions surprisingly well. The fall-off in performance occurs at spatial frequencies only slightly less than the values that are constrained by the sampling theorem, as shown in Figures 55 and 61. The modest effect of stimulus-form occurring in the experiments reported here should be compared to the null effect reported by Barlow (1978) and the very small effect reported by Uttal (1983) for two-dimensional stimuli consisting of randomly arrayed dots. It must be remembered however, that the conclusions presented so far hold only for randomly-dotted forms and not for those generated from dotted or continuous outlines. If the stimulus-forms are constructed from regularly spaced dotted grids, as we saw in Experiments 14 through 17, then the results are quite different in several regards. First, even the relatively small yet significant stimulus-form effect with random-dot-array stimuli as seen in Figures 40 and 45 disappears completely with grid stimuli as seen in Figures 71 and 75. Second, the effect of the signal-to-noise ratio becomes much more complicated. As Figures 72, 76, and 80 indicate, the most dense grid (consisting of 81 dots arranged in a 9 x 9 matrix) is so powerful, compelling, and detectable that it becomes totally resistant to masking even when the highest masking-dot densities are used. Yet, paradoxically, the less-dense grid stimuli are much more easily affected by the mask than are the random-dot stimuli, a phenomenon clearly shown in these same figures. Both of these phenomena become explicable if the observer is not using the stereoscopic

information that is available to him.

That this is the case is supported by the results of Experiment 17. Figures 81 and 83 demonstrate that the observer responds to monocularly viewed stimuli in much the same way as to the stereoscopic stimuli in Experiment 14. Thus, it seems that the observer either ignores, or does not have available to him, the same information he used or had available to him in the stereoscopic experiments using randomly dotted surfaces. Given that both the stimulus-form and the masking-dot densities are the same in both kinds of experiments, those that use randomly-dotted surfaces and those that use grids, it seems plausible to reject the hypothesis that the information is not available to the observer and to attribute the performance decline instead to nonutilization of available cues.

This, then, leads to an interesting conclusion. It seems that the observer is attending to or utilizing only selected portions of the information available to him in the stereoscopic grid experiments. Is it possible that responses to the prepotent rectangular grids are being reinforced in a way that is inducing the observer to use only monocular cues in this experiment? If so, the observer is maladaptively perpetuating a less-than-optimum monocular strategy even when the stereoscopic information would be extremely useful (i.e., when the signal-to-noise levels are low and dedensification of the masking-dots in depth would be helpful). If this is actually what is happening, then this is an unusual example of a situation in which the observer is failing to adapt optimally to the visual needs of the task.

A most interesting aspect of this failure to optimize strategies and use all available cues is that it is possible to make such selections at all. Indeed, given that all observers report strong phenomenological depth for these grided stimulus-forms, their ability to reach back into previous states of encoding (i.e., the two-dimensional retinotopic map of the stimulus-form) as a basis for their decisions is quite remarkable. Obviously, two-dimensional information patterns for each eye

are also being transmitted to central analytical mechanisms as well as fused stereoscopic information. The extraordinary fact is that the observer has some kind of attentively controlled selectivity available to him to choose either the three-dimensional stereoscopic cues or the two-dimensional retinotopic ones. Such an ability represents a level of control that had not previously been considered to be a likely characteristic of this kind of processing. I, for one, had comfortably referred to these phenomena earlier as being "preattentive : automatic." This terminology may no longer be appropriate in the light of the ew results.

Another particularly surprising and disconcerting ou ne of this study is that the apparent three-dimensional surface area of the s. .ulus-form does not appear to be an important variable in determining detectability, even though distribution of masking-dots into depth by the stereoscopic procedure does affect performance. Given a constant number of dots, the apparent density of a nonplanar surface must progressively decline as its apparent surface increases, but the effect that would logically follow from this bit of perceptual geometry does not appear in the obtained psychophysical data. This is so in spite of the fact the real density (as determined by the number of dots in the mask or in the stimulus-form) exerts a powerful influence on detectability. On the other hand, the overwhelming superiority of the stereoscopic viewing situation over the monocular control when randomly dotted stimuli are used argues strongly for some kind of a phenomenological "dedensification" of the masking-dots or some other equivalent kind of an improvement in the effective signal-to-noise relationships, as dots are distributed more widely throughout the apparent three-dimensional space. At the present time, there seems to me to be no way to resolve this dilemma. Future research is necessary to unravel these seemingly inconsistent and paradoxical results.

Finally, let's look back at some of the original questions asked on page ___.

and suggest plausible answers to them in light of the results that have been obtained.

1. Dotted nonplanar surfaces formed from random-dot arrays vary in their detectability as a function of the kind of shape, but only to a modest and idiosyncratic degree.

2. Dotted nonplanar surfaces of a single kind formed from random-dot arrays vary in their detectability as a function of the deformation away from a plane only if two or more maxima and minima are present, but only to a modest degree. More substantial effects are largely attributable to sampling density limits, not to shape or to the number of maxima and minima per se.

3. Nonplanar surfaces formed from grids do not display any detectability changes as a function of the kind of shape or the magnitude of the distortion in these experiments. This result, however, may be artifactual and due to unusual observer strategies (i.e., ignoring available three-dimensional attributes of the stimulus) stimulated by the prepotency of dense grid patterns even when viewed monocularly.

In sum, hypotheses 1 and 2a on page ___ are more likely to be valid than 2b and 3. Specifically, three-dimensional randomly dotted surfaces do behave like two-dimensional planar surfaces. In this psychophysical context, a plane is not the analog of a line.

C. A Test of The Autocorrelation Model -- The Model Finally Fails.

In the past an autocorrelational model had been used with great success to predict the performance of the human observer in this dotted-stimulus-in-dotted-mask type of task when two-dimensional stimuli were used. The model, as described earlier in this monograph, is based upon a discrete approximation to a convolution-type integral (see Equation 1) in which a simulation of a stimulus-form is essentially compared (by a point-by-point cross-multiplication) with a set of shifted replicas of itself. For two-dimensional stimuli, the evaluation of the autocorrelation integral for all possible shifts produces a function $A(\Delta x,\Delta y)$ that forms a three-dimensional space. The dimensions of this space are the magnitude of the shifts in the x and y dimensions (Δx and Δy) and the value $A(\Delta x,\Delta y)$ at each of those shifts in the $\Delta x, \Delta y$ space. The visual appearance of such a space was shown earlier in Figure 3. The magnitude of each peak and their spatial interrelationships are presumed to reflect in a quantitative manner the nature of the original stimulus-form that had been transformed by the autocorrelation integral.

Although it seems likely that this spatial pattern is itself a coded message that should be possible for the nervous system to process directly, it is helpful for the theoretician observing such an autocorrelogram to measure it in a more quantitative way. In this study, we accomplished this by using the Figure of Merit (F_m) — the outcome of a further transformation in accord with the expression denoted in Equation 2. This artbitrary, ad hoc, and yet empirically validated (in two-dimensional space) expression operates on the relative heights of the various peaks in the autocorrelogram space, their distances from each other, and their number to generate a single F_m that had been hitherto highly successful in predicting the relative psychophysical detectability of a set of two-dimensional stimulus-forms sharing certain common properties such as dot numerosity and

average interdot spacing.

An interesting sidenote concerning the Figure of Merit is that while it had been considered to be merely an arbitrary convenience to be used in the theoretical analysis, a collaborative experiment carried out in recent months between this laboratory and that of Professor Ken Goryo of Chiba University in Japan has produced results that suggest that F_m may have much more of a biological reality than had been previously suspected. Goryo, his students Mari Oki, Eiji Kimura, and Yoshiro Okazaki, and I measured evoked-brain potentials to exact replicas of some of the two-dimensional stimuli used in the experiments on rectangles (Experiment 12 and Supplementary Experiments 1 and 2 reported in Uttal, 1983).

Preliminary results indicate that there is a very strong inverse correlation between the predicted Figures of Merit and the amplitude of a strong evoked potential occurring about 200 msec following the stimulus! The Figure of Merit, therefore, may reflect something more fundamental (than simply an arbitrary number) concerning the way in which the individual computations are synthesized into a global measure of detectability by the central nervous system. The results obtained were admittedly preliminary, but were strong enough to suggest that further work is necessary on this important psychobiological correlate of what had previously been considered to be only a mathematical artifice.

Whatever the biological significance of the Figure of Merit, it is obvious that the computational problem grows rapidly as dimensions are added to the stimulus-form. When a two-dimensional form is autocorrelated, the result is a three-dimensional space. However, when a three-dimensional stimulus-form is analyzed with the autocorrelation model, the resulting autocorrelogram is itself no longer three-dimensional, as is the one shown in Figure 3, but rather becomes (mathematically) four-dimensional. Such a space is, of course, not displayable in the static snapshot-like graphics of Figure 3. Rather, something comparable to a

motion picture would be required to display the four-dimensional nature of the autocorrelogram. Alternatively, these transforms need not be displayed at all, but can simply be presented as arrays of numbers to the Figure of Merit evaluation algorithm.

Another problem still exists, however. The computational requirements grow exponentially with the linear increase in the number of dimensions. Indeed, when we attempted to expand the two-dimensional autocorrelation procedure to its three-dimensional analog, the computation time went from a few minutes to many hours, depending on the complexity of the form and the number of dots in the simulated stimulus-form. Furthermore, the discrete points on the grid had to be limited to avoid even more catastrophic computing requirements. Even though we did use a 15 x 15 x 15 matrix in the three-dimensional cases to be described shortly, and a 15 x 15 matrix in the two-dimensional case, the two matrix densities are not equally useful. It is very difficult to get a good approximation to a curving, nonplanar surface in such a coarsely discretized space, and therefore the calculated Figures of Merit are probably less satisfactory approximations in the three-dimensional than in the two-dimensional case.

For these reasons it has not been possible to carry out full-scale calculations for as varied a sampling of the stimuli used in this study as in the previous work. However, a mini-simulation was carried out in which four different stimulus-forms were compared — a plane consisting of regularly spaced dots, a plane consisting of irregularly spaced dots, a cylinder consisting of regular spaced dots, and a cylinder consisting of irregularly spaced dots. Two of these four simulated stimuli, the ones consisting of irregularly spaced dots, corresponded to the prototype plane and the most deformed stimulus-form used in Experiment 3. The other two simulated stimuli consist of a regularly spaced, grid-like plane and the closest obtainable approximation to a grid-like cylinder. The grid-like cylinder is transformed in the

same way as the randomly dotted cylinder. When calculations of the Figure of Merit were made for these four stimuli, the values obtained were 222,572 and 73,085 for the random plane and the random cylinder, respectively. Similarly, Figures of Merit of 699,878 and 149,754 were obtained for the analogous regularly spaced grid like stimuli.

Obviously, these values do not approximate the psychophysical data obtained in this study. The large differences in detectability between the plane and cylinder predicted in both the random and grid cases do not appear in the response data. This can be verified by inspecting Figures 15 and 16 for the random-dot array stimulus-forms and Figure 86 for the grid-like stimulus-forms. Figures 86 and 87 are presented here without further documentation or analysis; it is hoped, that by now their meaning should be self-evident. Simply stated, they are the results of an experiment in which the prototype planes were regular grids of dots.

Nor for that matter, do the predicted differences between the irregular and regular patterns occur in the psychophysical response. The model not only predicts that either cylinder should be seen less well than either plane, but also that a grid-like cylinder should be seen better than one constructed from a random array of dots. This result obtains only in some of the conditions of the comparable experiments. Obviously, other factors are becoming more important in the stereoscopic, three-dimensional case than those few organizational factors incorporated into the autocorrelation model. It seems likely, therefore, that the autocorrelation model will not be useful in modelling the three-dimensional stimulus situation in spite of its great success with two-dimensional stimuli unless it is modified to include these additional factors. A major future activity of this project will be to develop an alternative theoretical model of the stereoscopic viewing condition.

D. The Influence of the Signal-to-Noise Ratio

The most cursory visual examination of the data presented so far makes it immediately clear that even though the influence of the stimulus-form on detectability is modest, the influence of the numbers of dots in the stimulus-form and in the mask can be quite large. It is of considerable interest, therefore, to consider the nature of the dot-density effects in greater detail to ascertain the nature of the relationship between the stimulus-form and masking-dot densities and their respective influences on detectability.

Before doing so, it must be reiterated that the raw numbers of dots in the stimulus-form are probably not totally accurate indicators of "signal" attributes as required by a formal signal-to-noise ratio type of analysis: The influence of several other informational factors is not included in these simple dot counts. In addition to simple numerosity, other characteristics of the distribution of the dots may also play a role that is ignored in the simple analysis presented here. These other attributes include the linearity (as demonstrated in our earlier studies to be a compelling cue) and other aspects of clustering and local geometry (as demonstrated, for example, in Julesz', (1975; 1978; 1981, distinguished studies of texture perception). A further attribute that is ignored when one simply counts dots, of course, is the global organization of the dots that has been imposed on the stimulus-form itself.

The fact that the form effects are generally modest and insignificant for all of the types of forms with less than two maxima or minima however, does permit us to approximate signal information content by a simple count of the number of dots. The mask, on the other hand, is probably quite accurately characterized simply by the number of constituent dots since it is designed to be a purely random process. This is true to a degree that is dependent upon the accuracy of the

random number generators used in our programs.

It is, of course, true that even a random-number generator will occasionally construct an array of masking-dots that has some local geometrical property that may influence its efficiency as a mask or make a stimulus-form particularly detectable. Since the masking-dot arrays are generated anew for each experimental trial, any such effects will be washed out by the large number of trials performed during each experiment in this study. The possibility that some of the stimulus-forms used in this study have peculiar local geometries that may make them especially detectable cannot be ignored, however.

In the following section, how good an approximation the use of the raw number of dots actually is will be evaluated by considering the signal-to-noise ratio effects. This will be done by examining in detail one set of data — that set dealing with the parabolic arches obtained in Experiment 4. To begin, it is useful to replot the data of that example in a form that more directly depicts the signal and noise dot density relationships.

One useful form in which the data may be replotted is as a psychometric function in which the percent-correct performance scores are plotted against the ratio of the stimulus-form (signal) and mask (noise) dot numerosities. Of the several possible measures that could have been used, I have chosen to represent the signal-to-noise ratio, S/N, by the following expression

$$S/N = 10 \ln S_n/N_n \qquad (16)$$

where S_n is the number of dots in the stimulus-form and N_n is the number of dots in the mask. This equation is a modification of the signal-to-noise ratio expression used by Green and Swets (1966) for a comparable two-alternative, forced-choice paradigm in which any one of a set of possible signals had to be detected. Other

definitions of the signal-to-noise ratio could be used without qualitatively distorting the outcome of this analysis.

To demonstrate this analysis the data for the effects of stimulus-form and masking-dot densities from Experiment 4, and shown in Figure 24 will be transformed in accord with Equation 15 and then replotted. This produces a new independent variable —the signal-to-noise ratio — that is plotted against the performance scores for each of the original points. This transformation produces Figure 88 in which the parametric family of curves have been collapsed into a single scatter-plot using a packaged set of statistical routines.

A visual inspection of these replotted data reinforces the general impression already obtained; namely, that the signal-to-noise ratio (even as roughly and arbitrarily as it is defined here) accounts for a substantial amount of the variance in this part of this experiment. The resulting scatter-plot has been subjected to a multiple regression correlation analysis using S/N and $(S/N)^2$ as predictor variables. This analysis yields a correlation with the surprisingly high coefficient (r) of .95. This indicates that .90 of the variance of these data is accounted for by a curvilinear function of the signal-to-noise ratio. While this is not indicative in any way of internal mechanisms, it is clear that a good fit between the curvilinear regression line and the data is obtained and that one need not look much further to account for the remaining variance. The insignificant magnitude of the form effect in this particular experiment also argues for the fact that detectability is predominantly a function of the signal-to-noise ratio as simply defined by Equation 15 and the number of dots in the stimulus-form and mask, respectively.

Inspection of the sample psychometric function shown in Figure 88 yields some further insights about the form detection capability of human observers. At the upper end of the curve (as indicated by the arrow labeled A), it appears that performance asymptotes close to a S/N of -3.88, a value that corresponds to

approximately .7 stimulus-form dots for each dot of the mask. Therefore, the absolute detectability of stimulus-forms may be considered to be quite good even though the differential detectability as a function of form varies so slightly. In sum, a dotted form may be detected in dotted masks with nearly 100 percent probability when it is only a little more than two thirds as dense as the masking-dots.

At the other end of the graph (as indicated by the arrow labeled B), performance declines but does not reach the theoretical minimum at which it must be constrained in the limiting case when masking-dot densities are very high. Rather, there is still some residual detectability present even when S/N is -23, a value corresponding to roughly ten times as many masking-dots as stimulus-form dots. Since the scores at this point have not yet approached the 50 percent level that they ultimately must, it is clear that there is considerable residual detection ability at even more severe signal-to-noise ratios.

Finally, a brief comment is appropriate concerning the relationship between the real observer's performance and that of a putative ideal observer. It would be quite delightful if it were possible to develop a theoretical model of what criteria could be used to specify optimum detection performance. However, the complexity of the stimulus stituation faced here is much greater than that of most comparable detection tasks in which signal-detection theory has been successfully applied. Even armed with the heurstic suggestions, if not specific predictive successes, from the autocorrelation theory, it is not obvious (at least to this commentator) how such a theory might be developed and how the ideal observer might be defined. It is not possible, therefore, to draw the same kind of conclusions that Barlow and his co-workers (Barlow, 1978; Barlow and Reeves, 1979; Van Meeteren and Barlow, 1981; Burgess, Wagner, Jennings, and Barlow, 1981; Burgess and Barlow, 1983) drew concerning the exact efficiency exhibited by

the real observer relative to the predicted performance of an ideal observer. It is of no small interest to note, however, that they repeatedly found evidence of a 50 percent efficiency level in their studies in two dimensions.)

For these reasons, we are limited to the mainly qualitative judgment that, given the intrinsic difficulty of this signal-in-noise type of task, the human observer does "remarkably" well in extracting the hidden stimulus-form from the random-dots of the mask. There is some suggestion in these data that the observer actually approaches the limits set by the sampling theorem and the signal-to-noise relationships. For the moment, however, this intuition remains unquantified, no artificial system capable of performing this task yet being at hand, nor any ideal observer yet described.

E. Conclusions

1. Different stimulus types are detected with varying degrees of ease in the dotted-surface-in-dotted-mask type of task. A parabolic arch is detected slightly better than the average, and a double cubic and hyperbolic paraboloid are detected slightly less well than the average. However, these results are admittedly idiosyncratic and are qualified by our acknowledgment of a possible, though unidentified, artifact.

2. Distributing the dots of the mask throughout the perceived space by means of disparity-controlled stereopsis has the effect of dedensifying the mask and increasing performance when the stimulus-forms are generated from random-dot arrays but not when they are generated from regular grids.

3. The degree of deformation of simple types of polynominal-generated surfaces, however, has little effect on detectability. Simple types are those in which the surfaces have less than two maxima or minima. This null result obtains in spite of the fact that the apparent surface may have a greatly enlarged area and thus lower stimulus-form dot density.

4. The degree of deformation from a plane to a nonplanar stimulus surface, however, does exert a measurable, though modest, influence on detectability when more than a single maximum or minimum is present on the nonplanar surface.

5. As the number of maxima and minima increases — for example, as regulated by the spatial frequency of a sinusoidal surface undulating in depth — detectability decreases further. However, close examination of such stimulus-forms indicates

that a major portion of the effect of this parameter of form can be attributed to inadequate information being available to define the shape. At lower stimulus-form dot densities, the sampling density is insufficient for even an ideal observer to reconstruct the form. The human observer does only slightly less well than the limits imposed by the sampling theorem — a remarkable outcome in itself.

6. The signal-to-noise ratio is a strong determinant of the detectability of a form. Either increasing the stimulus-form dot density or decreasing the masking-dot density increases the detectability of the form. In sample experiments in which the effect of form is negligible over 90 percent of the variance in performance scores is accounted for by the signal-to-noise ratio alone.

7. It seems possible for an observer to attend selectively to different attributes of the stimulus. In experiments in which regular, grid-like dotted arrays are used as the planar prototypes, the monocular cues are so strong that observers seem to adopt a mode of viewing in which they ignore information available to them in the stereoscopic display even when it is necessary to perform the assigned task. At high stimulus-form dot densities, the grids are seen monocularly as well as they are binocularly in all levels of masking. At low stimulus-form dot densities, however, observers become unusually suspectible to masking in a way that suggests their strategy has actually degenerated to a monocular, two-dimensional mode from a dichoptic, stereoscopic one. It is especially noteworthy that the observers seem to be using the monocular, two-dimensional information even while reporting the subjective appearance of the three-dimensional shape of the grided, nonplanar surface. Thus, the suggestion of attentive or active control over what had previously been thought to be an automatic or passive process is raised.

8. In general, even though the effects of form may be small or insignificant, performance scores do tend to decrease as stimulus-forms deviate further from a plane.

9. There are some paradoxical or puzzling results in these experiments that cannot be explained at the present time:

a. Dedensifying the dots of a random-dot array stimulus-form by stretching it into three-dimensional space does not reduce the form's detectability. However, the stereoscopic procedure does strongly reduce the effect of a given number of masking-dots compared to monocular viewing. These two, seeming, contradictory findings remain among the most distressing and inconsistent outcomes of this study.

b. The size and mix of the stimulus set often influences the detectability of individual members of the set.

c. The autocorrelation model, which had been so successful with two-dimensional stimuli, fails to predict the outcome when three-dimensional stimuli are tested.

d. Grid stimulus-forms have no sensitivity to nonplanar shape comparable to that exhibited by forms generated from random-dot arrays. Yet, the grid stimulus-forms are both less and more susceptible to masking depending upon the number of stimulus dots present. In this case, stereoscopic dedensification seems to offer no advantage at high densities and to even be detrimental at low densities.

e. Obviously, there are multiple ways in which the various attributes of these dotted stimuli interact. Some of them remain obscure and are not yet well understood.

ADDENDUM

From a theoretical point of view, the most interesting implication of the surprising and counterintuitive outcome that grid-like stimuli are more strongly influenced by masking dots than are the random array stimuli is that a random sampling procedure is used more effectively by the visual system than is a regular or systematic sampling procedure to reconstruct the sampled surface. While initially startling and unexpected, this result is not totally unprecedented in the literature of sampling theory. Madow and Madow (1944) and Madow (1946) have studied this problem and have ascertained that there do indeed exist certain conditions in which random sampling procedures provide better estimates of the properties of a population than does systematic sampling.

Similar results have been obtained by Quenouille (1949) and Das (1950) who have both described statistical tests that show that random or unaligned samples are often more precise means of determining the characteristics of a surface than regularly placed grids. Even more relevant is a report by Milne (1959) in which it was reported that for those situations in which regular grid sampling definitely worked best, the "autocorrelation effects are weak". Weak autocorrelation means that there is no tendency for nearby samples to be related, a situation that assuredly does not obtain with the geometric surfaces used as stimulus-forms in this study. Mathematically, if not perceptually, nearby points on these surfaces are more highly correlated than distant ones. Thus, Milne's results are also consistent with both the other statistical studies and the present psychophysical results.

It seems in general, therefore, that if the points on a surface are themselves unrelated, then a systematic sample is more precise. If, on the other hand, nearby

points are related (for example, by being more likely to be at the same depth than distant points are likely to be) then the random sample is more precise. This statistical subtlety is reflected in the psychophysical performance of our observers. It is quite probably also associated with a reduced tendency to create pseudoforms, a process better known as aliasing.

Thus, the obtained superiority of random arrays over grid arrays in these experiments make sense from a statistical sampling theory point of view. This explanation rings true at least for the lower density stimuli. At higher densities, the grid stimuli are very resistant to masking for another reason — the monocular advantage provided by the rule of linear periodicity mentioned many pages ago. The reason that the loss of stereoscopic information is so devastating to random-dot stimuli and so much less significant with the grid stimuli may also be related to this interaction between the monocular cue of linear periodicity and the loss of the advantage enjoyed by randomly sampled stimuli as stereoscopic information is lost. Nevertheless, there are still many mysteries concerning these data. Statistical considerations like these only begin to shed some light on a few of the more counterintuitive outcomes of this study.

Though it is still too early to provide a complete theoretical analysis, there is some useful advice emerging from these data, both paradoxical and consistant, that may be of some utility in some of those practical applications I listed at the beginning of this book. First, if it is possible to extrude an image into three dimensions by stereoscopic viewing, a definite advantage accrues in signal-in-noise detection tasks of this genre. This advantage apparently results from the effective dedensification of the visual masking-dots. The surface to be detected, however, seems not to be affected as greatly by the dedensification of the sampled granularities by means of which it is defined. Nevertheless, the net outcome is a definite advantage of 3-dimensional over 2-dimensional viewing condition,

particularly with randomly sampled stimulus-forms.

A second practical outcome of this study is that there is not likely to be any shape that is detectable at a level that is substantialy greater than any other in this type of dot masking situation; shape effects obtained in this study were modest in amplitude. There is, therefore, no need or advantage to be gained by any attempt to organize stimuli into planes or any other particular surface in an effort to enhance the detectability of a region, surface, and by extrapolation, a solid. Any surface is seen virtually as well as any other.

Third, a serious question has been raised by these results concerning the type of sampling strategy that should be pursued to define a surface. For the reasons that I have already mentioned, it turns out that randomly sampled, continuous surfaces are detected more easily (i.e., are less influenced by visual masks) than are systematically or regularly sampled surfaces if the densities are medium or low. The practical implication of this finding is obvious. In the human observer, signal-in-noise, continuous surface, detection task of the genre being studied here or its analogs in the real world, it is preferable to sample a putative surface at random rather than with regular, systematically distributed dots.

Addendum To References

1. Madow, W.G. and Madow, L.H. On the theory of systematic sampling. Annals of Mathematical Statistics (1944), 15, 1-24.

2. Madow, L.H. Systematic sampling and its relation to other sampling designs. Journal of the American Statistical Association (1946), 41, 204-217.

3. Quenouille, M.H. Problems in plane sampling. Annals of mathematical statistics (1949), 20, 355-375.

4. Das, A.C. Two-dimensional systematic sampling and the associated stratified and random sampling. Sankhya, (1950), 10, 95-108.

5. Milne, A. The centric systematic area sample treated as a random sample. Biometrics, 15, 270-297.

Paradoxes and problems of this genre are the grist of future research efforts in this laboratory. There are many unknowns and uncertainties still existing in this rich and complex stimulus situation.

FOOTNOTES

[1]I qualify this sentence by introducing the word "primarily" since, in some of the previous work (Uttal, 1983), even though some stimulus-forms were presented in three-dimensional masking spaces the forms themselves were confined to a plane and thus were essentially two-dimensional. In the present series of studies, I deal with stimulus shapes that are actually nonplanar and thus have their own three-dimensional properties, in addition to those of the cubical volume in which they are presented.

[2]To achieve this highspeed conversion, however, I had to modify the delivered system by removing capacitors C10, C13, C16, and C19 from the four digital-to-analog-converter output stages. These capacitors are identified on the circuit diagrams provided by the manufacturer, California Data Corporation of Newburg Park, California. With the capacitors in place, the rise time of the system was seriously degraded.

[3]Luminosity, however, does not play an important role in determining the level of detectability. Performance is much more strongly related to the signal (stimulus-form dot numerosity)-to-noise (masking-dot numerosity) ratio and to the spatio-temporal form of the stimulus dots than to the physical properties of the dots.

[4]I have elsewhere (Uttal, 1983, p. 9) discussed the great difficulty that generally exists in any attempt to quantify form. The experiments reported here are an exception to that generality in that the stimuli are in fact systematically represented by formal (polynominal, sinusoidal, and topological) expressions.

[5]The exact number of masking-dots that are used in the experiments varies for reasons that are not entirely rational or logical. Some groups of observers simply performed better than others and required more masking-dots to comparably degrade their performance. Furthermore, as the series of experiments reported here were sequentially executed (not necessarily in the order presented here), a good deal was learned about the masking effects of these random-dots. Various step sizes and various dot numerosities were chosen in accord with this developing knowledge and with the varying abilities of groups of observers. In some cases this becomes an inconvenience in that identical masking levels are not available for comparison, but in no case do we believe it obscures or distorts the general trend of the results. This potential difficulty is even further ameliorated by the fact that interexperiment absolute levels are not compared in this study.

[6]Although it is somewhat against current tradition, I have chosen to present a tabular representation of the ANOVA because of the way these values will be used in subsequent analyses. The F ratios emerging from these analyses will be used as a kind of metadependent variable to compare the outcomes of the various experiments.

[7]I indicate that the signal-to-noise level is arbitrary because the number of dots alone, as is well-established from earlier research, does not entirely define the detectability of the stimulus-form. Detectability is also a function of the form itself. Simple numerosity ratios however, are, useful in a less precise sense and also are known to influence detectability. They are, therefore, used here merely as a general approximation to the relationship between the signal (the stimulus-form) and the noise (the masking-dots), not as an exact measure. Nevertheless, we will see later that they do a fair job of accounting for the variance in detectability

scores.

[8]My use of the average F ratio as a metadependent variable in this case may displease some of my more statistically purist colleagues. But, to the degree that the F ratio does represent the degree of significance of variations in the dependent variables, it seems appropriate for use as a measure of the strength of the effects obtained in this study. Because of interexperimental differences due to individual observer differences and stimulus sampling, no direct comparison between the absolute values of the various experiments would be meaningful. Since this measure of "effect" -- the F ratio -- is largely independent of the absolute magnitudes of the scores in these experiments, it is a convenient means of comparing the strength of the effect with a single numerical Figure of Merit.

REFERENCES

Appelle, S. Perception and discrimination as a function of stimulus orientation: The "oblique effect" in man and animals. Psychological Bulletin, 1972, 78, 266-278.

Barlow, H. B. The efficiency of detecting changes of density in random dot patterns. Vision Research, 1978, 18, 637-650.

Barlow, H. B. & Reeves, B. C. The versatility and absolute efficiency of detecting mirror symmetry in random dot displays, Vision Research, 1979, 19, 783-793.

Burgess, A. & Barlow, H. B. The precision of numerosity discrimination in arrays of random dots, Vision Research, 1983, 23, 811-820.

Burgess, A. E., Wagner, R. F., Jennings, R. J., & Barlow, H. B. Efficiency of human visual signal discrimination. Science, Oct. 2, 1981, 214, 93-94.

Caelli, T. On discriminating visual textures and images. Perception & Psychophysics, 1982, 31, 149-159.

Chen, L. Topological structure in visual perception. Science, Nov. 12, 1982, 218, 699-700.

Chen, L. What are the units of figure perceptual representation? Studies in the

Cognitive Sciences. University of California, Irvine, February 1983.

Dodwell, P. C. The Lie transformation group model of visual perception. Perception & Psychophysics, 1983, 34, 1-16.

Falzett, M. & Lappin, J. S. Detection of visual forms in space and time, Vision Research, 1983, 23, 181-189.

Foster, D. H. A description of discrete internal representation schemes for visual pattern discrimination. Biological Cybernetics, 1980(a), 38, 151-157.

Foster, D. H. A spatial perturbation technique for the investigation of discrete internal representation of visual patterns. Biological Cybernetics, 1980(b), 38, 159-169.

Foster, D. H. & Mason, R. J. Transformation and relational-structure schemes for visual pattern recognition. Biological Cybernetics, 1979, 32, 85-93.

Foster, D. H. & Mason, R. J. Irrelevance of local position information in visual adaptation to random arrays of small geometric elements. Perception, 1980, 9, 217-221.

French, R. S. Pattern recognition in the presence of visual noise. Journal of Experimental Psychology, 1954, 47, 27-31.

Green, D. M. & Swets, J. A. Signal Detection Theory and Psychophysics. New York, London, Sydney: John Wiley & Sons, Inc., 1966.

Helson, H. H. & Fehrer, E. The role of form in perception. American Journal of Psychology, 1932, 44, 79-102.

Hilbert, D. & Cohn-Vossen, S. Geometry and the Imagination. New York: Chelsea Publishing Company, 1952.

Hoffman, W. C. The Lie algebra of visual perception. Journal of Mathematical Psychology, 1966, 3, 65-98.

Hoffman, W. C. The Lie transformation group approach to visual neurophysiology. In Leeuwenberg, E. L. J. & Buffart, H. F. J. M. (Eds.), Formal theories of visual perception, Chichester, England: John Wiley & Sons, 1978.

Hoffman, W. C. Subjective geometry and geometric psychology. Mathematical Modelling, 1980, 1, 349-367.

Hughes, H. C. Search for the neural mechanisms essential to basic figural synthesis in the cat. In Ingle, D. J., Goodale, M. A., & Mansfield, R. J. W. (Eds.), Analysis of Visual Behavior. London, England: The MIT Press, Cambridge, Mass., 1982, 771-800.

Julesz, B. Binocular depth perception of computer generated patterns. Bell System Technical Journal, 1960, 39, 1125-1162.

Julesz, B. Foundations of cyclopean perception. Chicago: The University of Chicago Press, 1971.

Julesz, B. Experiments in the visual perception of texture. Scientific American, 1975, 232, 34-43.

Julesz, B. Perceptual limits of texture discrimination and their implications to figure-ground separation. In Leeuwenberg, E. L. J. & Buffart, H. F. J. M. (Eds.), Formal theories of visual perception. New York: Wiley, 1978.

Julesz, B. Textons, the elements of texture perceptions, and their interactions. Review Articles, March 12, 1981, 290, 91-97.

Kaniza, G. Contours without gradients or cognitive contours. Italian Journal of Psychology, 1974, 1, 93-112.

Krumhansl, C. L. Concerning the applicability of geometric models to similarity data: The interrelationship between similarity and spatial density. Psychological Review, 1978, 85, 445-463.

Monahan, J. S. & Lockhead, G. R. Identification of integral stimuli. Journal of Experimental Psychology: General, 1977, 106, 94-110.

Ohshima, T. Effects of Configurational Factors on Visual Pattern Discrimination. Unpublished Report. Department of Psychology, University of Tokyo, 1983.

Rogers, B. J. & Graham, M. E. Anisotropies in the perception of three-dimensional surfaces. Science, Sept. 30, 1983, 221, 1409-1412.

Scanlan, L. A. & Roscoe, S. N. Time-compressed displays for target detection. In

Roscoe, S. N. (Ed.), Aviation Psychology, 1980, The Iowa State University Press. 108-124.

Shannon, C. E. & Weaver, W. The Mathematical Theory of Communication. Urbana, Ill: University of Illinois Press, 1949.

Sutherland, N. S. Comments on the session. In Wathen-Dunn, W. (Ed.), Models for the perception of speech and visual form. Cambridge: MIT Press, 1967.

Tversky, A. Features of similarity. Psychological Review, 1977, 84, 327-352.

Tyler, C. W. Stereoscopic vision: Cortical limitations and a disparity scaling effect. Science, 1973, 181, 276-278.

Uttal, W. R. Masking of alphabetic character recognition by dynamic visual noise (DVN). Perception & Psychophysics, 1969, 6, 121-128.

Uttal, W. R. The character in the hole experiment: Interaction of forward and backward masking of alphabetic character recognition by dynamic visual noise (DVN). Perception & Psychophysics, 1969, 6, 177-181.

Uttal, W. R. Masking of alphabetic character recognition by ultrahigh-density dynamic visual noise. Perception & Psychophysics, 1970, 7, 19-22.

Uttal, W. R. Violations of visual simultaneity. Perception & Psychophysics, 1970, 7, 133-136.

Uttal, W. R. On the physiological basis of masking with dotted visual noise. Perception & Psychophysics, 1970, 7, 321-327.

Uttal, W. R. A masking approach to the problem of form perception. Perception & Psychophysics, 1971, 9, 296-298.

Uttal, W. R. The effect of deviations from linearity on the detection of dotted line patterns. Vision Research, 1973, 13, 2155-2163.

Uttal, W. R. The effect of interval and number on masking with dot bursts. Perception & Psychophysics, 1971, 9, 469-473.

Uttal, W. R. An Autocorrelation Theory of Form Detection. Hillsdale, NJ: Lawrence Erlbaum Associates, Publishers, 1975.

Uttal, W. R. Visual spatial interactions between dotted line segments. Vision Research, 1976, 16, 581-586.

Uttal, W. R. Complexity effects in form detection. Vision Research, 1977, 17, 359-365.

Uttal, W. R. A Taxonomy of Visual Process. Hillsdale, NJ: Lawrence Erlbaum Associates, Publishers, 1981.

Uttal, W. R. Visual Form Detection in 3-Dimensional Space. Hillsdale, NJ: Lawrence Erlbaum Associates, Publishers, 1983.

Uttal, W. R., Bunnel, L. M., & Corwin, S. On the detectability of straight lines in visual noise: An extension of French's paradigm into the millisecond domain. Perception & Psychophysics, 1970, 8, 385-388.

Uttal, W. R. & Hieronymous, R. Spatio-temporal effects in visual gap detection. Perception & Psychophysics, 1970, 8, 321-325.

van Meeteren, A. & Barlow, H. B. The statistical efficiency for detecting sinusoidal modulation of average dot density in random figures. Vision Research, 1981, 21, 765-777.

van Oeffelen, M. P. & Vos, P. G. An algorithm for pattern description on the level of relative proximity. Pattern Recognition, Jan. 7, 1983, 16, 341-348.

Yodogawa, E. Symmetropy, an entropy-like measure of visual symmetry. Perception & Psychophysics, 1982, 32, 230-240.

Young, M. J. Detection of dotted forms in a structured visual noise environment. Unpublished master's thesis distributed as: Perlab Report No. 3, Institute for Social Research, University of Michigan, Ann Arbor, March, 1984.

Zusne, L. Visual Perception of Form. New York and London: Academic Press, 1970.

Zusne, L. Form perception bibliography 1968-1973. JSAS Catalog of Selected Documents in Psychology, 1975, 5, 272. (Ms. No. 998).

Zusne, L. Form perception bibliography 1974-1978. JSAS Catalog of Selected Documents in Psychology, 1981, 11, 48-49, (Ms. No. 2286).

TABLE CAPTIONS

Table 1. The generating equations and coefficients for the seven stimulus forms used in Experiments 1 and 2.

Table 2. The generating equation and the coefficients for the stimulus set used in Experiment 3.

Table 3. The results of the ANOVA for the surface-shape dimension in Experiment 3.

Table 4. The results of the ANOVA for the number-of-surface-dots dimension in Experiment 3.

Table 5. The generating equation and the coefficients for the stimulus set used in Experiment 4.

Table 6. The results of the ANOVA for the surface-shape dimension in Experiment 4.

Table 7. The results of the ANOVA for the number-of-surface-dots dimension in Experiment 4.

Table 8. The generating equation and the coefficients for the stimulus set used in Experiment 5.

Table 9. The results of the ANOVA for the surface-shape dimension in Experiment 5.

Table 10. The results of the ANOVA for the number-of-surface-dots dimension in Experiment 5.

Table 11. The generating equation and the coefficients for the stimulus set used in Experiment 6.

Table 12. The results of the ANOVA for the surface-shape dimension in Experiment 6.

FIGURE CAPTIONS

Figure 1. A sample stimulus-form constructed from dotted outlines.

Figure 2. A sample stimulus-form constructed from an array of randomly positioned dots.

Figure 3. A sample two-dimensional autocorrelation analysis. (a) The simulated stimulus. the three-dimensional autocorrelation space, and the figure of merit for a noise free straight line. (b) The simulated stimulus, the three-dimensional autocorrelation space, and the figure of merit for a straight line embedded in random dotted visual noise.

Figure 4. Four samples of a stereoscopic, nonplanar stimulus-form hidden in four densities of masking dots (1, 25, 50, and 75, respectively). L indicates the left-eye image and R the right-eye image. If these four stereograms are viewed dichotpically a three dimensional dotted parabolic arch similar in shape to the one shown in Figure 10 will appear.

Figure 5. A photograph of the observer's viewing station in this study.

Figure 6. A diagram indicating the timing relations in each trial in this study.

Figure 7. A diagram showing the interconnnections between the analog components of the hybrid computer system used to control the proceedure and display the styimulus-forms in this study.

Figure 8. Projective drawings showing the several different kinds of poloynomial generated shapes used in this study. In the actual stimulus-form neither the outlines of the cube nor the network of lines in these drawings were actually present. The limits of the cubes and the surfaces were only suggested by the arrangement of arrays of dots. A. Cylinder. B. Parabolic arch. C. Hemisphere. D. Paraboloid of rotation. E. Cubic in one dimension. F. Cubic

in two dimensions. G. Hyperbolic paraboloid -- a saddle.

Figure 9. A set of projective drawings showing the progresive stages in the deformation of a plane into parabolic arch. Once again, it must be remembered that neither the outline of the cube nor the network on the surface is actually viewed by the observer — they are only suggested by the arrangement of an array of dots.

Figure 10. A projective drawing of a sample parabolic arch showing the usual line of sight in this study. Most stimulus-forms were concave towards the subject. Again, the network shown here is only for illustrative purposes and is not visible to the observer.

Figure 11. The results of Experiment 1 analyzed as a function of the surface shape. The family of curves is parametric as a function of the masking-dot density. In this case the tics on the horizontal axis refer to the seven different stimulus-forms used. Specifically, 1 = Cylinder; 2 = Parabolic arch; 3 = Hemisphere; 4 = Paraboloid of rotation; 5 = Cubic in the x dimension; 6 = Cubic in both the x and y dimensions; 7 = Hyperbolic Paraboloid.

Figure 12. The data from Figure 11 pooled to show the overall trend at all masking-dot densities. The numbers on the horizontal axis have the same meaning as in Figure 11.

Figure 13. The results of Experiment 2 analyzed as a function of the surface shape. The family of curves are parametric as a function of the masking-dot density. The numbers on the horizontal axis have the same meaning as in Figure 11.

Figure 14. Diagram showing the cross-sectional shapes of family of cylinders used in Experiment 3.

Figure 15. The results of Experiment 3 analyzed as a function of the surface shape. The family of curves is parametric as a function of the masking-dot density. In this case the tics on the horizontal axis refer to the degree of distortion from a plane to the cylinder with the smallest diameter as shown in Figure 14.

Figure 16. The data from Figure 15 pooled to show the overall trend at all masking-dot densities.

Figure 17. The results of Experiment 3 analyzed as a function of the number of surface dots in the stimulus form. The family of curves is parametric as a function of masking-dot density.

Figure 18. The data from Figure 17 pooled to show the overall trend at all masking-dot densities.

Figure 19. The results of Experiment 3 analyzed as a function of the surface shape, but only for the lowest stimulus-form dot density. The family of curves is parametric as a function of the masking-dot density.

Figure 20. Diagram showing the cross-sectional shapes of family of parabolic arches used in Experiment 4.

Figure 21. The results of Experiment 4 analyzed as a function of the surface shape. The family of curves is parametric as a function of the masking-dot density. In this case the tics on the horizontal axis refer to the degree of distortion from a plane to the most extreme parabolic arch as shown in Figure 20.

Figure 22. The data from Figure 21 pooled to show the overall trend at all masking-dot densities.

Figure 23. The results of Experiment 4 analyzed as a function of the surface shape, but only for the lowest stimulus-form dot density. The family of curves is parametric as a function of the masking-dot density.

Figure 24. The results of Experiment 4 analyzed as a function of the number of surface dots in the stimulus form. The family of curves is parametric as a function of masking-dot density.

Figure 25. The data from Figure 24 pooled to show the overall trend at all masking-dot densities.

Figure 26. Diagram showing the cross-sectional shapes of family of parabolic arches used in Experiment 5.

Figure 27. The results of Experiment 5 analyzed as a function of the surface shape. The family of curves is parametric as a function of the masking-dot density. In this case the tics on the horizontal axis refer to the degree of distortion from a plane to the hemisphere with the smallest diameter as shown in Figure 26.

Figure 28. The data from Figure 28 pooled to show the overall trend at all masking-dot densities.

Figure 29. The results of Experiment 5 analyzed as a function of the surface shape, but only for the lowest stimulus-form dot density. The family of curves is parametric as a function of the masking-dot density.

Figure 30. The results of Experiment 5 analyzed as a function of the number of surface dots in the stimulus form. The family of curves is parametric as a function of masking-dot density.

Figure 31. The data from Figure 30 pooled to show the overall trend at all masking-dot densities.

Figure 32. Diagram showing the cross-sectional shapes of family of paraboloids of rotation used in Experiment 6.

Figure 33. The results of Experiment 6 analyzed as a function of the surface shape. The family of curves is parametric as a function of the

masking-dot density. In this case the tics on the horizontal axis refer to the degree of distortion from a plane to the to the most extreme paraboloid of rotation as shown in Figure 32.

Figure 34. The data from Figure 33 pooled to show the overall trend at all masking-dot densities.

Figure 35. The results of Experiment 6 analyzed as a function of the surface shape, but only for the lowest stimulus-form dot density. The family of curves is parametric as a function of the masking-dot density.

Figure 36. The results of Experiment 6 analyzed as a function of the number of surface dots in the stimulus form. The family of curves is parametric as a function of masking-dot density.

Figure 37. The data from Figure 36 pooled to show the overall trend at all masking-dot densities.

Figure 38. Diagram showing the cross-sectional shapes of family of cubics in one dimension used in Experiment 7.

Figure 39. The results of Experiment 7 analyzed as a function of the surface shape. The family of curves is parametric as a function of the masking-dot density. In this case the tics on the horizontal axis refer to the degree of distortion from a plane to the cubic with the most extreme distortion as shown in in Figure 38.

Figure 40. The data from Figure 39 pooled to show the overall trend at all masking-dot densities.

Figure 41. The results of Experiment 7 analyzed as a function of the number of surface dots in the stimulus form. The family of curves is parametric as a function of masking-dot density.

Figure 42. The data from Figure 41 pooled to show the overall trend at all masking-dot densities.

Figure 43. Diagram showing some of the cross-sectional shapes of the family of cubics in two dimensions used in Experiment 8. This is only a sample of the many different cross-sections that might be cut in this complex form.

Figure 44. The results of Experiment 8 analyzed as a function of the surface shape. The family of curves is parametric as a function of the masking-dot density. In this case the tics on the horizontal axis refer to the degree of distortion from a plane to the cubic in two dimensions with the most extreme distortion as shown in in Figure 43.

Figure 45. The data from Figure 44 pooled to show the overall trend at all masking-dot densities.

Figure 46. The results of Experiment 8 analyzed as a function of the number of surface dots in the stimulus form. The family of curves is parametric as a function of masking-dot density.

Figure 47. The data from Figure 46 pooled to show the overall trend at all masking-dot densities.

Figure 48. Diagram showing some of the cross-sectional shapes of the family of hyperbolic paraboloids (saddles) used in Experiment 9. This is only a sample of the many different cross-sections that might be cut in this complex form.

Figure 49. The results of Experiment 9 analyzed as a function of the surface shape. The family of curves is parametric as a function of the masking-dot density. In this case the tics on the horizontal axis refer to the degree of distortion from a plane to the hyperbolic paraboloid with the most extreme distortion as shown in in Figure 43.

Figure 50. The data from Figure 49 pooled to show the overall trend at all masking-dot densities.

Figure 51. The results of Experiment 9 analyzed as a function of the surface shape, but only for the lowest stimulus-form dot density. The family of curves is parametric as a function of the masking-dot density.

Figure 52. The results of Experiment 9 analyzed as a function of the number of surface dots in the stimulus form. The family of curves is parametric as a function of masking-dot density.

Figure 53. The data from Figure 52 pooled to show the overall trend at all masking-dot densities.

Figure 54. Diagram showing a sample of a spatial sinusoidal stimulus to exemplify those used in Experiments 10, 11, and 12.

Figure 55. The results of Experiment 10 plotted as a function of the spatial frequencies of the sinusoidal stimuli. The family of curves is parametric as a function of the masking-dot density.

Figure 56. The data from Figure 55 pooled to show the overall trend at all masking-dot densities.

Figure 57. The results of Experiment 11 plotted as a function of the spatial frequencies of the sinusoidal stimuli. The family of curves is parametric as a function of the masking-dot density.

Figure 58. The data from Figure 57 pooled to show the overall trend at all masking-dot densities.

Figure 59. The results of Experiment 12 plotted as a function of the amplitudes of the sinusoidal stimuli. The family of curves is parametric as a function of the masking-dot density.

Figure 60. The results of Experiment 12 plotted as a function of the spatial frequencies of the sinusoidal stimuli. The family of curves is parametric as a function of the masking-dot density. The elevated results for the .37 cycles per degree condition are believed to be idiosyncratic.

Figure 61. The data from Figure 60 pooled to show the overall trend at all masking-dot densities.

Figure 62. The results of Experiment 12 plotted as a function of the number of surface dots in the stimulus forms. The family of curves is parametric as a function of the masking-dot density.

Figure 63. The data from Figure 62 pooled to show the overall trend at all masking-dot densities.

Figure 64. Diagram showing the five stimuli with varying connectivity used in Experiment 13.

Figure 65. The results of Experiment 13 plotted as a function of the connectivity of the five utilized stimuli. The family of curves is parametric as a function of the masking-dot density.

Figure 66. The data from Figure 65 pooled to show the overall trend at all masking-dot densities.

Figure 67. The results of Experiment 13 plotted as a function of the number of surface dots in the stimulus forms. The family of curves is parametric as a function of the masking-dot density.

Figure 68. The data from Figure 67 pooled to show the overall trend at all masking-dot densities.

Figure 69. (A) The stereogram for a grid-type cubic in one dimension with a substantial degree of distortion. (B) The dummy dots for the same stimulus condition. See text for details.

Figure 70. The results of Supplementary Experiment 14 analyzed as a function of the surface shape. The family of curves is parametric as a function of the masking-dot density. In this case the ties on the horizontal axis refer to the degree of distortion from a plane to the cubic in one dimension with the most extreme distortion as shown in in Figure 38. The cubic stimulus-forms in this case, however, are generated from a prototype plane that consists of a regular grid of dots rather than a random array.

Figure 71. The data from Figure 70 pooled to show the overall trend at all masking-dot densities.

Figure 72. The results of Supplementary Experiment 14 plotted as a function of the number of surface dots in the stimulus forms. The family of curves is parametric as a function of the masking-dot density.

Figure 73. The data from Figure 72 pooled to show the overall trend at all masking-dot densities.

Figure 74. The results of Supplementary Experiment 15 analyzed as a function of the surface shape. The family of curves is parametric as a function of the masking-dot density. In this case the ties on the horizontal axis refer to the degree of distortion from a plane to the cubic in two dimensions with the most extreme distortion as shown in in Figure 43. The cubic stimulus-forms in this case, however, are generated from a prototype plane that consists of a regular grid of dots rather than a random array.

Figure 75. The data from Figure 74 pooled to show the overall trend at all masking-dot densities.

Figure 76. The results of Supplementary Experiment 15 plotted as a function of the number of surface dots in the stimulus forms. The family of curves is parametric as a function of the masking-dot density.

Figure 77. The data from Figure 76 pooled to show the overall trend at all masking-dot densities.

Figure 78. The results of Supplementary Experiment 16 analyzed as a function of the surface shape. The family of curves is parametric as a function of the masking-dot density. In this case the ties on the horizontal axis refer to the degree of distortion from a plane to the hyperbolic paraboloid with the most extreme distortion as shown in in Figure 48. The stimulus-forms in this case, however, are generated from a prototype plane that consists of a regular grid of dots rather than a random array.

Figure 79. The data from Figure 78 pooled to show the overall trend at all masking-dot densities.

Figure 80. The results of Supplementary Experiment 16 plotted as a function of the number of surface dots in the stimulus forms. The family of curves is parametric as a function of the masking-dot density.

Figure 81. The data from Figure 80 pooled to show the overall trend at all masking-dot densities.

Figure 82. The results of Supplementary Experiment 17 analyzed as a function of the surface shape. The family of curves is parametric as a function of the masking-dot density. In this case the ties on the horizontal axis refer to the degree of distortion from a plane to the cubic in one dimension with the most extreme distortion as shown in in Figure 38.

The cubic stimulus-forms in this case, however, are generated from a prototype plane that consists of a regular grid of dots rather than a random array. In this experiment the observer viewed the stimulus-form monocularly.

Figure 83. The data from Figure 82 pooled to show the overall trend at all masking-dot densities.

Figure 84. The results of Supplementary Experiment 17 plotted as a function of the number of surface dots in the stimulus forms. The family of curves is parametric as a function of the masking-dot density.

Figure 85. The data from Figure 84 pooled to show the overall trend at all masking-dot densities.

Figure 86. The results of unnumbered supplementary experiment analyzed as a function of the surface shape of a set of cylinders. The family of curves is parametric as a function of the masking-dot density. In this case the tics on the horizontal axis refer to the degree of distortion from a plane to the cylinder with the most extreme distortion as shown in in Figure 14. The stimulus-forms in this case, however, are generated from a prototype plane that consists of a regular grid of dots rather than a random array.

Figure 87. The results of an unnumbered supplementary experiment plotted as a function of the number of surface dots in a set of cylindrical stimulus-forms. The family of curves is parametric as a function of the masking-dot density. Figure 88. The data of Experiment 4 replotted as a scatter-plot with all levels of stimulus-form and masking dot densities collapsed together. S/N is the signal-to-noise ratio as defined in the text. As indicated the horizontal axis runs from a minimum value of -25 to a maximum value

of 8, while the vertical axis runs from 50 percent to 100 percent in the manner to which the reader is accustomed. The points marked A and B indicate the assymptotic values of this function as interpreted in the text.

TABLE 1

Stimulus Form	Generating Equation	Coefficients
Cylinder	$z=G(-y^2+W)^{\frac{1}{2}}+H$	W=948676 H=2535 G=-1
Parabolic Arch	$z=Gy^2+H$	G=.002 H=1099
Hemisphere	$z=G(-x^2-y^2+W)^{\frac{1}{2}}+H$	W=948676 H=2535 G=-1
Paraboloid of Rotation	$z=G(x^2+y^2)+H$	G=.002 H=1085
Cubic in one dimension	$z=G(.001y^3-948.67y)+H$	G=.0025 H=2048
Cubic in two dimensions	$z=G(.001x^3-948.6x+.001y^3-948.6y)+H$	G=.001 H=2048
Hyperbolic Parabaloid	$z=G(x^2-y^2)+H$	G=-.001 H=2048

TABLE 2

Cylinder

$$z=G(-y^2+W)^{\frac{1}{2}}+H$$

Stim#	G	W	H
1	0	0	2048
2	-1	6400912	4480
3	-1	1991630	3265
4	-1	1217346	2859
5	-1	996254	2657
6	-1	948676	2535

Experiment: CYLRAN

Surface Shape

Masking Dot Density	d.f.	F Ratio	p
40	5, 210	.78	n.s.
100	5, 210	1.93	n.s.
150	5, 210	3.22	<.01
200	5, 210	1.00	n.s.
250	5, 210	1.79	n.s.

TABLE 3

Number of Surface Dots

Masking Dot Density	d.f.	F Ratio	p
40	4, 210	10.21	<.001
100	4, 210	24.23	<.001
150	4, 210	32.41	<.001
200	4, 210	28.08	<.001
250	4, 210	31.84	<.001

TABLE 4

TABLE 5

Parabolic Arch

$$Z = Gy^2 + H$$

Stim#	G	H
1	0	2048
2	.0004	1950
3	.0008	1669
4	.0012	1479
5	.0016	1289
6	.002	1099

Experiment: BOLRAN

Surface Shape

Masking Dot Density	d.f.	F Ratio	p
40	5, 210	1.07	n.s.
100	5, 210	.19	n.s.
150	5, 210	.76	n.s.
200	5, 210	.48	n.s.
250	5, 210	.70	n.s.

TABLE 6

Number of Surface Dots

Masking Dot Density	d.f.	F Ratio	p
40	4, 210	11.42	<.001
100	4, 210	42.74	<.001
150	4, 210	36.36	<.001
200	4, 210	35.97	<.001
250	4, 210	27.02	<.001

TABLE 7

TABLE 8

Hemisphere

$$z=G(-x^2-y^2+W)^{\frac{1}{2}}+H$$

Stim#	G	W	H
1	0	0	2048
2	-1	6400912	4480
3	-1	1991630	3265
4	-1	1217346	2859
5	-1	996254	2657
6	-1	948700	2537

Experiment: Hemis

Surface Shape

Masking Dot Density	d.f.	F Ratio	p
50	5, 150	1.20	n.s.
100	5, 150	.34	n.s.
150	5, 150	.70	n.s.
200	5, 150	.52	n.s.
250	5, 150	.53	n.s.

TABLE 9

Number of Surface Dots

Masking Dot Density	d.f.	F Ratio	p
50	4, 150	7.40	<.001
100	4, 150	21.99	<.001
150	4, 150	16.25	<.001
200	4, 150	17.23	<.001
250	4, 150	21.30	<.001

TABLE 10

TABLE 11

Paraboloid of Rotation

$$Z = G(x^2 + y^2) + H$$

Stim#	G	H
1	0	2048
2	.0004	1858
3	.0008	1669
4	.0012	1478
5	.0016	1289
6	.002	1085

Experiment: PARABS

Surface Shape

Masking Dot Density	d.f.	F Ratio	p
40	5, 210	1.19	n.s.
80	5, 210	.26	n.s.
120	5, 210	.52	n.s.
160	5, 210	1.96	n.s.
200	5, 210	.20	n.s.
240	5, 210	1.86	n.s.
255	5, 210	4.97	<.001

TABLE 12

Number of Surface Dots

Masking Dot Density	d.f.	F Ratio	p
40	4, 210	19.70	< .001
80	4, 210	52.15	< .001
120	4, 210	83.91	< .001
160	4, 210	87.20	< .001
200	4, 210	55.26	< .001
240	4, 210	51.00	< .001
255	4, 210	80.27	< .001

TABLE 13

TABLE 14

Cubic in One Dimension

$z=G(.001y^3-948.676y)+H$

Stim#	G	H
1	0	2048
2	.0005	2048
3	.001	2048
4	.0015	2048
5	.002	2048
6	.0025	2048

Experiment: CUBRAN1

Surface Shape

Masking Dot Density	d.f.	F Ratio	p
50	5, 150	.46	n.s.
100	5, 150	7.72	< .001
150	5, 150	6.52	< .001
200	5, 150	3.90	< .01
250	5, 150	7.75	< .001

TABLE 15

Number of Surface Dots

Masking Dot Density	d.f.	F Ratio	p
50	4, 150	24.53	< .001
100	4, 150	40.70	< .001
150	4, 150	59.53	< .001
200	4, 150	41.00	< .001
250	4, 150	65.53	< .001

TABLE 16

TABLE 17

Cubic in Two Dimensions

$$Z = G(.001x^3 - 948.6x + .001y^3 - 948.6y) + H$$

Stim#	G	H
1	0	2048
2	.0002	2048
3	.0004	2048
4	.0006	2048
5	.0008	2048
6	.001	2048

Experiment: CUBRAN2

Surface Shape

Masking Dot Density	d.f.	F Ratio	p
50	5, 210	5.47	< .001
100	5, 210	8.58	< .001
150	5, 210	8.25	< .001
200	5, 210	5.89	< .001
250	5, 210	12.00	< .001
300	5, 210	5.93	< .001
350	5, 210	6.88	< .001

TABLE 18

Number of Surface Dots

Masking Dot Density	d.f.	F Ratio	p
50	4, 210	22.45	< .001
100	4, 210	32.85	< .001
150	4, 210	34.42	< .001
200	4, 210	37.80	< .001
250	4, 210	61.57	< .001
300	4, 210	42.92	< .001
350	4, 210	56.13	< .001

TABLE 19

TABLE 20

Hyperbolic Parabaloid

$$z=G(x^2-y^2)+H$$

Stim#	G	H
1	0	2048
2	-.0002	2048
3	-.0004	2048
4	-.0006	2048
5	-.0008	2048
6	-.001	2048

Experiment: HYPARB

Surface Shape

Masking Dot Density	d.f.	F Ratio	p
50	5, 150	.53	n.s.
100	5, 150	2.29	< .05
150	5, 150	.34	n.s.
200	5, 150	.65	n.s.
250	5, 150	.66	n.s.
300	5, 150	1.61	n.s.
350	5, 150	.98	n.s.

TABLE 21

Number of Surface Dots

Masking Dot Density	d.f.	F Ratio	p
50	4, 150	15.46	<.001
100	4, 150	39.25	<.001
150	4, 150	16.31	<.001
200	4, 150	21.33	<.001
250	4, 150	11.53	<.001
300	4, 150	11.02	<.001
350	4, 150	9.64	<.001

TABLE 22

TABLE 23

Sinusoid

$Z = A \cos w \cdot x$

Stim#	A	W
1	650	0
2	650	.5
3	650	1.0
4	650	1.5
5	650	2.0
6	650	3.0
7	650	5.0

Experiment: SIN4

Surface Shape

Masking Dot Density	d.f.	F Ratio	p
50	5, 210	13.75	<.001
75	5, 210	8.27	<.001
100	5, 210	9.56	<.001
125	5, 210	6.60	<.001
150	5, 210	9.23	<.001
175	5, 210	8.03	<.001
200	5, 210	3.81	<.01

TABLE 24

Number of Surface Dots

Masking Dot Density	d.f.	F Ratio	p
50	4, 210	31.01	<.001
75	4, 210	28.89	<.001
100	4, 210	21.07	<.001
125	4, 210	30.03	<.001
150	4, 210	26.93	<.001
175	4, 210	23.96	<.001
200	4, 210	22.91	<.001

TABLE 25

Experiment: CON1

Surface Shape

Masking Dot Density	d.f.	F Ratio	p
50	4, 175	1.22	n.s.
100	4, 175	2.02	n.s.
150	4, 175	1.26	n.s.
200	4, 175	1.18	n.s.
300	4, 175	2.47	<.05
400	4, 175	.94	n.s.
450	4, 175	2.13	n.s.

TABLE 26

Number of Surface Dots

Masking Dot Density	d.f.	F Ratio	p
50	4, 175	1.49	n.s.
100	4, 175	8.19	<.001
150	4, 175	12.24	<.001
200	4, 175	25.58	<.001
300	4, 175	35.06	<.001
400	4, 175	28.89	<.001
450	4, 175	33.91	<.001

TABLE 27

Experiment: CUBGRID1

Surface Shape

Masking Dot Density	d.f.	F Ratio	p
50	5, 180	.81	n.s.
100	5, 180	.35	n.s.
150	5, 180	.26	n.s.
200	5, 180	1.16	n.s.
250	5, 180	.60	n.s.
300	5, 180	.93	n.s.

TABLE 28

Number of Surface Dots

Masking Dot Density	d.f.	F Ratio	p
50	4, 180	52.47	< .001
100	4, 180	115.55	< .001
150	4, 180	138.05	< .001
200	4, 180	143.50	< .001
250	4, 180	113.22	< .001
300	4, 180	131.89	< .001

TABLE 29

Experiment: CUBGRID2

Surface Shape

Masking Dot Density	d.f.	F Ratio	p
50	5, 210	1.62	n.s.
100	5, 210	.97	n.s.
150	5, 210	.41	n.s.
200	5, 210	1.24	n.s.
250	5, 210	.85	n.s.
300	5, 210	.35	n.s.

TABLE 30

Number of Surface Dots

Masking Dot Density	d.f.	F Ratio	p
50	4, 210	40.22	< .001
100	4, 210	77.26	< .001
150	4, 210	119.07	< .001
200	4, 210	109.74	< .001
250	4, 210	105.84	< .001
300	4, 210	107.90	< .001

TABLE 31

Experiment: HYGRID

Surface Shape

Masking Dot Density	d.f.	F Ratio	p
50	5, 210	2.26	<.05
100	5, 210	.38	n.s.
150	5, 210	.99	n.s.
200	5, 210	.79	n.s.
250	5, 210	.35	n.s.
300	5, 210	1.21	n.s.

TABLE 32

Number of Surface Dots

Masking Dot Density	d.f.	F Ratio	p
50	4, 210	29.16	< .001
100	4, 210	66.83	< .001
150	4, 210	75.45	< .001
200	4, 210	84.02	< .001
250	4, 210	95.32	< .001
300	4, 210	75.37	< .001

TABLE 33

Experiment: MONOGRID

Surface Shape

Masking Dot Density	d.f.	F Ratio	p
50	5, 210	.85	n.s.
100	5, 210	1.80	n.s.
150	5, 210	.56	n.s.
200	5, 210	1.09	n.s.

TABLE 34

Number of Surface Dots

Masking Dot Density	d.f	F Ratio	p
50	4, 210	96.25	< .001
100	4, 210	144.93	< .001
150	4, 210	144.81	< .001
200	4,210	133.19	< .001

TABLE 35

TABLE 36

Experiment #	Average F Ratios	
	Stimulus Form	Dot Density
3	1.74	25.35
4	.64	30.70
5	.66	16.83
6	1.57	61.36
7	5.27	46.26
8	7.56	41.23
9	1.01	17.70
12	8.46	26.40
13	1.60	20.77
14	.65	115.78
15	.91	93.34
16	1.00	70.98
17	1.08	129.80

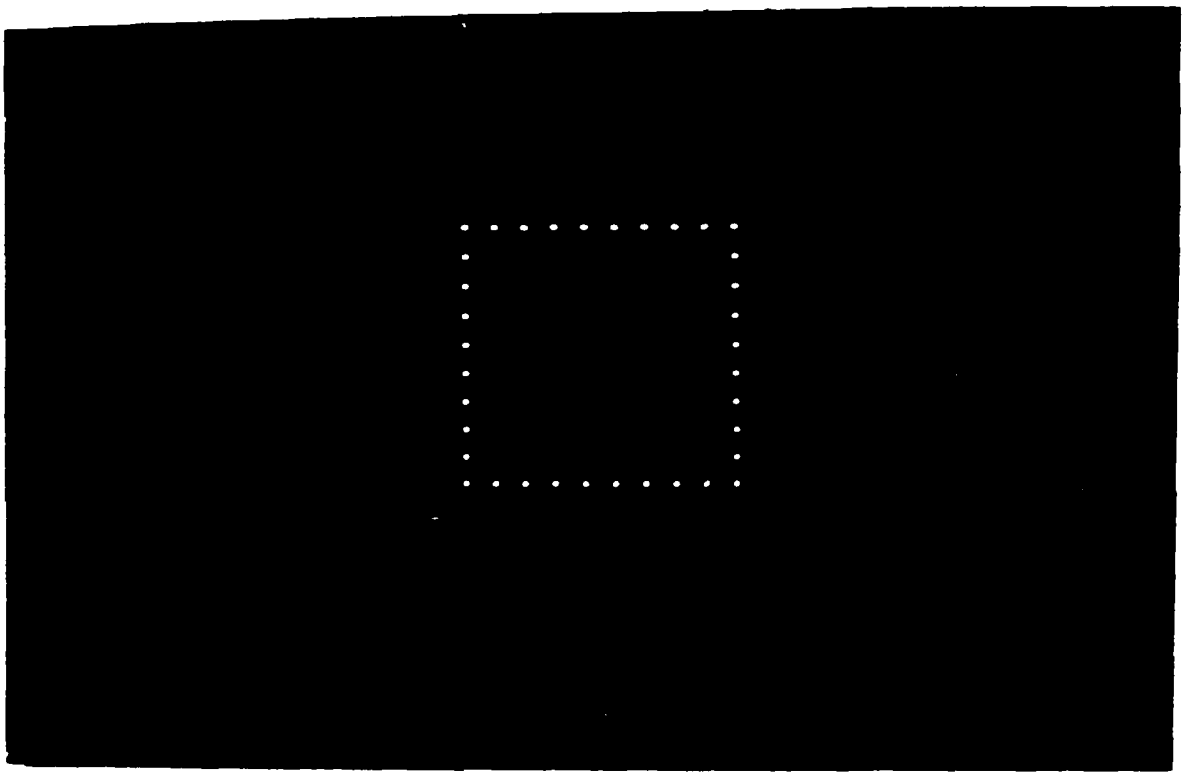

Figure 1

Figure 2

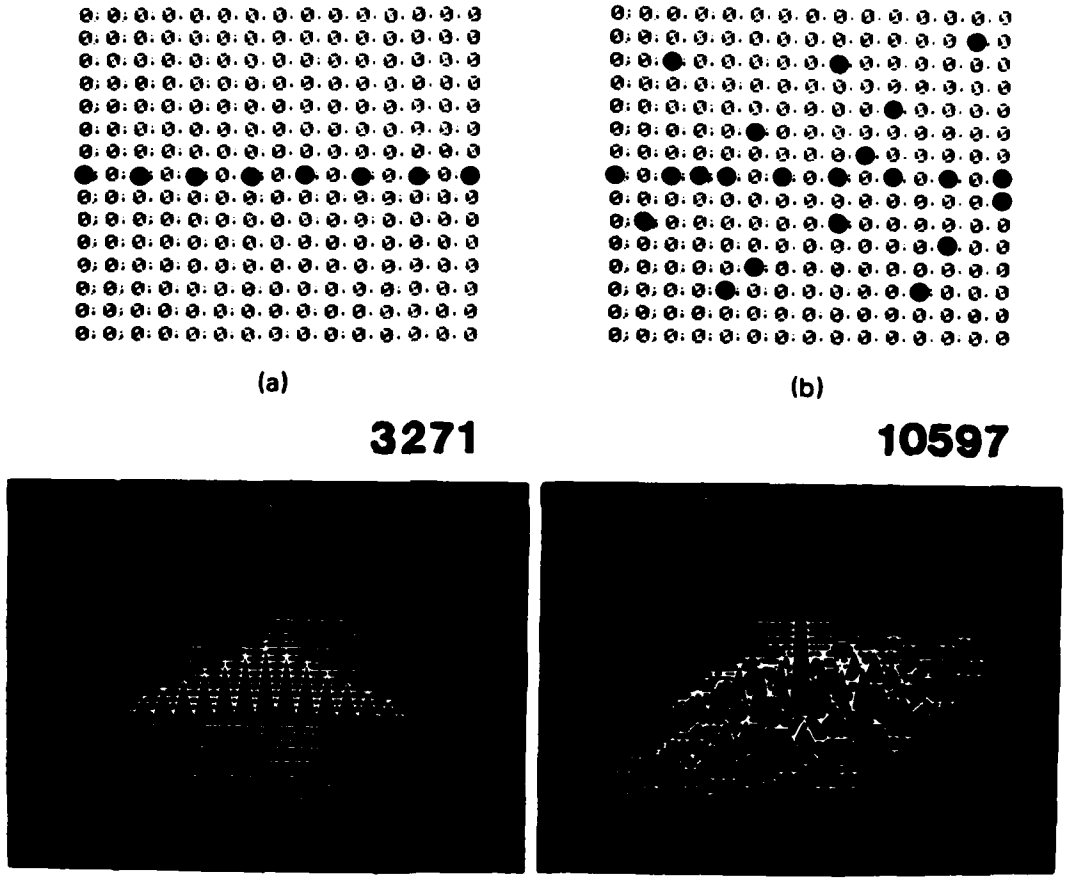

Figure 3

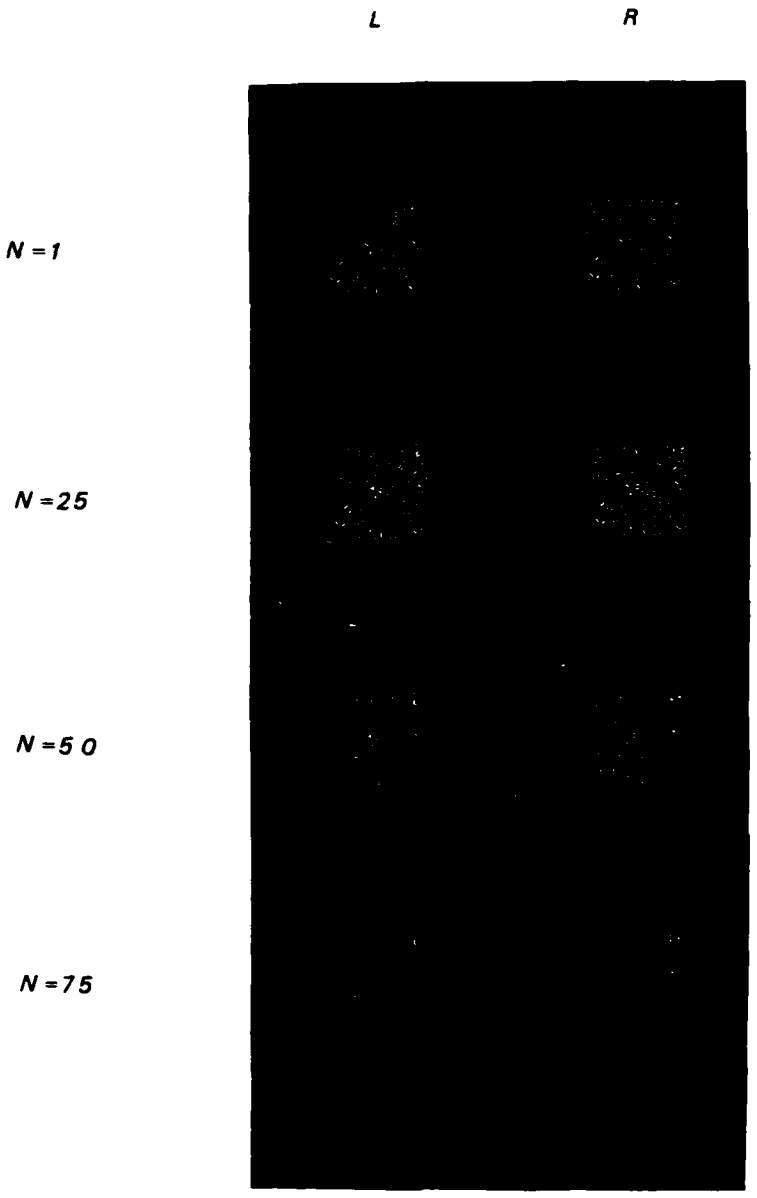

Figure 4

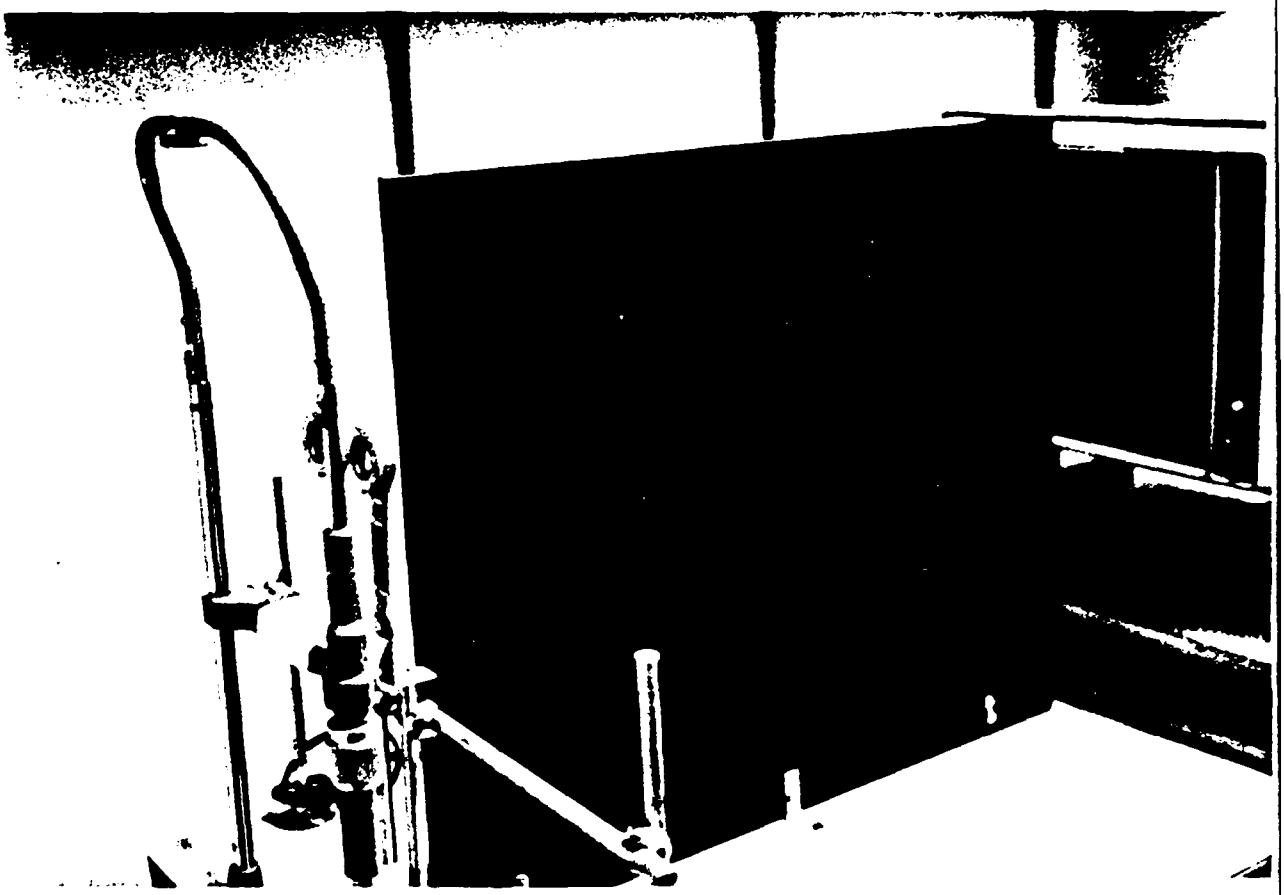

Figure 5

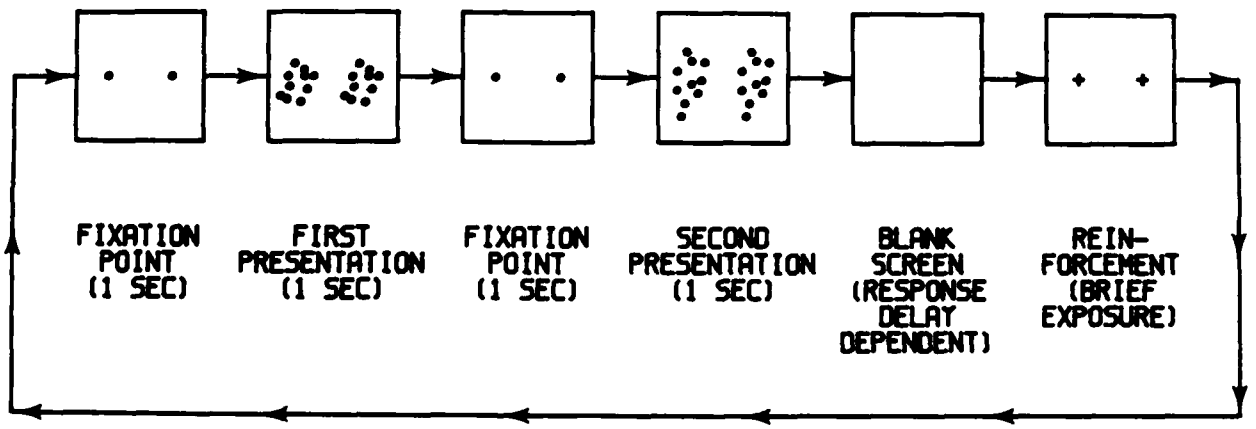
FIXATION POINT (1 SEC)
FIRST PRESENTATION (1 SEC)
FIXATION POINT (1 SEC)
SECOND PRESENTATION (1 SEC)
BLANK SCREEN (RESPONSE DELAY DEPENDENT)
REIN-FORCEMENT (BRIEF EXPOSURE)

Figure 6

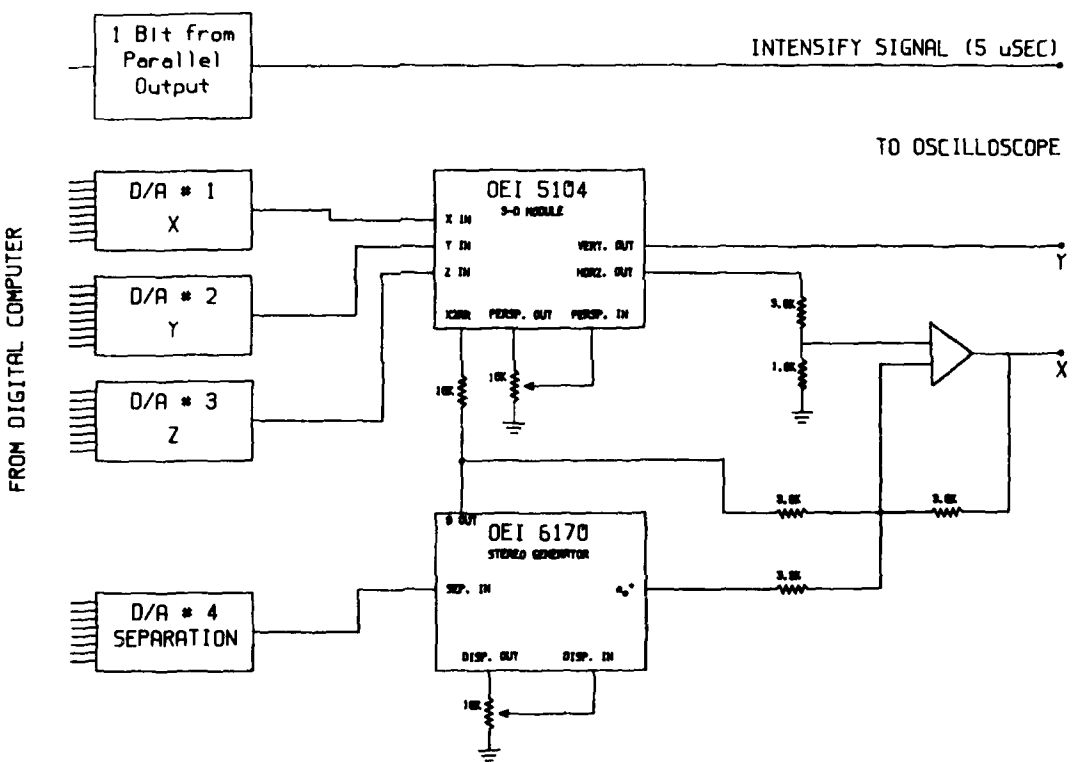
1 Bit from Parallel Output
INTENSIFY SIGNAL (5 uSEC)
TO OSCILLOSCOPE
FROM DIGITAL COMPUTER
D/A # 1 X
D/A # 2 Y
D/A # 3 Z
D/A # 4 SEPARATION
OEI 5104
OEI 6170
Y
X

Figure 7

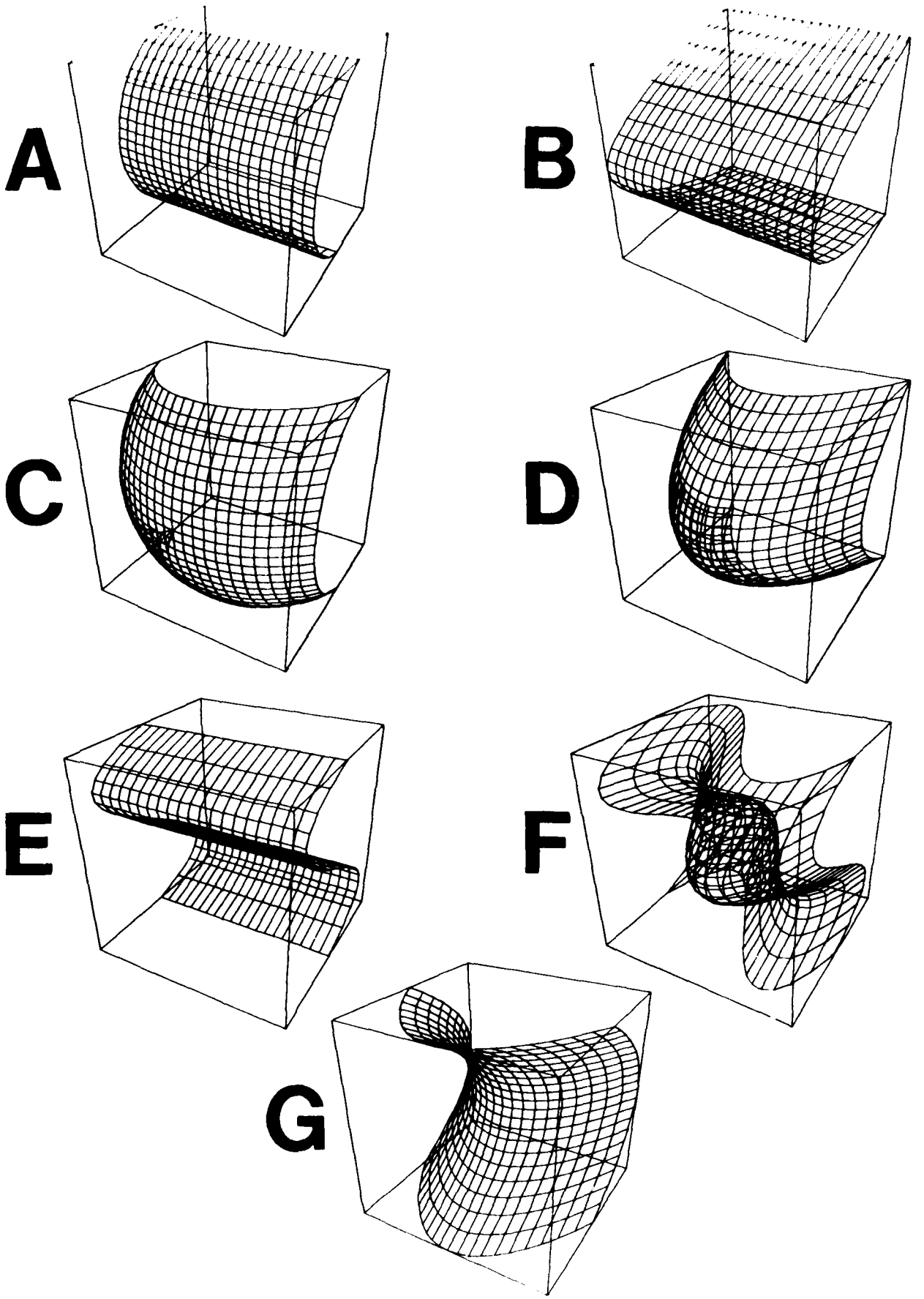
A
B
C
D
E
F
G

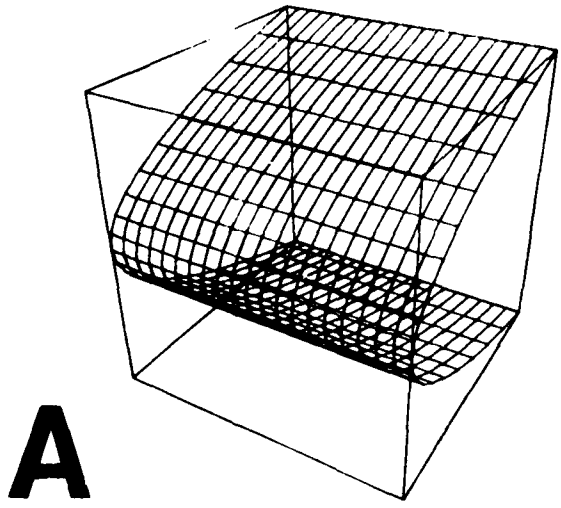

A

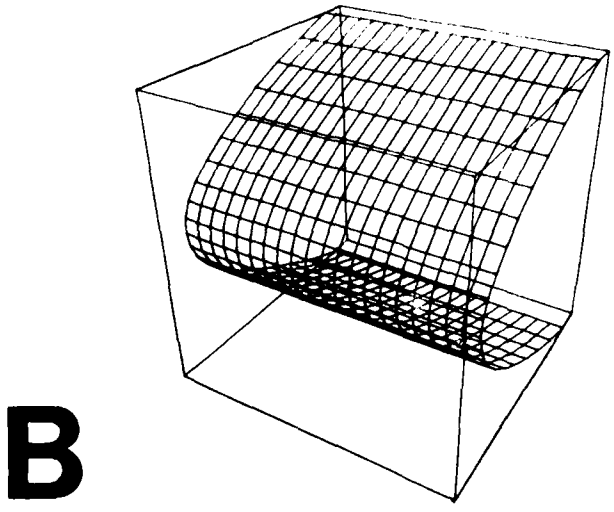

B

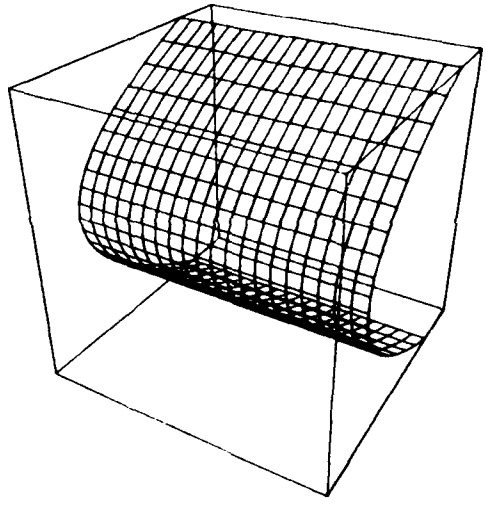

C

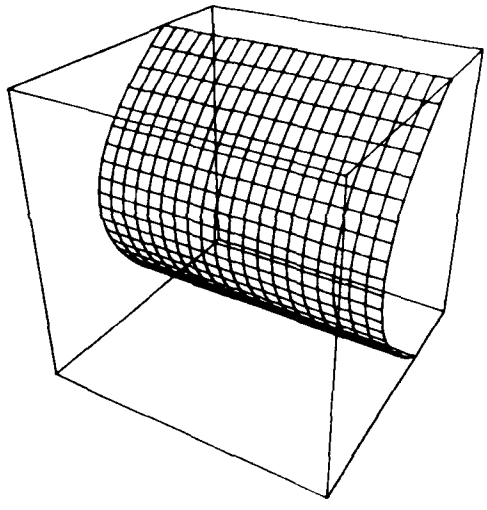

D

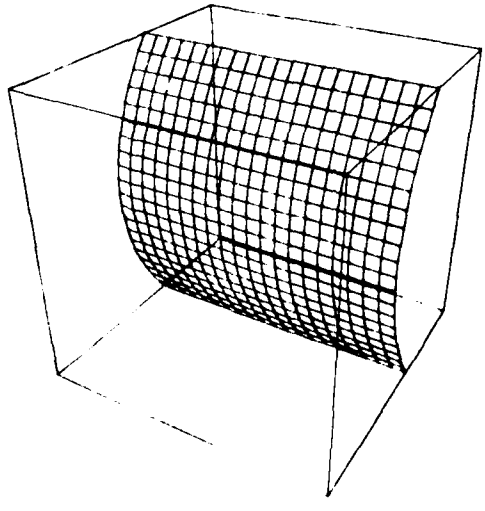

E

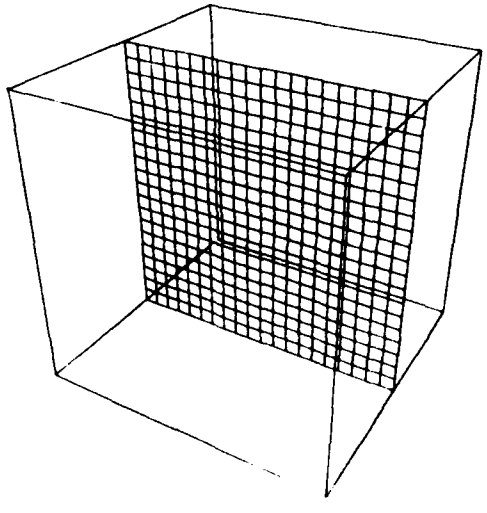

F

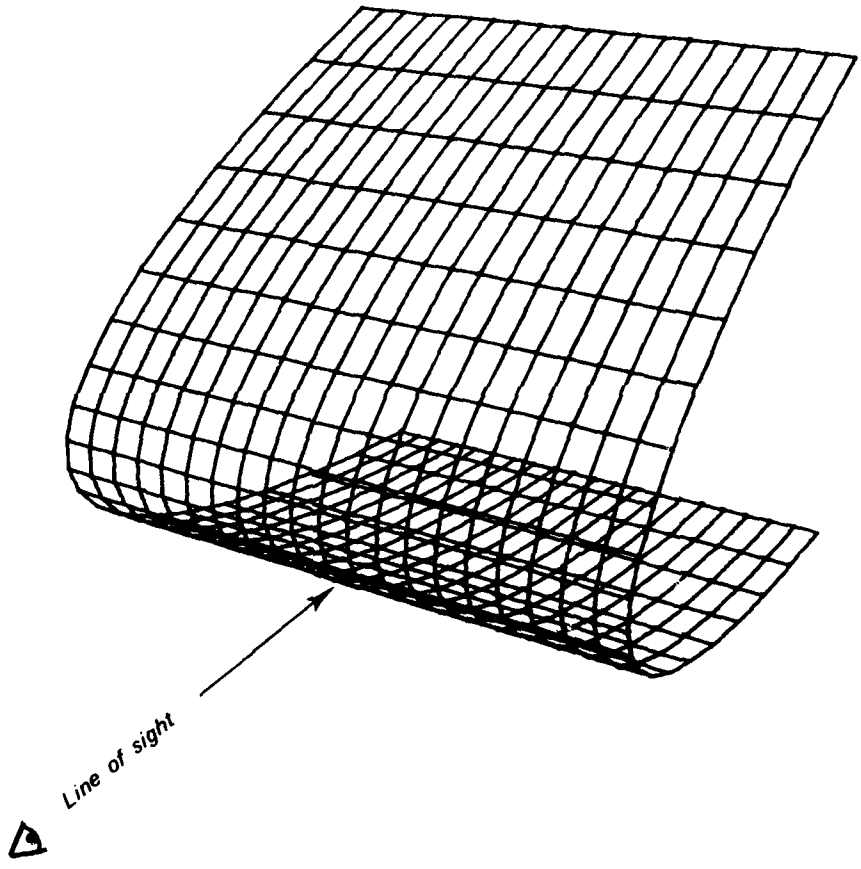

Figure 10

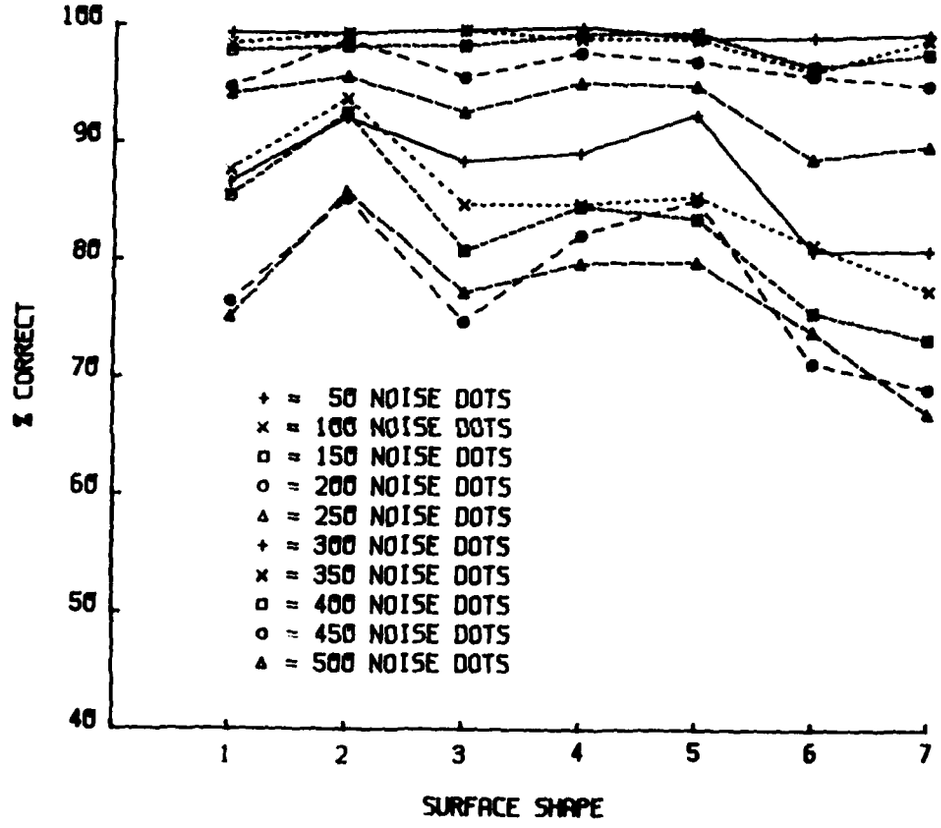
100
90
80
70
60
50
40
% CORRECT
1
2
3
4
5
6
7
SURFACE SHAPE
+ = 50 NOISE DOTS
× = 100 NOISE DOTS
□ = 150 NOISE DOTS
○ = 200 NOISE DOTS
△ = 250 NOISE DOTS
+ = 300 NOISE DOTS
× = 350 NOISE DOTS
□ = 400 NOISE DOTS
○ = 450 NOISE DOTS
△ = 500 NOISE DOTS

Figure 11

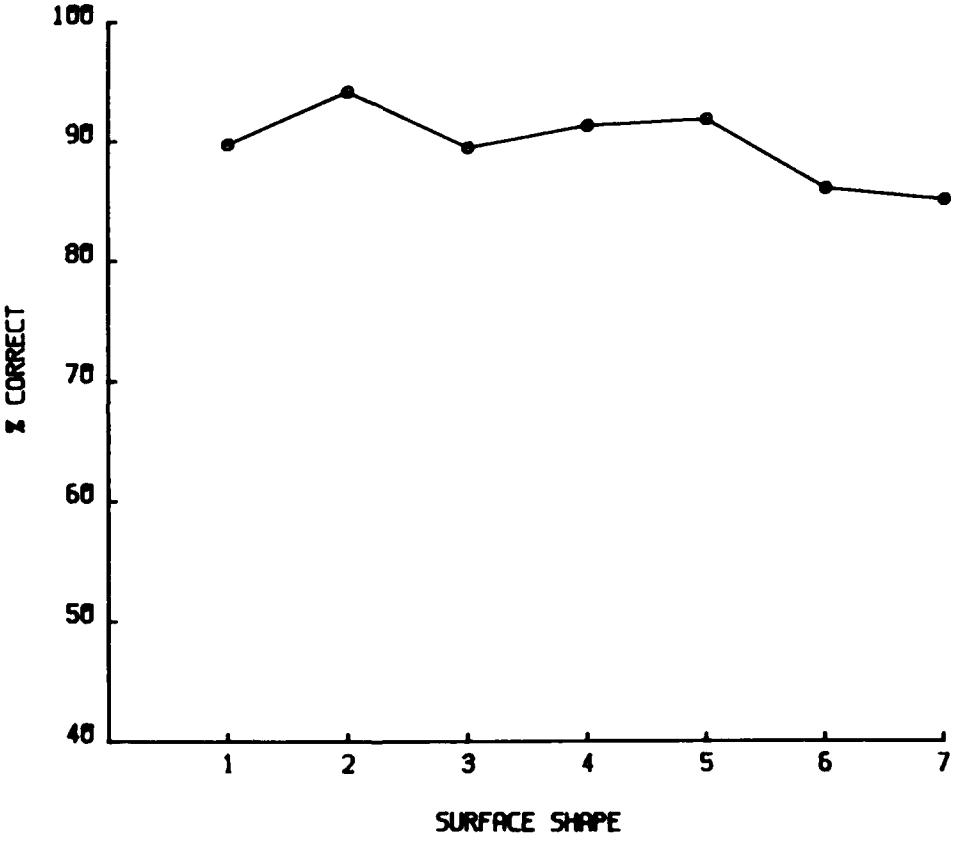

Figure 12

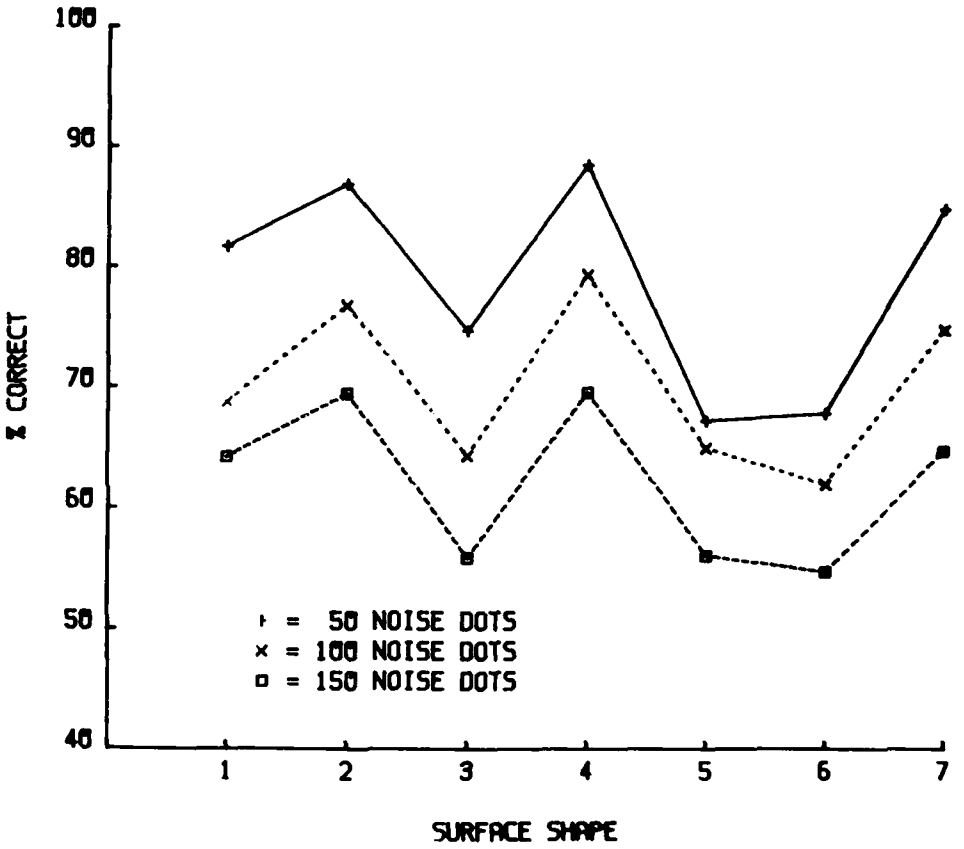
100
90
80
70
60
50
40
% CORRECT
1
2
3
4
5
6
7
SURFACE SHAPE
+ = 50 NOISE DOTS
× = 100 NOISE DOTS
□ = 150 NOISE DOTS

Figure 13

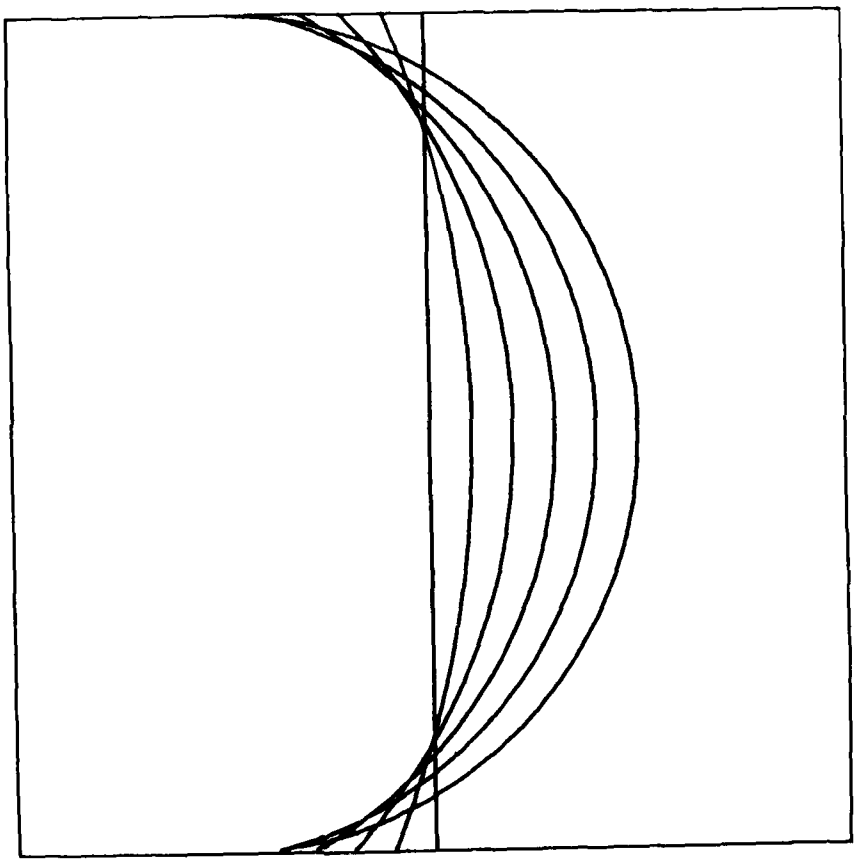

Figure 14

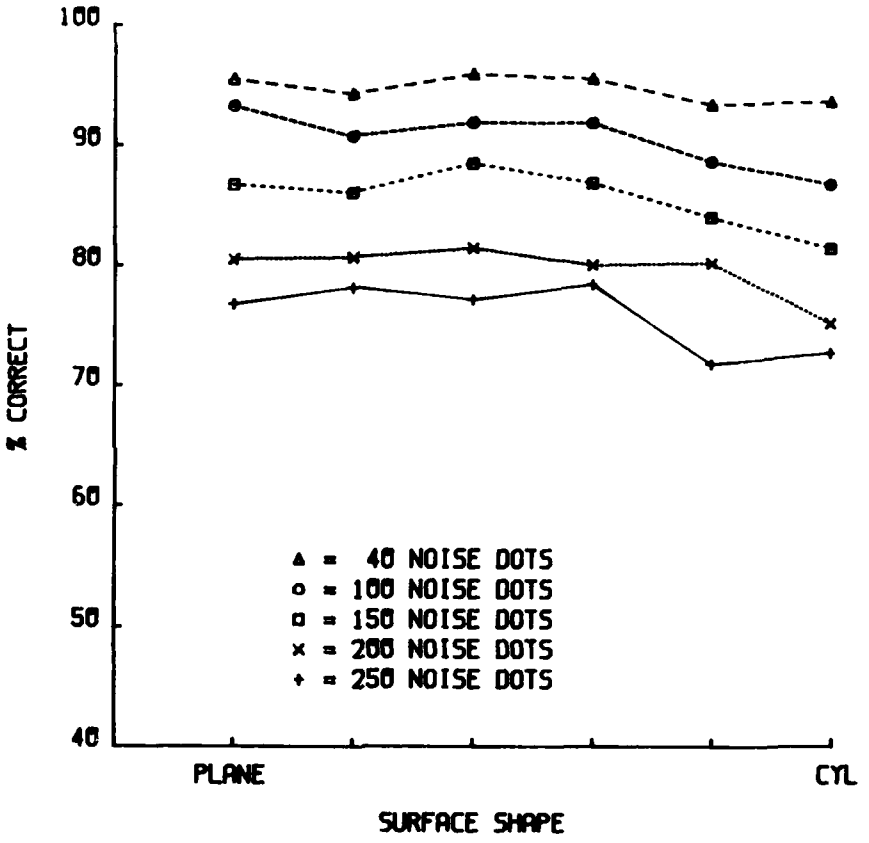
100
90
80
70
60
50
40
% CORRECT
▲ = 40 NOISE DOTS
○ = 100 NOISE DOTS
□ = 150 NOISE DOTS
× = 200 NOISE DOTS
+ = 250 NOISE DOTS
PLANE
CYL
SURFACE SHAPE

Figure 15

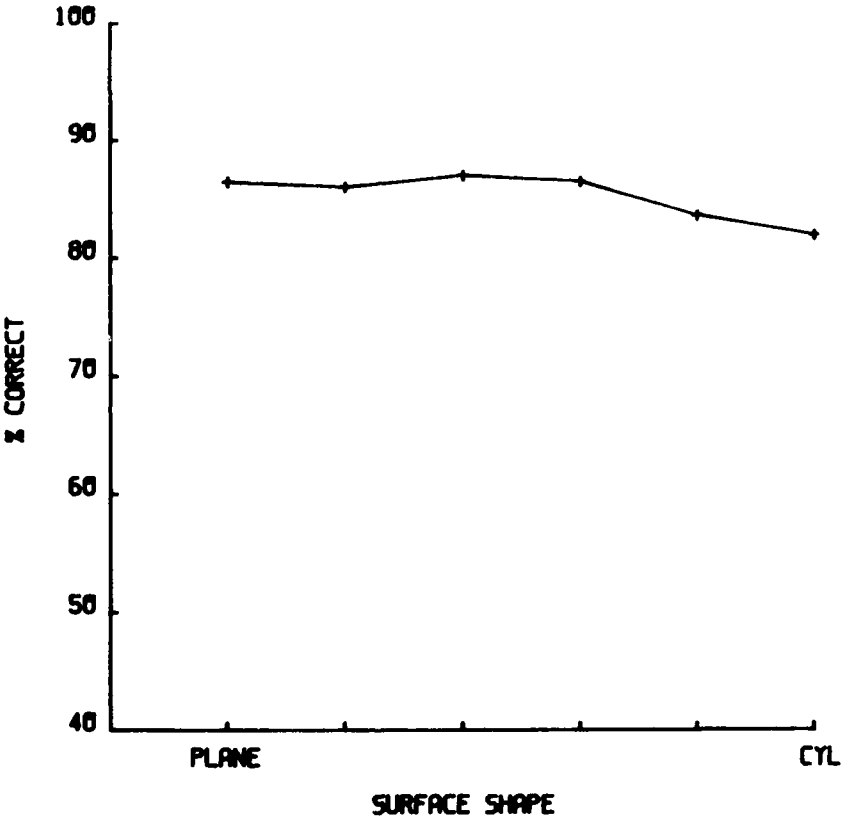

Figure 16

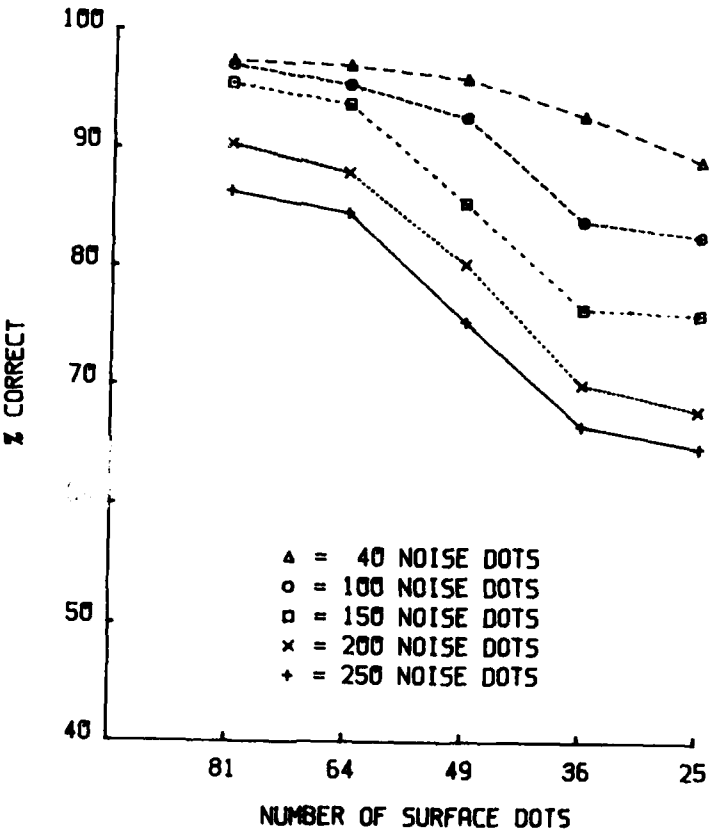
100
90
80
70
50
40
% CORRECT
Δ = 40 NOISE DOTS
o = 100 NOISE DOTS
□ = 150 NOISE DOTS
× = 200 NOISE DOTS
+ = 250 NOISE DOTS
81
64
49
36
25
NUMBER OF SURFACE DOTS

Figure 17

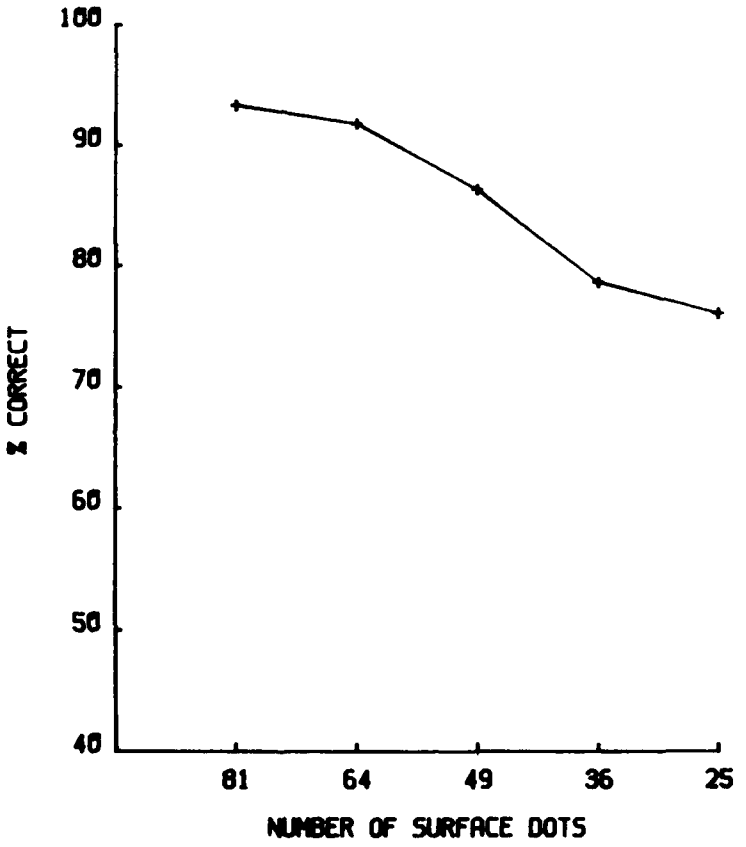
100
90
80
70
60
50
40
% CORRECT
81
64
49
36
25
NUMBER OF SURFACE DOTS

Figure 18

AD-A138 761 THE DETECTION OF NONPLANAR SURFACES IN VISUAL SPACE(U) 3/3
MICHIGAN UNIV ANN ARBOR PERCEPTION LAB
W R UTTAL ET AL. 01 MAR 84 PERLAB-4 N00014-81-C-0266
UNCLASSIFIED F/G 6/16 NL

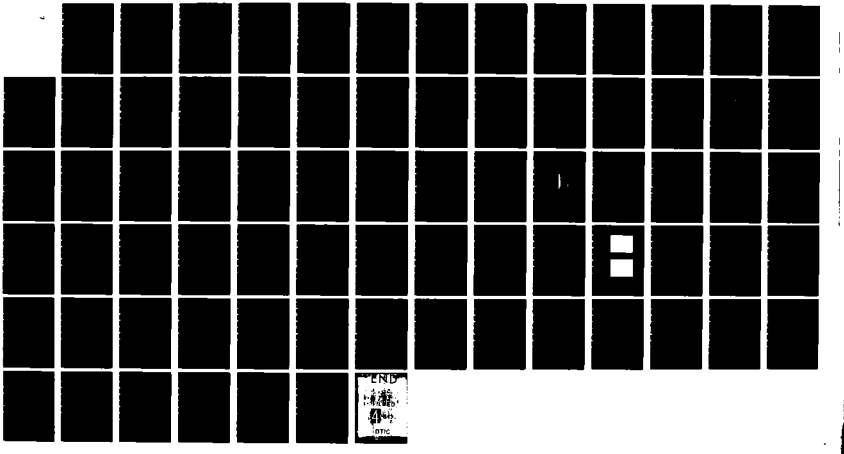

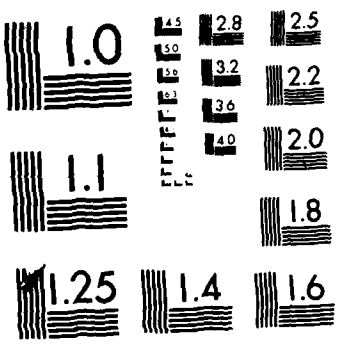

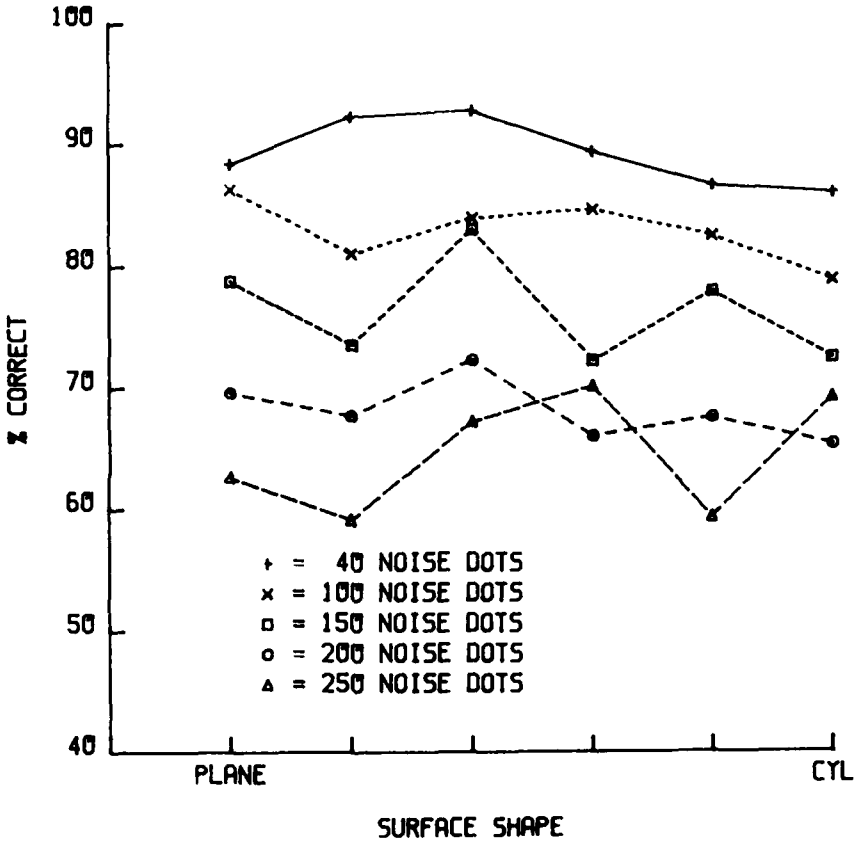
100
90
80
70
60
50
40
% CORRECT
+ = 40 NOISE DOTS
× = 100 NOISE DOTS
□ = 150 NOISE DOTS
○ = 200 NOISE DOTS
△ = 250 NOISE DOTS
PLANE
CYL
SURFACE SHAPE

Figure 19

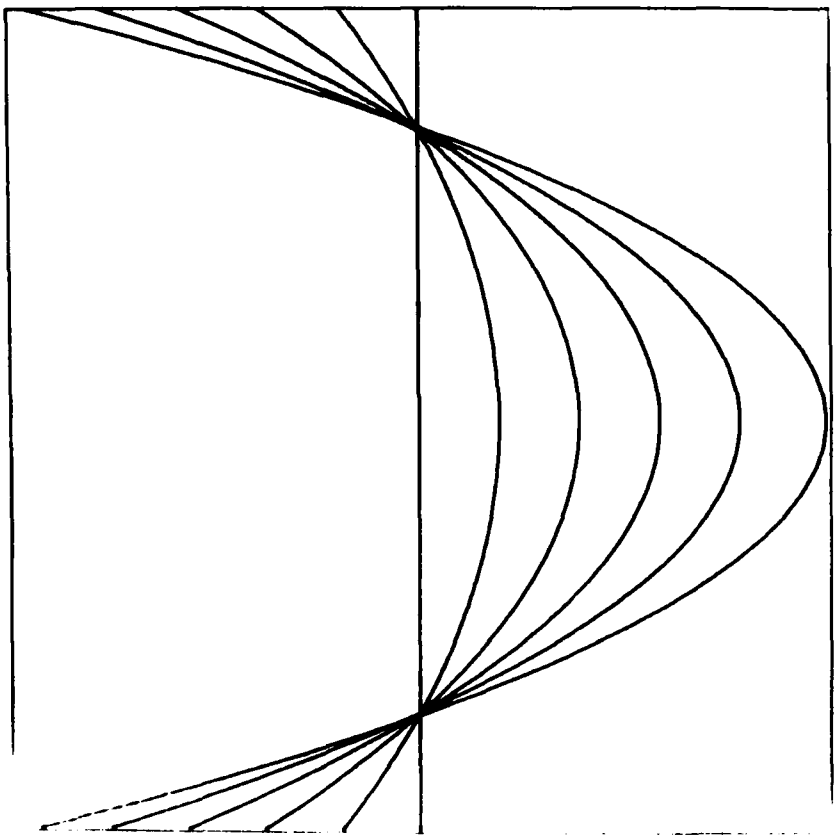

Figure 20

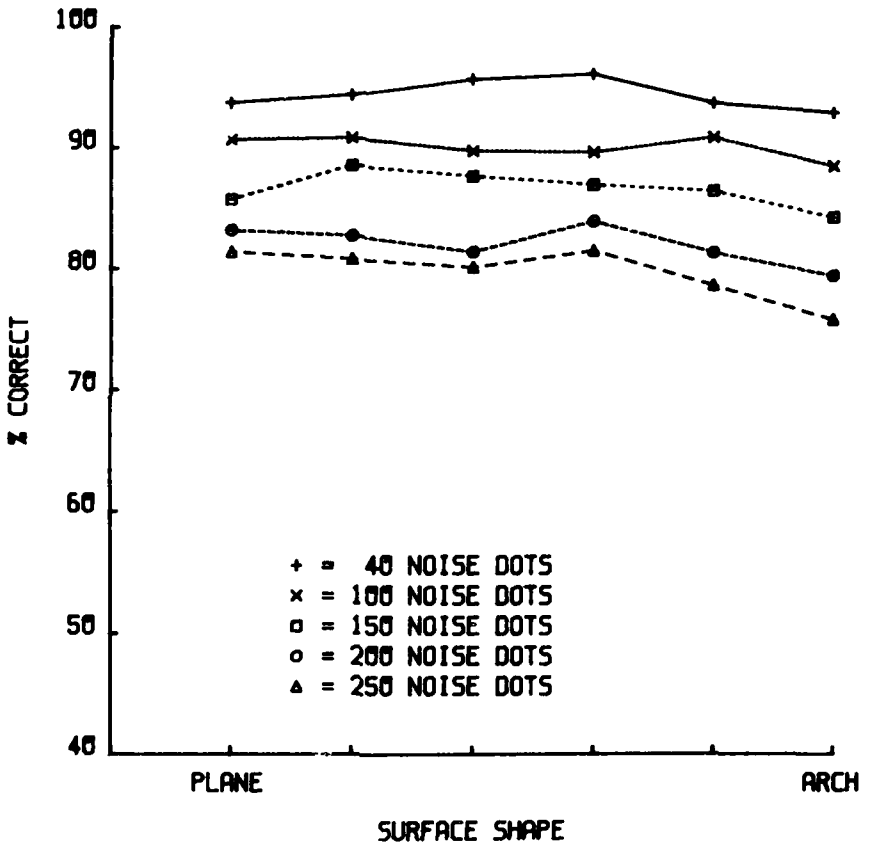
100
90
80
70
60
50
40
% CORRECT
+ = 40 NOISE DOTS
× = 100 NOISE DOTS
□ = 150 NOISE DOTS
○ = 200 NOISE DOTS
△ = 250 NOISE DOTS
PLANE
ARCH
SURFACE SHAPE

Figure 21

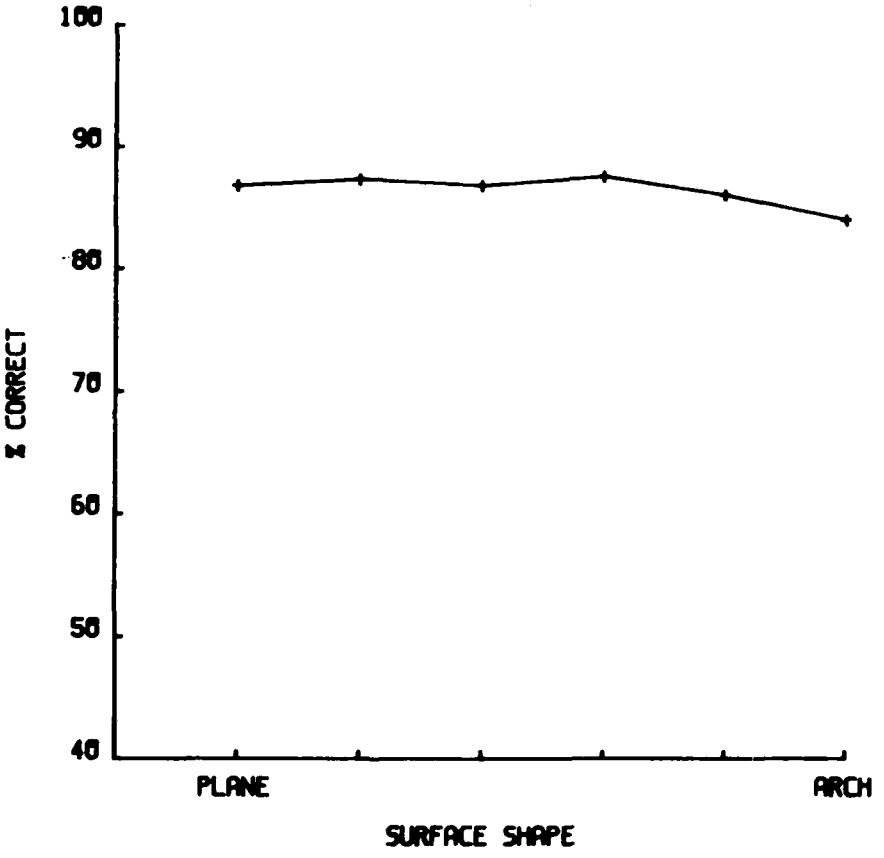

Figure 22

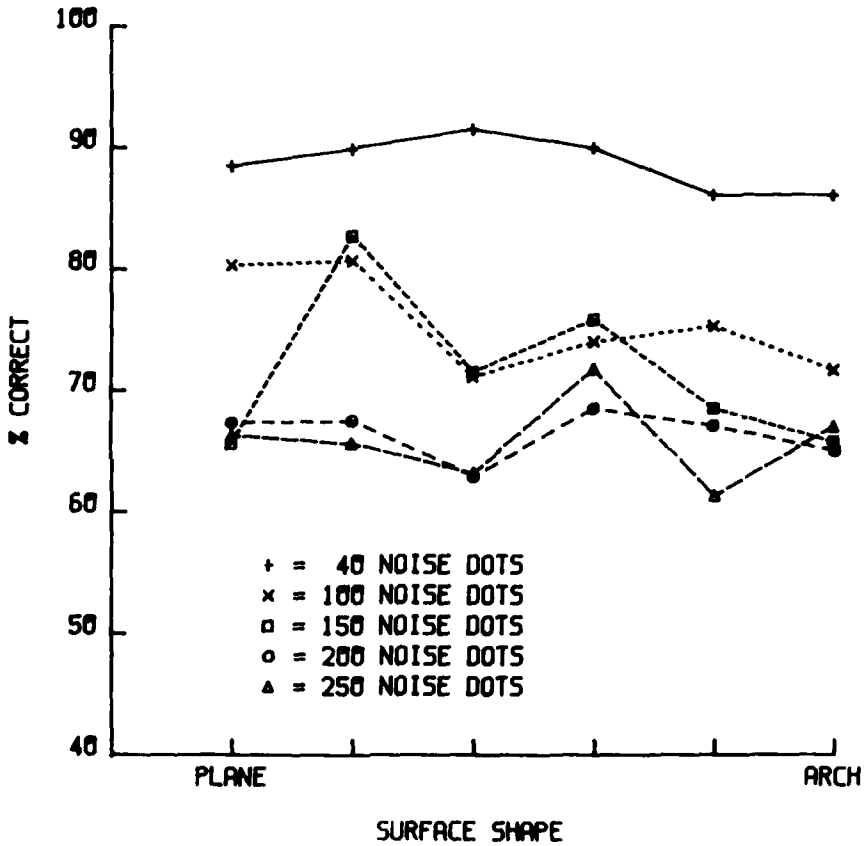
100
90
80
70
60
50
40
% CORRECT
+ = 40 NOISE DOTS
× = 100 NOISE DOTS
□ = 150 NOISE DOTS
○ = 200 NOISE DOTS
△ = 250 NOISE DOTS
PLANE
ARCH
SURFACE SHAPE

Figure 23

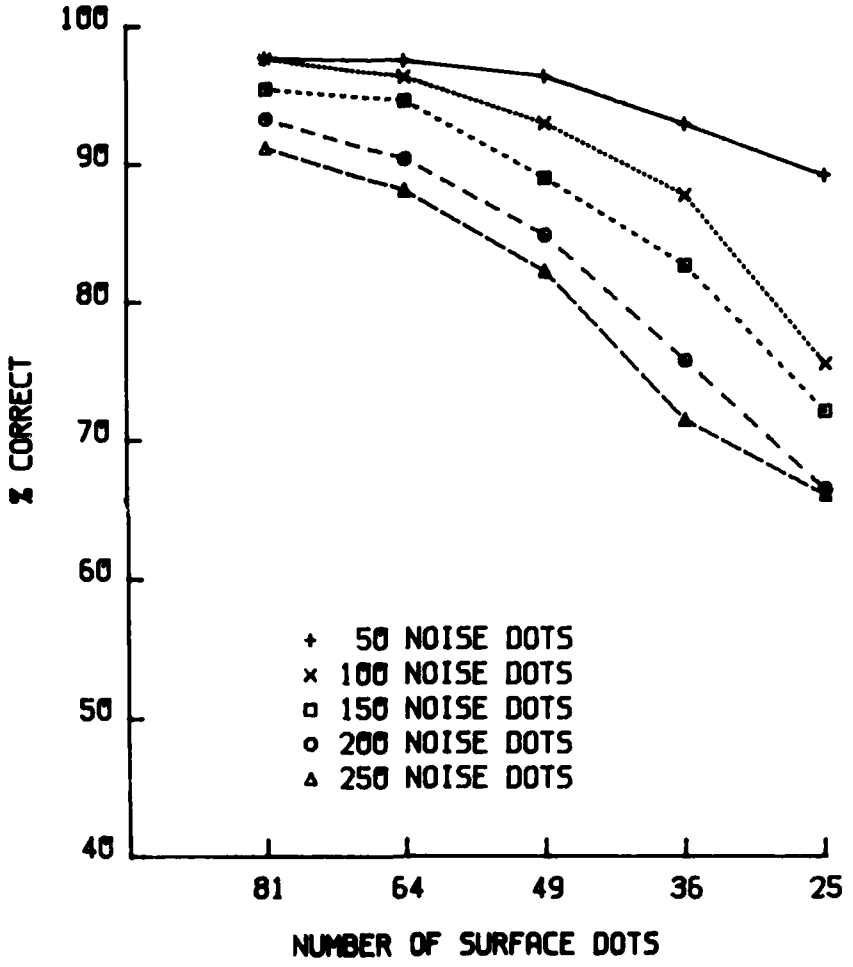
100
90
80
70
60
50
40
% CORRECT
+ 50 NOISE DOTS
× 100 NOISE DOTS
□ 150 NOISE DOTS
○ 200 NOISE DOTS
△ 250 NOISE DOTS
81
64
49
36
25
NUMBER OF SURFACE DOTS

Figure 24

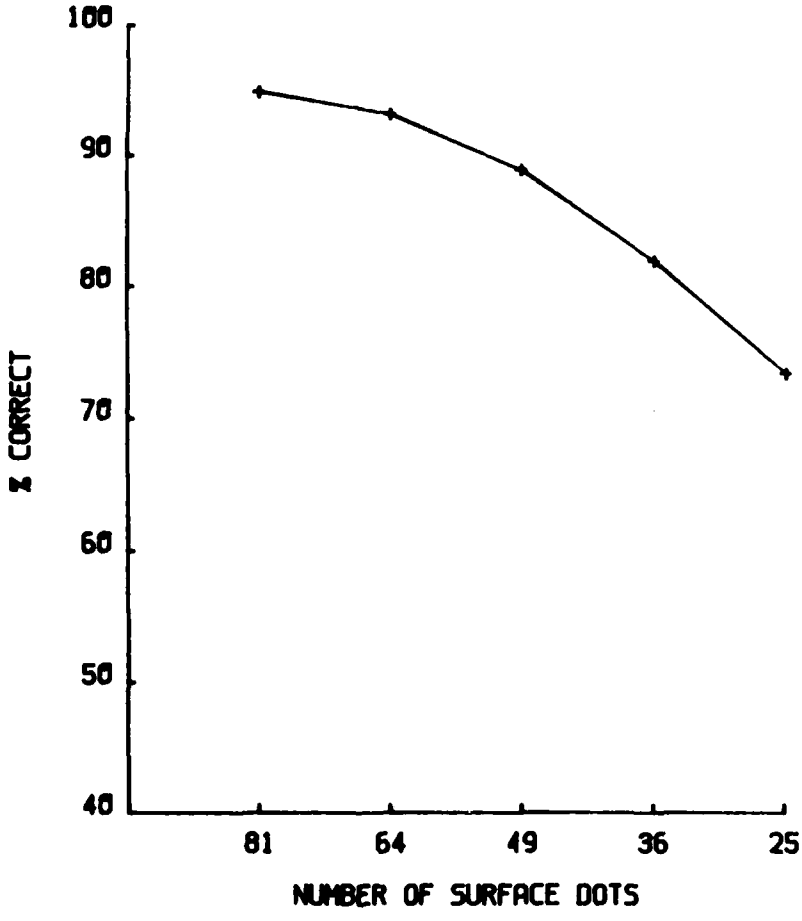
100
90
80
70
60
50
40
% CORRECT
81
64
49
36
25
NUMBER OF SURFACE DOTS

Figure 25

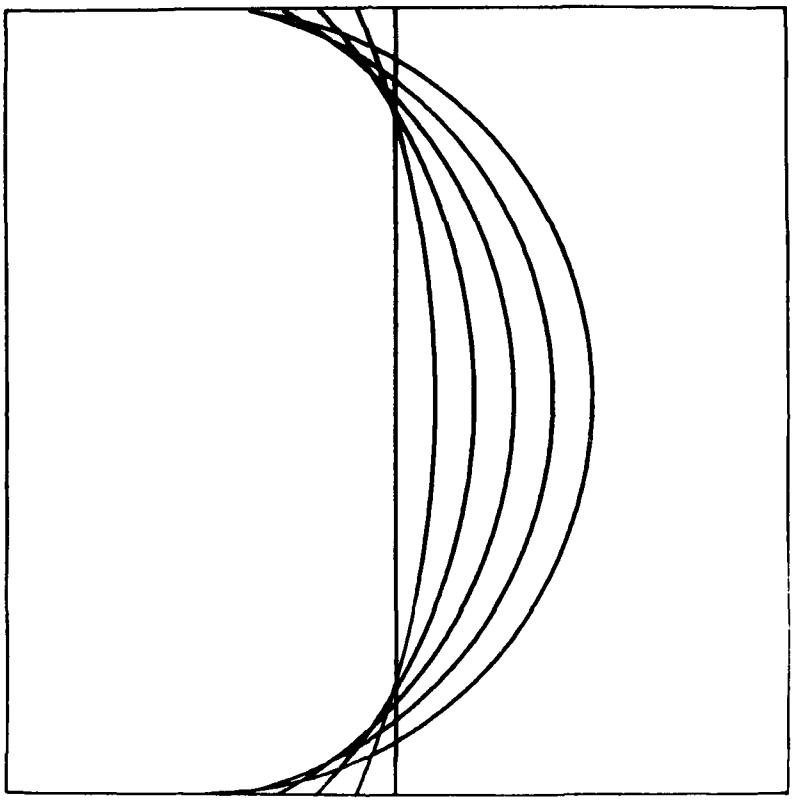

Figure 26

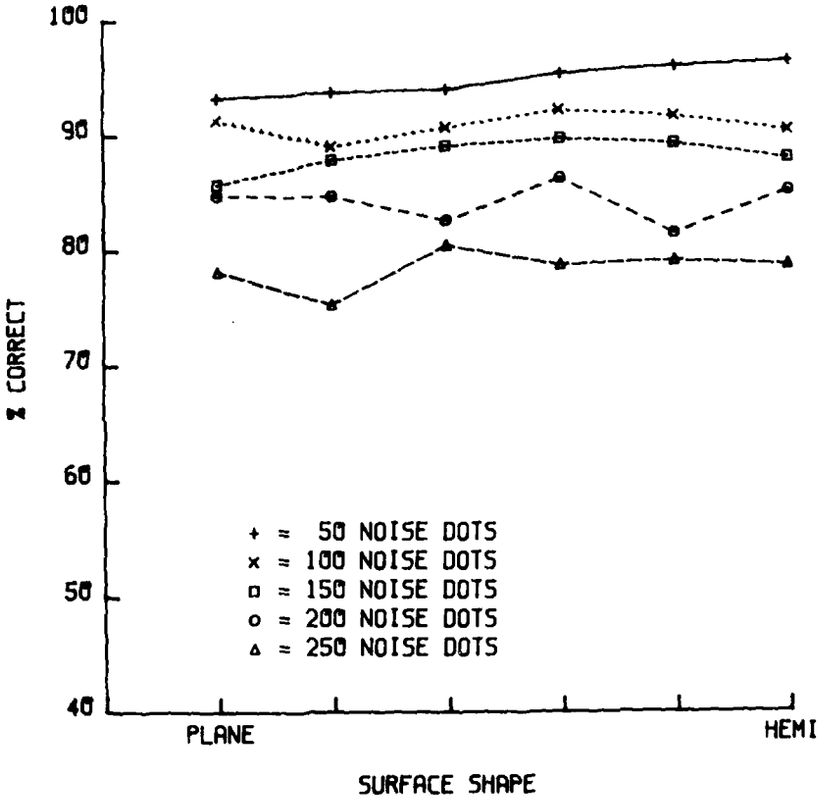
100
90
80
70
60
50
40
% CORRECT
+ = 50 NOISE DOTS
x = 100 NOISE DOTS
□ = 150 NOISE DOTS
o = 200 NOISE DOTS
△ = 250 NOISE DOTS
PLANE
HEMI
SURFACE SHAPE

Figure 27

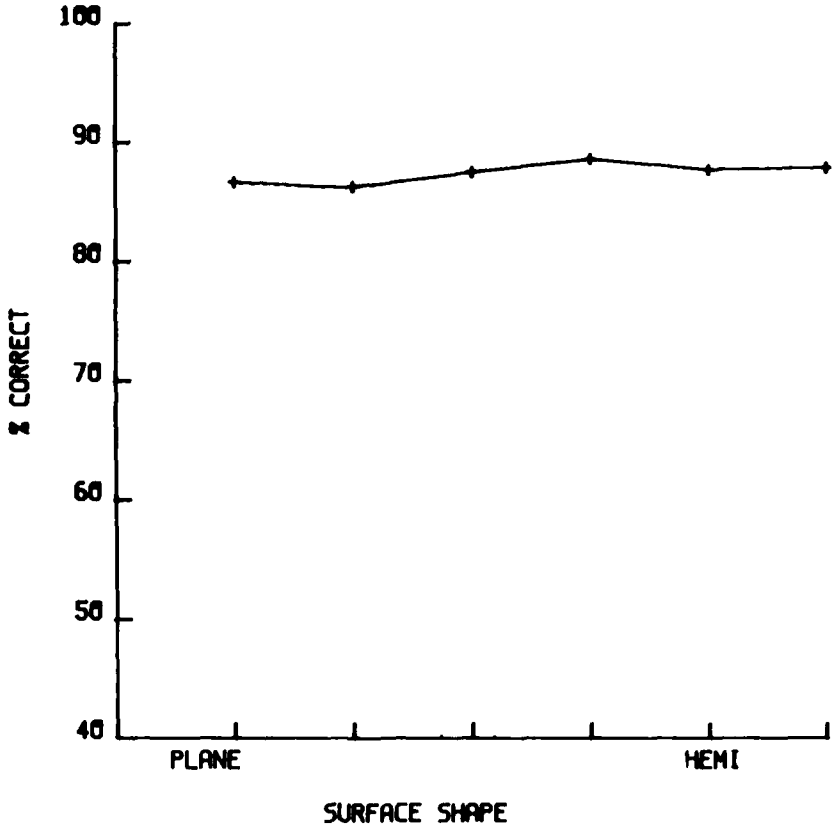

Figure 28

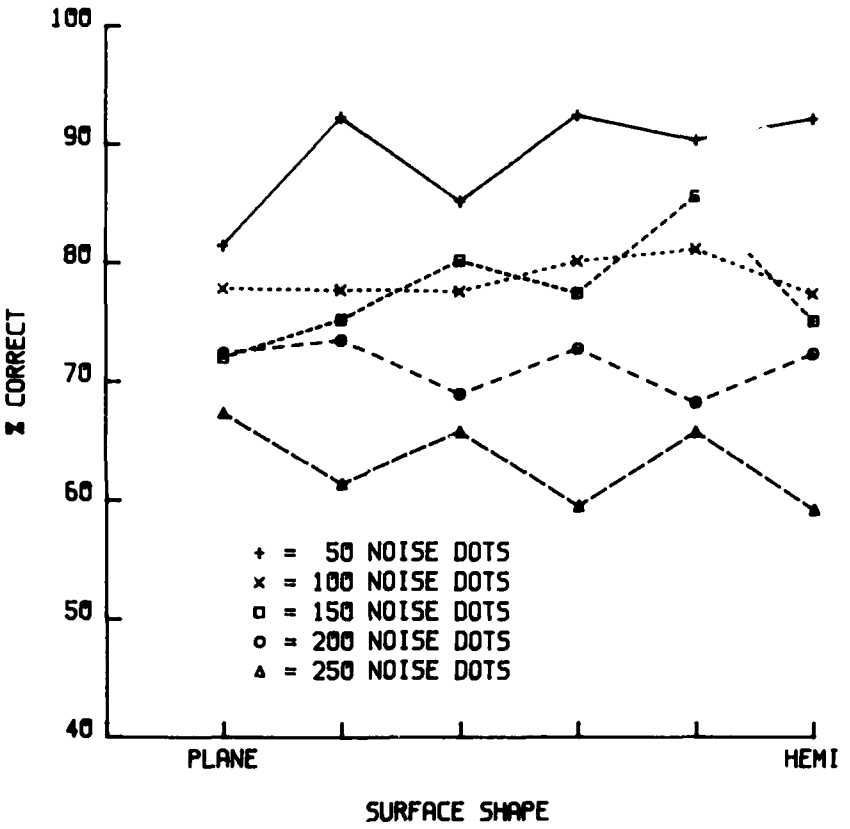
100
90
80
70
60
50
40
% CORRECT
+ = 50 NOISE DOTS
× = 100 NOISE DOTS
□ = 150 NOISE DOTS
○ = 200 NOISE DOTS
△ = 250 NOISE DOTS
PLANE
HEMI
SURFACE SHAPE

Figure 29

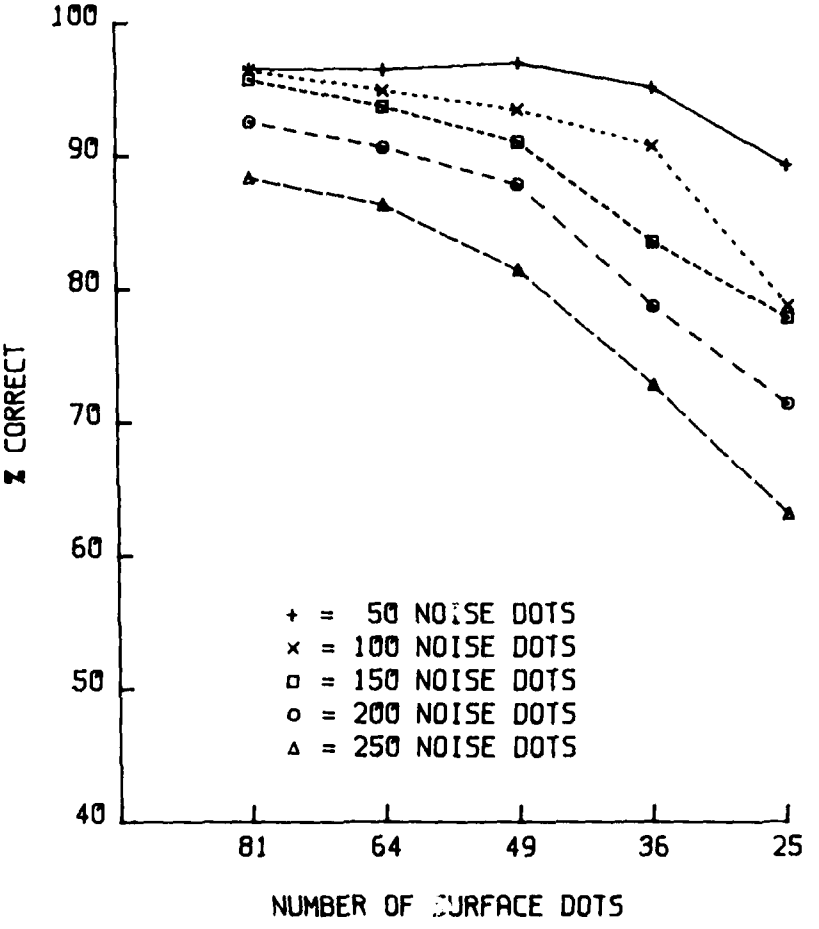
100
90
80
70
60
50
40
% CORRECT
+ = 50 NOISE DOTS
× = 100 NOISE DOTS
□ = 150 NOISE DOTS
○ = 200 NOISE DOTS
△ = 250 NOISE DOTS
81
64
49
36
25
NUMBER OF SURFACE DOTS

Figure 30

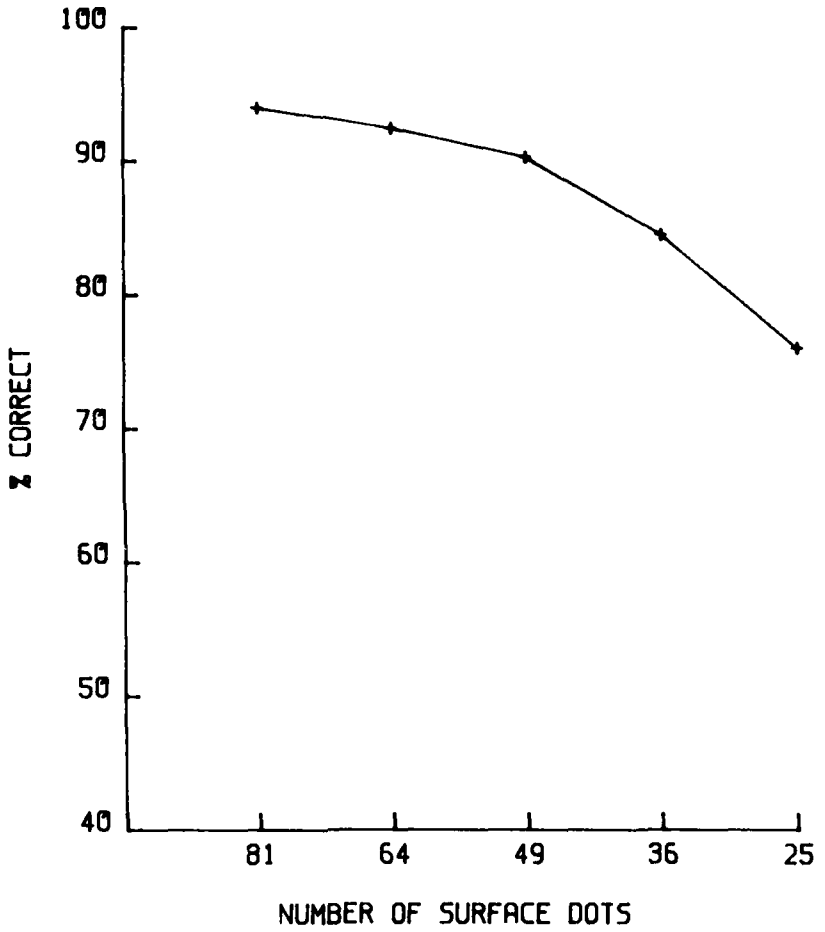
100
90
80
70
60
50
40
% CORRECT
81
64
49
36
25
NUMBER OF SURFACE DOTS

Figure 31

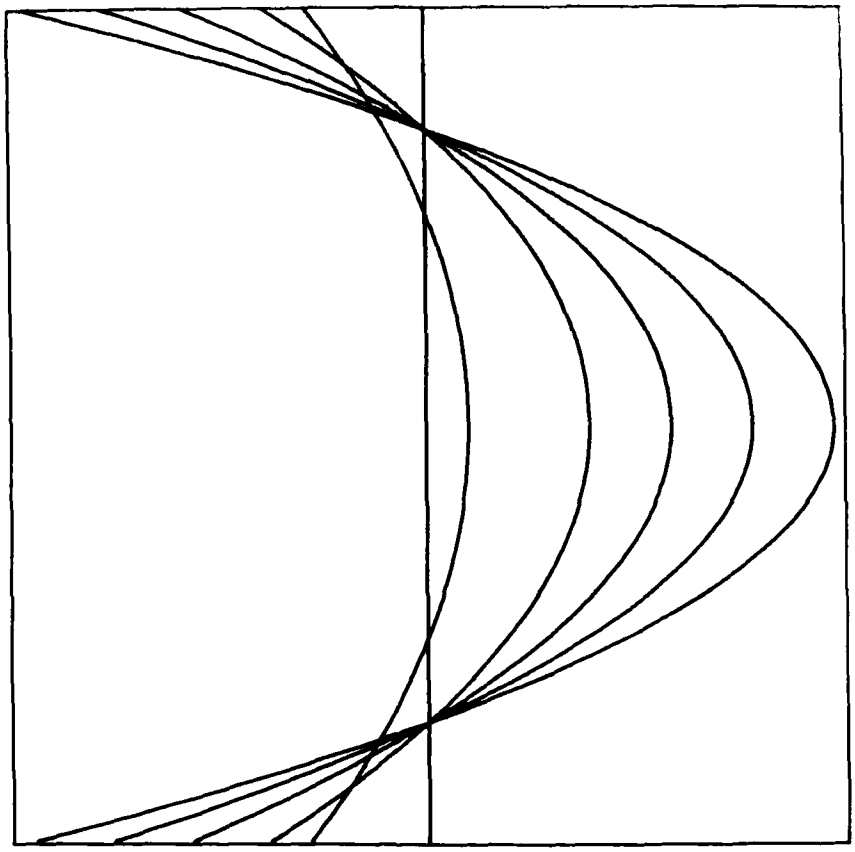

Figure 32

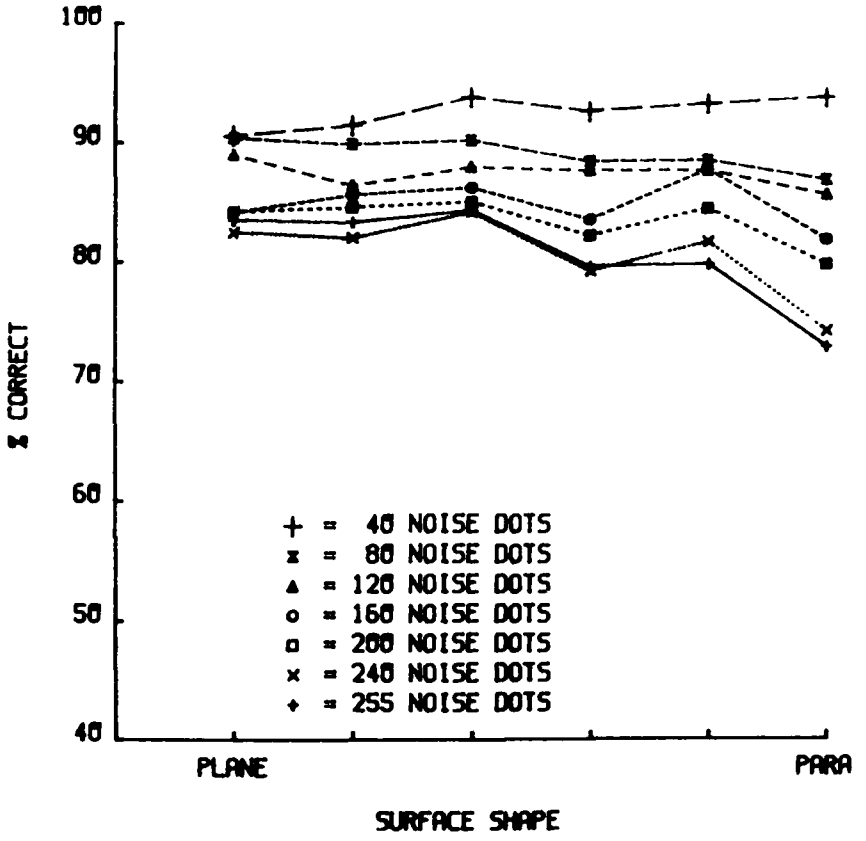
100
90
80
70
60
50
40
% CORRECT
+ = 40 NOISE DOTS
x = 80 NOISE DOTS
▲ = 120 NOISE DOTS
o = 160 NOISE DOTS
□ = 200 NOISE DOTS
× = 240 NOISE DOTS
♦ = 255 NOISE DOTS
PLANE
PARA
SURFACE SHAPE

Figure 33

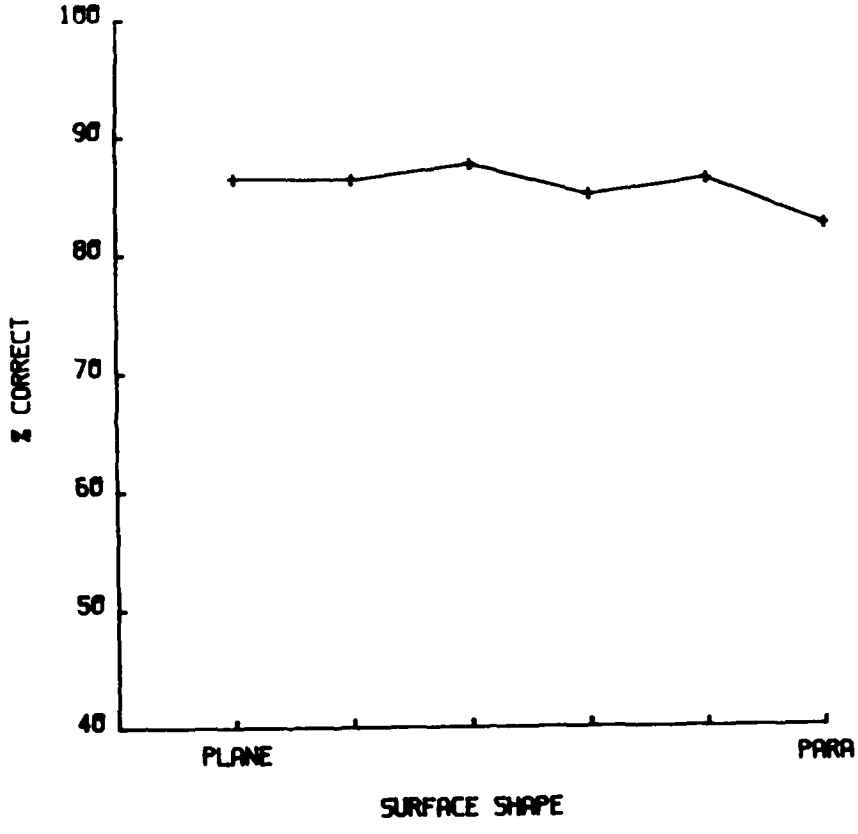

Figure 34

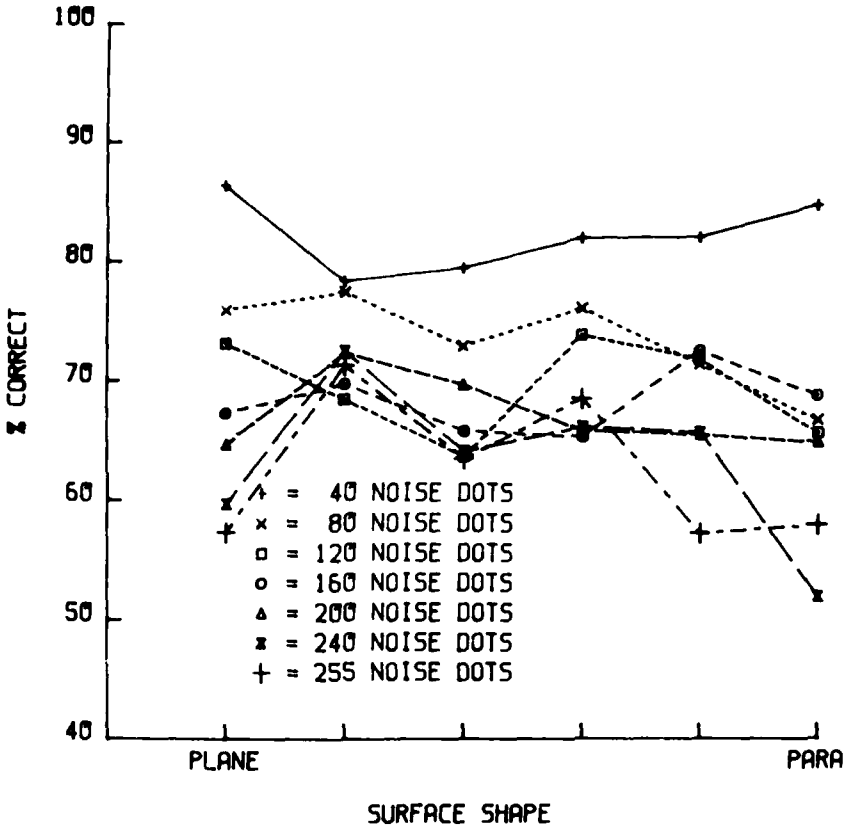
100
90
80
70
60
50
40
% CORRECT
+ = 40 NOISE DOTS
× = 80 NOISE DOTS
□ = 120 NOISE DOTS
○ = 160 NOISE DOTS
△ = 200 NOISE DOTS
⧗ = 240 NOISE DOTS
+ = 255 NOISE DOTS
PLANE
PARA
SURFACE SHAPE

Figure 35

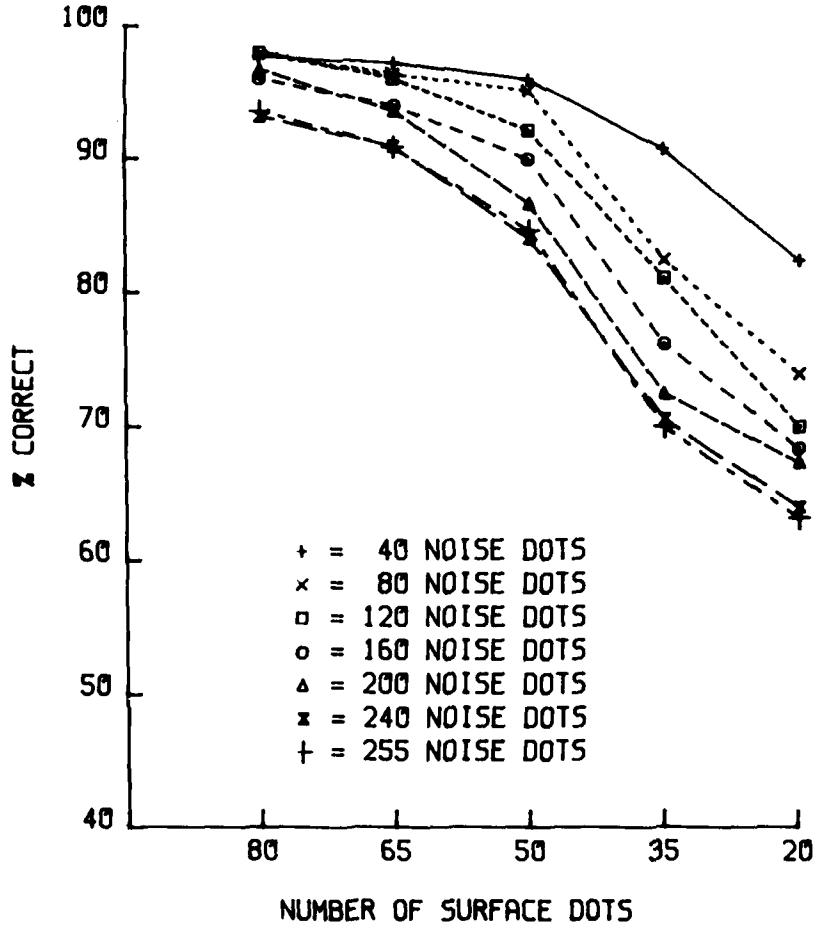
100
90
80
70
60
50
40
% CORRECT
+ = 40 NOISE DOTS
× = 80 NOISE DOTS
□ = 120 NOISE DOTS
o = 160 NOISE DOTS
△ = 200 NOISE DOTS
⧗ = 240 NOISE DOTS
+ = 255 NOISE DOTS
80
65
50
35
20
NUMBER OF SURFACE DOTS

Figure 36

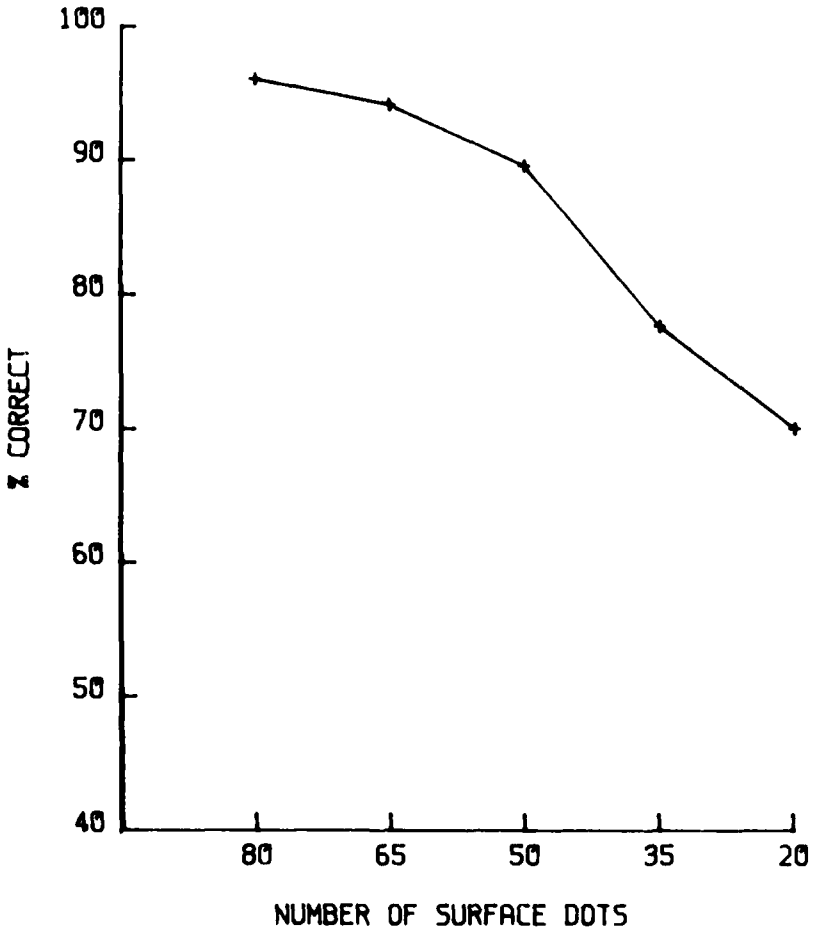
100
90
80
70
60
50
40
% CORRECT
80
65
50
35
20
NUMBER OF SURFACE DOTS

Figure 37

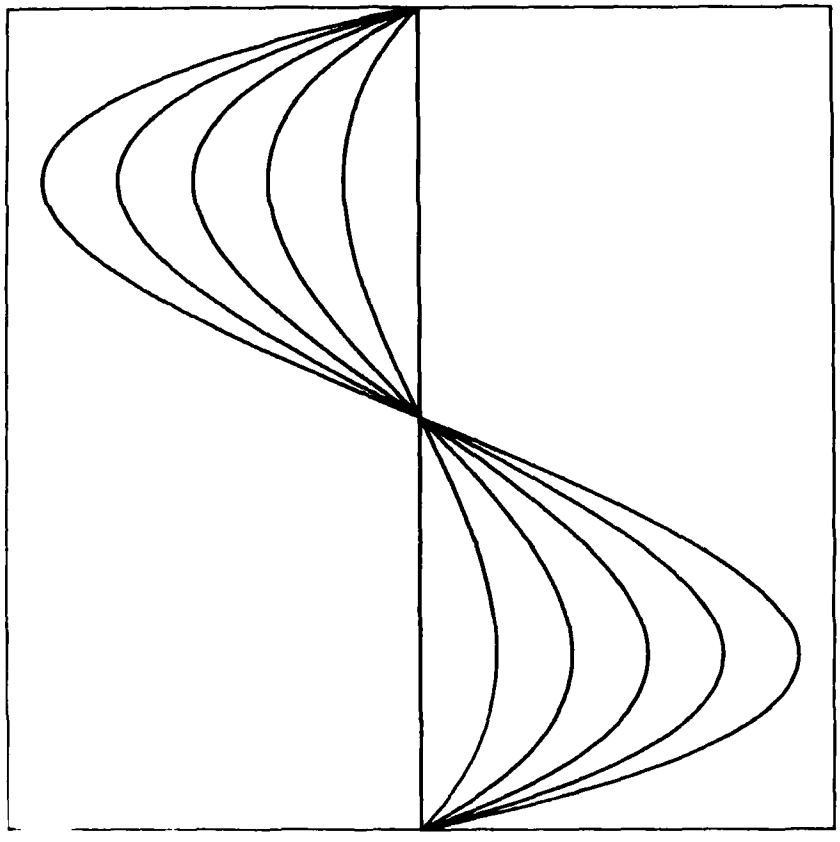

Figure 38

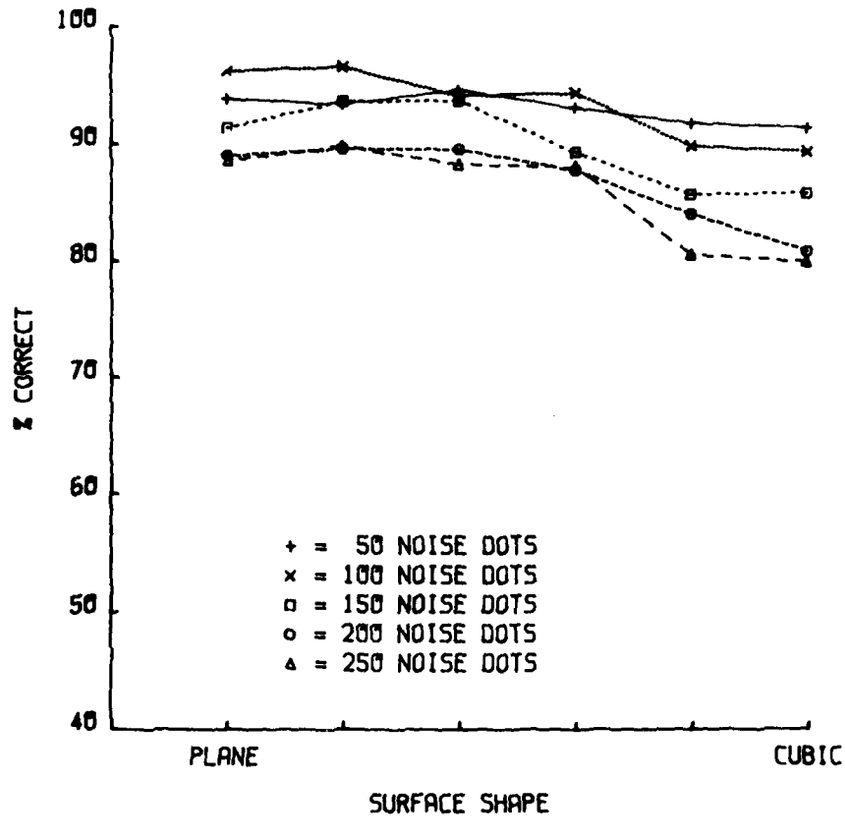
100
90
80
70
60
50
40
% CORRECT
+ = 50 NOISE DOTS
× = 100 NOISE DOTS
□ = 150 NOISE DOTS
○ = 200 NOISE DOTS
△ = 250 NOISE DOTS
PLANE
CUBIC
SURFACE SHAPE

Figure 39

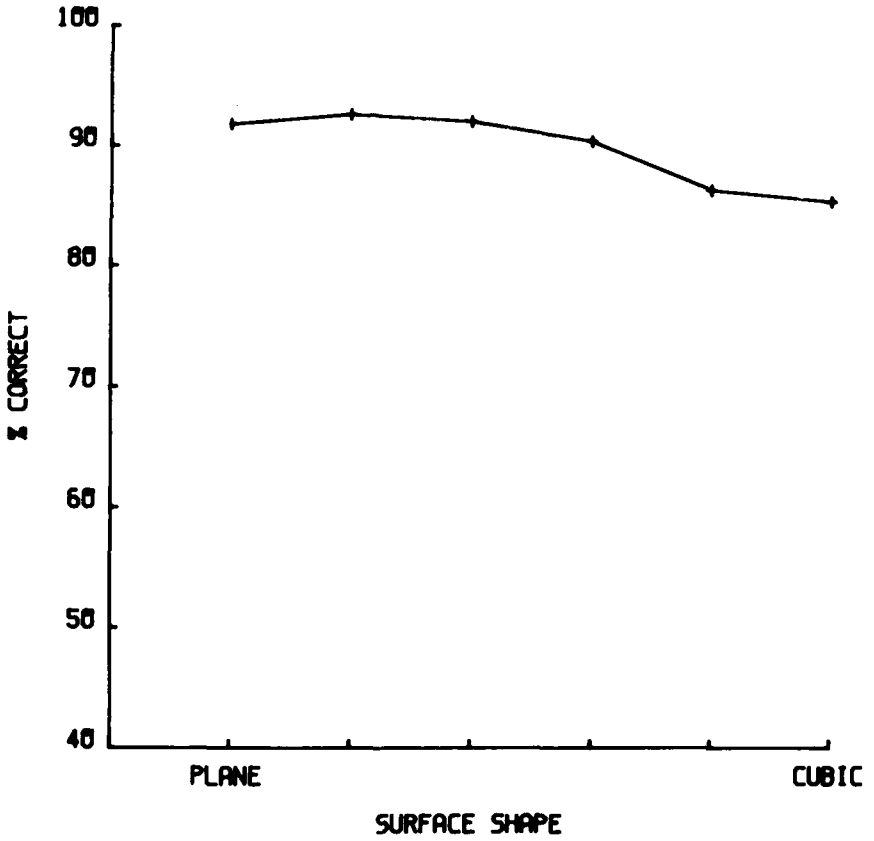

Figure 40

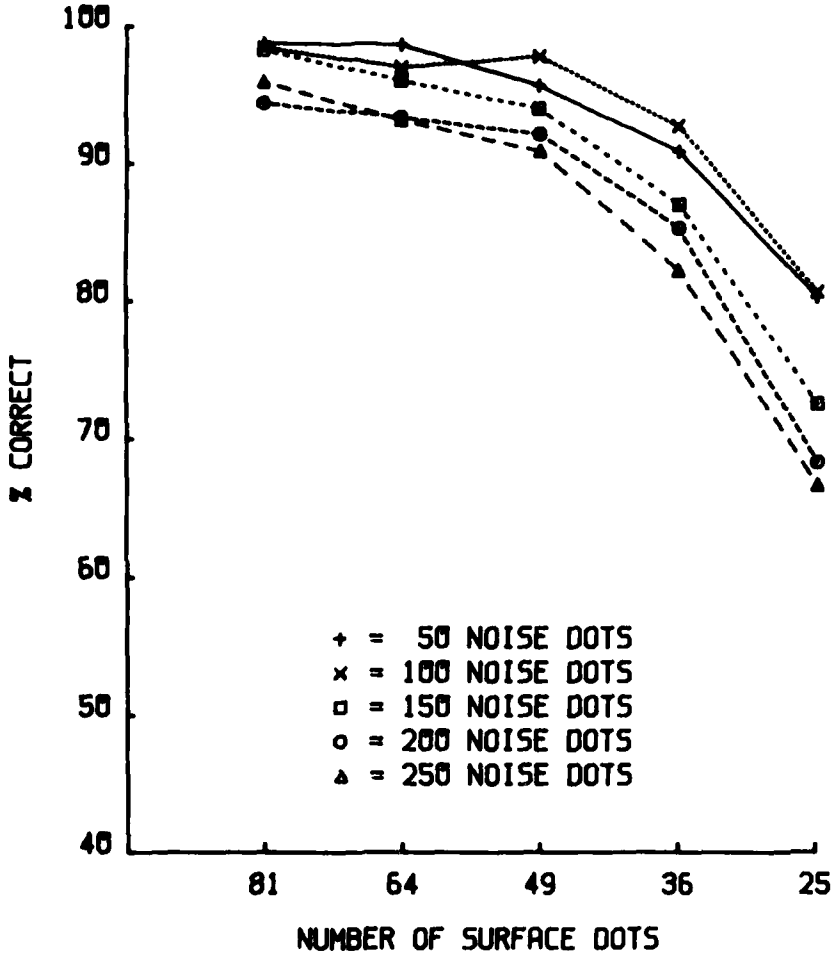
100
90
80
70
60
50
40
% CORRECT
+ = 50 NOISE DOTS
× = 100 NOISE DOTS
□ = 150 NOISE DOTS
○ = 200 NOISE DOTS
△ = 250 NOISE DOTS
81
64
49
36
25
NUMBER OF SURFACE DOTS

Figure 41

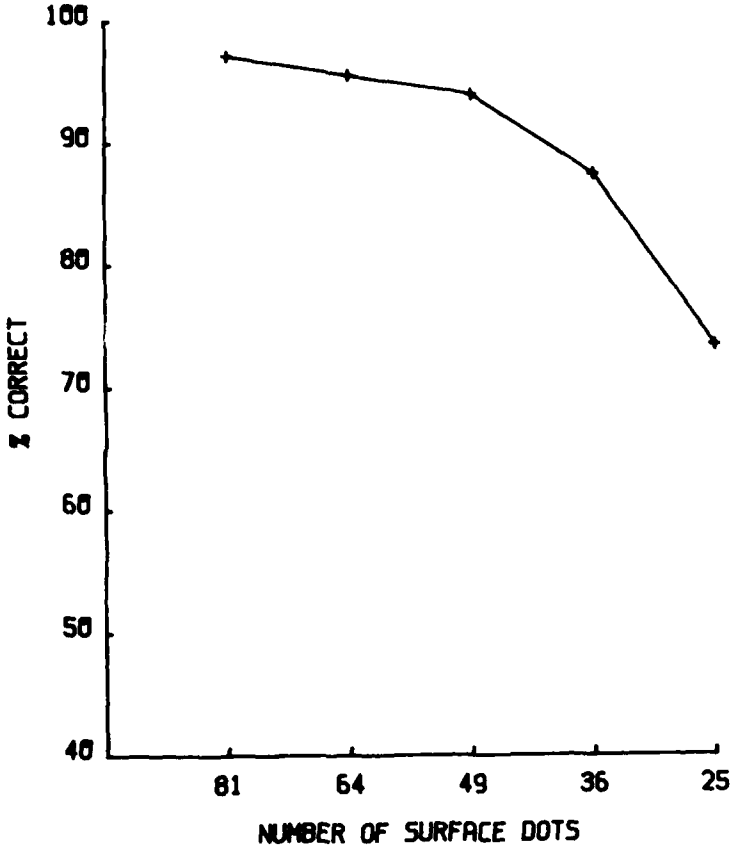
100
90
80
70
60
50
40
% CORRECT
81
64
49
36
25
NUMBER OF SURFACE DOTS

Figure 42

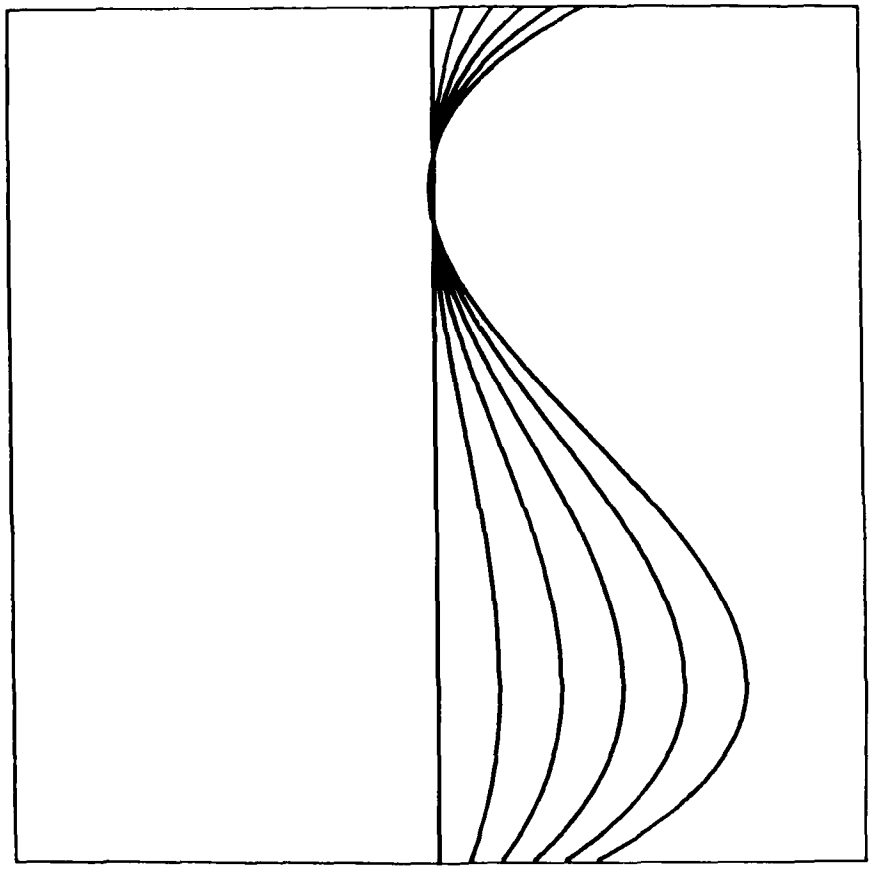

Figure 43

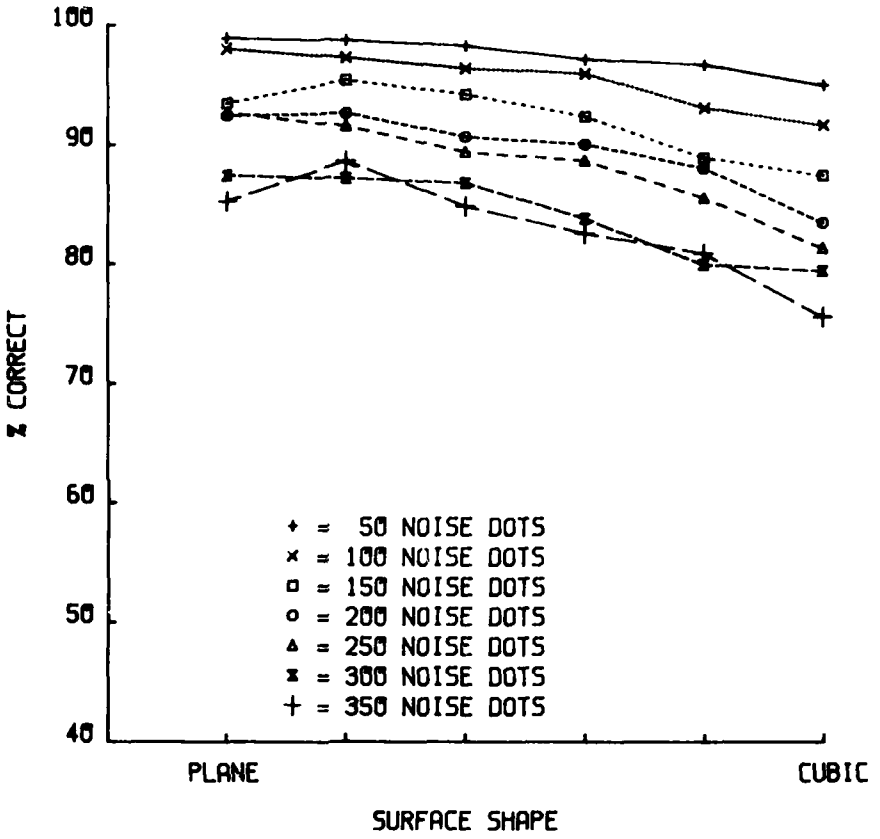
100
90
80
70
60
50
40
% CORRECT
+ = 50 NOISE DOTS
× = 100 NOISE DOTS
□ = 150 NOISE DOTS
○ = 200 NOISE DOTS
△ = 250 NOISE DOTS
⧗ = 300 NOISE DOTS
+ = 350 NOISE DOTS
PLANE
CUBIC
SURFACE SHAPE

Figure 44

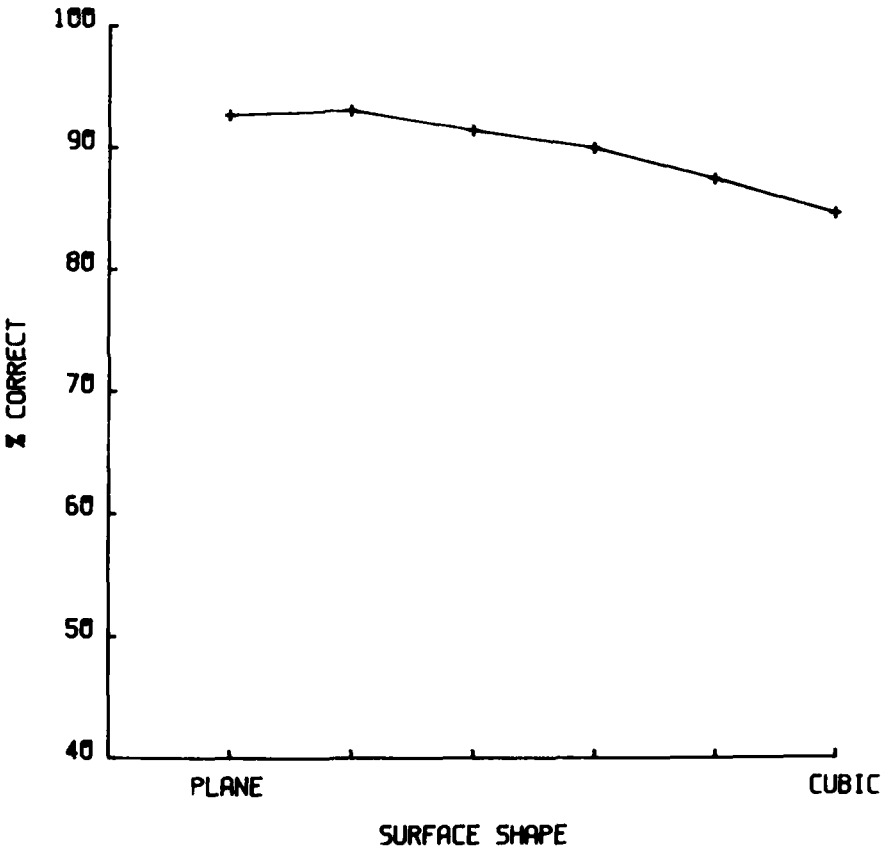

Figure 45

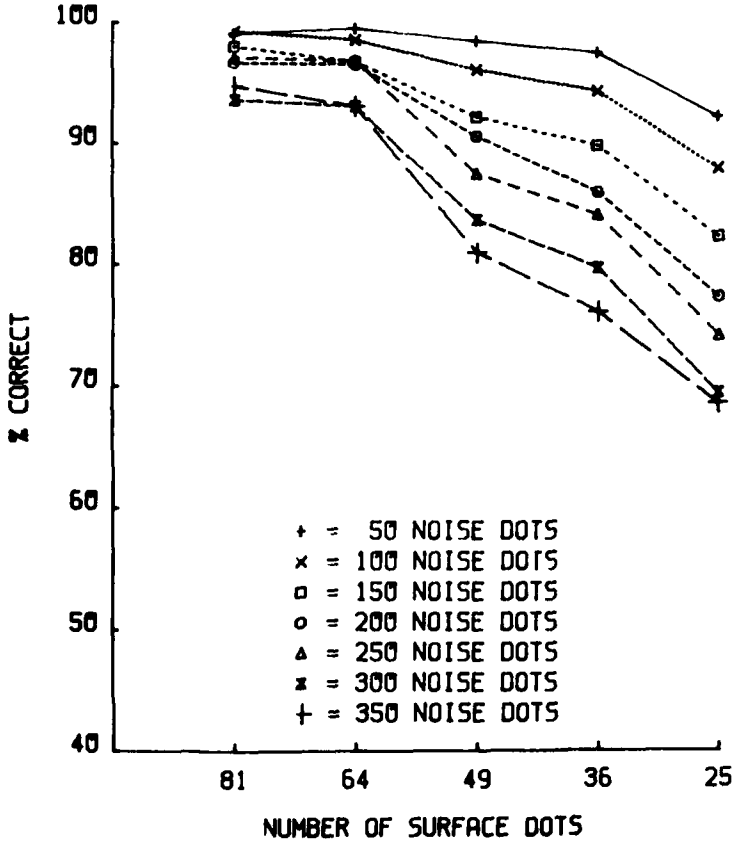
100
90
80
70
60
50
40
% CORRECT
+ = 50 NOISE DOTS
× = 100 NOISE DOTS
□ = 150 NOISE DOTS
o = 200 NOISE DOTS
△ = 250 NOISE DOTS
⧗ = 300 NOISE DOTS
+ = 350 NOISE DOTS
81
64
49
36
25
NUMBER OF SURFACE DOTS

Figure 46

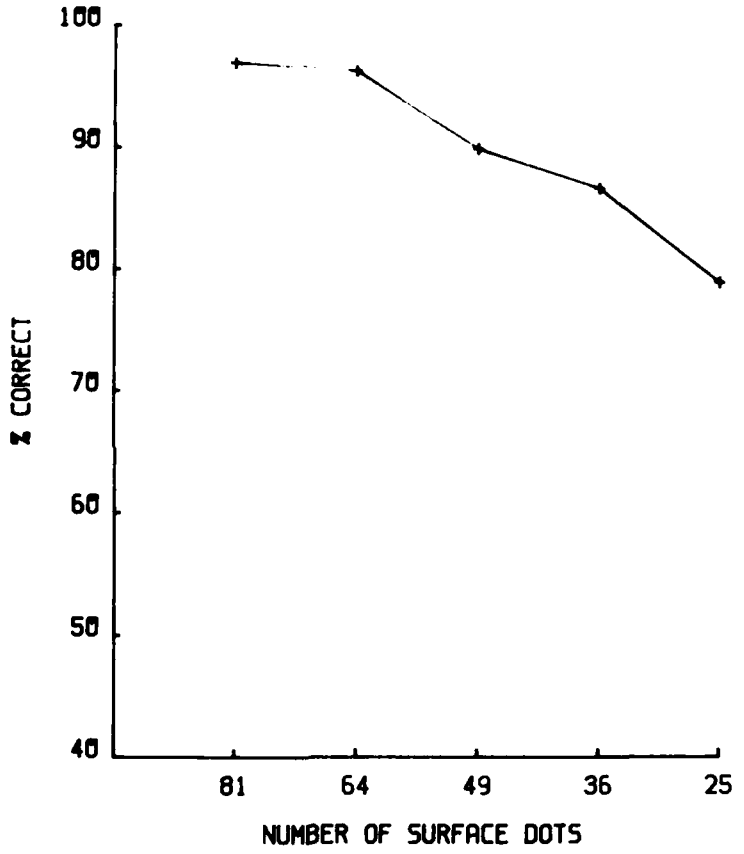
100
90
80
70
60
50
40
% CORRECT
81
64
49
36
25
NUMBER OF SURFACE DOTS

Figure 47

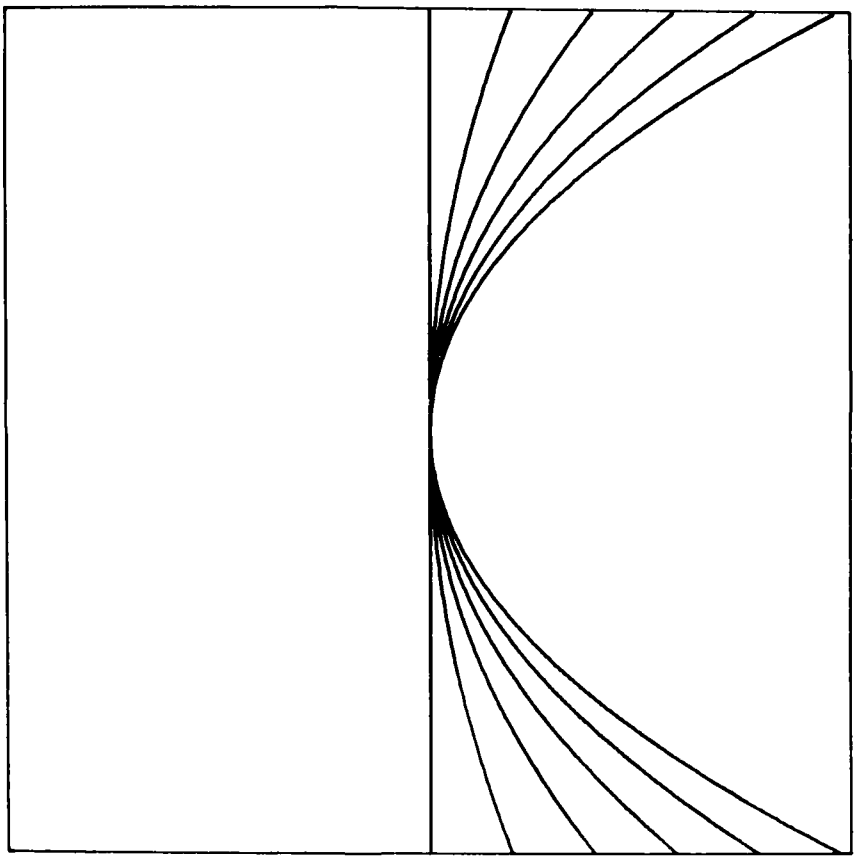

Figure 48

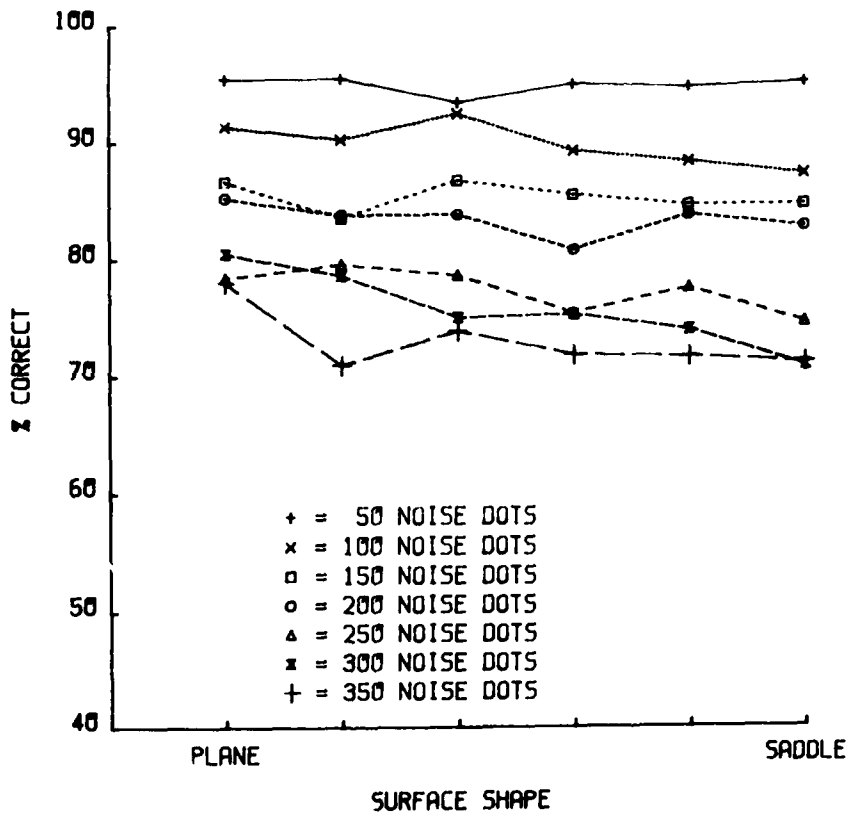
100
90
80
70
60
50
40
% CORRECT
+ = 50 NOISE DOTS
× = 100 NOISE DOTS
□ = 150 NOISE DOTS
○ = 200 NOISE DOTS
△ = 250 NOISE DOTS
⧗ = 300 NOISE DOTS
+ = 350 NOISE DOTS
PLANE
SADDLE
SURFACE SHAPE

Figure 49

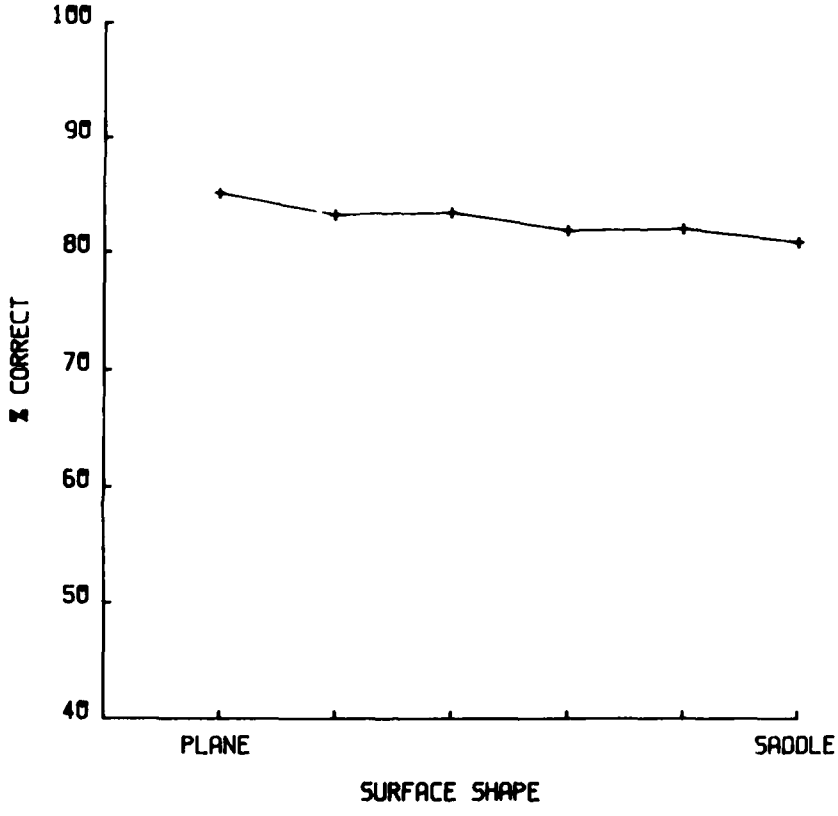

Figure 50

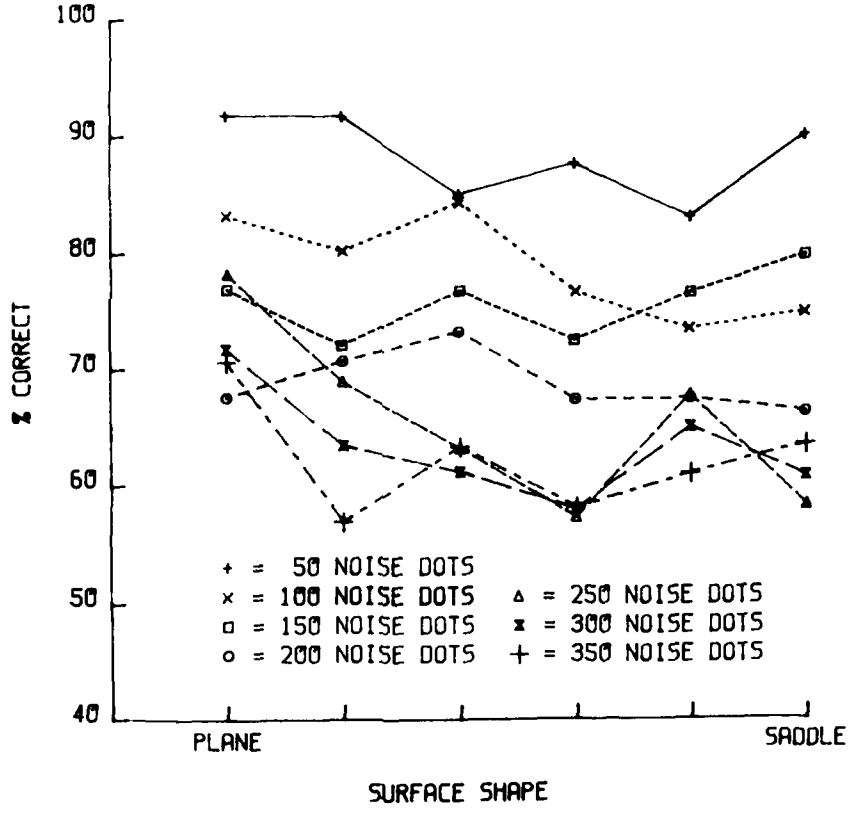
100
90
80
70
60
50
40
% CORRECT
+ = 50 NOISE DOTS
× = 100 NOISE DOTS
□ = 150 NOISE DOTS
○ = 200 NOISE DOTS
△ = 250 NOISE DOTS
⧗ = 300 NOISE DOTS
+ = 350 NOISE DOTS
PLANE
SADDLE
SURFACE SHAPE

Figure 51

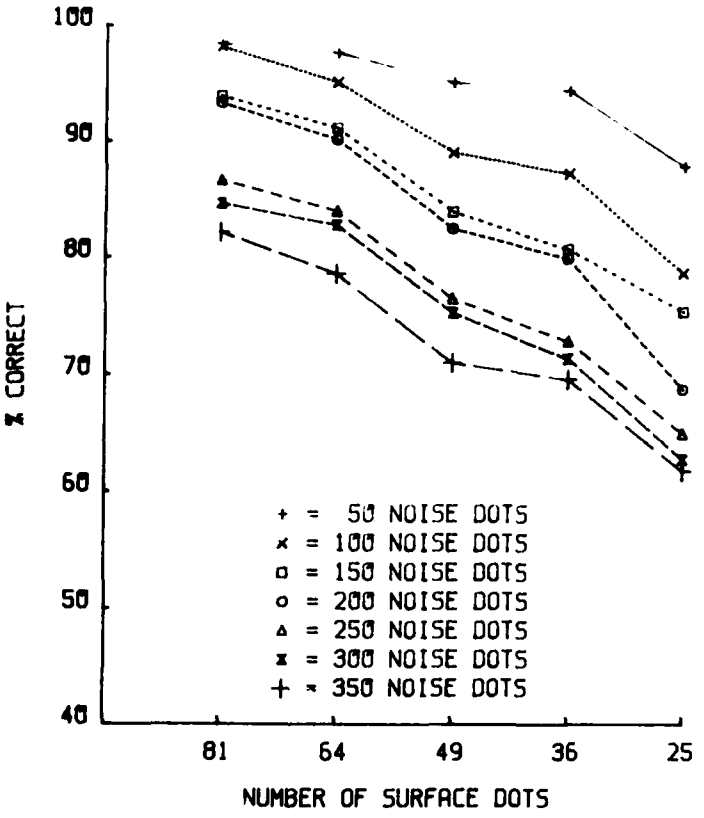
100
90
80
70
60
50
40
% CORRECT
+ = 50 NOISE DOTS
× = 100 NOISE DOTS
□ = 150 NOISE DOTS
○ = 200 NOISE DOTS
△ = 250 NOISE DOTS
⧗ = 300 NOISE DOTS
+ = 350 NOISE DOTS
81
64
49
36
25
NUMBER OF SURFACE DOTS

Figure 52

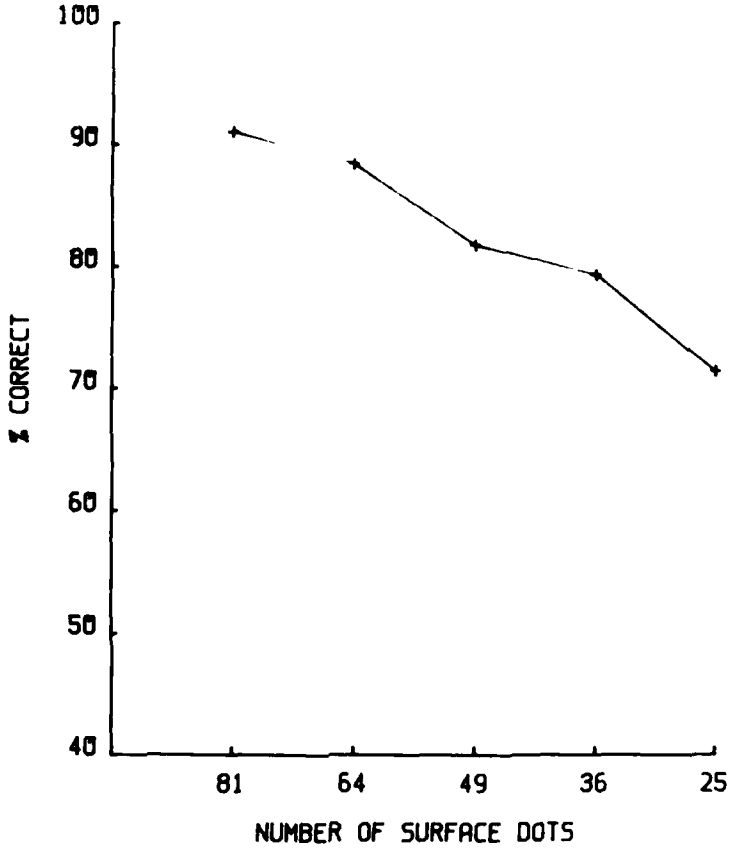
100
90
80
70
60
50
40
% CORRECT
81
64
49
36
25
NUMBER OF SURFACE DOTS

Figure 53

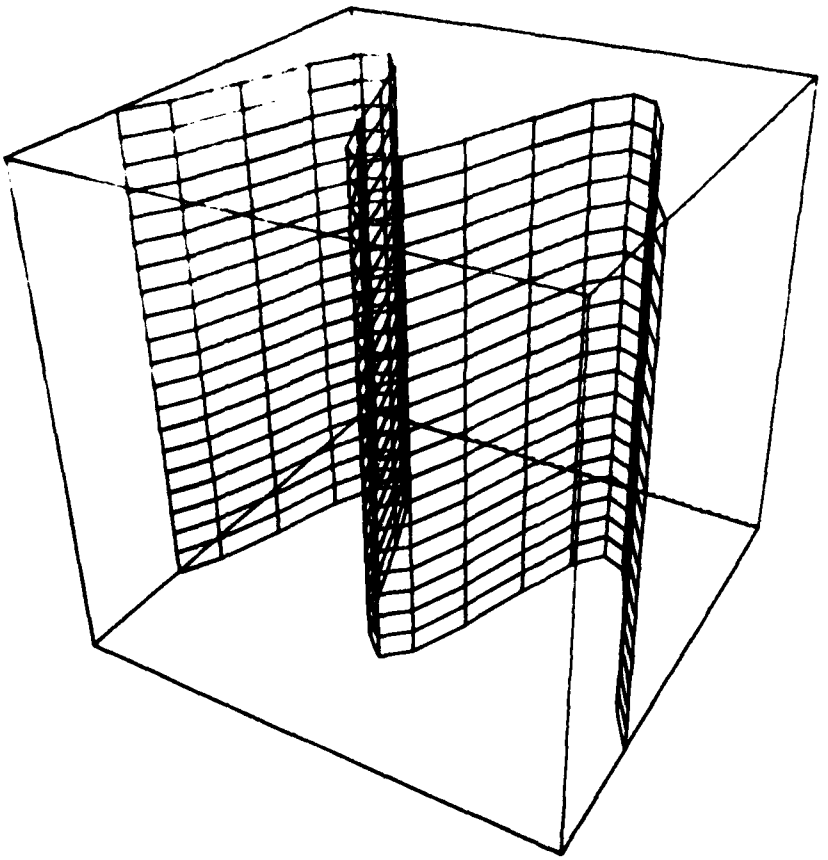

Figure 54

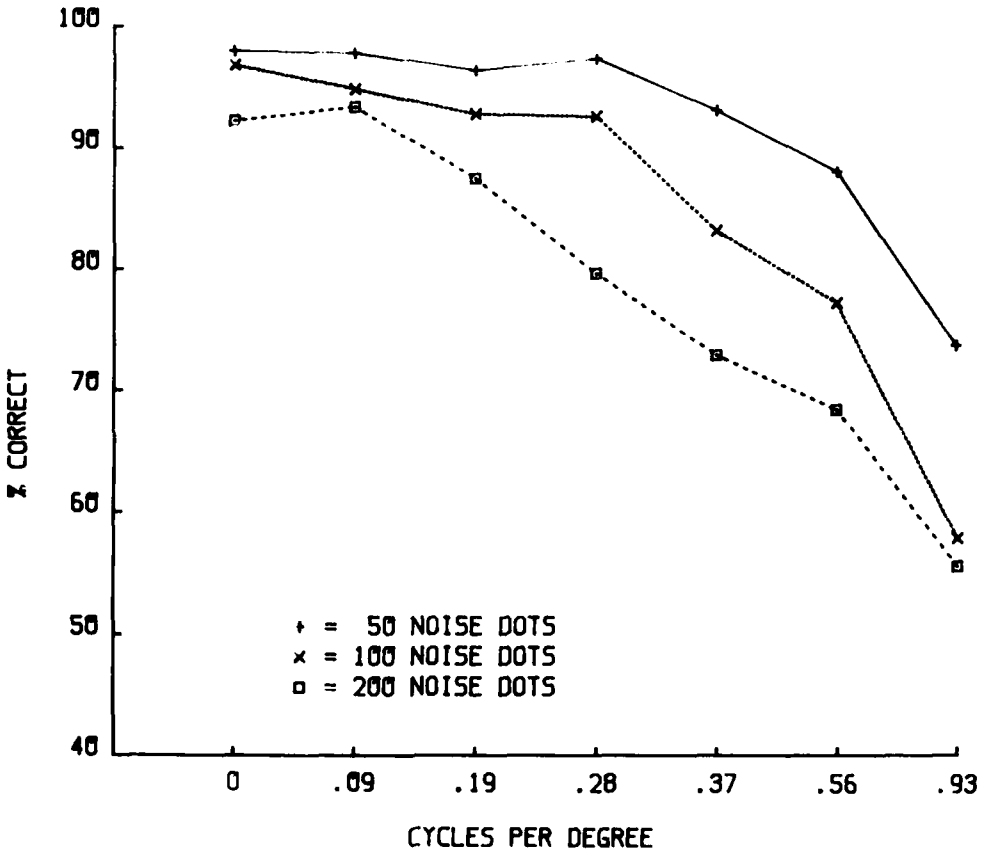
100
90
80
70
60
50
40
% CORRECT
+ = 50 NOISE DOTS
× = 100 NOISE DOTS
□ = 200 NOISE DOTS
0
.09
.19
.28
.37
.56
.93
CYCLES PER DEGREE

Figure 55

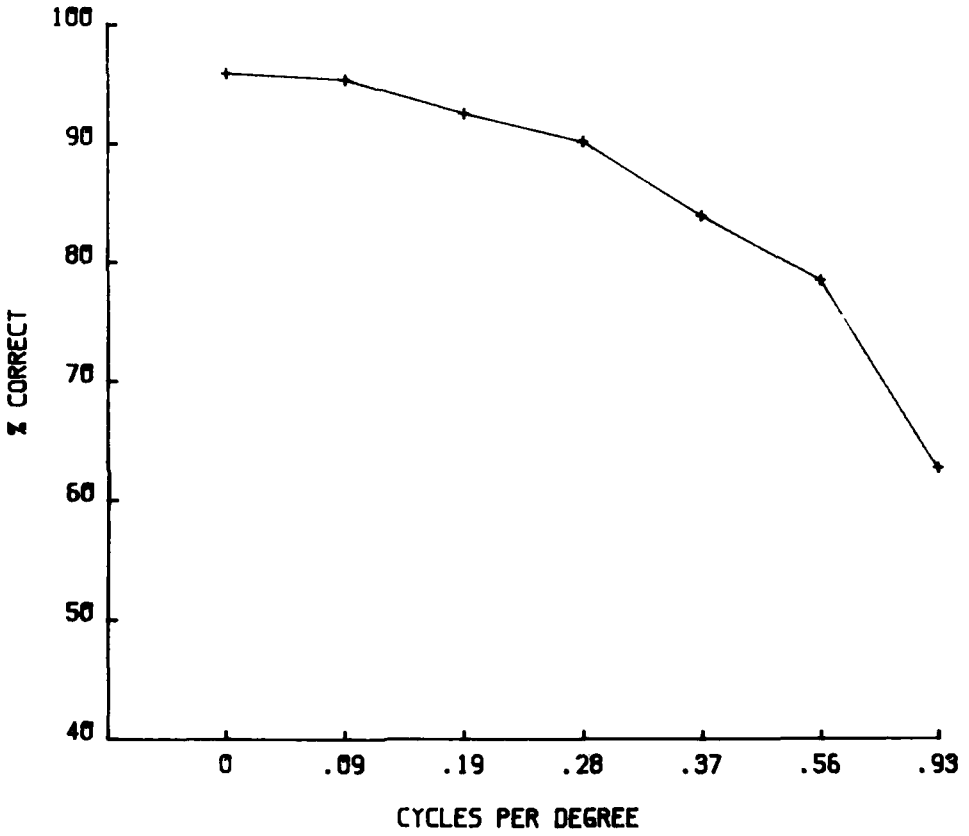
100
90
80
70
60
50
40
% CORRECT
0
.09
.19
.28
.37
.56
.93
CYCLES PER DEGREE

Figure 56

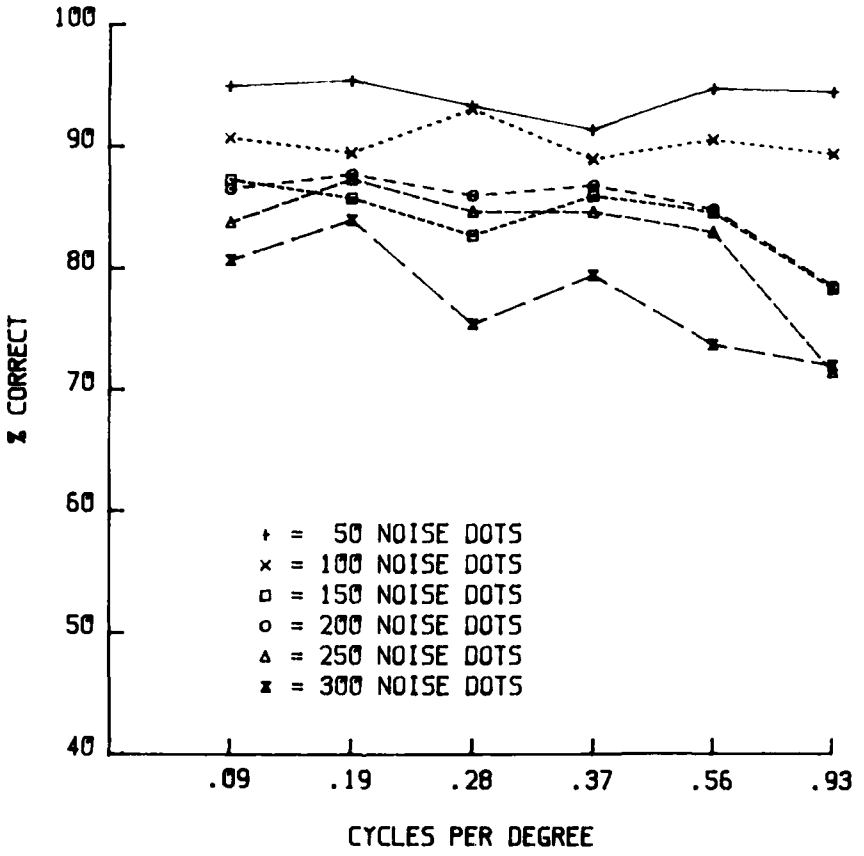
100
90
80
70
60
50
40
% CORRECT
+ = 50 NOISE DOTS
× = 100 NOISE DOTS
□ = 150 NOISE DOTS
○ = 200 NOISE DOTS
△ = 250 NOISE DOTS
⧗ = 300 NOISE DOTS
.09
.19
.28
.37
.56
.93
CYCLES PER DEGREE

Figure 57

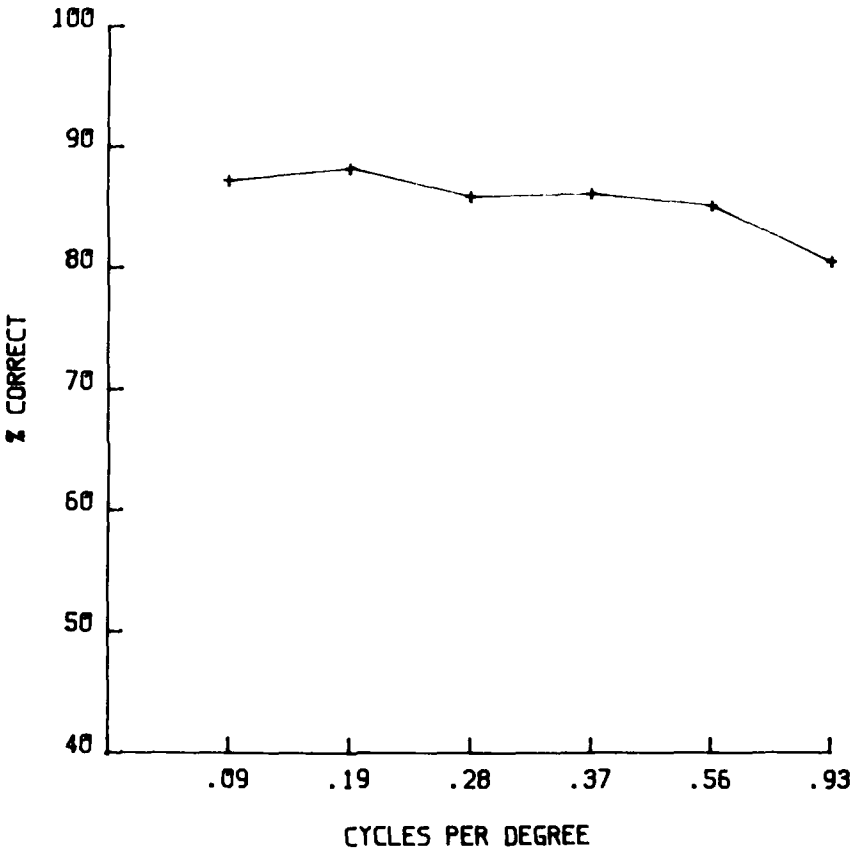

Figure 58

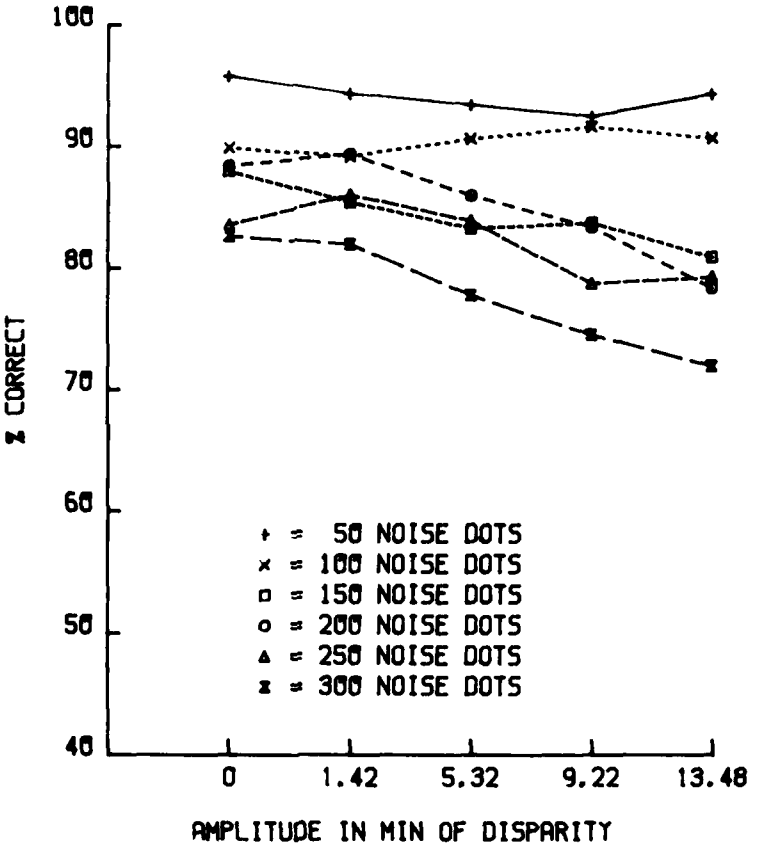
100
90
80
70
60
50
40
% CORRECT
+ = 50 NOISE DOTS
× = 100 NOISE DOTS
□ = 150 NOISE DOTS
○ = 200 NOISE DOTS
△ = 250 NOISE DOTS
⧗ = 300 NOISE DOTS
0
1.42
5.32
9.22
13.48
AMPLITUDE IN MIN OF DISPARITY

Figure 59

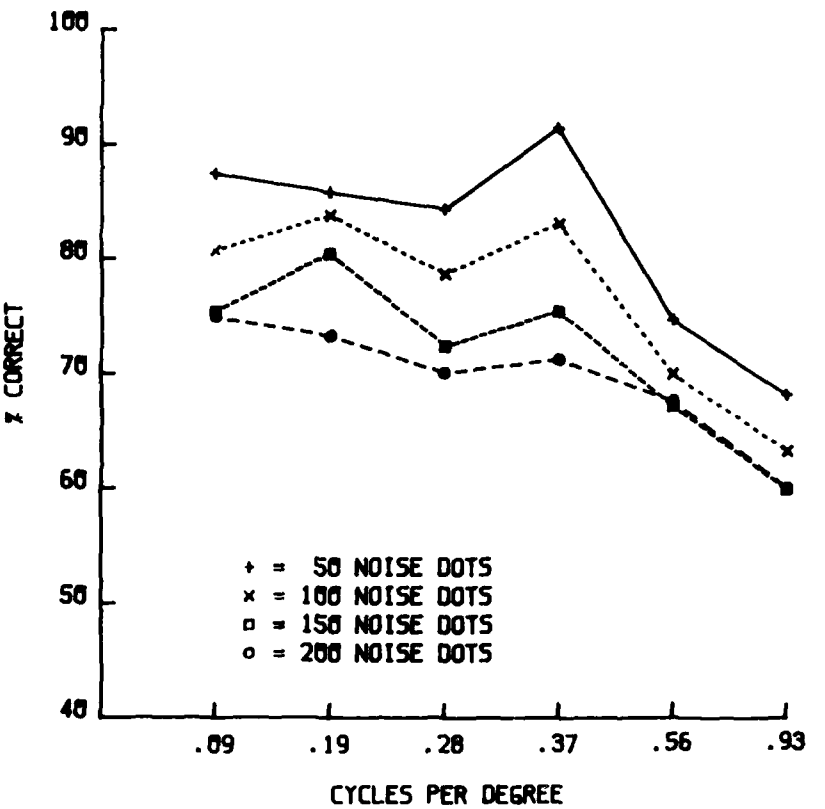
100
90
80
70
60
50
40
% CORRECT
+ = 50 NOISE DOTS
× = 100 NOISE DOTS
□ = 150 NOISE DOTS
○ = 200 NOISE DOTS
.09
.19
.28
.37
.56
.93
CYCLES PER DEGREE

Figure 60

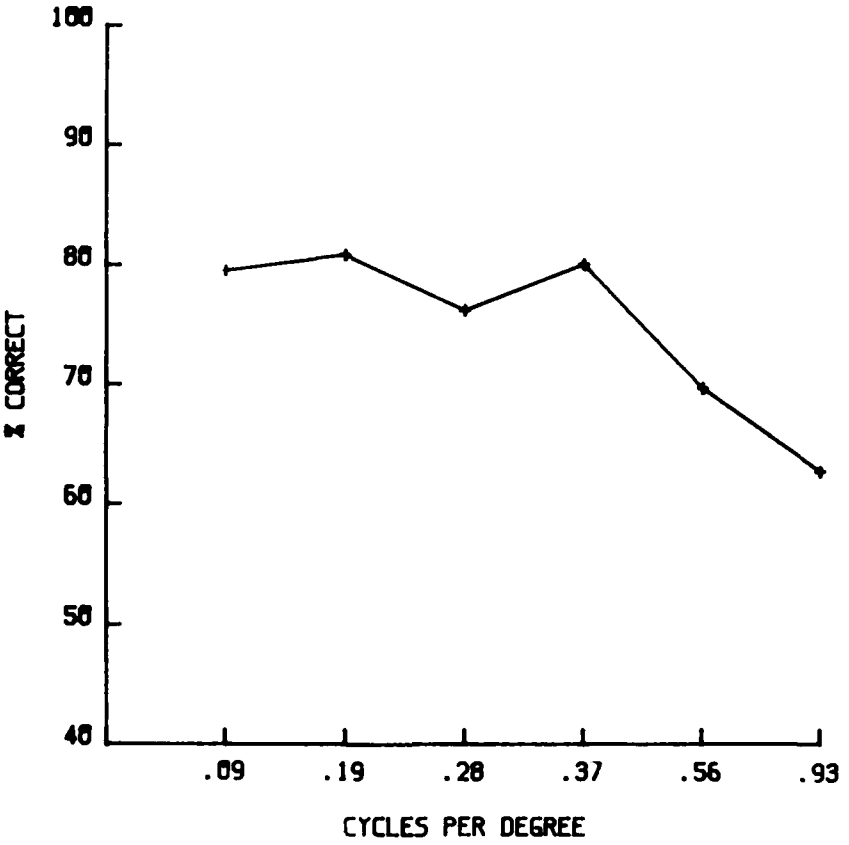

Figure 61

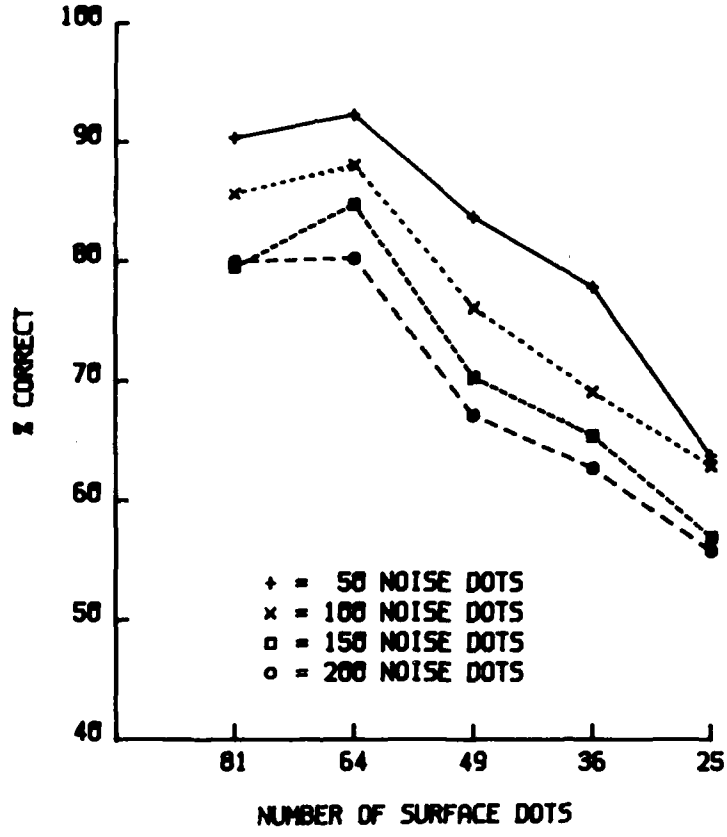
100
90
80
70
60
50
40
% CORRECT
+ = 50 NOISE DOTS
× = 100 NOISE DOTS
□ = 150 NOISE DOTS
○ = 200 NOISE DOTS
81
64
49
36
25
NUMBER OF SURFACE DOTS

Figure 62

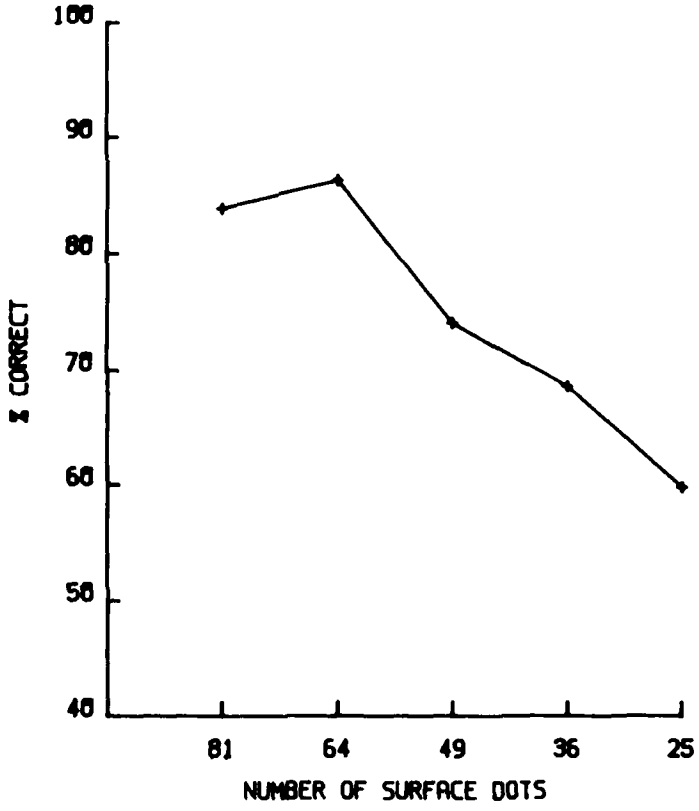
100
90
80
70
60
50
40
% CORRECT
81
64
49
36
25
NUMBER OF SURFACE DOTS

Figure 63

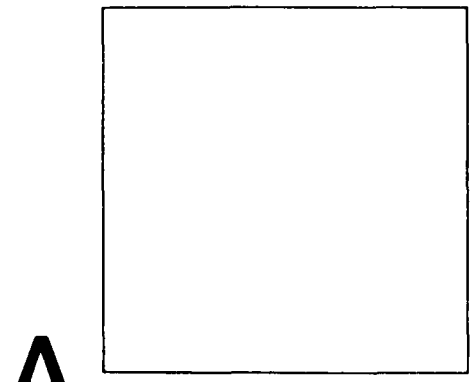
A

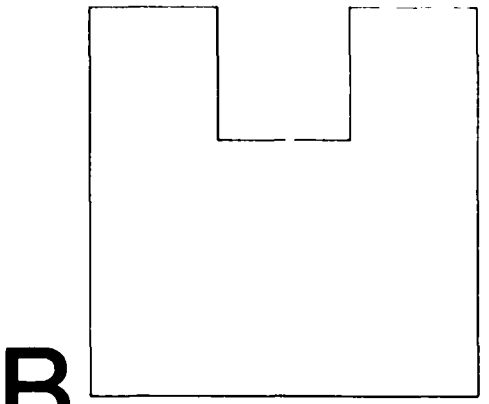
B

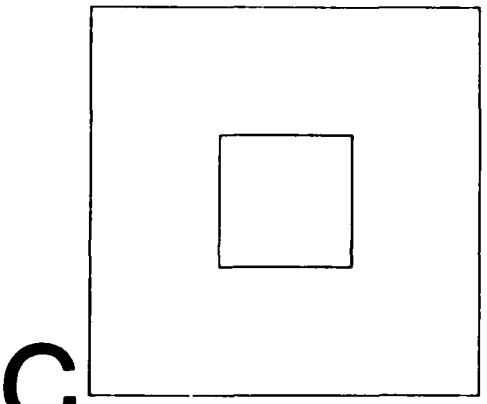
C

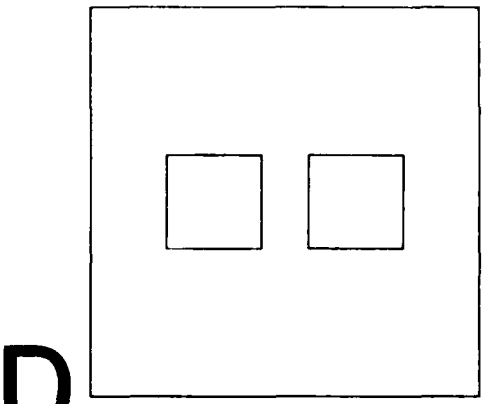
D

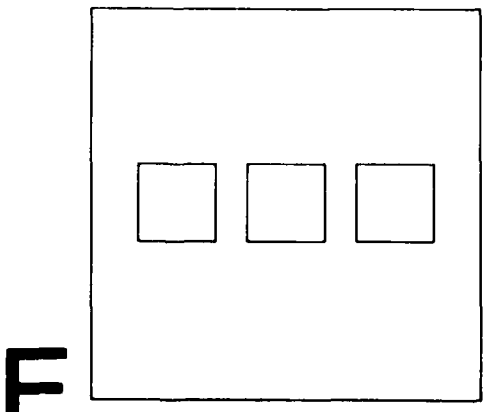
E

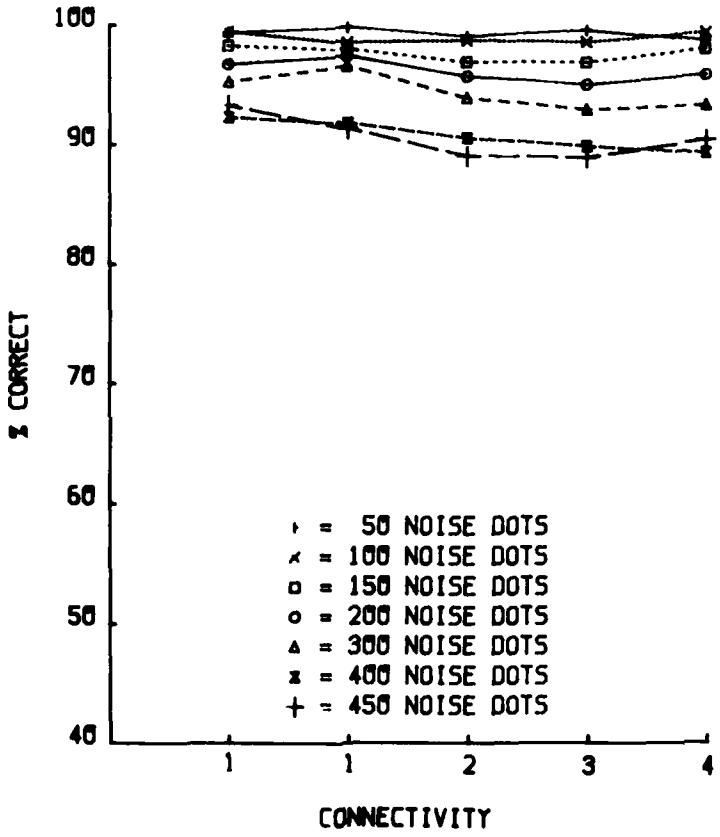
100
90
80
70
60
50
40
% CORRECT
1
1
2
3
4
CONNECTIVITY
= 50 NOISE DOTS
= 100 NOISE DOTS
= 150 NOISE DOTS
= 200 NOISE DOTS
= 300 NOISE DOTS
= 400 NOISE DOTS
= 450 NOISE DOTS

Figure 65

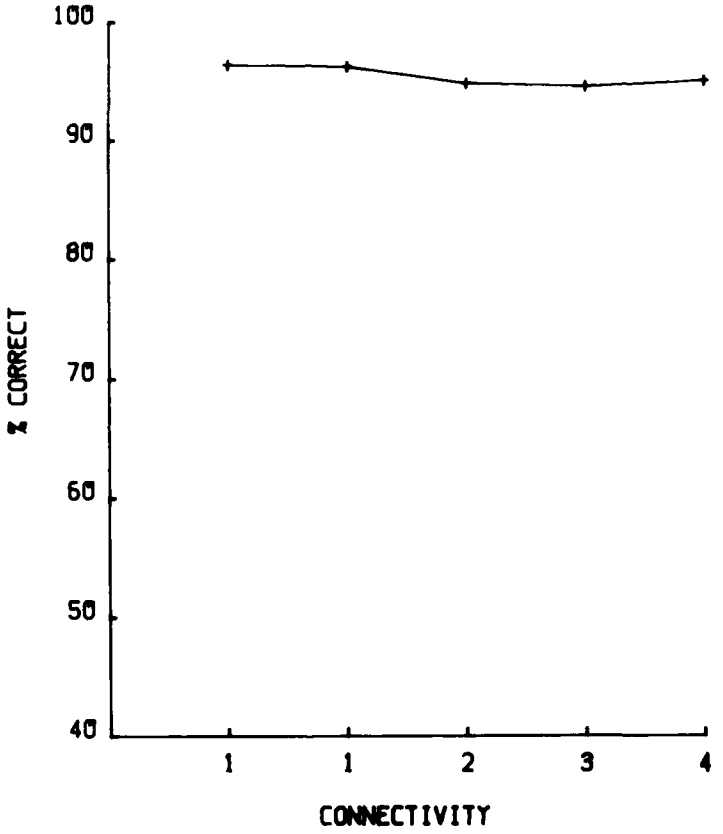

Figure 66

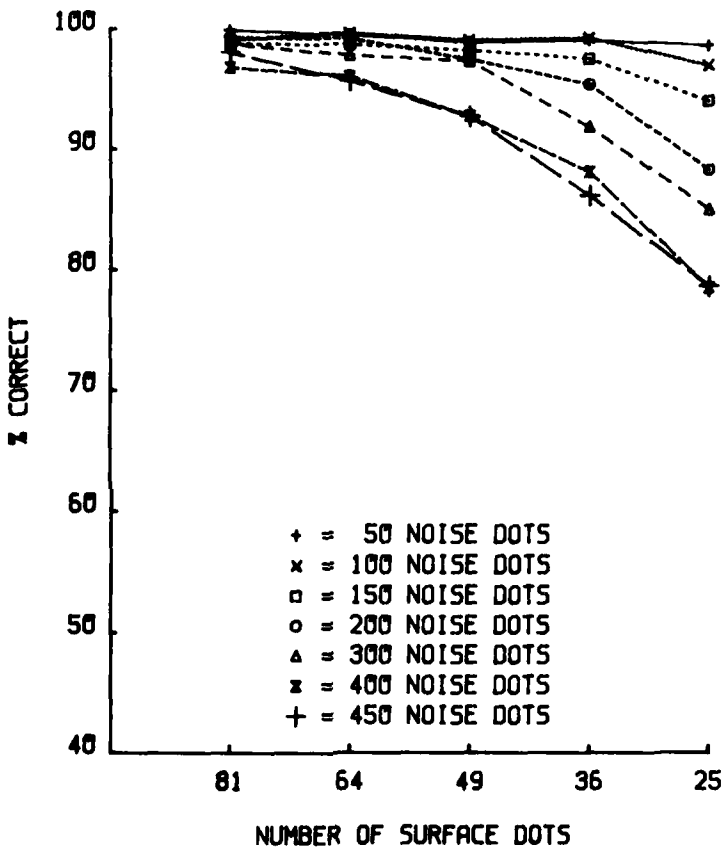
100
90
80
70
60
50
40
% CORRECT
+ = 50 NOISE DOTS
x = 100 NOISE DOTS
□ = 150 NOISE DOTS
o = 200 NOISE DOTS
△ = 300 NOISE DOTS
⧗ = 400 NOISE DOTS
+ = 450 NOISE DOTS
81
64
49
36
25
NUMBER OF SURFACE DOTS

Figure 67

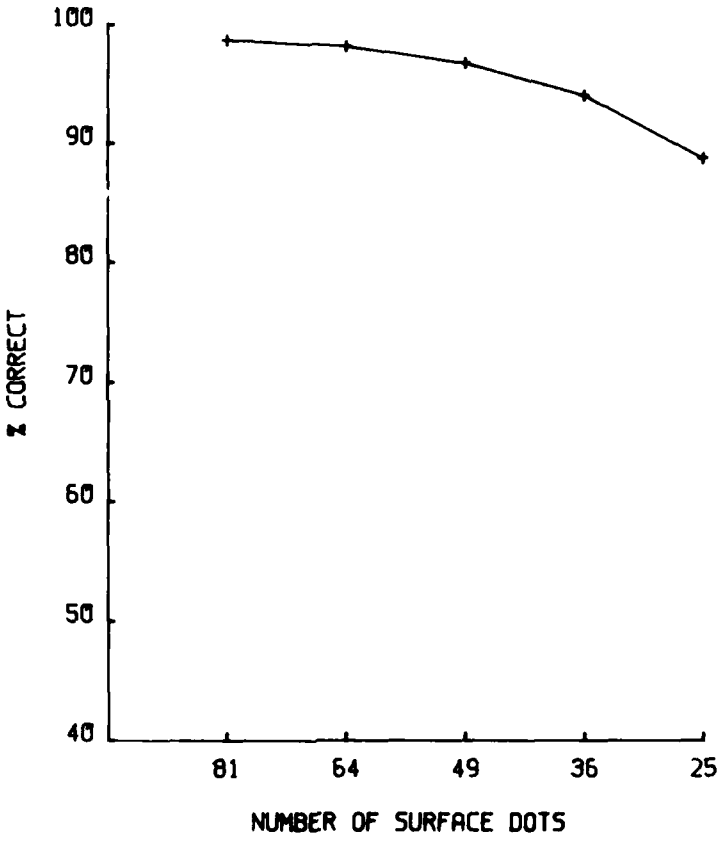
100
90
80
70
60
50
40
% CORRECT
81
64
49
36
25
NUMBER OF SURFACE DOTS

Figure 68

A

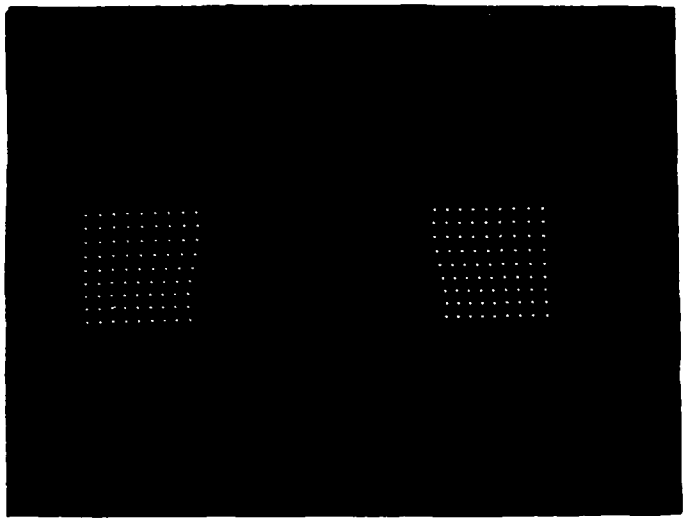

B

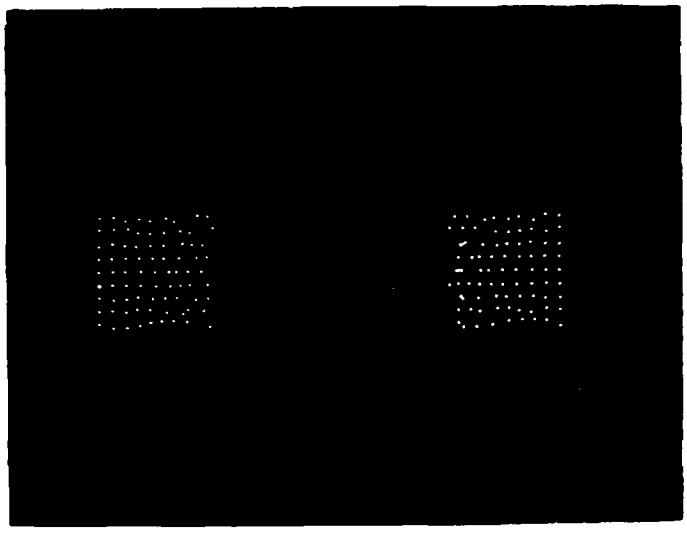

Figure 69

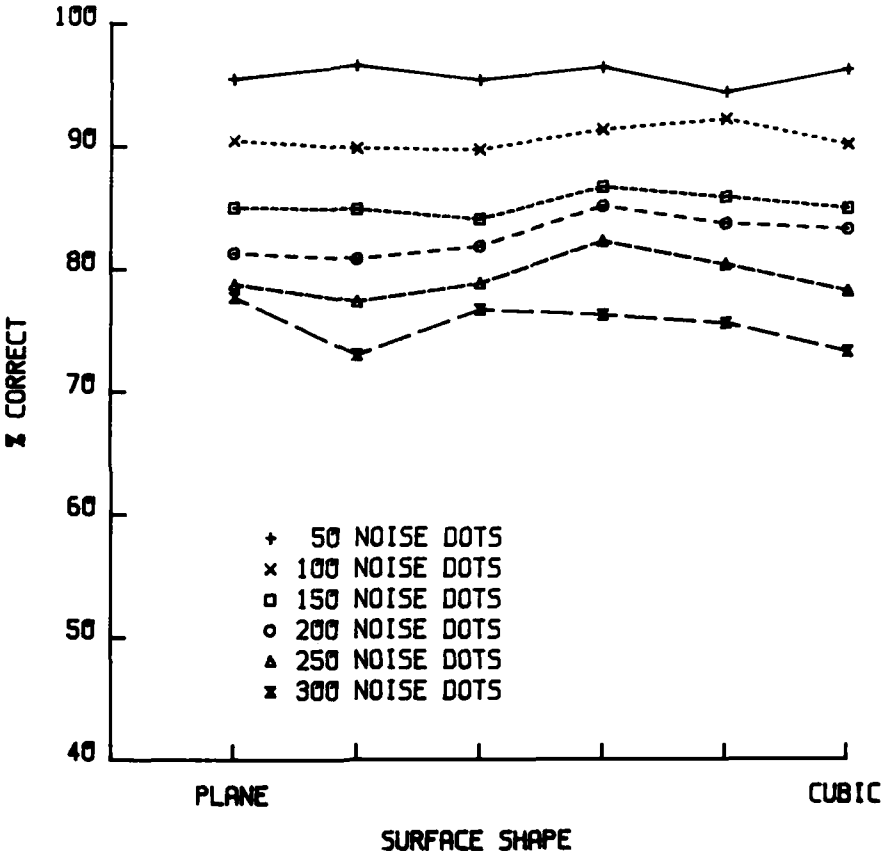
100
90
80
70
60
50
40
% CORRECT
+ 50 NOISE DOTS
× 100 NOISE DOTS
□ 150 NOISE DOTS
○ 200 NOISE DOTS
△ 250 NOISE DOTS
⧗ 300 NOISE DOTS
PLANE
CUBIC
SURFACE SHAPE

Figure 70

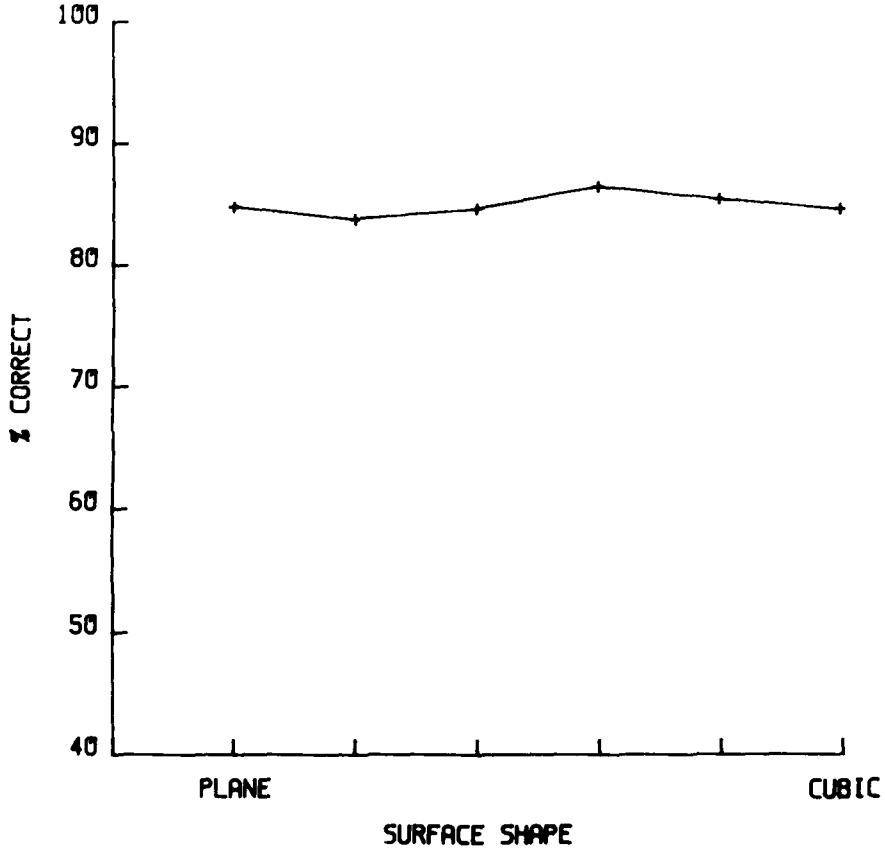

Figure 71

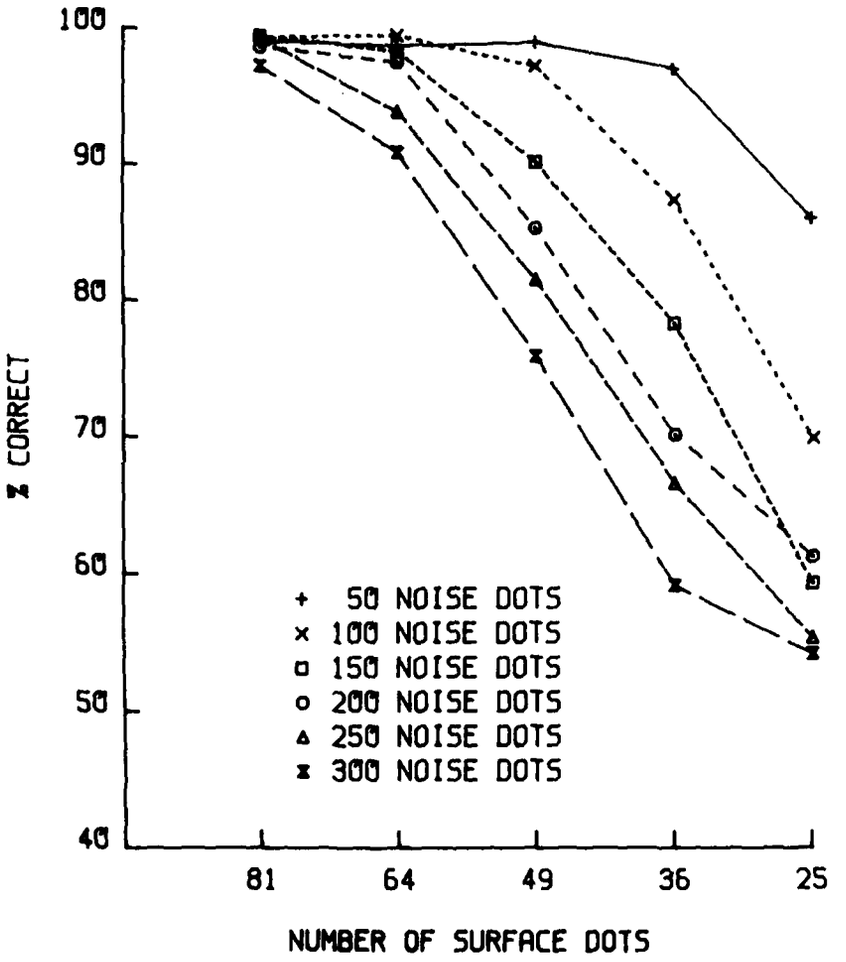
100
90
80
70
60
50
40
% CORRECT
+ 50 NOISE DOTS
× 100 NOISE DOTS
□ 150 NOISE DOTS
○ 200 NOISE DOTS
△ 250 NOISE DOTS
⧗ 300 NOISE DOTS
81
64
49
36
25
NUMBER OF SURFACE DOTS

Figure 72

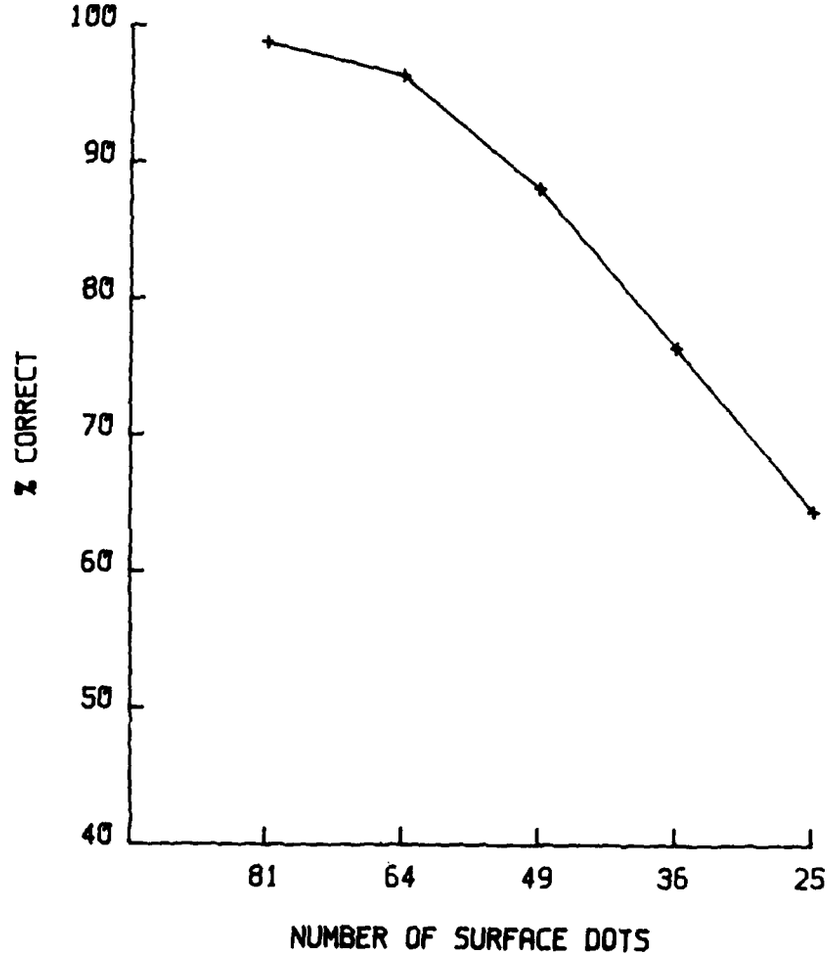
100
90
80
70
60
50
40
% CORRECT
81
64
49
36
25
NUMBER OF SURFACE DOTS

Figure 73

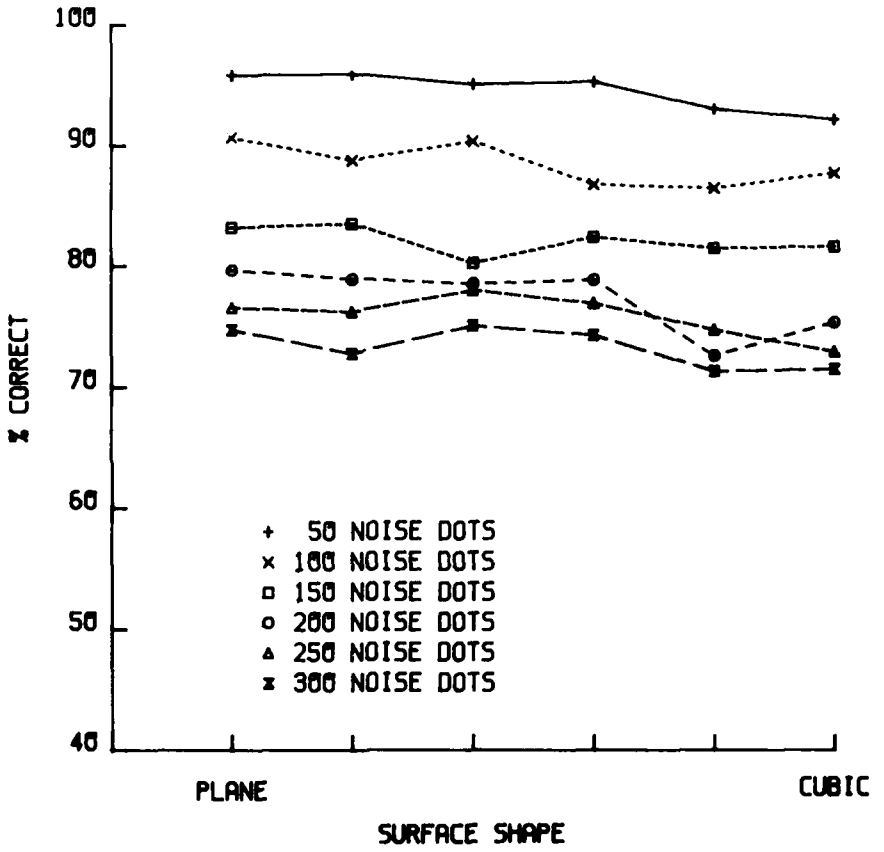
100
90
80
70
60
50
40
% CORRECT
+ 50 NOISE DOTS
× 100 NOISE DOTS
□ 150 NOISE DOTS
○ 200 NOISE DOTS
△ 250 NOISE DOTS
⧗ 300 NOISE DOTS
PLANE
CUBIC
SURFACE SHAPE

Figure 74

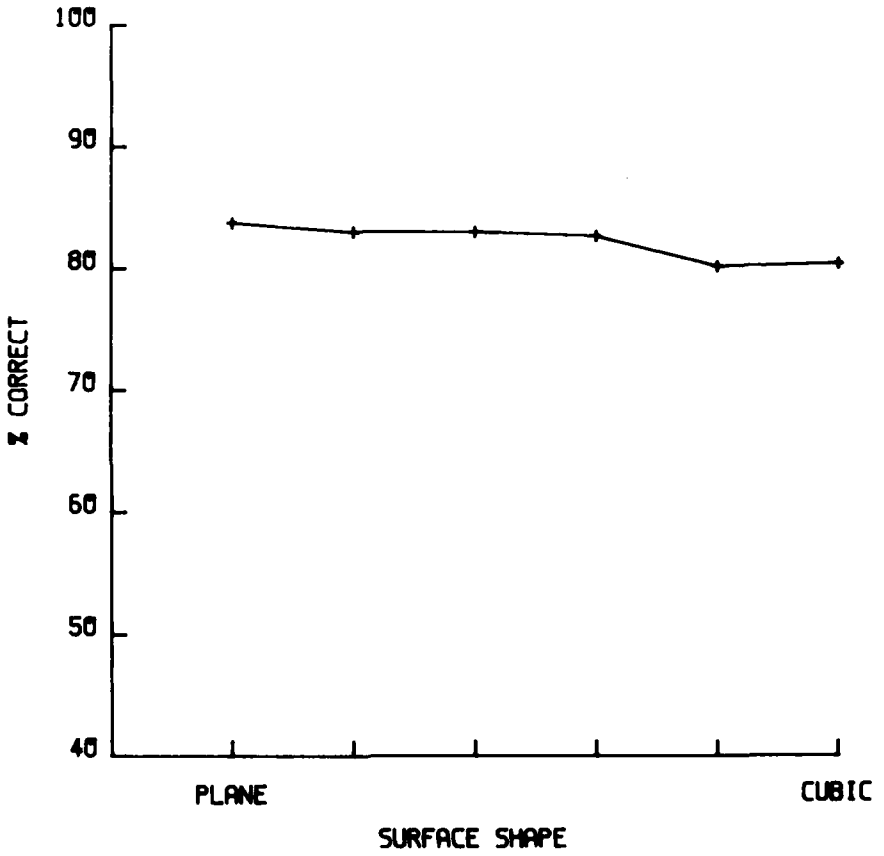

Figure 75

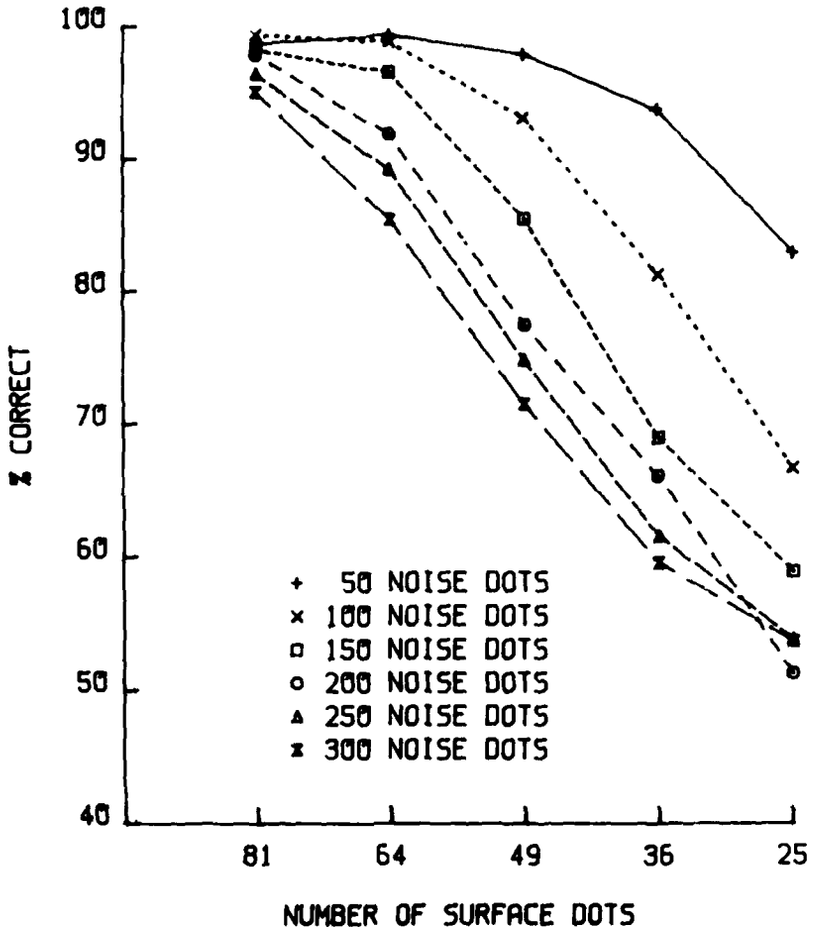
100
90
80
70
60
50
40
% CORRECT
+ 50 NOISE DOTS
× 100 NOISE DOTS
□ 150 NOISE DOTS
○ 200 NOISE DOTS
▲ 250 NOISE DOTS
⧗ 300 NOISE DOTS
81
64
49
36
25
NUMBER OF SURFACE DOTS

Figure 76

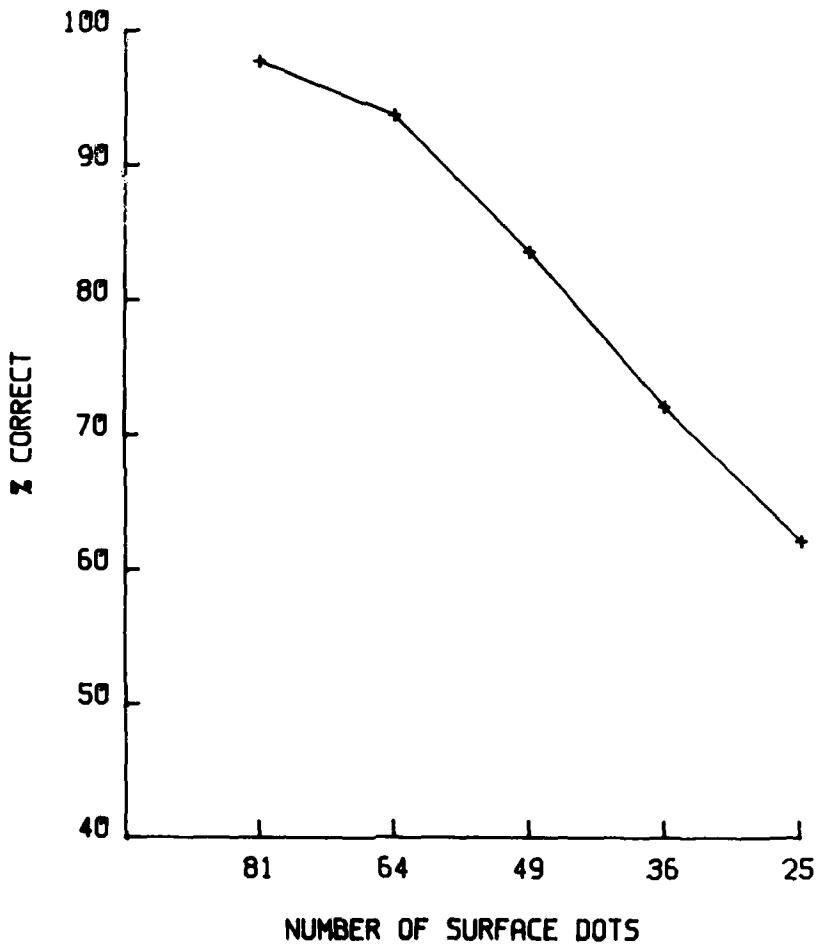
100
90
80
70
60
50
40
% CORRECT
81
64
49
36
25
NUMBER OF SURFACE DOTS

Figure 77

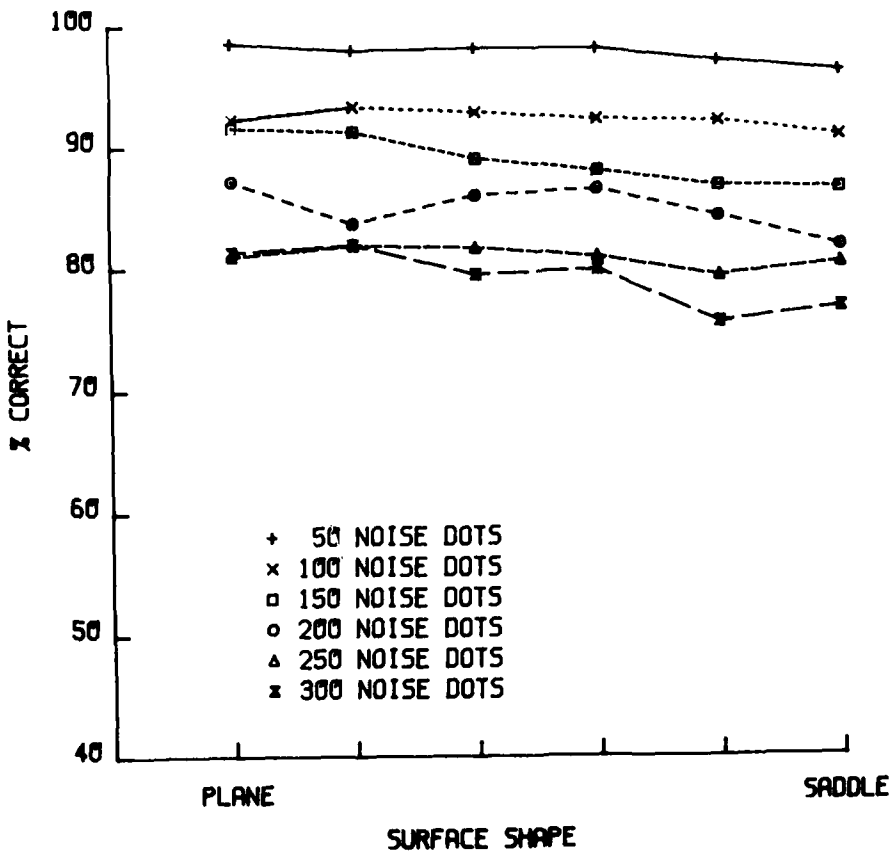
100
90
80
70
60
50
40
% CORRECT
+ 50 NOISE DOTS
× 100 NOISE DOTS
□ 150 NOISE DOTS
○ 200 NOISE DOTS
△ 250 NOISE DOTS
⧗ 300 NOISE DOTS
PLANE
SADDLE
SURFACE SHAPE

Figure 78

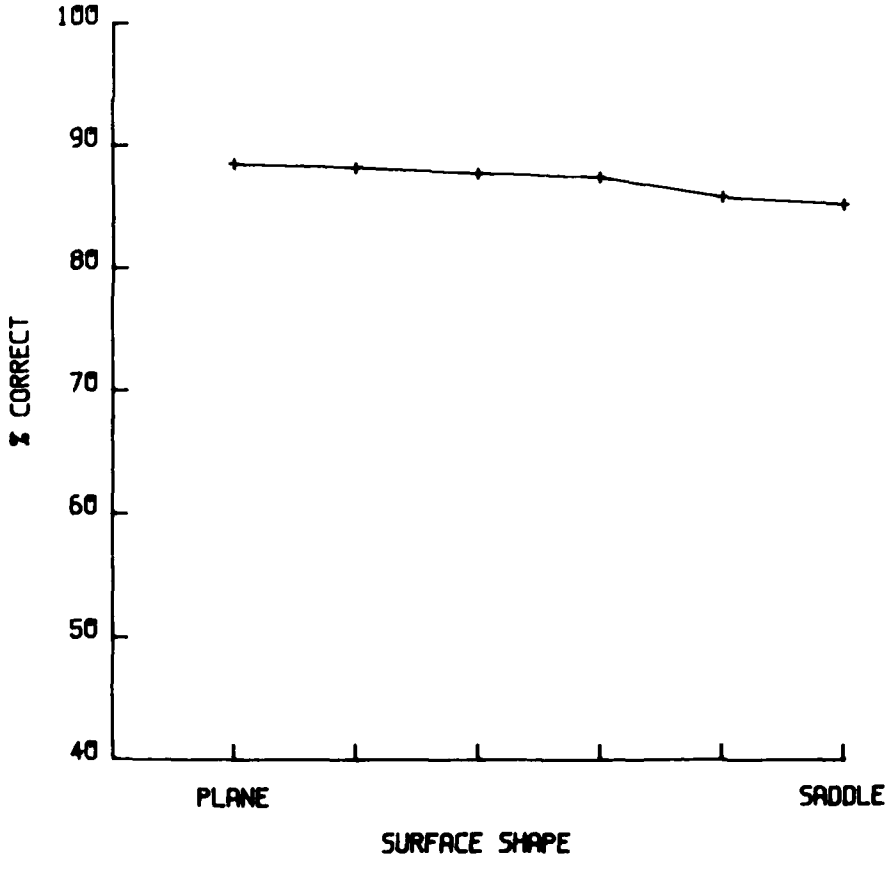

Figure 79

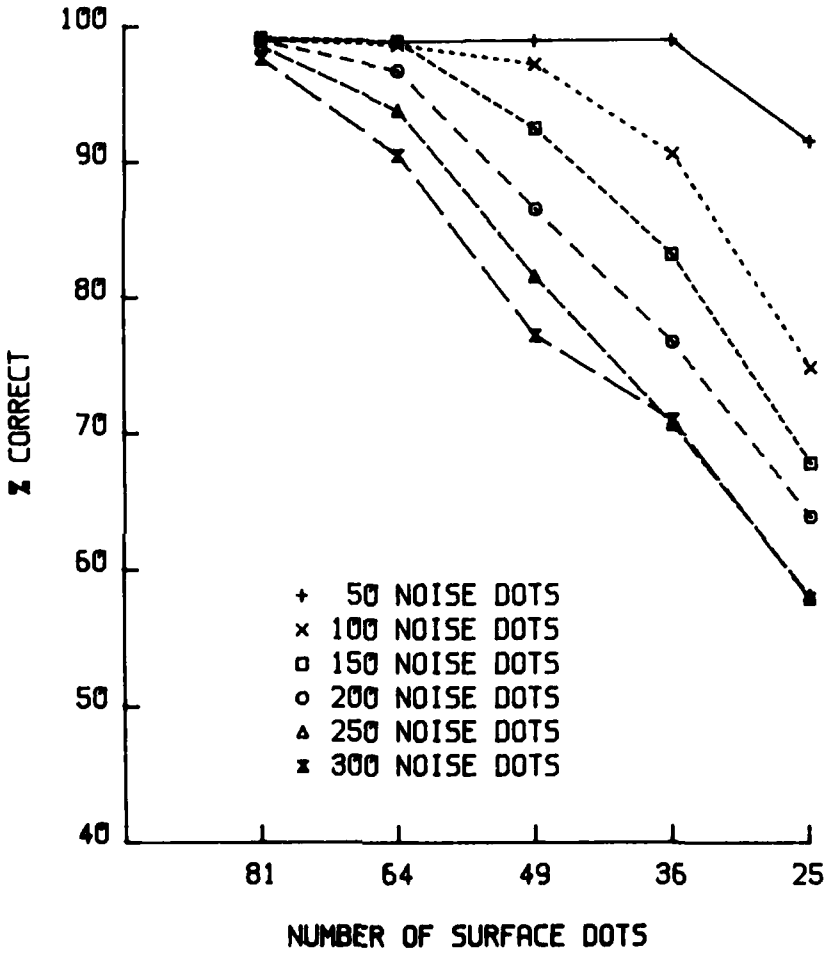
100
90
80
70
60
50
40
% CORRECT
+ 50 NOISE DOTS
× 100 NOISE DOTS
□ 150 NOISE DOTS
○ 200 NOISE DOTS
△ 250 NOISE DOTS
⧗ 300 NOISE DOTS
81
64
49
36
25
NUMBER OF SURFACE DOTS

Figure 80

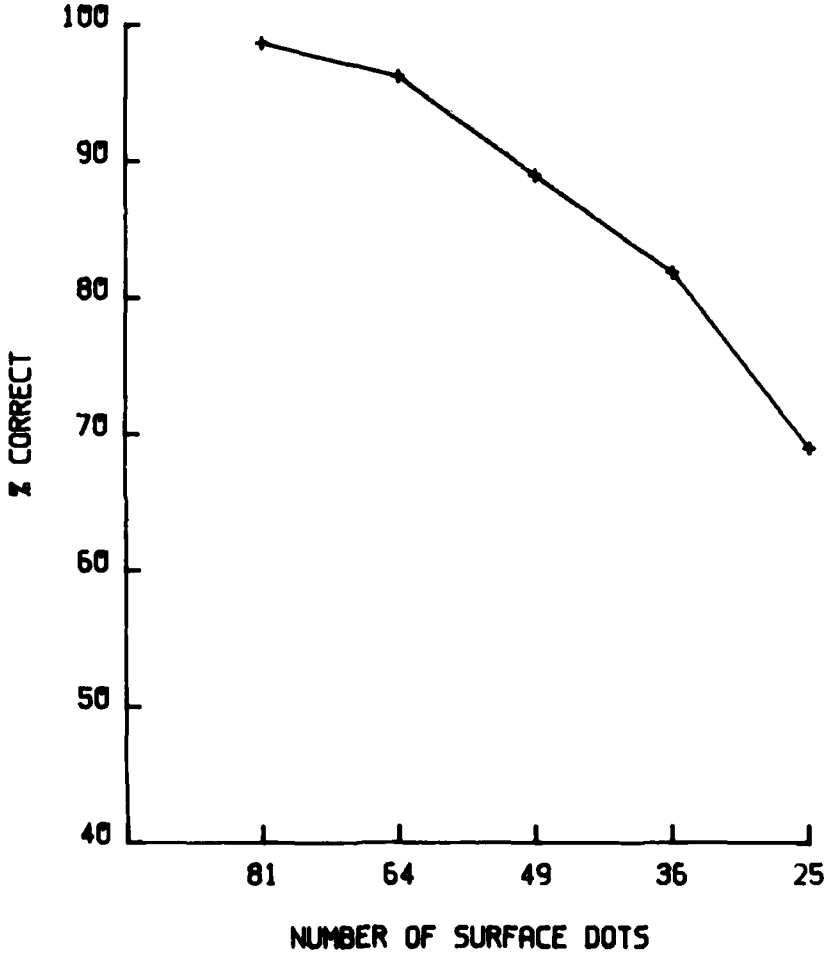
100
90
80
70
60
50
40
% CORRECT
81
64
49
36
25
NUMBER OF SURFACE DOTS

Figure 81

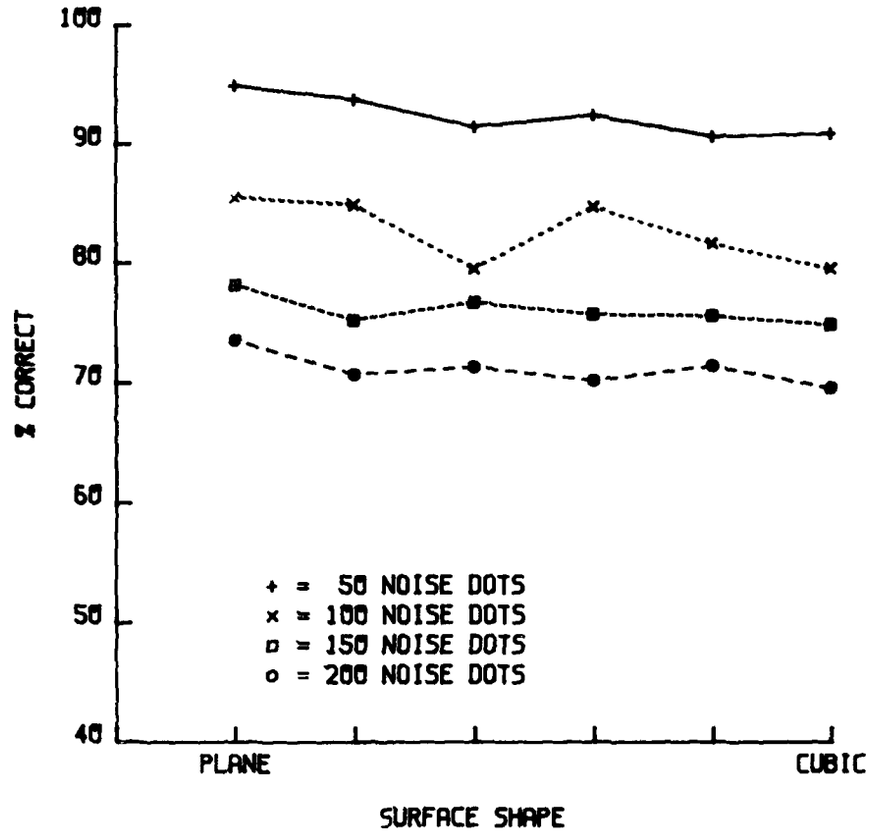
100
90
80
70
60
50
40
% CORRECT
+ = 50 NOISE DOTS
× = 100 NOISE DOTS
□ = 150 NOISE DOTS
o = 200 NOISE DOTS
PLANE
CUBIC
SURFACE SHAPE

Figure 82

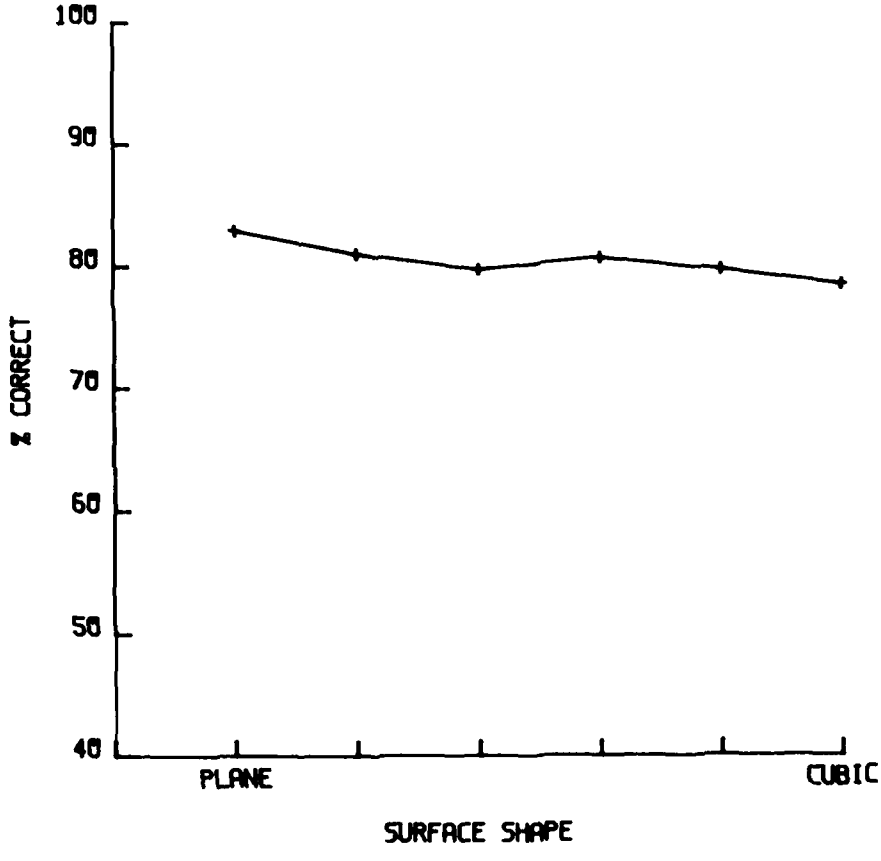

Figure 83

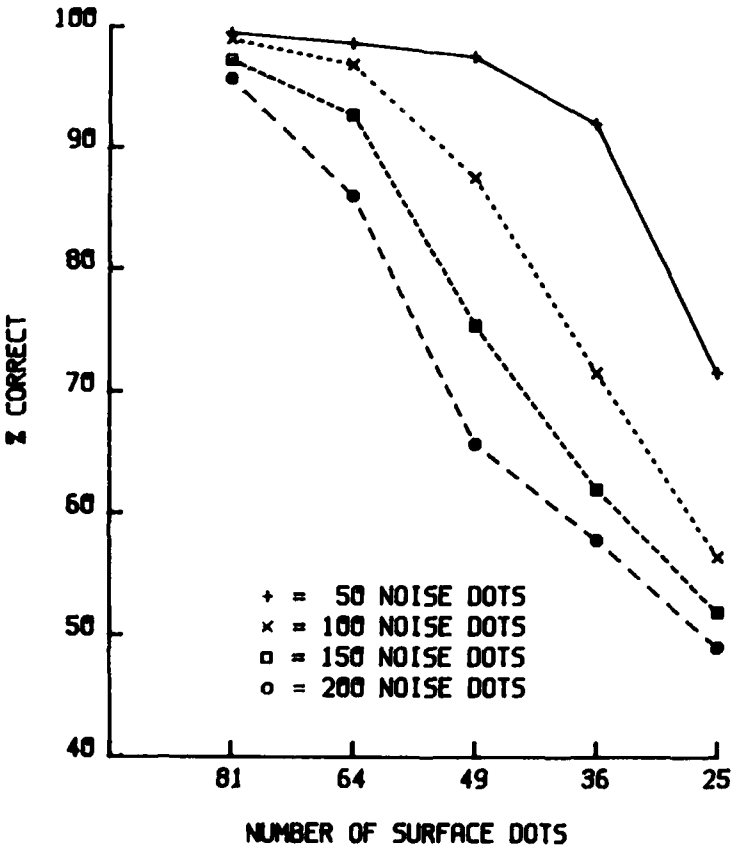
100
90
80
70
60
50
40
% CORRECT
+ = 50 NOISE DOTS
× = 100 NOISE DOTS
□ = 150 NOISE DOTS
o = 200 NOISE DOTS
81
64
49
36
25
NUMBER OF SURFACE DOTS

Figure 84

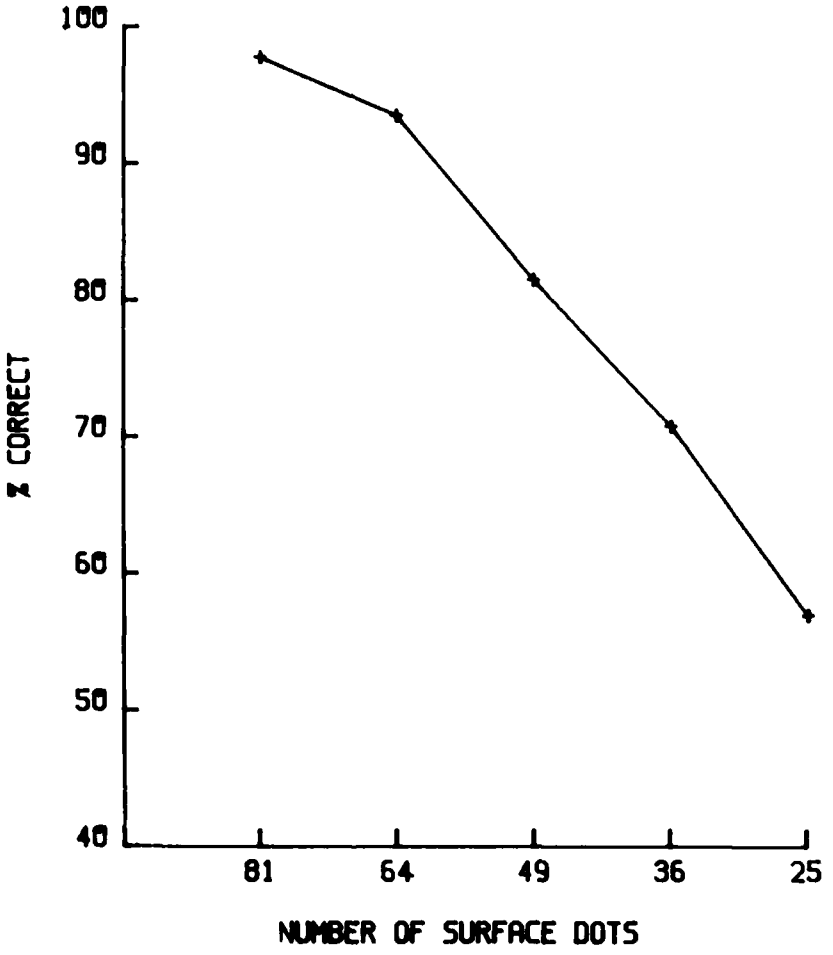
100
90
80
70
60
50
40
% CORRECT
81
64
49
36
25
NUMBER OF SURFACE DOTS

Figure 85

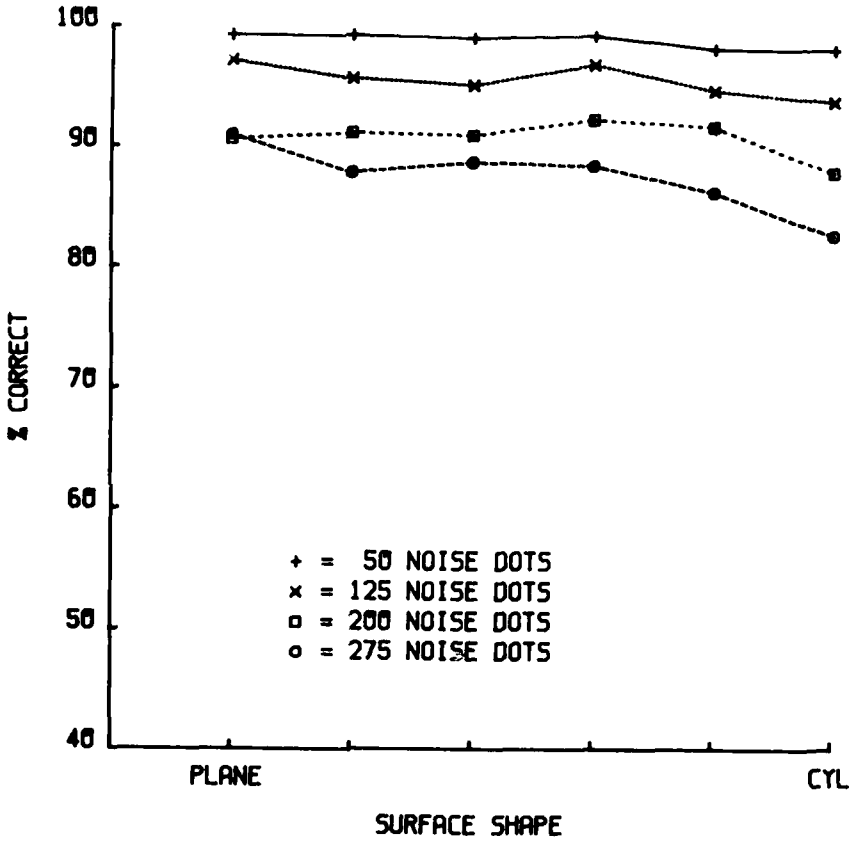
100
90
80
70
60
50
40
% CORRECT
+ = 50 NOISE DOTS
× = 125 NOISE DOTS
□ = 200 NOISE DOTS
○ = 275 NOISE DOTS
PLANE
CYL
SURFACE SHAPE

Figure 86

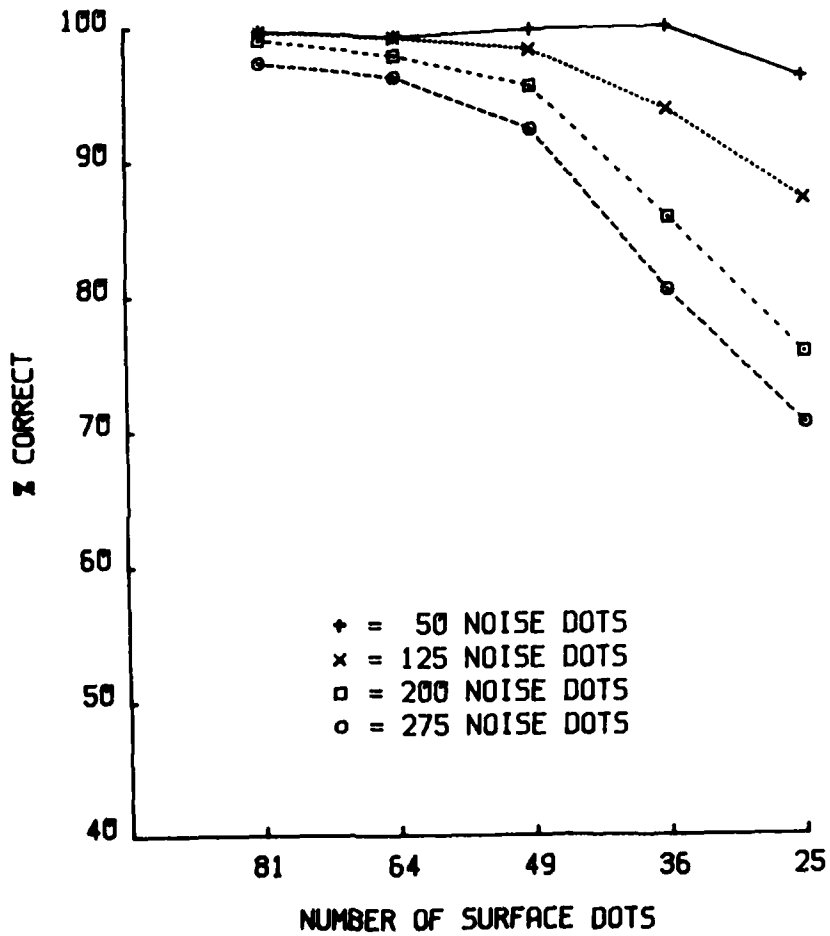
100
90
80
70
60
50
40
% CORRECT
+ = 50 NOISE DOTS
× = 125 NOISE DOTS
□ = 200 NOISE DOTS
o = 275 NOISE DOTS
81
64
49
36
25
NUMBER OF SURFACE DOTS

Figure 87

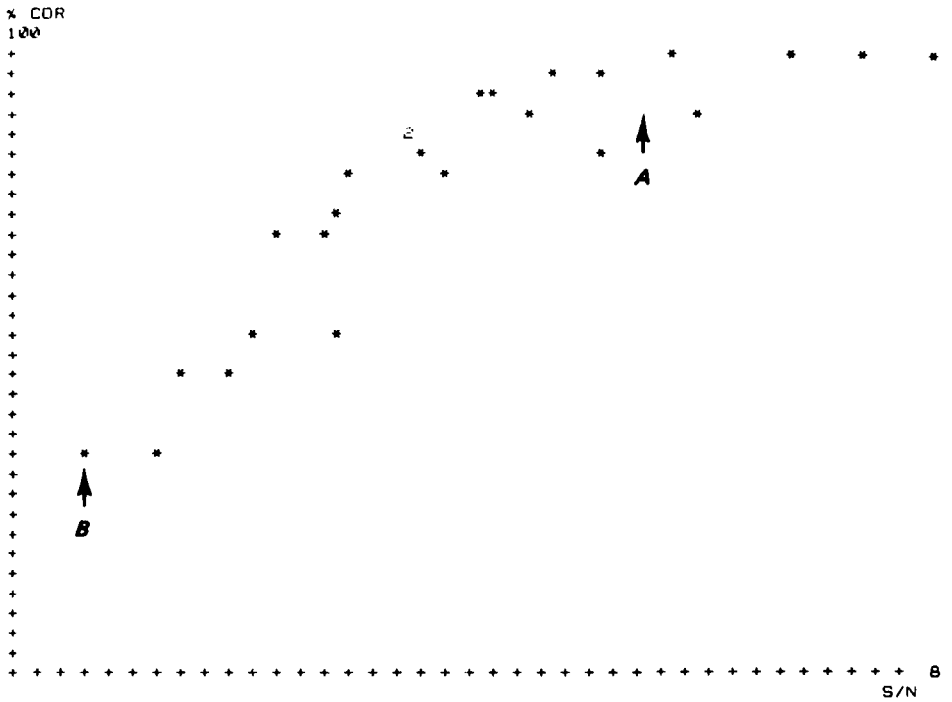

HORIZONTAL AXIS: S/N
LEFT ENDPOINT: -25 RIGHT ENDPOINT: 8

VERTICAL AXIS: % COR
LOWER ENDPOINT: 50 UPPER ENDPOINT: 100

Figure 88

OFFICE OF NAVAL RESEARCH

Engineering Psychology Group

TECHNICAL REPORTS DISTRIBUTION LIST

OSD

CAPT Paul R. Chatelier
Office of the Deputy Under Secretary
of Defense
OUSDRE (E&LS)
Pentagon, Room 3D129
Washington, D.C. 20301

Dr. Dennis Leedom
Office of the Deputy Under Secretary
of Defense (C^{3}I)
Pentagon
Washington, D.C. 20301

Department of the Navy

Engineering Psychology Group
Office of Naval Research
Code 442EP
800 North Quincy Street
Arlington, VA 22217 (3 cys)

Dr. Edward H. Huff
Man-Vehicle Systems Research Division
NASA Ames Research Center
Moffett Field, CA 94035

Dr. Andrew Rechnitzer
Office of the Chief of Naval
Operations, OP952F
Naval Oceanography Division
Washington, D.C. 20350

Manpower, Personnel & Training
Programs
Code 270
Office of Naval Research
800 North Quincy Street
Arlington, VA 22217

Department of the Navy

Statistics and Probability Group
Code 411-S&P
Office of Naval Research
800 North Quincy Street
Arlington, VA 22217

Information Sciences Division
Code 433
Office of Naval Research
800 North Quincy Street
Arlington, VA 22217

CDR Kent S. Hull
Helicopter/VTOL Human Factors Office
NASA-Ames Research Center
MS 239-21
Moffett Field, CA 94035

Special Assistant for Marine Corps
Matters
Code 100M
Office of Naval Research
800 North Quincy Street
Arlington, VA 22217

CDR James Offuff, Officer-in-Charge
ONR Detachment
1030 East Green Street
Pasadena, CA 91106

Director
Naval Research Laboratory
Technical Information Division
Code 2627
Washington, D.C. 20375

Dr. Michael Melich
Communications Sciences Division
Code 7500
Naval Research Laboratory
Washington, D.C. 20375

Department of the Navy

Naval Training Equipment Center
ATTN: Technical Library
Orlando, FL 32813

Dr. Robert G. Smith
Office of the Chief of Naval Operations, OP987H
Personnel Logistics Plans
Washington, D.C. 20350

Combat Control Systems Department
Code 35
Naval Underwater Systems Center
Newport, RI 02840

Human Factors Department
Code N-71
Naval Training Equipment Center
Orlando, FL 32813

Dr. Alfred F. Smode
Training Analysis and Evaluation Group
Naval Training & Equipment Center
Orlando, Fl 32813

CDR Norman E. Lane
Code N-7A
Naval Training Equipment Center
Orlando, FL 32813

Dean of Research Administration
Naval Postgraduate School
Monterey, CA 93940

Human Factors Engineering
Code 8231
Naval Ocean Systems Center
San Diego, CA 92152

Dr. Ross Pepper
Naval Ocean Systems Center
Hawaii Laboratory
P. O. Box 997
Kailua, HI 96734

Dr. A. L. Slafkosky
Scientific Advisor
Commandant of the Marine Corps
Code RD-1
Washington, D.C. 20380

Department of the Navy

CDR C. Hutchins
Code 55
Naval Postgraduate School
Monterey, CA 93940

Human Factors Technology Administrator
Office of Naval Technology
Code MAT 0722
800 North Quincy Street
Arlington, VA 22217

Commander
Naval Air Systems Command
Human Factors Programs
NAVAIR 334A
Washington, D.C. 20361

Commander
Naval Air Systems Command
Crew Station Design
NAVAIR 5313
Washington, D.C. 20361

Mr. Phillip Andrews
Naval Sea Systems Command
NAVSEA 61R
Washington, D.C. 20362

Commander
Naval Electronics Systems Command
Human Factors Engineering Branch
Code 81323
Washington, D.C. 20360

Dr. George Moeller
Human Factors Engineering Branch
Submarine Medical Research Lab
Naval Submarine Base
Groton, CT 06340

Head
Aerospace Psychology Department
Code L5
Naval Aerospace Medical Research Lab
Pensacola, FL 32508

Navy Personnel Research and Development Center
Planning & Appraisal Division
San Diego, CA 92152

Department of the Navy

Dr. Robert Blanchard
Navy Personnel Research and
Development Center
Command and Support Systems
San Diego, CA 92152

CDR J. Funaro
Human Factors Engineering Division
Naval Air Development Center
Warminster, PA 18974

Mr. Stephen Merriman
Human Factors Engineering Division
Naval Air Development Center
Warminster, PA 18974

Mr. Jeffrey Grossman
Human Factors Branch
Code 3152
Naval Weapons Center
China Lake, CA 93555

Human Factors Engineering Branch
Code 4023
Pacific Missile Test Center
Point Mugu, CA 93042

Dean of the Academic Departments
U. S. Naval Academy
Annapolis, MD 21402

Department of the Army

Dr. W. Moroney
Human Factors Section
Systems Engineering Test
Directorate
U.S. Naval Air Test Center
Patuxent River, MD 20670

Dr. Edgar M. Johnson
Technical Director
U.S. Army Research Institute
5001 Eisenhower Avenue
Alexandria, VA 22333

Technical Director
U.S. Army Human Engineering Labs
Aberdeen Proving Ground, MD 21005

Department of the Army

Director, Organizations and
Systems Research Laboratory
U.S. Army Research Institute
5001 Eisenhower Avenue
Alexandria, VA 22333

Mr. J. Barber
HQS, Department of the Army
DAPE-MBR
Washington, D.C. 20310

Department of the Air Force

U.S. Air Force Office of Scientific
Research
Life Sciences Directorate, NL
Bolling Air Force Base
Washington, D.C. 20332

AFHRL/LRS TDC
Attn: Susan Ewing
Wright-Patterson AFB, OH 45433

Chief, Systems Engineering Branch
Human Engineering Division
USAF AMRL/HES
Wright-Patterson AFB, OH 45433

Dr. Earl Alluisi
Chief Scientist
AFHRL/CCN
Brooks AFB, TX 78235

Foreign Addressees

Dr. Kenneth Gardner
Applied Psychology Unit
Admiralty Marine Technology
Establishment
Teddington, Middlesex TW11 OLN
England

Director, Human Factors Wing
Defence & Civil Institute of
Environmental Medicine
Post Office Box 2000
Downsview, Ontario M3M 3B9
Canada

Foreign Addressees

Dr. A. D. Baddeley
Director, Applied Psychology Unit
Medical Research Council
15 Chaucer Road
Cambridge, CB2 2EF England

Other Government Agencies

Defense Technical Information Center
Cameron Station, Bldg. 5
Alexandria, VA 22314 (12 cps)

Other Government Agencies

Dr. M. D. Montemerlo
Human Factors & Simulation
Technology, RTE-6
NASA HQS
Washington, D.C. 20546

Other Organizations

Ms. Denise Benel
Essex Corporation
333 North Fairfax Street
Alexandria, VA 22314

Dr. Jesse Orlansky
Institute for Defense Analysis
1801 N. Beauregard Street
Alexandria, VA 22311

Dr. Robert T. Hennessy
NAS - National Research Council (COHF)
2101 Constitution Avenue, N.W.
Washington, D.C. 20418

Dr. Robert Fox
Department of Psychology
Vanderbilt University
Nashville, TN 37240

Dr. James H. Howard, Jr.
Department of Psychology
Catholic University
Washington, D.C. 20064

Other Organizations

Dr. Christopher Wickens
Department of Psychology
University of Illinois
Urbana, IL 61801

Dr. Babur M. Pulat
Department of Industrial Engineering
North Carolina A&T State University
Greensboro, NC 27411

National Security Agency
Attn: N-32, Marie Goldberg
9800 Savage Road
Ft. Meade, MD 20722

Dr. Stanley N. Roscoe
New Mexico State University
Box 5095
Las Cruces, NM 88003

Dr. Richard Pew
Bolt Beranek & Newman, Inc.
50 Moulton Street
Cambridge, MA 02238

Dr. David J. Getty
Bolt Beranek & Newman, Inc.
50 Moulton Street
Cambridge, MA 02238

END

FILMED

4-84

DTIC